Developing a systemic monoclonal antibody therapy for the treatment of large burn injuries

by

Alireza Hassanshahi

Bachelor of Molecular Genetics

Master of Molecular Genetics

A thesis submitted for the degree of

Doctor of Philosophy
(Biomaterials Engineering and Nanomedicine)

Regenerative Medicine

Clinical and Health Sciences

Future Industries Institute

University of South Australia



University of
South Australia

February 2023

Contents

List of Figures vii
List of Tables x
List of Abbreviations xi
Project Summary xiv
Declaration xvi
Acknowledgments xvii
Chapter 1: Introduction 1
1.1 Skin Structure 2
1.2 Cutaneous wound healing 4
1.2.1 Haemostasis 6
1.2.2 Inflammation 6
1.2.3 Proliferation 8
1.2.4 Matrix remodelling 9
1.3 Burns 11
1.3.1 Pathophysiology of burn wounds 11
1.3.2 Depth of the Burn 12
1.4 The complications of burn injury healing 13
1.4.1 Prolonged inflammation 14
1.4.2 Infection 14
1.4.3 Hypertrophic scarring 15
1.5 Current management for burn patients 15
1.5.1 Wound grafting 16
1.5.2 Management of inflammation 16
1.5.3 Management of infection 17
1.5.4 Transforming growth factor-β modulators 17
1.5.5 Botulinum toxin A 17
1.6 Challenges of extensive burn injuries 18
1.6.1 Treatment of extensive burn injuries with topical agents and dressings 19
1.7 The need for novel therapeutics for the treatment of burn injuries 19
1.8 Flightless I 20
1.8.2 LRR and gelsolin domains of Flii interact with various binding partners 24
1.9 Flii is a negative regulator of wound repair 27

1.10 Flii affects proliferation migration, and apoptosis 28
1.11 Flii and the immune response during wound healing 29
1.12 Flii and TGFβ/Smad-dependent signalling pathway 30
1.13 The expression of Flii in burn wounds and hypertrophic scarring 30
1.14 Targeting Flii to improve healing outcomes 31
1.14.1 Antibody strategies for decreasing level of Flii 32
1.15 Therapeutic antibodies 32
1.15.1 Therapeutic monoclonal antibodies 32
1.16 Antibody therapy 33
1.17 Monoclonal antibodies against Flii protein 34
1.17.1 Targeting Flii using Flii neutralizing antibody to improve the healing process 34
1.18 The impact of FliiL FnAbs on burn wound and hypertrophic scarring 37
1.20 Systemic delivery of FnAbs to burn wounds 39
1.21 Knowledge gap, aims and hypotheses 40
1.21.1 Hypotheses and aims 40
Chapter 2: Materials and Methods 41
2.1 Generating new Flii neutralizing antibodies against Flii 42
2.1.1 General FnAb purification method 43
2.2 Cell culture and *in vitro* assays 44
2.2.1 Cell culture 44
2.2.2 Cell passaging 46
2.2.3 Cell proliferation assay 46
2.2.4 Scratch wound closure assay 47
2.2.5 Matrigel tube formation assay 47
2.2.6 siRNA knockdown 48
2.2.7 Gene expression studies 49
2.2.8 Protein expression studies 51
2.3 Animal Studies 54
2.3.1 Murine model of excisional wound healing 54
2.3.2 Rapid antibody labelling 56
2.3.3 Murine model of second-degree partial-thickness scald burn 56
2.4 Animal tissue processing and analysis 59
2.4.1 Tissue fixation and processing 59
2.4.2 Haematoxylin and eosin staining (H&E) 60

2.4.3 Immunohistochemistry 61
2.5 Measurement and analysis 63
2.5.1 Macroscopic wound measurement 63
2.5.2 IVIS analysis 63
2.5.3 Histology and immunohistochemistry measurement/analysis 64
2.6 Preparation of protein lysates 67
2.7 ELISA 67
2.8 Statistical analysis 68
Chapter 3: The impact of LRRFnAb and MFnAb on the function of human skin cells 69
3.1 Introduction 70
3.2 Results 72
3.2.1 MFnAbs improved the proliferation of keratinocytes 72
3.2.2 LRRFnAbs and MFnAbs increased the migration of keratinocytes 75
3.2.3 MFnAbs improved the proliferation of fibroblasts 78
3.2.4 MFnAbs improved the migration of fibroblasts 81
3.2.5 LRRFnAb improved the proliferation of dermal endothelial cells 84
3.2.6 LRRFnAb and MFnAb improved the migration of dermal endothelial cells 87
3.2.7 LRRFnAb and MFnAb stimulated tube formation of endothelial cells and increased half-life of formed capillaries 90
3.3 Discussion 96
Chapter 4: Systemic delivery of FnAbs raised against LRR and middle domains of Flii improves excisional wound healing in an acute wound murine model 100
4.1 Introduction 101
4.2 Results 103
4.2.1 Wound healing was accelerated in LRRFnAb and MFnAb treated mice 103
4.2.2 Flii expression was reduced in LRRFnAb and MFnAb treated mice 106
4.2.3 Inflammation was reduced in LRRFnAb and MFnAb treated mice 108
4.2.4 Angiogenesis was enhanced in LRRFnAb and MFnAb treated mice 111
4.2.5 VEGF expression was elevated in MFnAb treated mice 114
4.2.6 FGF-2 expression was increased in LRRFnAb treated mice 116
4.2.7 PDGF-BB expression was stimulated in LRRFnAb treated mice 118
4.3 Discussion 120
Chapter 5: Systemically administered FnAbs are effective at improving burn repair in a mouse model of partial-thickness scald injury 125

5.1 Introduction 126
5.2 Results 128
5.2.1 IP injected FnAbs localized to the site of burn injury 128
5.2.2 Effects of LRRFnAb and MFnAb treatment on wound healing in mice 131
5.2.3 Systemically administered MFnAb significantly reduced the expression level of Flii in the burn area 134
5.2.4 The number of myofibroblasts was elevated in the dermis of MFnAb treated mice. 136
5.2.5 Systemic delivery of LRRFnAb and MFnAb attenuated local inflammation in burn wounds 138
5.2.6 Systemic delivery of LRRFnAb and MFnAb increased the number of endothelial cells in the burn wounds 141
5.2.7 The number of mature blood vessels was elevated in LRRFnAb treated mice 143
5.2.8 Systemic delivery of LRRFnAb and MFnAb promoted the expression of VEGF within the burn wound 146
5.2.9 Systemic administration of LRRFnAb and MFnAb increased the expression of FGF-2 within the burn wound 148
5.2.10 TGF-β1 production was significantly reduced in MFnAb treated mice 150
5.3 Discussion 152
Chapter 6: Investigating the signalling pathways that lead to the pro-angiogenic effects of intracellular and extracellular Flii 158
6.1 Introduction: 159
6.2 Results 161
6.2.1 VEGF-A was upregulated in both LRRFnAb and MFnAb treated endothelial cells while the expression of PDGF-BB was downregulated in LRRFnAb and MFnAb treated endothelial cells 161
6.2.2 The effect of rFlii on the expression of pro-angiogenic genes in dermal endothelial cells 163
6.2.3 Knockdown of Flii by siRNA significantly decreased Flii RNA in dermal endothelial cells 165
6.2.4 Flii Knockdown attenuated intracellular Flii protein level in dermal endothelial cells 166
6.2.5 Flii knockdown by siRNA significantly upregulates FGF-2 and PDGF-BB levels in dermal endothelial cells 167
6.2.6 VEGF-A was elevated in MFnAb treated keratinocytes and FGF-2 was upregulated in LRRFnAb treated keratinocytes 169
6.2.7 The effect of rFlii on the expression of pro-angiogenic genes in keratinocytes 171
6.2.8 Knockdown of Flii by siRNA significantly attenuated Flii RNA in keratinocytes ... 173

6.2.9 Flii knockdown by siRNA promoted VEGF-A and FGF-2 expression and attenuated the PDGF-BB levels in skin keratinocytes 174
6.2.10 The effect of rFlii and MFnAb on the gene expression of pro-angiogenic factors in fibroblasts 176
6.3 Discussion 178
Chapter 7: General Discussion 183
7.1 Project significance 184
7.2 Systemic delivery of LRRFnAb in wound healing 185
7.3 Systemic delivery of MFnAb in wound healing 188
7.4 LRRFnAbs vs MFnAbs in wound healing 191
7.5 Extracellular and intracellular Flii interfere with the expression of pro-angiogenic factors and regulate angiogenesis 198
7.5.1 The effect of extracellular Flii on the expression of pro-angiogenic factors 198
7.5.2 The effect of intracellular Flii on the expression of pro-angiogenic factors 199
7.6 Limitations and Future Outlook 201
References 204

List of Figures

Figure 1. 1: Schematic representation of epidermis and dermis 3
Figure 1. 2: The stages of wound repair 5
Figure 1. 3: Illustration of different depths of burn injury 13
Figure 1. 4: Schematic diagram of Flii 20
Figure 1. 5: Interactions of the LRR and gelsolin domains of Flii: orchestrating cellular dynamics and molecular signalling 26
Figure 1. 6: Flii is elevated in acute burns and hypertrophic scars 31
Figure 1. 7: Structure of an IgG monoclonal antibody. 33
Figure 1. 8: Topical application of first generation Flii neutralising antibody (FliiL FnAb) to incisional and excisional wounds 36
Figure 1. 9: Local delivery of first generation Flii neutralizing antibody (FliiL FnAb) to burn wounds 38
Figure 2. 1: FnAbs production method using DNA super-immunization method. 43
Figure 2. 2: Portions of Flightless I protein that were used to generate LRRFnAb and MFnAb. 43
Figure 2. 3: The assessment of LRRFnAb and MFnAb affinity with Flii 44
Figure 2. 4: Human skin cells 45
Figure 2. 5: Matrigel-based tube formation assay 48
Figure 2. 6: Schematic of FnAb delivery to a murine model of excisional wound healing by IP injection 55
Figure 2. 7: The procedures of a murine model of second-degree partial-thickness scald burn .. 58
Figure 2. 8: Fluorescence *in vivo* imaging and analysis by IVIS Lumina S5 Imaging System 63
Figure 2. 9: Histological measurements of wound healing 65
Figure 2. 10: Fluorescent immunohistochemical staining 66
Figure 3. 1: Effect of LRRFnAb and MFnAb on the proliferation of keratinocytes 74
Figure 3. 2: Effect of LRRFnAb and MFnAb on the migration of keratinocytes 77
Figure 3. 3: Effect of LRRFnAb and MFnAb on the proliferation of fibroblasts 80
Figure 3. 4: Effect of LRRFnAb and MFnAb on the migration of fibroblasts 83
Figure 3. 5: Effect of LRRFnAb and MFnAb on the proliferation of endothelial cells 86

Figure 3. 6: Effect of LRRFnAb and MFnAb on the migration of endothelial cells..... 89
Figure 3. 7: Effect of LRRFnAb and MFnAb on angiogenesic tube formation..... 93
Figure 3. 8: Effect of LRRFnAb and MFnAb on vascular organization 95
Figure 4. 1: Macroscopic assessment: Effect of LRRFnAb and MFnAb on the rate of murine excisional wound healing..... 104
Figure 4. 2: Histological assessment: Effect of LRRFnAb and MFnAb on the rate of excisional wound healing..... 106
Figure 4. 3: Effect of LRRFnAb and MFnAb on Flii expression..... 107
Figure 4. 4: Impact of LRRFnAb and MFnAb on neutrophil infiltration..... 109
Figure 4. 5: Impact of LRRFnAb and MFnAb on macrophage infiltration and polarization in the wound site..... 110
Figure 4. 6: Impact of LRRFnAb and MFnAb on angiogenesis in excisional wounds..... 113
Figure 4. 7: Effect of LRRFnAb and MFnAb on VEGF expression..... 115
Figure 4. 8: Effect of LRRFnAb and MFnAb on FGF-2 expression in the wound site 117
Figure 4. 9: Effect of LRRFnAb and MFnAb on PDGF-BB expression..... 119
Figure 5. 1: Localization of systemically administered LRRFnAb and MFnAb in murine burn wounds..... 129
Figure 5. 2: Antibody localization of systemically administered LRRFnAb and MFnAb in murine burn wounds..... 130
Figure 5. 3: Macroscopic assessment: Effect of IP injected LRRFnAb and MFnAb on the rate of burn injury healing..... 133
Figure 5. 4: Histological assessment: Effect of LRRFnAb and MFnAb on the rate of burn injury healing..... 134
Figure 5. 5: Effect of LRRFnAb and MFnAb on Flii expression..... 135
Figure 5. 6: Effect of LRRFnAb and MFnAb on myofibroblasts in the partial-thickness burns 137
Figure 5. 7: Impact of LRRFnAb and MFnAb on neutrophil infiltration in the deep dermis 139
Figure 5. 8: Impact of LRRFnAb and MFnAb on macrophage infiltration and polarization in the burn site..... 140
Figure 5. 9: Effect of LRRFnAb and MFnAb on endothelial cells in the partial-thickness burns 142
Figure 5. 10: Impact of systemic delivery of LRRFnAb and MFnAb on angiogenesis in burns 145

Figure 5. 11: Effect of LRRFnAb and MFnAb on VEGF expression 147
Figure 5. 12: Effect of LRRFnAb and MFnAb on FGF-2 expression in the burn site 149
Figure 5. 13: Effect of LRRFnAb and MFnAb on TGF-β1 expression in burn wounds..... 151
Figure 6. 1: Effect of LRRFnAb and MFnAb on mRNA expression of pro-angiogenic factors in dermal endothelial cells 162
Figure 6. 2: Impact of rFlii and FnAb neutralizing rFlii on mRNA expression of pro-angiogenic factors in dermal endothelial cells 164
Figure 6. 3: Flii knockdown by siRNA significantly decreased Flii in dermal endothelial cells 165
Figure 6. 4: Impact of Flii knockdown on protein level of Flii in dermal endothelial cells 166
Figure 6. 5: Effect of Flii knockdown on mRNA expression of pro-angiogenic factors in dermal endothelial cells 168
Figure 6. 6: Impact of LRRFnAb and MFnAb on mRNA expression of pro-angiogenic factors in keratinocytes 170
Figure 6. 7: Impact of rFlii and FnAb binding rFlii on mRNA expression of pro-angiogenic factors in keratinocytes 172
Figure 6. 8: Flii knockdown by siRNA significantly attenuated Flii in keratinocytes 173
Figure 6. 9: Effect of Flii knockdown on mRNA expression of pro-angiogenic factors in keratinocytes 175
Figure 6. 10: Impact of MFnAb, rFlii, and MFnAb binding rFlii on mRNA expression of pro-angiogenic factors in fibroblasts 177
Figure 7. 1: *In vitro* and *in vivo* effects of LRRFnAb and MFnAb on wound healing compared to IgG antibody control 197

List of Tables

Table 1. 1: Flii binding partners 21
Table 2. 1: siRNA sequences for scrambled control siRNA (siControl) and siFlii conditions 49
Table 2. 2: PCR primers 51
Table 2. 3: Polyacrylamide gels for protein resolution 53
Table 2. 4: The standard protocol for tissue processing 60
Table 2. 5: List of the primary and secondary antibodies for Fluorescent Immunohistochemistry 62
Table 7. 1. *In vitro* and *in vivo* effects of LRRFnAb and MFnAb compared to IgG antibody control. 195

List of Abbreviations

Ang-1	Angiopoietin 1
Ang-2	Angiopoietin 2
AP-1	Activator protein 1
AR	Androgen receptor
ARC	Animal Resources Centre
BCA	Bicinchoninic acid
BCL-2	B-cell lymphoma 2
CARM1	Coactivator-associated arginine methyltransferase 1
CO2	Carbon dioxide
DAPI	4′,6-Diamidino-2-phenylindole
DC	Dendritic cell
DMEM	Dulbecco's Modified Eagle Medium
DNA	Deoxyribonucleic acid
ECM	Extracellular matrix
EDTA	Ethylenediaminetetraacetic acid
ELISA	Enzyme-linked immunosorbent assay
ER	Estrogen receptor
ERK	Extracellular signal-regulated kinase
EthoH	Ethanol
FBS	Fetal bovine serum
Fc	Fragment crystallizable
Flii	Flightless I
FliiL FnAb	First generation Flightless I neutralizing antibody
FnAb	Flightless I neutralizing antibody
Fv	Variable fragment
G3BP1	Ras GTPase-activating protein-binding protein 1
GR	Glucocorticoid receptor
GREB1	Growth regulation by estrogen in breast cancer 1

H&E	Hematoxylin and eosin
HaCaT	High sensitivity of human epidermal keratinocytes
HDMECs	Human dermal microvascular endothelial cells
HFFs	Human foreskin fibroblasts
HUVEC	Human umbilical vein endothelial cells
IFN	Interferon
IgG	Immunoglobulin G
IL	Interleukin
IP	Intraperitoneal
IQGAP1	Ras GTPase-activating-like protein
LRR	Leucine-rich repeat
LRRFIP	Leucine-rich repeat Flightless-interacting protein
LRRFnAb	Flightless I neutralizing antibody raised against the LRR of Flii
mAbs	Monoclonal antibodies
MFnAb	Flightless I neutralizing antibody raised against the middle domain of Flii
MMP	Matrix metalloproteinase
mRNA	Messenger ribonucleic acid
Myc	Myelocytomatosis viral oncogene
NLRP3	Nucleotide-binding domain-like receptor protein 3
PBS	Phosphate-buffered saline
PDGF	Platelet derived growth factor
pSiNPs	porous silicon nanoparticles
rFlii	Recombinant Flightless I
RNA	Ribonucleic acid
ROS	Reactive oxygen species
RT-PCR	Real-time reverse transcription–polymerase chain reaction
SDS-PAGE	Sodium dodecyl-sulfate polyacrylamide gel electrophoresis
siRNA	Small interfering RNA
TGF-β	Transforming growth factor beta
TLR4	Toll-like receptor 4
TNF-α	Tumour necrosis factor alpha

Tris	Trisaminomethane
VEGF	Vascular endothelial growth factor
VSMCs	Vascular smooth muscle cells
αSMA	Alpha smooth muscle actin
β-Cat	Beta-catenin

Project Summary

Despite many advances in burn care, management of burn injuries remains a challenge and slow wound repair, pain, and hypertrophic scarring are causes of ongoing patient morbidity. Flightless I (Flii) is a member of the gelsolin family of cytoskeletal proteins and consists of six gelsolin-like domains and a leucine-rich repeat (LRR) domain at the N-terminus. Flii is elevated in wounds including burns and reducing the level of Flii is a promising approach for improving wound repair. The most effective approach has been to neutralise Flii activity using application of function blocking monoclonal antibodies. LRR and gelsolin domains of Flii interact with various binding partners and enable Flii to interfere with various cellular events. The first Flii neutralizing antibodies (FliiL FnAbs) were generated against a specific antigen sequence corresponding to aa57-66 in the LRR of human Flii and has been shown to improve wound healing *in vitro* and *in vivo*. This research aimed to determine whether blocking different parts of the Flii protein would result in different cell functions so specific FnAbs were employed to target against LRR (LRRFnAb) and middle domain of Flii (MFnAb). Additionally, FliiL FnAbs have been used in localized, topical and intradermal applications, however, large surface area burns are difficult to treat by intradermal injection of therapeutics so LRRFnAbs and MFnAbs were tested systemically in an acute wound murine and a mouse model of partial-thickness scald injury in this study.

The impact of LRRFnAbs on wound healing was investigated both *in vitro* and *in vivo*. *In vitro*, Flii attenuation using LRRFnAbs enhanced migration of keratinocytes and promoted proliferation and migration of endothelial cells. LRRFnAbs also increased the angiogenic capacity of endothelial cells and improved capillary tube formation *in vitro*. *In vivo*, systemically administered LRRFnAbs reduced the expression of Flii and improved wound appearance in murine excisional wounds. This was mediated by reduced inflammation and improved angiogenesis. *In vivo*, LRRFnAbs delivered systemically localized at the site of burn injury and decreased Flii in a scald burn model. Systemically administered LRRFnAbs also decreased inflammation and improved angiogenesis in burn wounds.

The effect of MFnAbs on wound repair was studied using *in vitro* and *in vivo* approaches. *In vitro*, decreasing Flii using MFnAbs increased proliferation and migration of keratinocytes and fibroblasts. MFnAbs also enhanced cellular migration of endothelial cells and increased capillary

tube formation *in vitro*. *In vivo*, systemically delivered MFnAbs reduced Flii and wound area and increased the rate of re-epithelialization in an acute wound murine model. MFnAbs also resulted in attenuated inflammation and improved angiogenesis in excisional wounds. *In vivo*, systemic delivered MFnAbs localized at the site of burn injury and decreased Flii in a mouse model of partial-thickness scald injury. Systemically administered MFnAbs improved burn repair which was mediated by reduced inflammation and increased production of pro-angiogenic factors VEGF and FGF-2.

In vitro, the effect of extracellular and intracellular Flii on the expression of key pro-angiogenic factors was also investigated in this study. Both intracellular and extracellular Flii appeared to interfere with angiogenic signalling pathways involved in the expression of VEGF-A, FGF-2, and PDGF-BB genes.

Overall, results presented in this thesis suggest that attenuation of Flii using FnAbs against either LRR or middle domain of Flii can improve healing outcomes. LRRFnAbs and MFnAbs have the potential to enhance wound healing through controlling inflammation and increasing angiogenesis. The clinical application of systemically injected Flii monoclonal antibodies could therefore be a potential approach for promoting healing of large surface area wounds including burns immediately after injury.

Declaration

This thesis presents work carried out by myself and does not incorporate without acknowledgment any material previously submitted for a degree or diploma in any university; to the best of my knowledge, it does not contain any materials previously published or written by another person except where due reference is made in the text; and all substantive contributions by others to the work presented, including jointly authored publications, are clearly acknowledged.

Alireza Hassanshahi



February 2023

Acknowledgments

I would like to sincerely thank those who have supported and guided me during my PhD candidature and the establishment of this thesis. I want to thank my supervisors, Professor Allison Cowin, Dr Xanthe Strudwick, and Dr Zlatko Kopecki for their invaluable advice, support, and encouragement which they have given over the years. To my principal supervisor, Allison, it was an honour to join your team and I have been extremely lucky to have a supervisor who cared so much about my work. Thank you Xanthe and Zlatko for being so understanding and supportive during this project. I wouldn't have been able to complete this PhD without your help and the lending of your combined expertise.

I am grateful to all of those with whom I had the pleasure to work in regenerative medicine group during this project. In particular, Parinaz, your friendship and support have been a great help during my PhD, and I value all the support you have given me. I also thank Damian Adams for his help in the beginning of my research project.

This work would not have been possible without the financial support that made my PhD work possible. I must express my gratitude to the University of South Australia for the University President's Scholarship (UPS). I also gratefully acknowledge the University of South Australia and Australian Wound and Tissue Repair Society (AWTRS) for supplying the funds that assisted to present my research to international and national conferences. I would like to thank the staff and students both at Future Industries Institute and Clinical and Clinical & Health Sciences. In particular, Hattie, I am so thankful for your help and kindness.

My deepest and endless thanks to my family for giving me love and support in every moment of my life. Mom and Dad, you have been my light in the darkness. I love you beyond words, beyond poems, beyond melodies. Thank you Samaneh, Mohammadhossein and Saeid, you are the inspiration behind my endeavours. Thank you Mohammadhossein for all the help you have given me over the years; I appreciate all your support. To Samaneh, having a sister is like having a best friend with crazy wonderful moments. Thank you to Saeid, I'm super lucky to have you as a brother. I appreciate your immense kindness and am so thankful to have such an amazing family in my life.

Chapter 1: Introduction

1.1 Skin Structure

The skin acts as a fundamental interface between the body and the environment and has vital functions such as temperature regulation, maintenance of water and electrolytes, has important roles in immunity and the endocrine system (Romanovsky, 2014; Yannas, 2015). As shown in Figure 1.1, the skin consists of two main layers including the epidermis and the dermis (Romanovsky, 2014). The outermost layer of the skin is called the epidermis, keratinocytes are the main cell types in the epidermis, but it also contains of melanocytes, Langerhans cells, and Merkel cells (Clayton *et al*., 2017; Gilaberte *et al*., 2016; Hwa *et al*., 2011) (Figure1.1). Keratinocytes differentiate from the basal cells that are attached to or reside at the basement membrane, which separates the epidermis from the dermis (Gilaberte *et al*., 2016; Madison, 2003), into anucleated, flat cells (corneocytes) in the final stage of differentiation and form the corneocytes of the stratum corneum (Ishikawa *et al*., 2012) that acts as the skin barrier between the organism and the environment (Wickett and Visscher, 2006). Melanocytes are responsible for the pigmentation of the skin, contributing to the skin's appearance and providing protection against ultraviolet radiation (Tsatmali *et al*., 2002). Melanocytes possess dendrites by which they interact with keratinocytes (Tsatmali *et al*., 2002). Determining the adequate adaptive immune response is the role of Langerhans cells which are dendritic but unpigmented cells that reside in the epidermis (West and Bennett, 2018). Merkel cells are located in the basal layer of the epidermis close to the nerve endings and propagate the touch sensation (Boulais and Misery, 2007). Merkel cells, in addition to their sensory functions, also serve as neuroendocrine cells, producing and releasing various hormones and signalling molecules (Boulais and Misery, 2007). The dermis, which supports the epidermis, is composed of two layers: the thin papillary dermis, characterized by loosely arranged collagen fibers, and the thicker reticular dermis, characterized by irregularly arranged collagen bundles (Wong *et al*., 2016). Stromal cells including fibroblasts, fibrocytes, and lymph cells can be found in the dermis (Gilaberte *et al*., 2016; Zeng *et al*., 2011). Several types of myeloid and immune cells are also present in the dermis or move through this layer of the skin. The underlying dermis consists of blood and lymphatic vessels, fibroblasts, nerve fibers, and the extracellular matrix (ECM) (Pfisterer *et al*., 2021). The dermis is composed primarily of collagen fibers providing strength and toughness, along with elastin that preserves the flexibility, and the normal elasticity and proteoglycans that create viscosity and hydration (Zeng *et al*., 2011).

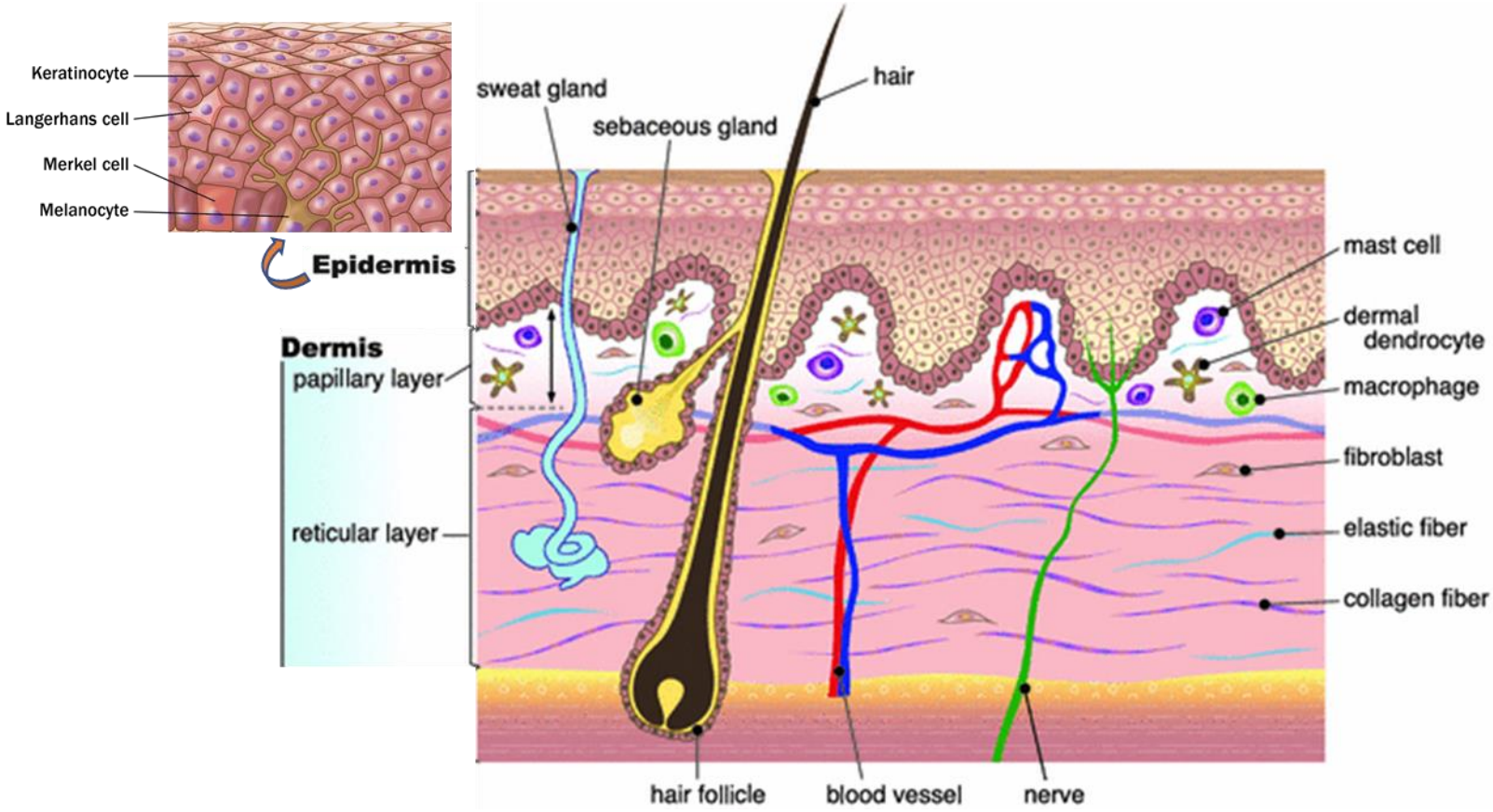


Figure 1. 1: Schematic representation of epidermis and dermis. Adapted from Kawasumi *et al*. (2013).

1.2 Cutaneous wound healing

Human skin has evolved quick and effective mechanisms to close breaches in response to injuries in a process termed wound healing (Broughton *et al*., 2006). Cutaneous wound healing is characterized by four main stages including haemostasis, inflammation, proliferation, and remodelling as shown in Figure 1.2. These classic phases lead to physiological and architectural restoration of the skin post-injury (Broughton *et al*., 2006).

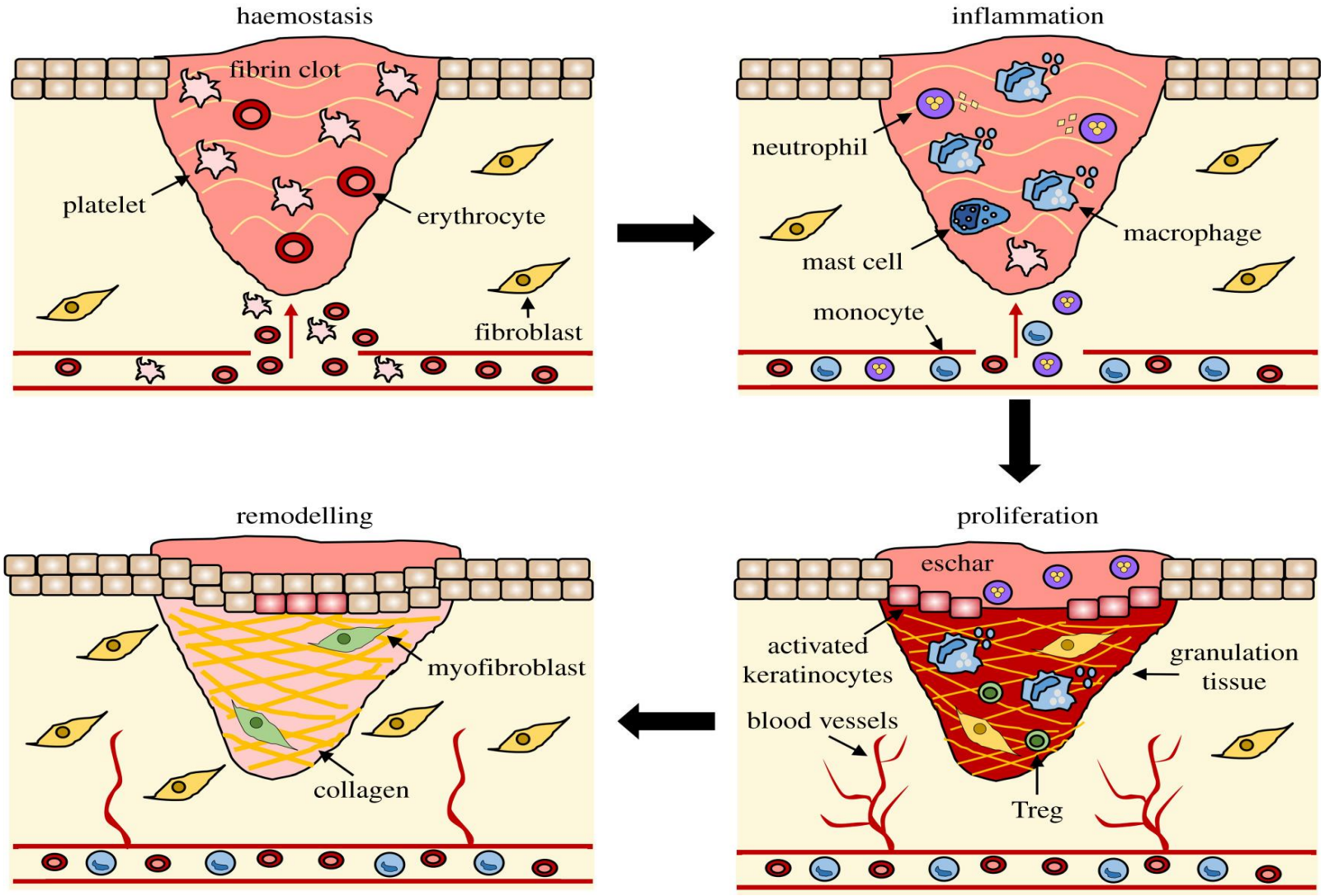


Figure 1. 2: The stages of wound repair including haemostasis, inflammation, proliferation, and remodelling and their major cellular components. Adapted from Wilkinson *et al.* (2020).

1.2.1 Haemostasis

The complex process of haemostasis involves the interaction and function of platelets, the cascade of plasma coagulation, fibrinolytic proteins, blood vessels, and cytokine mediators (Periayah *et al*., 2017). Platelets play a major role in haemostasis and coagulation as they contribute their haemostatic potential via adhesion and aggregation that are activated following the injury (Periayah *et al*., 2017). Following injury, damaged vessels immediately contract and clots form to prevent loss of blood from the damaged site (Velnar *et al*., 2009). This clot consists of fibrin, fibronectin, vitronectin, and thrombospondin plugging the wound and stopping bleeding (Zaidi and Green, 2019). This clot also carries out multiple secondary functions such as acting as a barrier against infection, supplying a scaffold for immune cells, and keeping storage of growth factors and cytokines to manage the cells involved in the early stage of wound repair (Mahdavian Delavary *et al*., 2011).

1.2.2 Inflammation

Neutrophils and monocytes are activated within the wound site through localized vasodilation and fluid extravasation following the initial inflammatory phase. An immune response is then initiated, which is sustained and supported by macrophages (Tiwari, 2012). This inflammatory response acts to prevent infection and degrade necrotic tissue and also to trigger signalling pathways during wound healing (Reinke and Sorg, 2012). The secretion of pro-inflammatory cytokines and chemokines stimulates circulating leucocytes to the wound site (Martin and Leibovich, 2005). Pro-inflammatory factors also attract vasodilatation to promote the adhesion of neutrophils and monocytes. This process is facilitated by the subsequent expression of endothelial cell adhesion molecules (Vestweber, 2015). Chemoattractants such as tumour necrosis factor-alpha (TNF-α), interleukin 1 (IL-1), and bacterial endotoxins attract neutrophils following injury (Kolaczkowska and Kubes, 2013). Neutrophils are recruited to the wound site from damaged vessels and release cytokines (Kolaczkowska and Kubes, 2013). Pro-inflammatory signals and signalling pathways involved in inflammation activate wound cells including neutrophils to secrete their cytokines (Kolaczkowska and Kubes, 2013). Neutrophils remove bacterial and necrotic tissues by phagocytosis and secretion of reactive oxygen species (ROS), proteolytic enzymes, and antimicrobial peptides (Kolaczkowska and Kubes, 2013; Segel *et al*., 2011).

Multiple intrinsic and extrinsic factors are involved in the inflammatory response which makes it a complex process. Excessive and uncontrolled inflammation can promote injury and result in impaired healing (Boniakowski *et al*., 2017). However, any failure in immune cell recruitment can also impair wound repair (Lin *et al*., 2011). Hence, an appropriate immune response is critical for an effective wound healing (Kim *et al*., 2008). In fact, the immune response must be elevated appropriately in response to infection and reduced effectively to allow the resolution stage, which signifies the restoration of normal tissue function and the return to haemostasis, to occur (Kim *et al*., 2008). The number of neutrophils reduce in the absence of infection within a few days of injury (Kim *et al*., 2008). Neutrophils are mostly extruded from the site of the wound since these cells are attached to the fibrin scab (Martin and Leibovich, 2005). Other neutrophils are removed by the mechanism of innate clearance including macrophage efferocytosis (Martin and Leibovich, 2005). Necrosis, phagocytosis, and apoptosis are other mechanisms of clearance for neutrophil removal within the wound site (Wang *et al*., 2017). Some neutrophils can leave inflamed tissue and come back to the blood circulatory system via reverse transendothelial migration as investigated in animal models such as zebrafish and mice and shown in human neutrophils *in vitro* (Buckley *et al*., 2006; Wang *et al*., 2017; Yoo and Huttenlocher, 2011).

Circulating monocytes are recruited to the wound site where they differentiate into macrophages. The first wave of monocytes enters the wound tissue simultaneously with neutrophils (Rodero *et al*., 2014). Macrophages have important roles in wound healing, exhibiting versatility and high plasticity (Das *et al*., 2015). Macrophages reach peak infiltration 7 days following injury in humans and 72 hours post-injury in mice (Baum and Arpey, 2005). Macrophages, like neutrophils, utilize evolutionarily conserved receptors to engulf pathogens and necrotic cellular debris. However, they undergo distinct morphological and behavioural changes in response to cytokine activity (Mantovani *et al*., 2005).

Based on phenotype, macrophages are separated into two classic groups including pro-inflammatory (M1) macrophages and anti-inflammatory (M2) macrophages (Ferrante and Leibovich, 2012; Murray *et al*., 2014). M1 macrophages which are stimulated by lipopolysaccharide (LPS) and interferon-gamma (IFN-γ) promote inflammation by releasing ROS, cytokines such as IL-12, IL-1β, IL-6, TNFα, and growth factors including Platelet-derived growth factor (PDGF) and vascular endothelial factor (VEGF). Apoptotic neutrophils are phagocytosed

by M1 macrophages and replaced as the major mediator of inflammation (Mahdavian Delavary *et al*., 2011). Inflammation progresses by a transition to alternative macrophage activation through recruited monocytes differentiation, or by *in situ* macrophages phenotypic transition to anti-inflammatory macrophages (Khallou-Laschet *et al*., 2010).

M2 macrophages release pro-resolutory cytokines such as IL-4, IL-10, IL-13, and arginase which have a prominent role in effective wound healing (Campbell *et al*., 2013). A multitude of growth factors, in order to improve re-epithelialization, angiogenesis, and fibroplasia are also secreted by M2 macrophages (Mahdavian Delavary *et al*., 2011). In addition, M2 macrophages promote ECM repair and inflammation resolution (Ferrante and Leibovich, 2012).

1.2.3 Proliferation

The proliferative phase of healing is activated by fibroblasts and keratinocytes stimulated by growth factors and cytokines (Werner *et al*., 2007). The orchestrated wound closure, matrix deposition, and angiogenesis occur during the proliferative phase of wound healing (Shaw and Martin, 2016). This phase is characterized by considerable activity of different cells such as keratinocytes, fibroblasts, endothelial cells, and macrophages (Pastar *et al*., 2014). In this stage, the migration of keratinocytes over the wound aids to reform the epithelial barrier which is a crucial step in the healing process (Pastar *et al*., 2014). Keratinocyte activation is triggered approximately 12 hours following injury onset by alterations in mechanical tension and electrochemical gradients (Shaw and Martin, 2016). This stimulates keratinocytes located at the wound edge to experience partial epithelial-mesenchymal transition and migrate across the wound to restore the epidermis in the process termed re-epithelialization (Haensel and Dai, 2018). The migration process terminates when keratinocytes from opposite edges reach each other (Baum and Arpey, 2005). In certain wound types, such as superficial burns, the migration process may vary, and the reconstitution of the epidermis can occur not only from keratinocytes from opposite edges but also from keratinocytes derived from hair follicles (Shpichka *et al*., 2019). A thin layer is created, and keratinocytes set up new adhesions to the basement membrane. Keratinocytes completely restore the basement membrane and undergo the final differentiation to reform the epidermal layer (Baum and Arpey, 2005).

Fibroblasts play a major role in replacing the provisional fibrin-rich matrix with new granulation tissue. Wound cells utilize the granulation tissue as a scaffold to facilitate migration and differentiation, promoting both the growth of blood vessels and ECM deposition (Wilkinson and Hardman, 2020). Different signalling molecules such as transforming growth factor (TGF-β) and PDGF are released from endothelial cells, platelets, and macrophages. These signals cause fibroblasts to respond and stimulate these cells to become pro-fibrotic or differentiate into myofibroblasts which are important in the contraction of the wound (Li *et al*., 2007).

In order to provide metabolic factors for the damaged tissue during the proliferative phase of healing, new blood vessels are formed in a process termed angiogenesis. Angiogenesis is regulated by several pro-angiogenic factors including fibroblast growth factor 2 (FGF-2), VEGF, TGF-β1, PDGF, and angiopoietins (Ang-1 and Ang-2) released by macrophages, fibroblasts, and keratinocytes (Demidova-Rice *et al*., 2012; Honnegowda *et al*., 2015). These factors stimulate endothelial cells to proliferate and migrate to the wound site. New blood vessels branch out and fuse with other sprouts to form stable tube networks (Honnegowda *et al*., 2015). Endothelial cells undergo multiple morphological alterations during capillary growth while they are under the control of chemotactic agents (Augustin *et al*., 1994; Velnar and Gradisnik, 2018). These factors act on the surface of endothelial cells to guide cell movements throughout the process of angiogenesis (Augustin *et al*., 1994; Velnar and Gradisnik, 2018). Anti-apoptotic proteins such as B-cell lymphoma 2 (BCL-2) are upregulated by VEGF to prevent the apoptosis of endothelial cells (Cai *et al*., 2003). In addition, angiogenesis is promoted by phenotypic changes in endothelial cells triggered by fibrin matrix (Kalebic *et al*., 1983). Macrophages play an important role in angiogenesis as they release proteases including matrix metalloproteinases (MMPs) to break down the network of fibrin and chemotactic factors such as TNF-α, VEGF, and TGF-β to promote migration of endothelial cells (Du Cheyne *et al*., 2020).

1.2.4 Matrix remodelling

Remodelling of the wound is the last phase of healing (Widgerow, 2011), where the scar matures. Elastin and collagen are deposited and fibroblasts differentiate into myofibroblasts (Singer and Clark, 1999). The contractile phenotype of myofibroblasts allows them to be involved in the contracture of the wound (Hinz, 2007). The balance between contraction and re-epithelialization

determines the pliability of the wound which is controlled by the phenotypic conversion of fibroblasts and myofibroblasts (Snowden, 1984).

ECM remodelling is the final phase of healing that results in the formation of a type I collagen-rich scar and can take up to several years (Li *et al*., 2007). Fibroblasts are also extensively involved in matrix remodelling and the formation of mature collagen fibrils (Darby *et al*., 2014). Proteoglycans facilitate the process of cell migration by acting as a conduit. These proteins assist in the formation of cross-linked collagen fibrils (Schultz and Wysocki, 2009). The composition of collagen in unwounded adult skin contains 80% collagen type I and 10% collagen type III, while the granulation tissue includes 30% collagen type III with 10% collagen type I (Witte and Barbul, 1997). During the remodelling phase of healing, collagen type III is replaced by type I collagen by which the tensile strength of the scar formation is increased (Diegelmann and Evans, 2004). The architecture and integrity of ECM under no circumstance returns to that of uninjured skin (Witte and Barbul, 1997). MMPs play key roles in the balance regulation of collagen degradation and synthesis in ECM. M2 macrophages, keratinocytes, and fibroblast express collagenase that are responsible for cleaving native helical collagens during the healing process (Darby *et al*., 2014). Injury repair responses are attenuated when macrophages, fibroblasts, and endothelial cells either exit the wound site or undergo apoptosis, leaving a scar (Larouche *et al*., 2018)

1.3 Burns

Burn injuries are an important global public health and an under-appreciated trauma that can affect anyone. The main causes of burn injuries are fire and heat from either hot liquids or solids. radiation, cold, electricity, friction, and chemical sources are the other causes of burn injuries (Jeschke *et al*., 2020). Even though all types of burn injuries are associated with tissue destruction as a result of energy transfer, different causes can lead to different responses (Lee, 1997). For instance, burn severity is influenced by various critical factors such as the temperature of the liquid, duration and extent of exposure, rather than solely being determined by the specific mechanism of injury. It is important to consider these factors comprehensively when assessing the initial depth and progression of burn injuries caused by different sources, including flames and scalding liquids (Jeschke *et al*., 2020). Severe burn injuries are associated with metabolic changes, immune and inflammatory responses, and vasodilatory shock (Jeschke *et al*., 2020; Lateef *et al*., 2019). These challenges are difficult to manage and can cause multiple organ failures (Jeschke *et al*., 2020). Partial thickness burn injuries, whether deep or superficial, are associated with pain and have the potential for infection. Superficial partial thickness burns typically form blisters and can be prone to infection if the blisters are broken or removed, and they may or may not result in scarring. Similarly, deep partial-thickness burns are accompanied by severe pain, infection, and hypertrophic scarring, significantly impacting physical and mental health as well as the overall quality of life. Full-thickness burns, too, are painful, susceptible to infection, and tend to scar (Church *et al*., 2006; Finnerty *et al*., 2016).

1.3.1 Pathophysiology of burn wounds

Regardless of the source of the burn, these injuries are categorized depending on the burn depth (Serrano *et al*., 2015) (Figure 1.3). Burn patients are susceptible to massive infection which may lead to sepsis as well as increased systemic inflammation (Farina *et al*., 2013). Delayed re-epithelialization following persistent inflammation impairs healing for burn patients (Edgar *et al*., 2011; Sommer *et al*., 2013). The range of inflammation is based on the burn depth since deep burns exhibit higher expression of cytokines and inflammatory response (Pereira and Herndon, 2005; Sakallioglu *et al*., 2006).

1.3.2 Depth of the Burn

Burns are classified based on how deep the injury penetrates the skin (Figure 1.3) and are classified as described below (Abazari *et al*., 2022):

- Superficial burns affect the epidermis. These are warm, painful, and soft when touched and there is no blistering.
- Superficial partial-thickness burns involve the epidermis and dermis. This class can affect either the superficial or deep dermis based on the depth of the injury. These burns are painful, blistered, red, moist, and blanch.
- Deep partial- thickness burns affect the epidermis, dermis, and subcutaneous fat or deeper. Deep partial burns have little or no pain due to the destroyed nerves. These burns can be white, charred, or brown and feel firm with no blanching.
- Full thickness burns penetrate both the epidermis and dermis layers of the skin, extending into the underlying tissues. This class of burns potentially affect muscle and bone, resulting in the absence of sensation in the area due to the destruction of nerve endings (Jeschke *et al*., 2020).

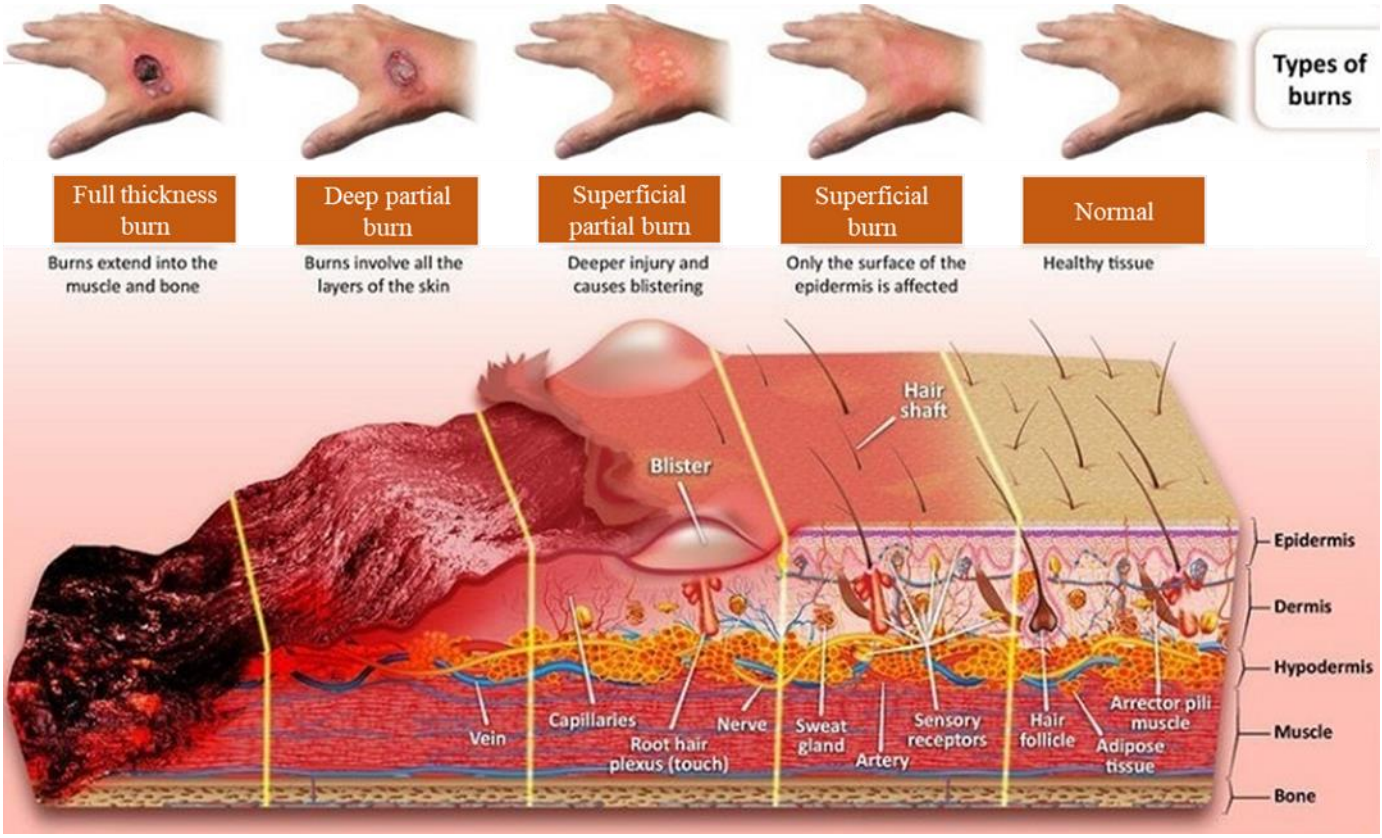


Figure 1. 3: Illustration of different depths of burn injury. Adapted from phoenix society (2022).

1.4 The complications of burn injury healing

Burn injury repair is a long-term and complex process and dependent on the immune system (Pucułek *et al*., 2021). The process of burn healing is associated with different healing processes and involves the reconstruction of injured tissue resulting from the incident (Kocik, 1996). A number of reactions occur immediately after burns including cascades of mediators involved in inflammation and the release of growth factors (Auger *et al*., 2017). The immune system plays a pivotal role in the process of burn repair and the impairment and stimulation of immune responses results in different healing outcomes in burn patients (Markiewicz-Gospodarek *et al*., 2022). Patients with deep burns can develop an acute immune response resulting in extensive inflammation, multi-organ dysfunction, and hypertrophic scarring which can significantly affect

physical and mental health. Additionally, the compromised barrier function of the skin in deep burn injuries can lead to an increased susceptibility to systemic infections (Heng *et al*., 2015; Markiewicz-Gospodarek *et al*., 2022).

1.4.1 Prolonged inflammation

Successful burn healing requires the inflammatory response and mediators including lipids, kinins, and cytokines. These mediators activate the proliferative phase of wound healing by recruiting macrophages and leukocytes (Singer and Clark, 1999). The inflammatory response is triggered immediately after the injury; however, in cases of severe or extensive burns, the inflammatory response can become uncontrolled, resulting in an augmented inflammatory response that does not promote the repair process but rather leads to a generalized catabolic state and impaired healing. It is important to note that localized superficial partial burns, depending on their nature and severity, may have a higher likelihood of healing well without significant complications (Jeschke *et al*., 2008; Stanojcic *et al*., 2018). This uncontrolled response, which is almost unique to burn injuries, leads to an increased risk of organ failure and mortality (Porter *et al*., 2016). The extravascular osmotic activity and vasodilation initiate significant and excessive oedema which frequently accompanies inflammation (Arturson, 2000). Prolonged oedema and inflammation aggravate pain (Edgar *et al*., 2011; Sommer *et al*., 2013). The correlation between the elevated inflammatory response and scar formation is also well established and improper inflammatory signalling and responses have been found to result in hypertrophic scarring (Wang *et al*., 2020). Particularly, the presence of increased macrophages observed within the wound site at specific times of the repair process leads to an increased incidence of fibrosis and hypertrophic scarring (Strudwick and Cowin, 2018).

1.4.2 Infection

Severe burn patients experience wound infection, particularly drug-resistant infections (Branski *et al*., 2009). This infection may result in prolonged hospital stays, impaired wound repair, higher costs, and mortality (Shupp *et al*., 2010). Burns infection can be associated with noticeable immune responses, sepsis, which lead to hypotension and inadequate perfusion of organs such as skin (Bloemsma *et al*., 2008).

1.4.3 Hypertrophic scarring

Hypertrophic scarring is an important concern and an abnormal response in deep partial thickness burn wounds. This scar is a common pathological feature which occurs within weeks after injury in 30–90% of cases with burn patients (Gauglitz *et al*., 2011). Patients with hypertrophic scarring have restricted movements, pain, itch, and may be dissatisfied with their appearance (Finnerty *et al*., 2016). The risk of hypertrophic scarring is hugely increased when wound healing is delayed (>3 weeks) (Gauglitz *et al*., 2011). These thick scars are typically limited to the confines of the initial wound and are associated with persistent inflammation (Finnerty *et al*., 2016). The overactivation of TGF-β1 signalling also has been linked to increased fibrosis and scar formation (Strudwick and Cowin, 2018). Furthermore, the elevated number of myofibroblasts and contracture formation are associated with hypertrophic scarring (Gabbiani, 2003; Shin and Minn, 2004). The dysfunction of endothelial cells have also been related to the development of hypertrophic scars (Molina *et al*., 2022).

1.5 Current management for burn patients

Burn injury management has evolved over the past decades via a wide range of research and clinical and preclinical studies. Significant advancements and new approaches have been developed for the treatment of burns such as novel skin grafts and antimicrobial dressings, the development of systemic delivery of drugs, improved pharmacological interventions, new surgical approaches, and management of inflammation and infection (Rowan *et al*., 2015; Wang *et al*., 2018). As a result of these advancements, the survival of patients has increased, and a reduction in the length of hospital stay has occurred, resulting in reduced costs for medical providers and patients. However, there are still multiple challenges that require to be solved to improve burn care (Rowan *et al*., 2015; Wang *et al*., 2018). Specifically, in the context of burn management, wound healing, excessive inflammation, systemic infection, and hypertrophic scarring must be prioritized, while considering other factors such as pain management, prevention of contractures, and minimizing functional impairment that should not be neglected.

1.5.1 Wound grafting

Early burn wound excision and skin grafting have been the conventional treatment of large burn injuries for decades (Desai *et al*., 1990; Puri *et al*., 2016). Studies have reported that excision within 24 to 48 hours post-injury have beneficial effects such as reduced blood loss, infection, mortality rate, and improved graft take (Puri *et al*., 2016). However, the reduction in mortality may only be observed in cases without inhalation injury (Ong *et al*., 2006). Autografts are defined as the grafting of tissue from an uninjured area on the same patient, providing adequate coverage with minimal risk of rejection (Schwanholt *et al*., 1993). Temporary skin graft with allograft, xenograft, dermal analogue, and skin substitute can be used for patients with larger and more extensive burns as the donor site are either insufficient or unavailable (Hermans, 2011). Allografts, the tissue taken from a human donor, and xenografts, tissue from other species, result in improved re-epithelialization (Hermans, 2011). These grafts prepare the wound for autograft which is associated with more healing outcomes when compared with traditional dressings (Hermans, 2011). However, there are multiple disavantages and complications of skin grafting including infection, blood or pus pooling beneath the transplanted skin, bleeding, problems with blood circulation, scar formation building up over the graft site, loss of skin sensation or increased pain sensitivity, uneven, discolored, patchy skin, and poor healing (Singh *et al*., 2015).

1.5.2 Management of inflammation

The application of therapeutic intervention can be used when excessive inflammation and edema have occurred in burns as inflammation have beneficial and destructive impacts on the management of burn healing (Rowan *et al*., 2015).

Studies have suggested that the treatment of inflammation is difficult for patients with large burns (Farina *et al*., 2013). The blockage of prostaglandin synthesis by anti-inflammatory drugs such as nonsteroidal drugs or glucocorticoids impairs the process of wound repair (Franz *et al*., 2007). In contrast, the administration of steroids has been found to attenuate inflammation in burn patients (Huang *et al*., 2015; Stubhaug *et al*., 2007). The standard treatment for patients with full and deep partial-thickness burns comprises early excision and grafting (Figure 1.5) as the risk of infection

and scarring is considerably reduced by early excision (Barret and Herndon, 2003; Engrav *et al*., 1983).

1.5.3 Management of infection

Infection caused by various bacteria remains one of the leading causes of death for burn patients, highlighting the significant risk posed by bacterial infections in this population (D'Avignon *et al*., 2010). Multiple approaches have been investigated to develop topical antimicrobial treatment and leading to reduced dressing changes and antibiotic resistance (Wang *et al*., 2018). These approaches are mainly focused on the delivery of well-established antibiotics and using alternative antimicrobial agents including curcumin or antimicrobial peptides (Krausz *et al*., 2015; Silva *et al*., 2015). Systemic antifungal drugs such as azoles, polyenes, and echinocandins are available for fungal infections (Pedrosa and Rodrigues, 2011).

1.5.4 Transforming growth factor-β modulators

Collagen synthesis and the formation of scars are worsened via the activation of TGF-β1 and TGF-β2, while TGF-β3 is known as an anti-scarring factor (Yamaguchi *et al*., 1990). Several investigations have shown that targeting the TGF-β signalling pathway can result in improved healing outcomes with reduce scarring. These studies aimed to attenuate TGF-β1 and TGF-β2 using inhibitors of TGF-β such as decorin and neutralizing antibodies (Wehrhan *et al*., 2004; Yamaguchi *et al*., 1990; Zhang *et al*., 2015). Furthermore, antisense oligonucleotides have been employed to inhibit the activation of TGF-β1 which was followed by the downregulation of TGF-β1 and TGF-β2 and upregulation of anti-scarring TGF-β3 (Bran *et al*., 2010; Viera *et al*., 2010). Despite these investigations, the injection of TGF-β3 into surgical sites has been the only therapeutic approach developed to modulate the TGF-β signalling pathway in clinical trials, but trials were not successful, and it never progressed into clinical use (Ferguson *et al*., 2009).

1.5.5 Botulinum toxin A

Botulinum toxin A which is released by the bacterium Clostridium botulinum is capable of suppressing acetylcholine production from a neuron and inducing the suppression of muscle contraction. This neurotoxin has been found to improve scar formation. Injection of botulinum

toxin into the wound site has been shown to promote wound healing and reduce scar formation in humans (Gassner and Sherris, 2003). Botulinum toxin can result in reduced wound tension, leading to decreased number of myofibroblasts differentiation (Block *et al*., 2015; Viera *et al*., 2010). These changes are associated with elevated expression of alpha-smooth muscle actin, causing the wound contraction (Zhibo and Miaobo, 2009). Clinical studies using botulinum toxin A reveal that scar regression was improved, and the lesions were flatter in patients who received botulinum toxin treatment. The investigations suggest that this neurotoxin inhibits the proliferation and differentiation of fibroblasts and suppresses the production of TGF-β1 (Xiao *et al*., 2010). There are several areas that remain to be determined in treatments using botulinum toxin including timing in the injections and dose characteristic of botulinum toxin A (Chambers, 2020). The precise biological effect of the applications using the toxin still requires additional investigations (Chambers, 2020).

1.6 Challenges of extensive burn injuries

Minor burns are normally superficial and do not lead to complications (van Baar *et al*., 2006). However, deep and extensive burns take more time to heal and cause scar formation (Procter, 2010). Although the scar contracts as it heals, if the scar forms across a joint in a limb or digit, the contracture may result in restricted movement (Procter, 2010). In addition, widespread burns can cause extensive fluid loss and dehydration as fluid seeps from the circulating blood into the burned site (Namdar *et al*., 2010). Dehydration is a common consequence of extensive burns and can potentially develop into shock can develop shock in patients. (Namdar *et al*., 2010). This particular aspect requires further attention due to its major impact on patient outcomes. Moreover, chemical imbalances are the other complication of this type of burns (Nielson *et al*., 2017). Extensive burns deserves immediate care as they may be associated with systemic infection which can spread throughout the body by blood stream and cause serious illnesses and death (Norbury *et al*., 2016). Systemic and uncontrolled inflammation is another complication of extensive burn injuries that causes severe health problems for patients (Nielson *et al*., 2017). Understanding the underlying mechanisms of inflammation is crucial for evaluating patient outcomes in the context of extensive burns. Additionally, considering new strategies for managing inflammation is essential in improving outcomes for these patients (Nielson *et al*., 2017).

1.6.1 Treatment of extensive burn injuries with topical agents and dressings

Treatment of extensive burn injuries includes cleansing, debridement, and burn dressings. Topical antimicrobial agents are typically incorporated in routine burn dressings changes; however, more investigations are required to determine which agent or dressing is ideal for coverage of the burn wounds to control infection and improve wound repair (Norman *et al*., 2017; Wasiak *et al*., 2013). Topical agents and dressings aim to protect the surface of the wound, preserve moist environment, enhance wound healing, and restrict wound progression while reducing discomfort for the burn patients (Norman *et al*., 2017; Wasiak *et al*., 2013). Honey-derived wound dressings can be used for extensive burns in order to improve healing outcomes and have been shown to be more effective than conventional treatments such as paraffin gauze, sterile linen, and polyurethane film (Aziz and Abdul Rasool Hassan, 2017). However, the safety and efficacy of honey-derived wound dressings for complex and severe burn injuries has not been established (Jull *et al*., 2015). The applications of povidone-iodine ointment have been also found to enhance wound repair in patients with extensive burns but multiple dressing changes during a day, delayed re-epithelialization, and cytotoxicity are drawbacks of use of povidone-iodine products (Norman, 2003; Steen, 1993; Vermeulen *et al*., 2010). Dakin's solution which contains 0.025% sodium hypochlorite has been also used for management of extensive burn injuries. However, there are a few well-defined investigations to strongly encourage Dakin's solution use in extensive burn injuries (Ahmed, 2011).

1.7 The need for novel therapeutics for the treatment of burn injuries

As mentioned, there are multiple options for management of burn injuries by which the mortality rates and the length of hospital stay have been reduced. However, the ongoing pain, hypertrophic scarring, and slow process of repair continue to pose serious challenges for burn management (Wang *et al*., 2018). These concerns generically result from excessive inflammation and poor healing features including impaired re-epithelialization, angiogenesis, and tissue remodelling (Veith *et al*., 2019). There is therefore a clear need for the development of new approaches that improve the way burns heal.

1.8 Flightless I

Flightless I (Flii) is a member of the gelsolin family of actin-binding proteins that are involved in numerous biological activities including ovulation and development, wound repair, and the progression of cancer (Strudwick and Cowin, 2020). Flii originally was identified in drosophila in which mutations in the gelsolin domain resulted in defects in flight muscles (Campbell *et al*., 1993; Straub *et al*., 1996). These defects are associated with an inability to fly and also gastrulation abnormality during embryogenesis in drosophila (Campbell *et al*., 1993; Straub *et al*., 1996). Flii has been found to have 95% homology between mice and humans which characterizes Flii as a highly conserved protein (Campbell *et al*., 1993). Flii has been shown to be expressed in various human tissues and has important roles in mammalian health (Nag *et al*., 2013). The absence of Flii has been found to be lethal in mice during embryogenesis, associated with failure in the formation of an early structure called the egg cylinder, which is crucial for proper development before gastrulation (Campbell *et al*., 2002).

As mentioned, Flii is a member of the gelsolin family of cytoskeletal proteins. There is a classic 6-fold gelsolin repeat at the C-terminal of Flii (Figure 1.4). Additionally, 16 tandem leucine-rich repeats (LRR) exist at the N-terminus (Liu and Yin, 1998) (Figure 1.4). Flii has been found to bind actin through its gelsolin domain. Flii protein binds globular and filamentous actin in mammalian cells and prevents polymerization and caps the barbed ends of filamentous actin; however, the ability of actin severing has not been observed in Flii (Mohammad *et al*., 2012).

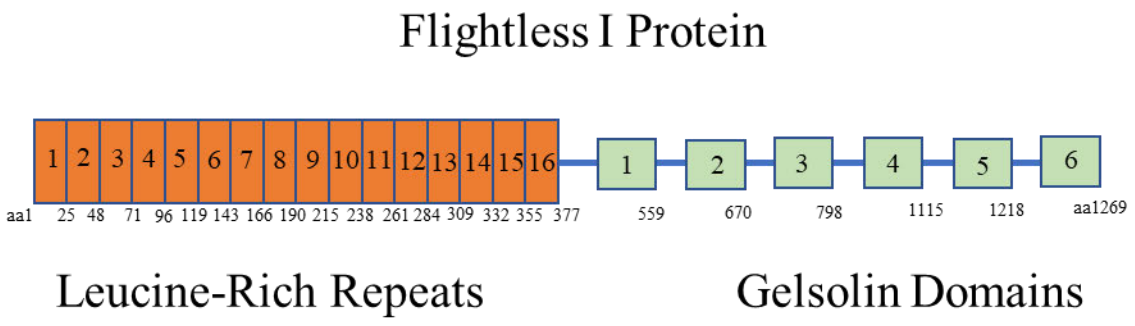


Figure 1. 4: Schematic diagram of Flii including the N-terminal Leucine Rich Repeats, C-terminal Gelsolin-like Domains, and amino acid locations.

Flii is known as a unique protein among other members of the gelsolin family as the additional N-terminal LRR of Flii provides it with the ability to be involved with molecular recognition via its interaction with several proteins or lipids (Liu and Yin, 1998). Multiple interacting partners have been reported that bind different domains of Flii, showing Flii is involved in numerous cellular activities (Strudwick and Cowin, 2020) (Table1.1).

Table 1. 1: Flii binding partners

Binding Partner	Flii Binding Domain	Function	Reference
Glucocorticoid receptor	LRR	Activate GR-mediated transcription	(Jin *et al*., 2017)
GRIP1	LRR	Nuclear receptor coactivator to promote transcription	(Lee *et al*., 2004)
Importin β	LRR	Involved in nuclear-cytoplasmic transport	(Lee *et al*., 2004)
LRRFIP1	LRR (aa1-427)	Inhibit B-catenin-dependent transcription Reduces TLR4 signallings	(Dai *et al*., 2009)
LRRFIP2	LRR (aa1-427)	Reduces TLR4 signalling Inhibits NLRP3 Inflammasome	(Dai *et al*., 2009; Jin *et al*., 2013)
Nup88	LRR	Involved in nuclear-cytoplasmic transport	(Liao *et al*., 2015)
Thyroid Receptor	LRR	Hormone-independent transcriptional regulation	(Gettemans *et al*., 2005)
LPS	LRR	Inhibit activation of macrophages	(Lei *et al*., 2012)
G3BP1	LRR	Facilitate Rac-1 mediated cell extention formation	(Arora *et al*., 2018)
IQGAP1	LRR	Facilitate cell extention and elongation	(Arora *et al*., 2020)

Binding Partner	Flii Binding Domain	Function	Reference
active RAC1	LRR	Mediate RhoA-ROCK-independent myosin II activation	(Marei *et al*., 2016)
active R-Ras	LRR	Facilitate Rac-1 mediated cell extention formation	(Arora *et al*., 2018)
Ras Gap	LRR	Facilitate Rac-1 mediated cell extention formation	(Arora *et al*., 2018)
Androgen Receptor	LRR (aa1-494) and gelsolin (aa495-822)	Nuclear receptor coactivator to promote transcription	(Wang *et al*., 2016)
CARM1	LRR and gelsolin	Nuclear receptor coactivator to promote transcription	(Lee *et al*., 2004)
ChREBP	LRR and gelsolin	Negative regulatory component of of the ChREBP transcriptional complex	(Wu *et al*., 2013)
Estrogen Receptor α	LRR and gelsolin	Hormone-independent transcriptional regulation	(Gettemans *et al*., 2005; Jeong *et al*., 2009)
Caspase 1	LRR and gelsolin	Prevent inflammatory activity and regulates caspase-1 induced cell death	(Li *et al*., 2008)
Caspase 11	LRR and gelsolin	Localise caspase-11 to F-actin rich leading edge Reduces TLR4 inflammatory signalling	(Li *et al*., 2008)
Actin	gelsolin	Actin filament assembly and stabilization	(Liu and Yin, 1998)

Binding Partner	Flii Binding Domain	Function	Reference
G-Actin	gelsolin	Prevent polymirisation	(Mohammad *et al.*, 2012)
F-Actin	gelsolin	Caps barbed end	(Mohammad *et al.*, 2012)
Ca^{2+}	gelsolin	Regulate actinomyosin dynamics	(Nag *et al.*, 2013)
Daam1	gelsolin	Enhance DRF-induced linear actin asssembly	(Higashi *et al.*, 2010)
mDia 1	gelsolin	Enhance DRF-induced linear actin asssembly	(Higashi *et al.*, 2010)
BAF53	gelsolin	Transcriptional regulation	(Jeong *et al.*, 2009)
MyD88	gelsolin	Interfere with formation of TLR4-Myd88 inflammatory signalling complex	(Wang *et al.*, 2006)

1.8.2 LRR and gelsolin domains of Flii interact with various binding partners

As shown in Table 1.1, multiple binding partners have been reported to interact with different domains of Flii (Strudwick and Cowin, 2020). Ras is a member of the Rho family of GTPases and is involved in the polymerization of actin via Rac1 (Olson and Marais, 2000). The LRR of Flii is involved in inducing the formation of Rac1-mediated cell extension by binding R-Ras (Arora *et al*., 2018). Furthermore, the LRR domain has been shown to interact with Ras GTPase-activating-like protein (IQGAP1), facilitating the formation of short cell extensions (Arora *et al*., 2020). Also, the LRR domain allows the Flii protein to detect bacteria as this domain of Flii can bind LPS, an important activator of macrophages (Lei *et al*., 2012). Flii appears to sequester LPS and inhibit macrophage activation (Lei *et al*., 2012). Flii is involved in the regulation of apoptosis as the LRR and gelsolin domains of Flii can bind caspase 1, resulting in limited caspase 1 induced cell death (Li *et al*., 2008). The LRR and gelsolin domains of Flii have also been found to regulate migration by their interaction with the p30 domain of Caspase-11 (Li *et al*., 2008).

It has been reported that Flii interacts with coactivator-associated arginine methyltransferase 1 (CARM1) through its LRR and gelsolin domains (Lee *et al*., 2004). The interaction between the LRR domain of Flii and the p160 coactivator glucocorticoid receptor-interacting protein 1 (GRIP1) has been also found (Archer *et al*., 2005; Lee *et al*., 2004). Flii binding to the estrogen receptor α via its LRR domain is also reported which induces the transcription of estrogen-responsive factors such as myelocytomatosis viral oncogene (Myc) and growth regulation by estrogen in breast cancer 1 (GREB1) (Gettemans *et al*., 2005; Jeong *et al*., 2009). Moreover, the LRR and gelsolin domains of Flii bind the androgen receptor (AR), forming a complex which competes with ligand binding to AR (Wang *et al*., 2016). Flii appears to prevent AR transactivation, leading to decreased AR nuclear localization (Wang *et al*., 2016). Flli binds Nup88 and Importin β proteins via its LRR domain (Liao *et al*., 2015). Nup88 as a component of the nuclear pore complex and importin β act as a nuclear transport receptor and plays major roles in nucleocytoplasmic transport of protein, mRNA, and the 60S ribosomal subunit (Bernad *et al*., 2006; Hutten and Kehlenbach, 2006; Strom and Weis). The LRR of Flii interacts with two important partners including Leucine-rich repeat Flightless-interacting protein (LRRFIP)1 and LRRFIP2 involved in a number of signalling pathways (Wilson *et al*., 1998). LRRFIP1 is involved in the regulation of epidermal growth factor receptor (EGFR), PDGF, and TNFα, acting as a transcriptional repressor (Jin *et al*., 2013; Ohtsuka

et al., 2011). LRRFIP1 has been found to induce type I interferon (IFN) in fibroblasts, macrophages, and hepatocytes while attenuating LRRFIP1 regulates the activation of inflammasome and expression of IL-1β (Liu *et al*., 2015; Yang *et al*., 2010). LRRFIP2 can interact with caspase-11 and also disrupt binding between Flii and MyD88, resulting in enhanced activity of Toll-like receptor 4 (TLR4) signalling (Jin *et al*., 2013). LRRFIP1 increases the proliferation of vascular smooth muscle cells (VSMCs) and enhances extracellular signal-regulated kinase (ERK) phosphorylation which are key pathological factors in atherosclerosis and restenosis (Choe *et al*., 2013). LRRFIP1 and LRRFIP2 have been known as trigger factors for β-catenin/TCF/LEF signalling pathway, p300, GRIP1, and β-catenin (Lee *et al*., 2004; Liu *et al*., 2005; Ohtsuka *et al*., 2011; Yang *et al*., 2010), resulting in c-myc and cyclinD1 transcription that is important for cellular proliferation and apoptosis (Lee and Stallcup, 2006; Liao *et al*., 2007). A comprehensive summary of these activities can be found in Figure 1.5, providing a visual representation of complex network of interactions orchestrated by the LRR and gelsolin domains of Flii.

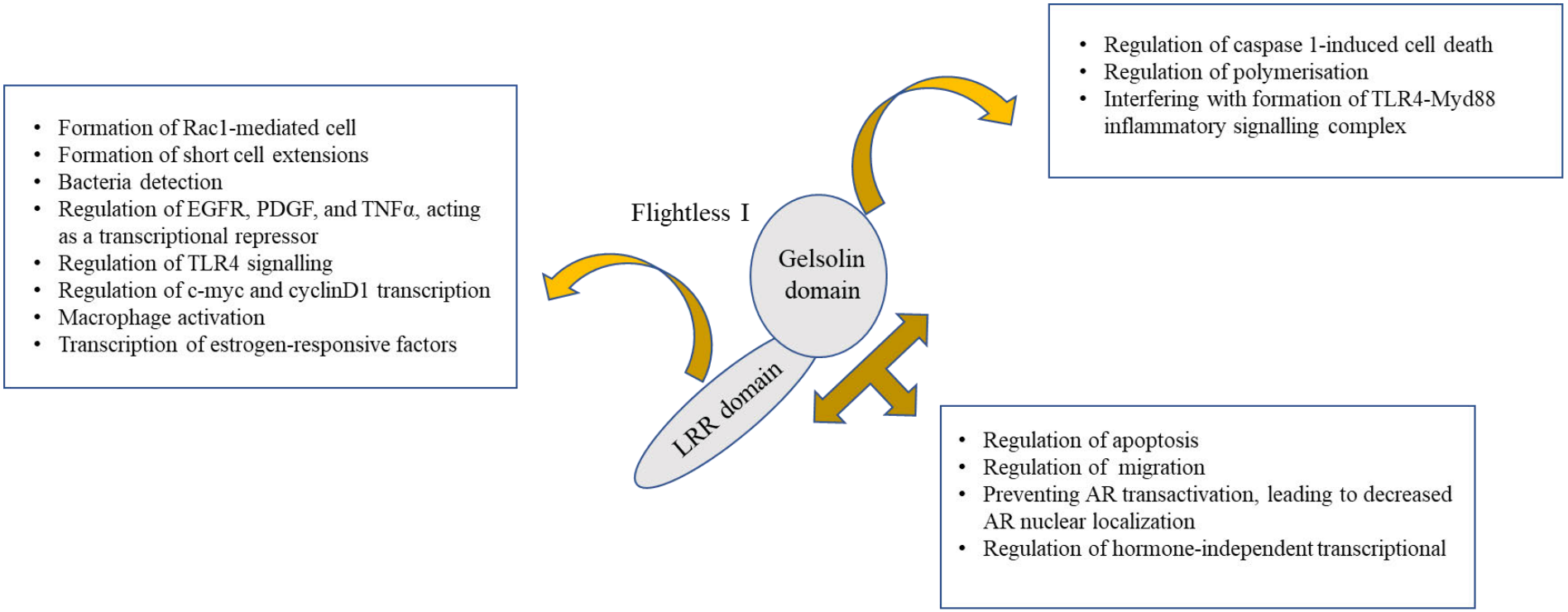


Figure 1. 5: Interactions of the LRR and gelsolin domains of Flii: orchestrating cellular dynamics and molecular signalling

1.9 Flii is a negative regulator of wound repair

Studies have suggested that Flii is considerably involved in the cytoskeletal mechanics needed for the migration of cells during the repair process (Ruzehaji *et al*., 2014). Flii is upregulated in wounded skin following injury (Ruzehaji *et al*., 2014). Flii negatively affects the process of healing as wounds in heterozygous knockout mice with reduced expression of Flii show an improved rate of healing (Cowin *et al*., 2007). This improvement is associated with lower collagen I deposition. Additionally, overexpression of Flii delays healing with higher collagen I deposition and increased scar formation (Cowin *et al*., 2007). The negative effect of Flii in wound healing has been related to its stimulatory effect on the inhibition of epidermal stem cell activation (Yang *et al*., 2020). The epidermal stem cells which are found in hair follicles close to the edge of the wound induce the proliferative potential required for the re-epithelisation of the wound (Plikus *et al*., 2012). These cells need to be activated, however, high expression of Flii disrupts this process by interrupting the Wnt-signalling pathway, resulting in delayed wound closure (Yang *et al*., 2020).

Flii expression is further elevated in diabetic foot wounds and venous leg ulcers that have delayed healing (Ruzehaji *et al*., 2014; Ruzehaji *et al*., 2013). Studies have revealed that overexpression of Flii aggravates the impaired healing processes associated with diabetes and aging (Adams *et al*., 2008; Ruzehaji *et al*., 2013).

Flii has been found to have a negative impact on angiogenesis in diabetic conditions. Reduced vessel sprouting and decreased formation of tight junctions are observed in endothelial cells isolated from mice that overexpressed Flii (Ruzehaji *et al*., 2014). Additionally, a decreased number of pericytes are observed in diabetic wounds, which show increased expression of Flii (Thomas *et al*., 2020). Pericytes aid endothelial cells to improve the stability and functionality of blood vessels (Thomas *et al*., 2020). The expression of pro-angiogenic VEGF is upregulated in diabetic mice with the heterozygous knockout of Flii (Ruzehaji *et al*., 2014). Also, the number of endothelial cells and pericytes was increased in these animal models, indicating the negative effect of Flii on angiogenesis during wound healing *in vivo* (Ruzehaji *et al*., 2014; Thomas *et al*., 2020). *In vitro*, capillary tube formation of human umbilical vein endothelial cells (HUVEC) was elevated following attenuation of Flii in cell media culture (Ruzehaji *et al*., 2014).

The expression of TGFβ1 is elevated in Flii overexpressing mice during wound healing, while Flii heterozygous knockout mice show increased expression of TGF-β3 that is known as an anti-scarring factor in the repair process (Chan *et al*., 2014). The expression of myofibroblast marker α-SMA was also attenuated in Flii heterozygous knockout mice with burn injuries (Adams *et al*., 2009). The expression level of TGF-β1 and TGF-β3 was also investigated in this model and a reduced level of TGF-β1 and elevated TGF-β3 was seen (Adams *et al*., 2009). Fibroblast-specific Flii overexpression has also been shown to delay healing with decreased expression of collagen I within the wound bed and elevated myofibroblasts number (Turner *et al*., 2015c). The impaired wound closure in Flii overexpressing mice was attributed to the disruption in the process that inhibit migration of cells over the provisional wound bed and via attenuated adhesion at the junction of dermal-epidermal (Kopecki *et al*., 2009).

1.10 Flii affects proliferation migration, and apoptosis

Flii recruits R-Ras to adhesion sites, aiding cell extension in the early phase of cell migration (Arora *et al*., 2018). Studies have revealed that the LRR domain of Flii interacts with R-Ras and acts as an adaptor protein to assemble R-Ras and GTPase-activating protein SH3 domain-binding protein. The formation of Rac1-mediated cell extension is activated following the interaction between Flii and R-Ras (Arora *et al*., 2018). Flii also stimulates migration by acting as an effector of Rac1, a mediator of the focal complexes assembly which facilitates cellular migration (Marei *et al*., 2016). Flii binds Rac1 to mediate the activation of RhoA-ROCK-independent myosin II, promoting migration (Marei *et al*., 2016).

Studies have demonstrated that Flii is involved in cellular proliferation and apoptosis (Cowin *et al*., 2007). Flii regulates apoptosis through its interaction with caspase 1 to suppress and limit the activity of caspase-1-induced cell death (Li *et al*., 2008). The negative role of Flii in the proliferation of fibroblasts and keratinocytes has been described as knockdown of Flii using siRNA resulted in increased proliferation. Additionally, isolated cells from mice with overexpressed Flii showed attenuated proliferation (Cowin *et al*., 2007). In addition, Flii has been found to negatively regulate canonical Wnt signalling transduction (Lei *et al*., 2012). This pathway plays a major role in the expression of genes involved in the process of proliferation. Studies have revealed that the

phosphorylation and degradation of cytosolic β-Cat, an important regulator of cellular proliferation is modulated by canonical Wnt-signalling pathway (Lei *et al*., 2012; Yang *et al*., 2017).

1.11 Flii and the immune response during wound healing

Flii is involved in the immune response by regulating innate immunity. Nucleotide-binding domain-like receptor protein 3 (NLRP3) inflammasome and MyD88-TLR4 are two major inflammatory pathways that are affected by Flii (Strudwick and Cowin, 2020; Wang *et al*., 2006). Studies have shown that the colocalization of NLRP3 with F-actin is attenuated while Flii silencing, illustrating that Flii is necessary for this interaction (Burger *et al*., 2016). Additionally, the activation of NLRP3 inflammasome is improved following Flii knockdown and the secretion and maturation of IL-1β are decreased whilst Flii is overexpressed (Jin *et al*., 2013; Kim *et al*., 2017; Li *et al*., 2008). These studies suggest that Flii negatively regulates NLRP3 inflammasome. Flii has been reported to be involved in the activity of MyD88-TLR4 signalling pathway, acting to regulate the early phases of inflammation following injury and pathogen recognition (Mogensen, 2009; Wang *et al*., 2005). *In vitro* results have demonstrated that Flii interacts with MyD88, interfering with the complex of TLR4-MyD88 signalling. Following this interaction, the activation of LPS induced NFκB is inhibited in macrophages (Wang *et al*., 2005).

Furthermore, LPS stimulated cells exhibit attenuated expression and secretion of TNFα in the presence of media enriched with Flii, suggesting the role of secreted Flii in this signalling pathway (Lei *et al*., 2012). Flii is detected in wound fluids from chronic and acute wounds and blisters (Cowin *et al*., 2007; Ruzehaji *et al*., 2014). The constitutive secretion of Flii is characterized by a non-classical late endosome/lysosome-mediated pathway through macrophages and fibroblasts (Cowin *et al*., 2007; Cowin *et al*., 2012; Lei *et al*., 2012). Secretion is elevated in response to both scratch wounding in fibroblasts and after the activation of LPS in macrophages (Cowin *et al*., 2007; Cowin *et al*., 2012; Lei *et al*., 2012). Flii binds LPS through its N-terminal LRR domain with a high homology to TLR4, playing an important role in bacteria detection (Bell *et al*., 2003; Lei *et al*., 2012). It has been suggested that secreted Flii may detach LPS from its binding sites to inhibit the activation of macrophages to decrease the production of cytokines (Lei *et al*., 2012).

1.12 Flii and TGFβ/Smad-dependent signalling pathway

Flii is involved in the regulation of the TGFβ/Smad-Dependent Signalling Pathway which regulates collagen I transcription and myofibroblast differentiation (Biernacka *et al*., 2011; Strudwick and Cowin, 2020). Studies have shown that attenuating Flii using siRNA in fibroblasts results in reduced TGF-β1 expression which is a promoter of fibrosis and scar formation by regulating collagen production (Adams *et al*., 2008; Biernacka *et al*., 2011). Furthermore, TGF-β1 mRNA is elevated in Flii overexpressing fibroblasts and reduced in Flii deficient cells (Chan *et al*., 2014). The expression level of TGF-β3 mRNA that has an anti-fibrotic role was also investigated in this study, showing no change of TGF-β3 mRNA in both Flii overexpressed and deficient cells (Chan *et al*., 2014). *In vitro* results showed that the expression of Smad 3 is decreased following attenuating Flii using siRNA, while the expression of Smad 7 is elevated (Chan *et al*., 2014). The expression of collagen I is decreased in fibroblasts treated with siRNA for Flii (Cowin *et al*., 2007). Additionally, estrogen-mediated collagen I is inhibited in these fibroblasts, suggesting that the expression of Flii is necessary for the adequate production of collagen I (Adams *et al*., 2008). These studies highlight the significance of Flii in fibrotic responses. Understanding the complex interactions involving Flii and its impact on TGFβ signalling could provide valuable insights for developing targeted interventions in fibrotic disorders.

1.13 The expression of Flii in burn wounds and hypertrophic scarring

Human skin burns and hypertrophic scars both exhibit high levels of Flii (Figure 1.5) (Cameron *et al*., 2016). Furthermore, increased expression of Flii was observed in a mouse model of hypertrophic scarring induced by bleomycin. Bleomycin, delivered subcutaneously to mice with heterozygous knockout of Flii, resulted in decreased fibrosis and reduced expression of TGF-β1. However, Flii overexpressing mice demonstrated increased scarring, elevated myofibroblasts, and increased collagen I/III ratio which is a promoter of fibrosis (Cameron *et al*., 2016). Moreover, the severity of scar formation was significantly increased in Flii overexpressing mice, while scarring was reduced in Flii heterozygous knockout mice, indicating the potential regulatory effect of Flii on hypertrophic scarring (Cameron *et al*., 2016).

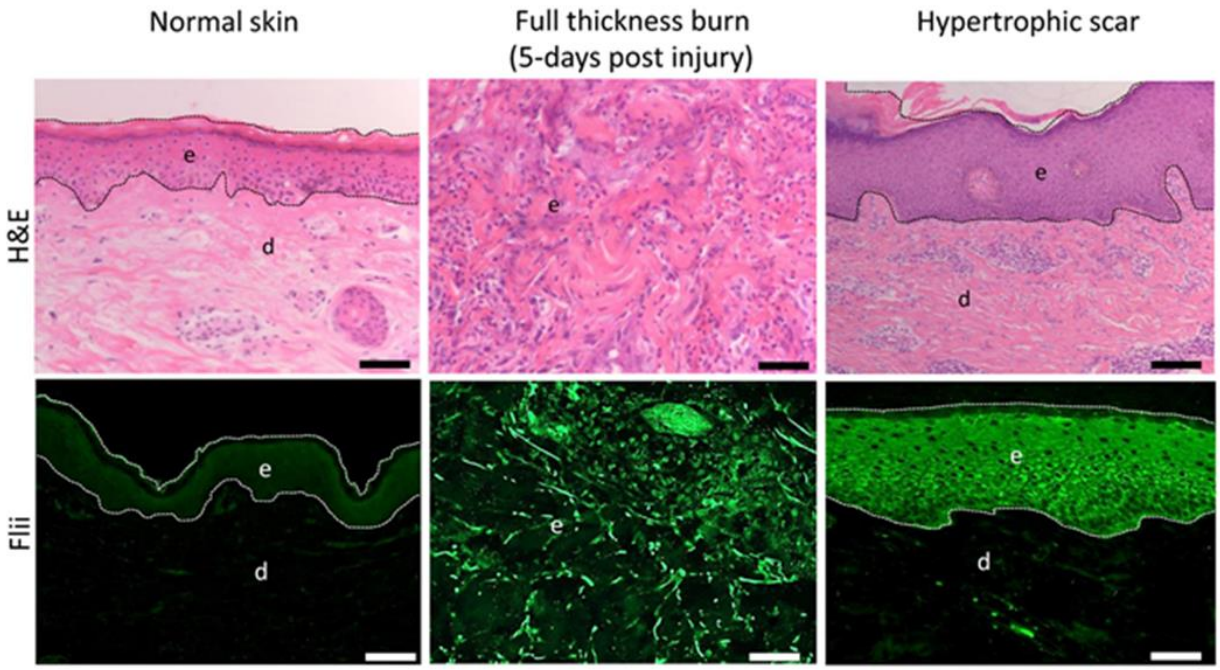


Figure 1. 6: Flii is elevated in acute burns and hypertrophic scars

H&E staining and Flii immunohistochemistry (green) on samples of human normal skin, acute burn, and hypertrophic scars. Adapted from Cameron *et al*. (2016).

1.14 Targeting Flii to improve healing outcomes

There are several studies that have investigated reducing the adverse impacts of Flii on the healing process (Strudwick and Cowin, 2020). In order to inhibit the activity of intracellular Flii (*in vivo*), small interfering RNA has been designed against Flii known as Flii siRNA (Martens *et al*., 2015). A layer-by-layer polymer surface was employed to deliver Flii siRNA to reduce fibrotic processes created by medical device implantation (Martens *et al*., 2015). The expression of Flii was attenuated within the tissue surrounding the implant, TGF-β1 was reduced, and anti-fibrotic TGF-β3 was elevated, indicating the beneficial effect of Flii siRNA on the fibrotic process (Martens *et al*., 2015). Another investigation showed that porous silicon nanoparticles (pSiNPs) loaded with Flii siRNA increased cellular migration and proliferation in keratinocytes (Turner *et al*., 2016).

Additionally, wound healing was significantly accelerated in murine models of acute excisional wounds treated with Flii siRNA-pSiNPs compared to control groups (Turner *et al*., 2016).

1.14.1 Antibody strategies for decreasing level of Flii

As previously mentioned, studies have identified Flii as an important regulator of healing process and suggested that decreasing Flii levels in the wound site could be a promising approach to promote wound healing. In order to attenuate the negative effect of extracellular Flii on healing process, new strategies based on neutralizing Flii activity using antibodies have been developed.

1.15 Therapeutic antibodies

Therapeutic antibodies are medications that employ antibodies to target disease-related factors (Lu *et al*., 2020; Suzuki *et al*., 2015). By using the specificity provided by therapeutic antibodies, only one antigen is recognized with high affinity (Lu *et al*., 2020). Applications that employed therapeutic antibodies are associated with a high level of efficacy and less side effects (Suzuki *et al*., 2015). These antibodies have the ability to bind a wide range of specific targets and the modes of action of the antibodies enable them to be used extensively in therapeutic targets (Suzuki *et al*., 2015).

1.15.1 Therapeutic monoclonal antibodies

Therapeutic monoclonal antibodies (mAbs) are specific antibodies developed to target particular proteins that are overexpressed in different diseases. mAbs are large multimeric proteins with a molecular weight of approximately 150 kDa. They contain multiple post-translational modifications and are composed of two types of polypeptide chains (Chames *et al*., 2009). The structure of immunoglobulin G (IgG), the most common mAb has been shown in Figure 1.6. IgGs consist of two heavy chains and two light chains. The variable fragment (Fv) binds the target protein which can be either a protein involved in pathology or a protein present on the surface of a target cell (Aranez and Ambrus, 2020; Turner *et al*., 2015b). The constant region enables the antibody to have a structure and contains Fc domain by which the antibody neutralises antigen

(Turner *et al*., 2015b). The Fc domain binds to the Fc receptor leading to inhibited target cell/protein (Aranez and Ambrus, 2020; Turner *et al*., 2015b). Off-target effects are significantly reduced using mAbs which provide considerably high target specificity and enable selective antigen binding (Golay and Introna, 2012).

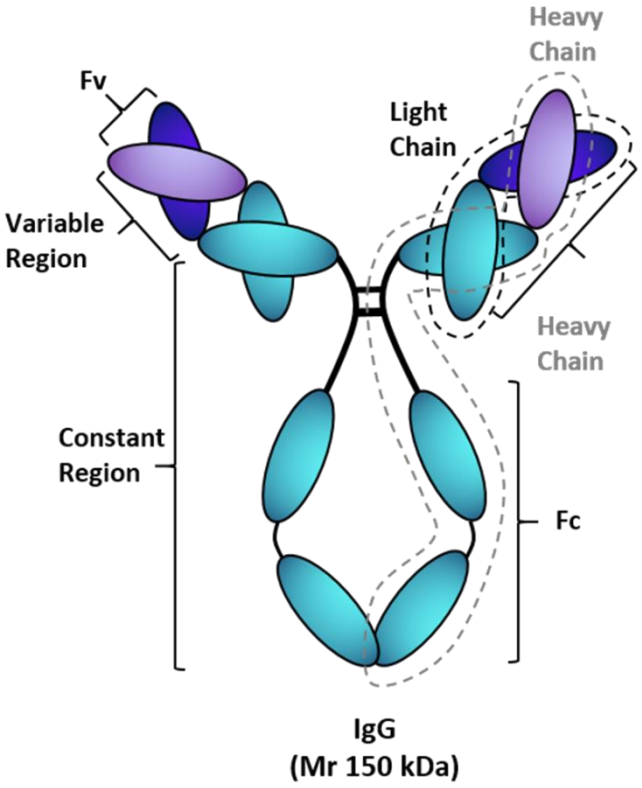


Figure 1. 7: Structure of an IgG monoclonal antibody. Adapted from Isabelle Topin -tebu-(2018).

1.16 Antibody therapy

A number of mAbs have been generated over the past decades which revolutionized the treatment of cancers, cardiovascular and autoimmune diseases, and infections (Singh *et al*., 2018). This has led to great interest in the wound field as there are several proteins that are detrimental to wound repair and are overexpressed in the different types of wounds (Turner *et al*., 2015a). Therapeutic mAbs have been used to bind to these proteins, thereby suppressing their activity and promoting healing responses (Turner *et al*., 2015a). Previous investigations have shown that anti-TGF-β1,2 mAbs improve wound healing including reduced scar formation and fibrosis, decreased macrophages and monocytes, and attenuated collagen deposition in different animal models (Shah

et al., 1992, 1994). The neutralisation of TNF-α using mAbs has been found to stimulate the formation of regulatory macrophages, leading to the activation of anti-inflammatory cytokines (Ordás *et al*., 2012; Vos *et al*., 2011). In a murine model of corneal alkali burns, Interleukin-6 has been neutralized with mAbs, resulting in reduced infiltration of inflammatory cells and suppression of cytokines (Sakimoto *et al*., 2012).

1.17 Monoclonal antibodies against Flii protein

To reduce extracellular Flii protein in the wounds, a mouse monoclonal antibody was raised against a specific antigen sequence corresponding to aa57-66 in the LRR of human Flii (Adams *et al*., 2009; Cowin *et al*., 2007). Several *in vitro* and *in vivo* studies were carried out to examine the impact of monoclonal antibodies against Flii protein on the process of wound repair. This antibody was also investigated in numerous wound healing studies to determine the role of extracellular Flii that is elevated in response to injury.

1.17.1 Targeting Flii using Flii neutralizing antibody to improve the healing process

Decreasing the adverse effect of Flii using first generation Flii neutralizing antibody (FliiL FnAb) was investigated in numerous wound healing studies. These FliiL FnAbs were delivered intradermally to incisional wound margins in wild type mice, resulting in a considerable improvement in wound appearance (Figure 1.7A) (Cowin *et al*., 2007; Jackson *et al*., 2012). Investigations also showed that treatment of cultured keratinocytes and fibroblasts with FliiL FnAb enhanced their proliferation and migration (Cowin *et al*., 2007). Furthermore, the addition of FliiL FnAb to cultured human endothelial cells increased capillary tube formation, indicating that reducing Flii using FliiL FnAb improved angiogenesis *in vitro* (Ruzehaji *et al*., 2014). The effect of FliiL FnAbs on wounds in large animal models was also investigated (Jackson *et al*., 2012). The injection of these antibodies into porcine excisional wounds enhanced the rate of re-epithelialisation and reduced the size of scars (Figure 1.7B) (Jackson *et al*., 2012). Intradermal injection of FliiL FnAbs into diabetic mice wounds was found to promote the secretion of VEGF within the wounds, indicating the effect of Flii on the angiogenesis process during wound healing (Ruzehaji *et al*., 2014; Ruzehaji *et al*., 2013).

Topical applications of multiple cream formulations have been developed to aid delivery of FliiL FnAb to wounded skin (Haidari *et al*., 2017). The development of these creams allowed for the prolonged FliiL FnAb release into the epidermis and dermis of porcine skin (Haidari *et al*., 2017). Topically applied FliiL FnAb cream into blistered skin in an epidermolysis bullosa acquisita (EBA) mouse model resulted in reduced inflammation (Kopecki *et al*., 2013). Moreover, treatment of FliiL FnAb creams during the early phases blistering led to attenuated severity of blister formation. Topical application of FnAb creams also decreased the severity of blisters when applied to established blisters, resulting in less fragile skin in this EBA mouse model (Kopecki *et al*., 2013). In another study, psoriasiform dermatitis in mice was induced by Chong *et al* and FliiL FnAb applied topically both prior to the induction and during the sensitisation of the skin (Chong *et al*., 2017). Inflammation and dermal cellular infiltration were reduced, resulting in decreased erythema and epidermal hyperplasia (Chong *et al*., 2017).

Porous silicon nanoparticles (pSi NPs) loaded with FliiL FnAb *in vitro* were found to increase the proliferation of keratinocytes and improve the recovery of wounded cells by electric cell-sensing impedance sensing (Turner *et al*., 2017). Incisional wounds were also delivered by a single dose of FliiL FnAb-pSi NPs in a mouse model, leading to a significant improvement in wound appearance (Turner *et al*., 2017).

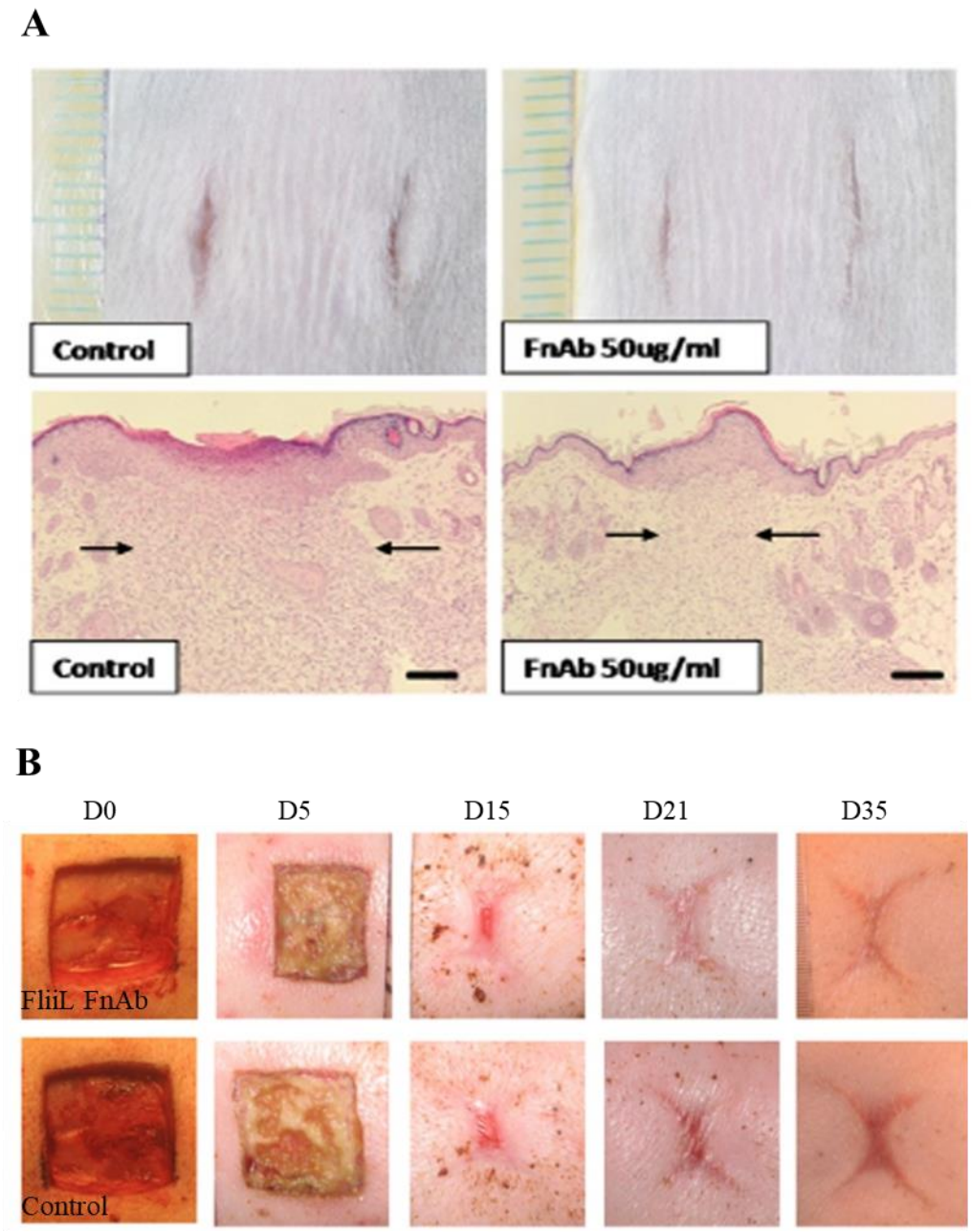


Figure 1. 8: Topical application of first generation Flii neutralising antibody (FliiL FnAb) to incisional and excisional wounds

A) a murine model of incisional wound and B) a porcine model of excisional wounds (Jackson *et al*., 2012).

1.18 The impact of FliiL FnAbs on burn wound and hypertrophic scarring

To determine the efficacy of FliiL FnAbs treatment on burn wounds and hypertrophic scarring, studies have been performed using scald burn injury model and bleomycin induced scarring model. As illustrated in Figure 1.8A, the intradermal injection of FliiL FnAbs to murine partial-thickness scald burns resulted in a significant improvement in the appearance of the burn wounds (Adams *et al*., 2009). The expression of TGF-β1 was reduced, while the level of anti-scarring TGF-β3 was elevated (Adams *et al*., 2009). Also, the expression of myofibroblast markers α-SMA and collagen (Figure 1.8A) was decreased in the developing scars (Adams *et al*., 2009). The effect of FliiL FnAbs on scar formation was investigated using a murine model of hypertrophic scarring (Figure 1.8B) (Cameron *et al*., 2016). The injection of FliiL FnAb into scars caused by the induction of bleomycin resulted in a significant improvement in the macroscopic appearance of scars, leading to a decreased dermal thickness and decreased ratio of collagen I/III (Figure 1.8B) (Cameron *et al*., 2016).

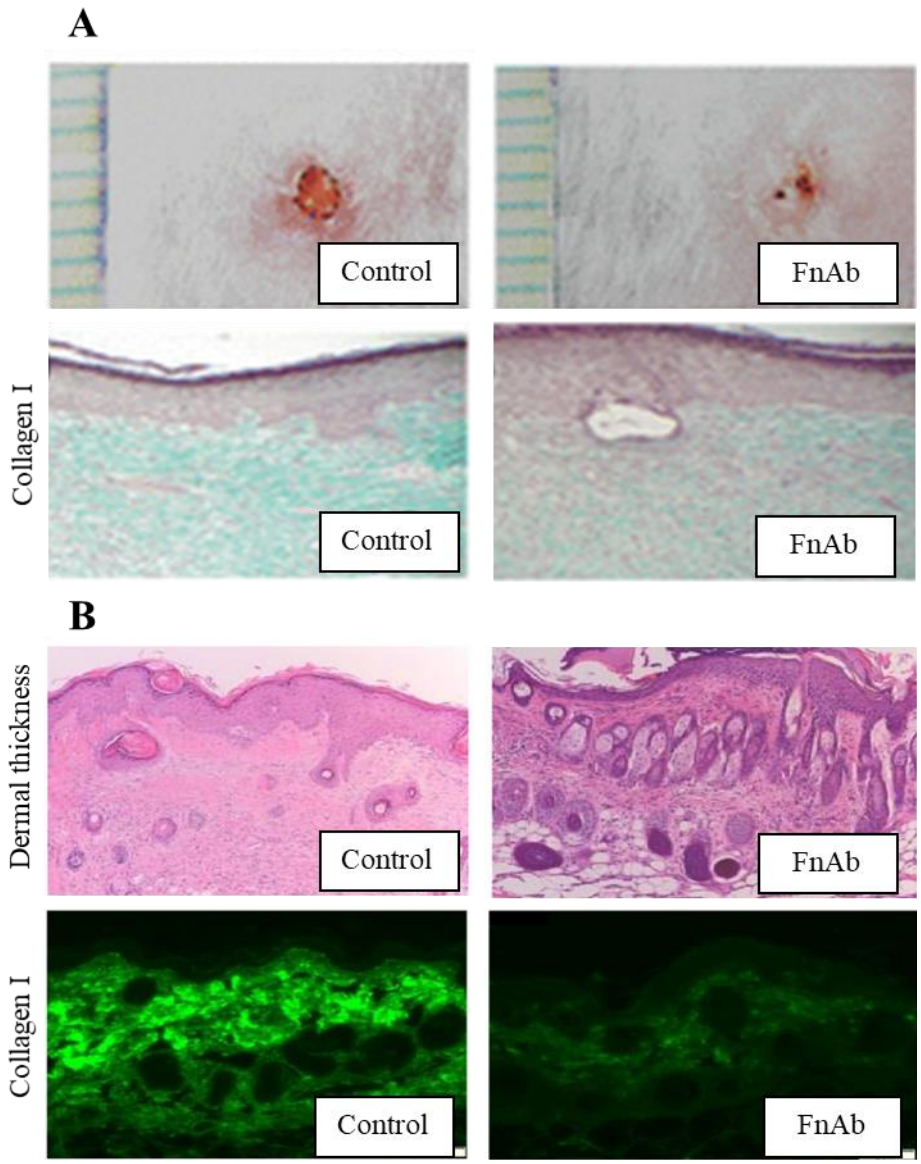


Figure 1. 9: Local delivery of first generation Flii neutralizing antibody (FliiL FnAb) to burn wounds

A) murine burn wounds (Adams *et al*. 2009) B) murine model of hypertrophic scarring (Cameron *et al*., 2016).

1.20 Systemic delivery of FnAbs to burn wounds

There are various routes of administration for medications, which depend not only on convenience but also on the properties of the substance being administered (e.g., an antibody). The choice of the route of administration also depends on the location at which the substance needs to be applied (Kim and De Jesus, 2022). The systemic route directly delivers the medications to the circulation (Kim and De Jesus, 2022). This administration route is used when a rapid effect of the substance is desired, and a precise serum drug level is needed, while the local delivery provides the potential to achieve high and sustained local concentrations of the medication without major systemic doses (Eccleston *et al*., 1996; Kim and De Jesus, 2022). Neutralizing Flii activity using localized, intradermal application of FliiL FnAbs has previously been shown to be a promising and effective approach to inhibit the activity of Flii (Adams *et al*., 2009; Cowin *et al*., 2007; Jackson *et al*., 2012). However, it is important to note that while this section primarily focuses on the systemic delivery of FnAbs to burn wounds, it is worth mentioning the challenges associated with local management of burn injuries. Burn injuries tend to cover large surface areas of the body such as the hand, faces, bony protuberances, and joints. Also, the management of burn wounds is a long-drawn-out process relying on various wound dressings which require regular and painful changes (Wall *et al*., 2019).

While burns dressings primarily focus on preventing infection, they face numerous challenges in effectively supporting wound repair. Although some dressings show enhancing wound healing, the complex nature of burn injuries and the extensive body areas they affect pose significant hurdles (Markiewicz-Gospodarek *et al*., 2022). Exploring the development of a simple and targeted antibody therapy for systemic administration in burn patients could be an exciting avenue to improve wound healing over larger body areas.

1.21 Knowledge gap, aims and hypotheses

Despite advances in burn care over past decades, management of burn injuries is still a challenge as there are limited options for improving healing outcomes for burn patients. Flii protein has been found to be a negative regulator of healing in many types of skin wounds including burns. FnAbs are being developed with preclinical studies showing that they reduce the activity of Flii which is elevated in wounds. Intradermal, local injection, and topical application of first generation FnAbs has been investigated in models of acute wound and burn models of wound healing, leading to improved healing processes. However, these applications are not a feasible and effective approach for patients with extensive burns that cover large surface areas of the body. New FnAbs raised against either LRR of Flii (LRRFnAb) or middle domain of Flii protein (MFnAb) were generated that were investigated in this research project to determine if the new generation of antibodies that target different parts of Flii can still improve wound healing while delivered systemically.

1.21.1 Hypotheses and aims

Based on the current literature, it was hypothesised that reducing Flii using the new generation of FnAbs (LRRFnAb and MFnAb) in skin cells will affect cellular proliferation, migration, and functionality. In addition, systemic administration and delivery of LRRFnAb and MFnAb would enable multiple and large wounds to be treated simultaneously. It was further hypothesised that FnAbs that bind to different domains of Flii would exert different healing effects in acute and burn wound repair.

The specific aims of this study were as follows:

1. To assess and compare the effect of LRRFnAb and MFnAb on the function of skin cells *in vitro*.
2. To investigate and compare the effect of systemic delivery of LRRFnAb and MFnAb to a murine model of excisional healing.
3. To investigate and compare the effect of systemic delivery of LRRFnAb and MFnAb to a murine model of second-degree scald burn.
4. To investigate the signalling pathways that led to the pro-angiogenic effect of intracellular and extracellular Flii.

Chapter 2: Materials and Methods

This chapter describes materials, methods of measurements/assessments, and statistical analysis conducted in this thesis. All standard laboratory chemicals were purchased from Sigma-Aldrich (Castle Hill, New South Wales, Australia) unless stated otherwise.

2.1 Generating new Flii neutralizing antibodies against Flii

Mouse monoclonal antibodies raised against different parts of human Flii protein were generated by Superview Biotechnology (Jiangsu, China) (Figure 2.1). The optimisation of target DNA codon was performed. Dendritic cell (DC) targeting sequences was applied to enhance the antigen uptake and T helper sequences were also added to facilitate the humoral immune response. Plasmid DNA was formulated and delivered by microparticles for controlled and long-lasting release. The clones were then screened using cell-based ELISA.

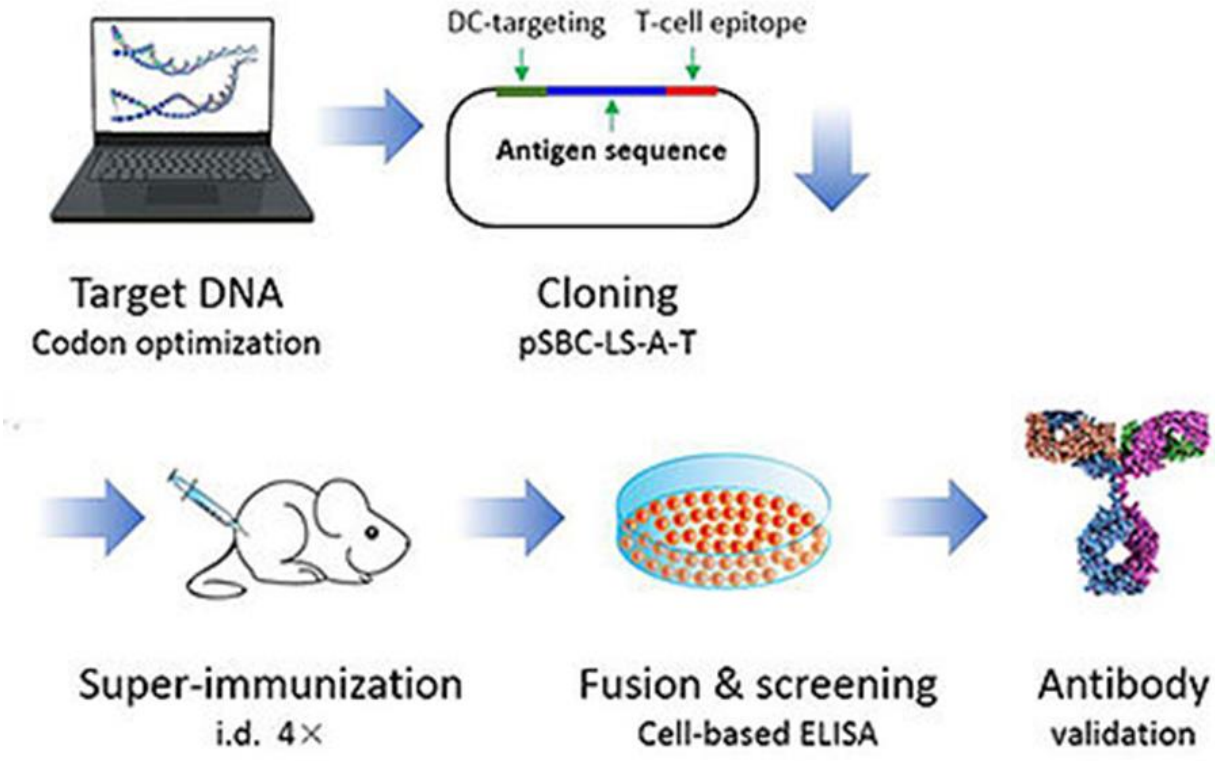


Figure 2. 1: FnAbs production method using DNA super-immunization method. Adapted from Superview Biotechnology website.

Optimising DNA sequence, applying DC-targeting sequences and T helper sequences were performed. Plasmid DNA was then delivered by microparticles for controlled and long-lasting release and antibodies were detected using ELISA.

A Flii neutralizing antibody (FnAb) raised against the peptide 1-403aa in the LRR domain of Flii protein is termed LRRFnAb (Figure 2.2). Another FnAb generated against the middle domain of Flii protein targeting 401-824aa includes three gelsolin domains of Flii protein is termed MFnAb (Figure 2.2).

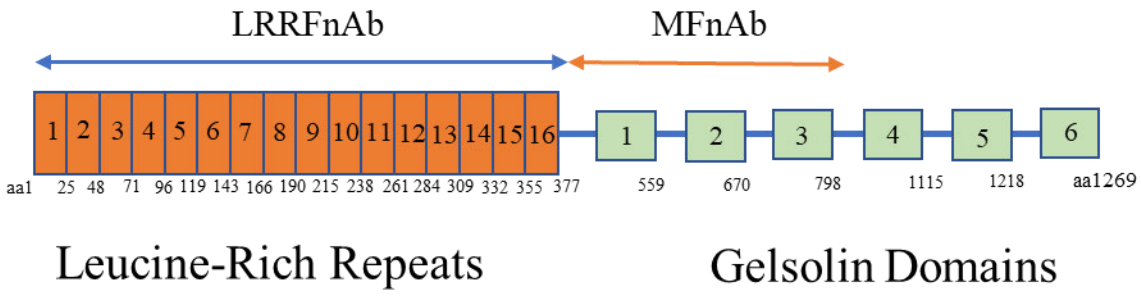


Figure 2. 2: Portions of Flightless I protein that were used to generate LRRFnAb and MFnAb.

2.1.1 General FnAb purification method

Mouse hybridoma cell lines were generated by Superview Biotechnology (Jiangsu, China) (Figure 2.1). Hybridomas were maintained in low serum medium (5% FBS) with culture supernatant decanted routinely for purification of secreted antibody. FnAbs were purified using a HiTrapTM protein G HP column and ÄKTA Pure chromatography system. Antibodies were eluted from the column with 0.1 M glycine-HCl, pH 2.7, and neutralized with 1 M Tris-HCl, pH 9.0, followed by buffer exchange into PBS and concentration to 1 mg/ml stock. Antibody concentrations were determined by absorbance at 280 nM. The hybridoma cell lines yielded 5 mg per litre and 9 mg per litre for LRRFnAb and MFnAb respectively. The affinity of LRRFnAb and MFnAb with Flii were confirmed using ELISA, Western blotting, and Immunofluorescent staining (Figure 2.3).

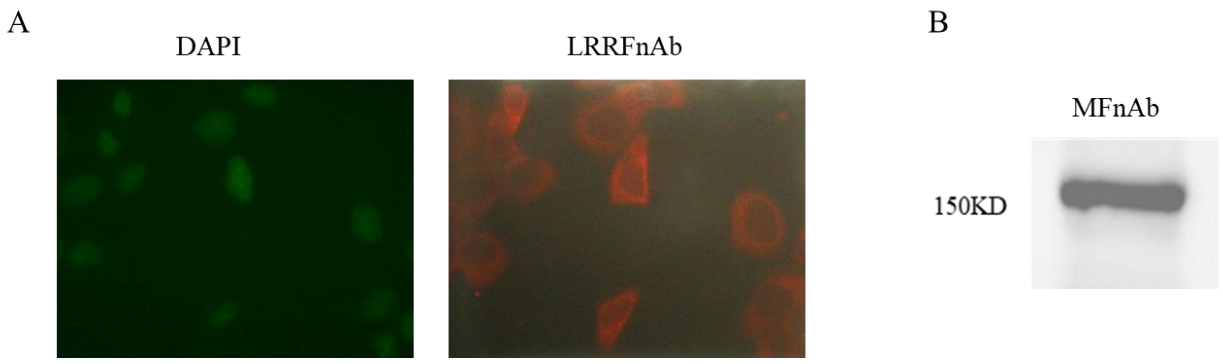


Figure 2. 3: The assessment of LRRFnAb and MFnAb affinity with Flii

A) Immunofluorescent assessments indicate the affinity between LRRFnAb and Flii protein in human embryonic kidney cells transfected with plasmid encoding human Flii. B) Western blotting assessments indicate the affinity between MFnAb and Flii protein in human immortalized keratinocytes.

2.2 Cell culture and *in vitro* assays

2.2.1 Cell culture

2.2.1.1 Human Foreskin Fibroblasts, Human Immortalized Keratinocytes, and Human Dermal Microvascular Endothelial Cells

The tubes containing human foreskin fibroblasts (HFFs) (ATCC, Manassas, USA) and human immortalized keratinocytes (HaCaTs) (CLS, Deutschland, Germany) were thawed in a 37°C water bath for 2 minutes, wiped, sterilized with 70% ethanol, and then the cells were cultured (seeded at 6.5×10^3 cells/cm^2). The medium for both HFFs and HaCaTs was composed of the following materials:

- Low-glucose DMEM medium (Thermo Fisher Scientific, VIC, Australia)
- 2 mM L-Glutamine (Lonza, Basel, Switzerland)
- 10% FBS (Atlas biologicals, Fort Collins, USA)
- 100 U/ml penicillin/streptomycin (Lonza, Basel, Switzerland)

A commercially available cryopreserved vial of human dermal microvascular endothelial cells (HDMECs) (0.5×10^6 cells) (Promocell, Heidelberg, Germany) was purchased and defrosted in a

37°C water bath for 2 minutes, wiped and sterilized with 70% ethanol. The contents were suspended in a 12 ml complete growth medium in a T75 tissue culture flask. HDMECs (seeded at 5×10^5 cells) were cultured in:

- Endothelial cell growth medium MV2 (PromoCell, Heidelberg, Germany)
- 10% FBS (Atlas biologicals, Fort Collins, USA)
- 2 mM L-Glutamine (Lonza, Basel, Switzerland)
- 100 U/ml penicillin/streptomycin (Lonza, Basel, Switzerland)

All three cell types were incubated at 37°C with 5% CO_2 and 95% humidity. The cells were washed with PBS and the medium replaced with warmed, fresh medium following 18 hours post-seeding incubation. Phase-contrast images of HFFs, HaCaTs, and HDMECs at 10X magnification are shown in Figure 2.4.

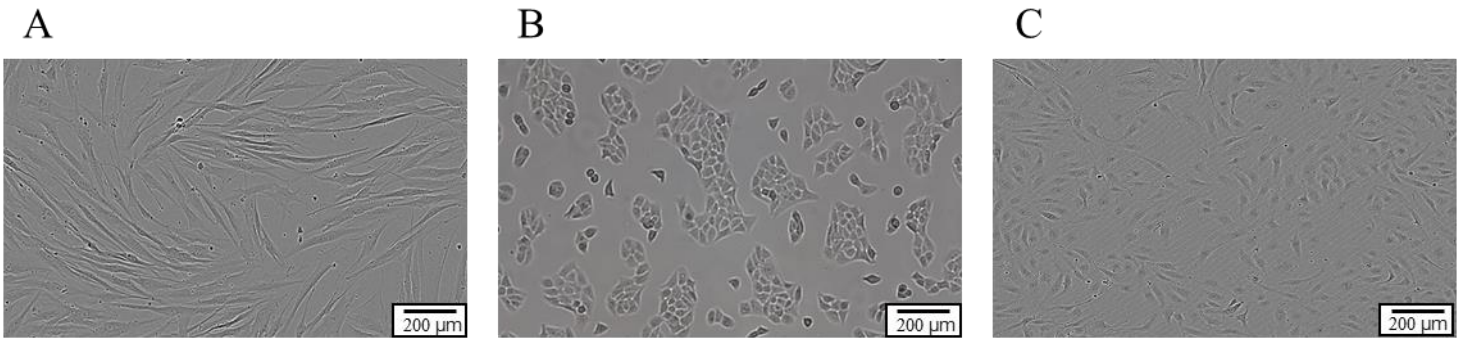


Figure 2. 4: Human skin cells

A) Human foreskin fibroblasts (HFFs), B) Human immortalized keratinocytes (HaCaTs) C) Human dermal microvascular endothelial cells (HDMECs) (10X)

2.2.2 Cell passaging

Cells were incubated until 90% confluent with fresh media every 3 days. To subculture, the cells were washed twice with 5 ml PBS following removal of the culture medium from T75 flasks. The cells were covered with 3 ml 0.05% trypsin-EDTA for HaCaTs and HDMECs and 3 ml 0.25% trypsin-EDTA for HFFs at 37°C. After 2 minutes, cells were detached from the surface following gentle tapping. After the cells were released, 9 ml culture medium was added to the cells to neutralize the trypsin effect, and the cell suspension was centrifuged at 350 x g for 5 minutes at room temperature to pellet the cells. The cells were diluted to a final volume of 1 ml of growth medium. NucleoCounter (Chemometec, Allerod, Denmark) was employed to count the cells and the split ratio of 1:5, 1:7, and 1:4 was used for HFFs, HaCaTs, and HDMECs respectively.

2.2.3 Cell proliferation assay

To determine the effect of different antibodies raised against Flii protein on the proliferation of HaCaTs, HFFs, and HDMECs, a non-invasive and label-free cell proliferation assay was performed using the IncuCyte Live-Cell Imaging System (Essen Bioscience, MI, USA). This assay enables real-time imaging, allowing for continuous monitoring of cellular processes. The confluency mask generated by the assay provides an assessment of the extent of cell proliferation that occurred within a 24-hour period. The confluency measurements were acquired at regular intervals of every 3 hours, enabling precise tracking of cellular growth dynamics over time. HaCaTs, HFFs, and HDMECs were seeded on a 96-well plate at a density of 5×10^3 cells/well and incubated for 24 hours at 37ºC. The cells were then treated with either normal media or IgG (Bio X Cell, Lebanon, USA) or LRRFnAb or MFnAb (Superview Biotechnology, Jiangsu, China) and photographed every 3 hours using a 10X objective (Essen Bioscience, MI, USA). Cell proliferation was monitored by analysing the occupied area (% of confluence) of cell images over time using IncuCyte ZOOM® Software (2015A, REV1). The IncuCyte cell proliferation assay allows every well of the plate to be imaged and analyzed automatically to provide a readout of cell proliferation over time based on confluency rate achieved in a specific time period.

2.2.4 Scratch wound closure assay

To assess the impact of LRRFnAb and MFnAb generated against LRR and middle domain of Flii respectively, on the migration of dermal fibroblasts, keratinocytes, and endothelial cells, scratch wound closure assay was conducted. The HaCaT, HFF, and HDMEC cells were seeded on a 96-well plate and incubated at 37^{o}C until they reached fully confluent. Cells were then wounded using a WoundMaker™ (Essen bioscience, MI, USA). Following wounding, cells were washed twice with PBS, and the media replaced with either control media or media containing IgG or media containing FnAbs. The plate was placed into the IncuCyte™ ZOOM (Essen BioScience) and the IncuCyte ZOOM® Software (2015A, REV1) was programmed to scan the entire plate every 3 hours with phase imaging using a 10X objective until complete wound closure. Each image was masked by the integrated analysis algorithm to detect the wounded and unwounded areas to measure wound width and wound confluence over the time of the experiment.

2.2.5 Matrigel tube formation assay

To evaluate the effect of LRRFnAb and MFnAb on blood vessel formation, an *in vitro* tube formation assay was carried out. This experiment demonstrates the angiogenic activity of vascular endothelial cells following incubation with FnAbs. As shown in Figure 2.5, 10 µl reduced growth factor Matrigel (Corning, New York, USA), was added to each well of an Ibidi u-slide angiogenesis 15-well plate (Ibidi GmbH, Bavaria, Germany) and incubated for 30 minutes at 37°C. HDMECs suspended in 50 µl of either untreated media or media containing IgG or media containing FnAb were seeded in each well. The plates were incubated and photographed every 3 hours using an Olympus IX81 microscope (Olympus, Tokyo, Japan). Pseudo vascular organization of endothelial cells cultured in gel medium was then detected and analysed by Image J Angiogenesis Analyzer. Number of nodes, segments, junctions, master junctions, and meshes were quantified using Image J Angiogenesis Analyzer.

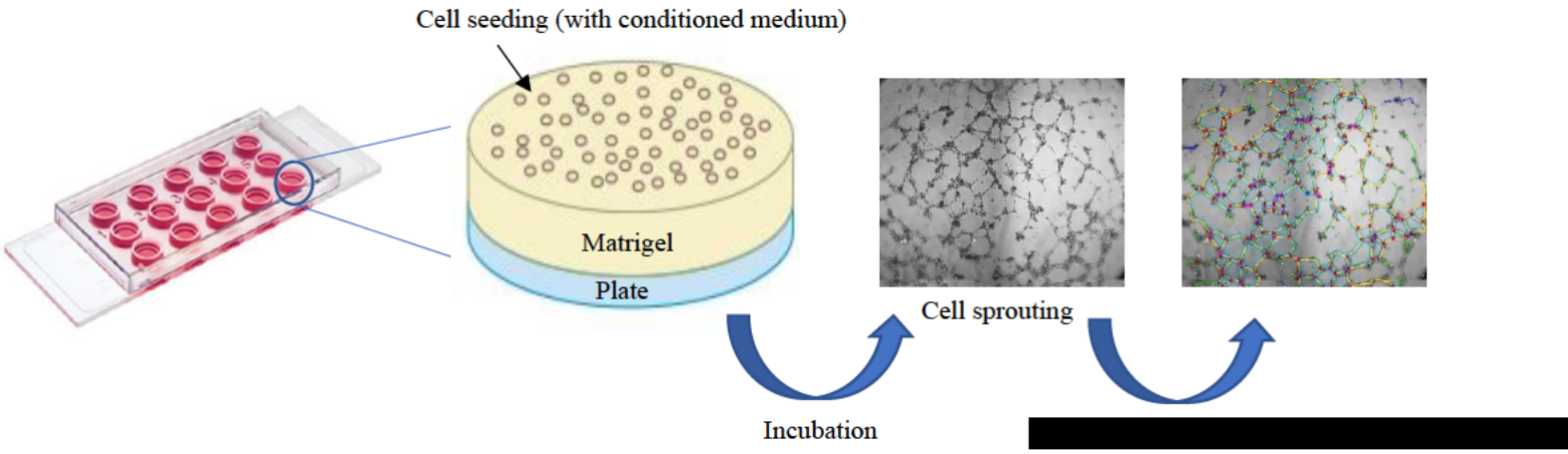


Figure 2. 5: Matrigel-based tube formation assay

2.2.6 siRNA knockdown

Human dermal endothelial cells and keratinocytes were treated with siRNA to attenuate Flii. For this purpose, the cells were seeded (2×10^5 cells) into 6-well plates and incubated for 24 hours in normal media. siRNA (0.5µL/well) (10.0 nmol) (Sigma Aldrich, Castle Hill, NSW, Australia) (Table 2.3) was diluted in 1 ml Opti-MEM (Life Technologies Australia, Scoresby, VIC, Australia) and incubated at room temperature for 30 min. Lipofectamine 2000 (Thermo Fisher Scientific, Scoresby, VIC, Australia) (0.3µL/well) was also combined with 1 ml Opti-MEM and incubated at room temperature for 30 min. siRNA and lipofectamine solution were combined to form an siRNA:Lipofectamine complex. The combined solution was left at room temperature for a further 30 min. A total of 2 ml solution was added to each well and the cells were incubated for 12 hours. The transfection media was then replaced with warm, fresh media and incubated for 24 hours for Flii Knockdown assessments.

Table 2. 1: siRNA sequences for scrambled control siRNA (siControl) and siFlii conditions

Treatment	Forward primer (5'-3')	Reverse primer (5'-3')
siControl	GGUUAGCCGCACGUUAGUU	AACUAACGUGCGGCUAACC
siFlii	GCUGGAACACUUGUCUGUG	CACAGACAAGUGUUCCAGC

2.2.7 Gene expression studies

2.2.7.1 RNA isolation

Endothelial cells, keratinocytes, and fibroblasts were treated with either LRRFnAb or MFnAb or human recombinant flightless I protein (rFlii) (Cusabio, Houston, US) +/- FnAbs (LRRFnAb or MFnAb) for 24 hours. Total RNA, including mRNA transcripts, were isolated from treated fibroblasts, keratinocytes, endothelial cells and also siFlii/siControl treated endothelial cells and keratinocytes using the Purelink RNAmini kit (Invitrogen, Carlsbad, CA, USA). Briefly, growth medium from the cultured cells was removed. The cells were incubated with trypsin-EDTA at 37°C for 3 minutes following washing cells with sterile PBS for 10 seconds. The cells were detached and centrifuged for 5 minutes in 360 x g. Lysis buffer (0.6 ml) with 2-mercaptoethanol (10 ul/ml) was added. The cell pellets were dispersed, and the cells lysed by vertexing. The lysate was passed through a 21-gauge syringe needle 5–10 times for homogenization. To each volume of cell homogenate, 0.6 ml of 70% ethanol was added. The sample was transferred to the spin cartridge (with the collection tube) following vortex. The spin cartridge with the collection tube was centrifuged at 12,000 × g for 15 seconds at room temperature and the flow-through was discarded. Wash buffer I was added to the spin cartridge and centrifuged at 12,000 × g for 15 seconds at room temperature. The flow-through was discarded and the spin cartridge was placed into a new collection tube. Wash buffer II was added to the spin cartridge and centrifuged at 12,000 × g for 15 seconds at room temperature and the flow-through was discarded. The previous step (adding wash buffer II, centrifuging, and discarding) was repeated and the spin cartridge was centrifuged at 12,000 × g for 1–2 minutes to dry the membrane with bound RNA. The spin cartridge was inserted into a recovery tube and 50 µl RNase-free water was added to the spin cartridge. The sample was incubated at room temperature for 1 minute. The spin cartridge was centrifuged for 2 minutes at 12,000 × g at room temperature to elute the RNA. The concentration

of purified RNA was measured by absorbance at 260nm using 2 µl of RNA diluted 1/10 in RNase-free water on the NanoDrop Lite Spectrophotometer (Thermo Fisher Scientific, VIC, Australia).

2.2.7.2 cDNA synthesis

cDNA was synthesized using Bio-Rad iScript kit (Bio-Rad, NSW, Australia) from purified RNA by combining 600 ng RNA diluted in nuclease-free water with 4 µl buffer mix and 1 µl iScript reverse transcriptase enzyme in a 20 µl reaction. The total mixture was incubated for 5 minutes at 25°C, followed by incubation for 30 minutes at 42°C, and 5 minutes at 80°C. The tubes were then cooled to 4 °C.

2.2.7.3 qRT-PCR

qRT-PCR was conducted in triplicate to quantify the level of the target gene expression on the BioRad CFX Connect Real-Time PCR System using SsoAdvanced SYBR Green Universal Supermix synthesis (Bio-Rad, NSW, Australia). To perform qRT-PCR for target genes, 200nM each of the forward and reverse primers (Table 2.2) were combined with 10 µl SYBR Green Universal Supermix and 1 µl cDNA template in a 20ul reaction. Each primer efficiency was calculated in a 20 µl reaction by a serial 1:5 dilution of cDNA from 250ng to 0ng, with an R^2 value of above 0.95 of greater than 0.95 considered acceptable. The step of amplification was initiated by 30 seconds at 90°C, which was followed by 32 cycles of 95°C for 5 seconds, and 60 °C for 20 seconds with the SYBR Green signal read after each repeat of annealing. To assess specificity of amplification in qPCR protocol, melting curve was analysed by cycling from 65 °C to 95 °C in 0.5 °C in 5 second increments.

Table 2. 2: PCR primers

Gene	Forward primer (5'-3')	Reverse primer (5'-3')	Primer Efficiency	R^2 value	Melt Peak
Flii	CATCCTACAGCAAACAGGTCATCAT	GTGTGTG CTGGATGTATACCTGG GAA	93.2%	0.994	85.5°C
VEGF-A	AGGGCAGAATCATCACGAAGT	AGGGTCTCGATTGGATGGCA	98.1%	0.967	86.0°C
FGF-2	AGAAGAGCGACCCTCACATCA	CGGTTAGCACACACTCCTTTG	97.4%	0.982	85.0°C
PDGF-BB	CTCGATCCGCTCCTTTGATGA	CGTTGGTGCGGTCTATGAG	98.3%	0.977	88.0°C
CypA	GGTTGGATGGCAAGCATGTG	TGCTGGTCTTGCCATTCCTG	92.5%	0.986	83.0°C

2.2.8 Protein expression studies

2.2.8.1 Preparation of protein lysates

In order to prepare lysate from cell culture, the cell layer was washed with precooled sterile PBS. The PBS was then aspirated and RIPA Buffer (150mM sodium chloride, 1% Triton X-100, 0.5% sodium deoxycholate, 0.1% sodium dodecyl sulfate and 50mM Tris base, pH 8.0,) with complete-mini protease inhibitor cocktail (Roche, Basel, Switzerland) (1 tablet per 10 ml of RIPA) was added for the efficient lysis of cells and solubilization of protein. The lysate was collected into the labelled cold tubes and centrifuged at 14,000 g for 15 minutes at 4°C. The supernatant was transferred into a fresh tube kept on ice for further analysis.

2.2.8.2 BCA assay for measurement of total protein concentration

Bicinchoninic Acid (BCA) assay was performed for quantitation of total protein in samples using a Pierce BCA Protein Assay Kit (Thermo Fisher Scientific, VIC, Australia). A set of diluted standards (2000, 1000, 500, 250, 125, 72.5, 36.25, 18.125 µg/ml) of bovine serum albumin (BSA) was employed in triplicate. Each lysate was diluted 1:1, 1:2, 1:4, and 1:16 and 25 µl of each sample was added to each well in triplicate in 96 well plates. BCA working reagent was also prepared by mixing 50 parts of BCA reagent A with 1 part of BCA reagent B. 200 µl of the BCA working

reagent was added to each well containing sample. The plate was covered and incubated at 37°C for 30 minutes. The plate was then cooled down to room temperature and the absorbance measured at 562nm on a plate reader (Tecan Group, Mannedorf, Switzerland). The total concentration of protein for each sample was calculated with reference based on the standard curve using a linear equation.

2.2.8.3 Western blotting

SDS-PAGE gel was prepared based on desired resolution and visualization of target protein (Table 2.3). Samples were made up to 20 ul and combined with 5 ul of 5 x SDS PAGE loading buffer (25nM Tris pH 6.8, 8% glycerol, 1% SDS, 0.02% bromophenol blue, 5% 2-mercaptoethanol). Protein lysates were loaded onto prepared SDS-Page gels following heat at 95°C for 5 min. The gel was run in 1 x Western Running Buffer at 100V until the dye front flew over the bottom of the gel. Blotting papers, transfer sponges, and nitrocellulose membrane (BioTraceTM NT, Pall Corporation, FL, USA) were transferred into 1 x cold Transfer Buffer. The gel was rinsed in western transfer buffer briefly before setting up in the holder. The holder containing gel, blotting papers, transfer sponges, and nitrocellulose membrane was set up and transfer was performed at 100V 1hr at 4°C. The membrane was then blocked in 12% skim milk for 15 mins while shaking. The membrane was incubated in 5% skim milk containing primary antibodies against Flii (1:500) (Superview Biotechnology, Jiangsu, China) and GAPDH (1:500) (sc-25778, Santa Cruz Biotechnology, Texas, USA) overnight at 4°C. The membrane was then washed twice with 1 x TTBS (TBS, 0.1% Tween20) for 5 minutes while shaking. The membrane was incubated in 5% skim milk containing Secondary antibodies (1:1000) (DAKO P0447 and P0448, Agilent, Santa Clara, CA, USA) for proteins of interest for 40 minutes at room temperature followed by washing twice with 1 x TTBS for 5 mins and once with TBS for further 5 mins at room temperature. The membrane was developed using a Westpico kit (Thermo Fisher Scientific, VIC, Australia) and visualized for protein detection by a SynGene G-Box (Syngene, Australia).

Table 2. 3: Polyacrylamide gels for protein resolution

	10% Separating gel	4% Stacking gel
30% Acrylamide	3.35 ml	0.5 ml
3M Tris, pH 8.9/9.5	1.25 ml	-
0.5M Tris, pH 6.8	-	0.276 ml
Distilled Water	5.25 ml	4.104 ml
10% SDS	125 µl	50 µl
10% APS	100 µl	40 µl
TEMED	6.25 µl	4 µl

2.3 Animal Studies

All animal studies were first approved by either the Women's and Children's Health Network or University of South Australia Animals Ethics committees, depending on the location where the animals were housed. The studies were conducted in accordance with the Australian code for the care and use of animals for scientific purposes.

2.3.1 Murine model of excisional wound healing

The approval with the Animal Ethics number AE1119 was provided and 8–10 weeks old female BALB/c mice (6 mice per group) (ARC, Perth, Australia) with weight of 20-25 g were subjected to a model of excisional wound healing. The mice were group housed on arrival and left to acclimatize for 7 days during which time there were no interventions. Mice were administered analgesia (Buprenorphine at 0.05 mg/kg) by subcutaneous injection 30 minutes prior to the surgery. After inducing anaesthesia by inhalation of 5% isoflurane and 5% oxygen at 2 L/minute, the mice were maintained on a mask delivering 2% isoflurane at a flow rate of 0.5 L/minute while placed on a heat pad. Following anaesthesia, the backs of mice (dorsum) were shaved and Veet cream applied to remove hair. After cleaning the skin with water, the exposed skin was sterilized using 70% alcohol swabs. A full thickness 10mm diameter excisional wound was then created through the skin using a disposable punch biopsy tool (AcuPunch, available from Acuderm) approximately 1.5 cm from the base of the skull and 0.5 cm on the midline. Each mouse received a single dose of either LRRFnAb or MFnAb or IgG (100µl ~ 5 mg/kg), injected into the abdominal cavity (Figure 2.6) whilst the animal was still anaesthetized. Mice were allowed to recover from anaesthesia on a heated pad and were returned to individual cages to recover in a warm, dry cage and given water and food *ad libitum*. A second administration of analgesia (Buprenorphine at 0.05 mg/kg) was delivered to mice 8 hours post-surgery, if necessary, which was determined by observation of any signs of pain or distress. For the duration of all experiments, the mice were also monitored daily for signs of discomfort or distress. Mice were photographed on days 0, 2, 4, and 7 to monitor wound size throughout the study. Finally, mice were humanely killed by CO_2 inhalation followed by cervical dislocation on day 7, and tissues were collected for wound healing analysis to assess the effect of systemic delivery of FnAbs on wound healing. This trial was carried out by Damian Adams and Xanthe Strudwick.

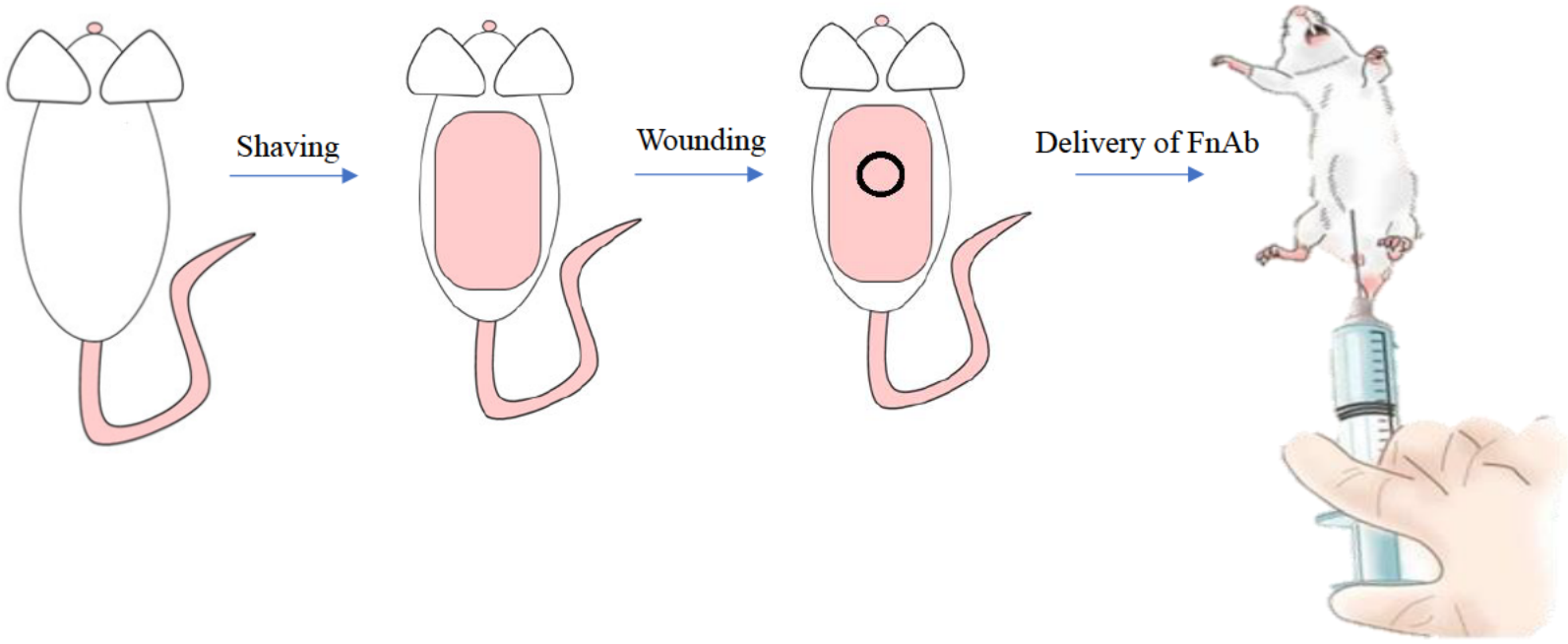


Figure 2. 6: Schematic of FnAb delivery to a murine model of excisional wound healing by IP injection

2.3.2 Rapid antibody labelling

A SAIVI Antibody Alexa Fluor 680 Labelling kit (Thermo Fisher Scientific, VIC, Australia) was used to label the antibodies following the manufacturer's description to determine the antibody localization of systemically of LRRFnAb and MFnAb in mice. All reactions were performed at room temperature and all solutions including the antibody solutions were equilibrated to room temperature before use. A solution of sodium bicarbonate, pH 8.3, was prepared by adding 1 ml of deionized water to the provided vial of sodium bicarbonate. The solution was completely dissolved by vertex mixing. 50 µl sodium bicarbonate buffer was then combined with 10 µl regulator solution and 500 µl antibody solution. The mixture was transferred to a reaction vial containing the lyophilized Alexa Fluor® reactive dye. The dye was completely dissolved through trituration. The antibody/dye solution was incubated 60 minutes at room temperature and protected from light. The reaction mixture was then layered on the top of the provided purification column bed using a clean column loading pipette. After allowing the reaction mixture to absorb into the column bed, a gentle layering of 1.3 ml of PBS was applied onto the column bed. PBS (900 µl) was applied to the column when stopped dripping and the eluate was collected in a clean, 1.5 ml Eppendorf tube. The dye-antibody eluate was stored at 2–6˚C prior to use while protected from the light.

2.3.3 Murine model of second-degree partial-thickness scald burn

Following the approval provided by Women's and Children's Health Network and the University of South Australia Animal Ethics Committee (Animal Ethics number: AE1088), 10–12-week-old female BALB/c mice (10 mice per group) with weight of 20-25 g were used for this trial. Mice were given a general health check and administered analgesia 30 minutes prior to burn induction (Buprenorphine at 0.05 mg/kg) injected under the skin (subcutaneous injection). For this model, anaesthesia was induced by subcutaneous injection of ketamine (75 mg/kg) and domitor (1mg/kg), with the mice being returned to their cage until becoming unconscious, after which time they were transferred to a heat pad to maintain core body temperature. The back of the mice (dorsum) was shaved with clippers and hair removal was applied with depilatory cream (Veet). The skin of mice was cleaned and sterilized with water and 70% ethanol (Chem-Supply, SA, Australia). Full anaesthesia then was confirmed by checking for a lack of foot pinch reflex. Mice were gently and

securely placed into the custom-made scald burn apparatus made from a 60 ml plastic syringe with a cut-out measuring 70 mm^2. In order to create a 7% total body surface area second degree scald burn, the apparatus was submerged in a hot water bath (65°C) for 45 seconds to expose the skin to hot water. The mouse was immediately placed into cold (15°C) water for another 45 seconds to arrest the burn process (Figure 2.7). Following burn injury, the mouse was removed from the burn apparatus and received systemic FnAbs via intraperitoneal (IP) injection (100µl ~ 5 mg/kg). FnAbs were labelled with a fluorescent dye to enable tracking as described in section 2.3.2. Anaesthesia was then reversed by subcutaneous administration of Antisedan (Atipamezole 1 mg/mL). Mice were returned to the heat pad until awakened post-surgery. The burn wounds were not dressed, and they were allowed to recover in a warm, dry cage and given water and food *ad libitum*. The second round of analgesia (Buprenorphine at 0.05 mg/kg) was delivered to mice (subcutaneous injection) 8 hours following burn surgery.

Mice were imaged using IVIS Lumina S5 Imaging System (PerkinElmer, Massachusetts, USA) to allow real-time monitoring of FnAb localization on days 0, 1, 2, 3, 4, and 7. For imaging, the mice were anaesthetised with gaseous isoflurane (2% isoflurane, 0.5 L/minute) and placed on a warmed heater pad within the imaging system. Anaesthesia time was 2-5 minutes to take the images. The mice were then removed from isoflurane exposure and recovered quickly. Mice were humanely killed by CO_2 on day 7 and death was confirmed by cervical dislocation. The wounds were collected from each mouse for histological analysis of wound healing parameters and to assess the effect of FnAbs on wound healing.



Figure 2. 7: The procedures of a murine model of second-degree partial-thickness scald burn

The back skin was shaved, and mouse was gently and securely placed into the custom-made scald burn apparatus. The apparatus was submerged in a hot water bath (65°C) for 45 seconds and the mouse was immediately placed into cold (15°C) water for 45 seconds to achieve the appropriate burn wound.

2.4 Animal tissue processing and analysis

2.4.1 Tissue fixation and processing

Tissue samples including wounded and unwounded tissues were placed in histological cassettes and fixed in 10% neutral buffered formalin solution overnight prior to transfer into 70% ethanol (EtOH). Fixed tissues were processed overnight using an Excelsior™ AS Tissue Processor (Thermo Fisher Scientific, Massachusetts, USA). The tissues were dehydrated by immersing samples in a series of EtOH solutions of increasing concentration until pure, water-free alcohol was reached. The tissue samples were then cleared in transitional solvent xylene (the cleaning solvent) (Fronine, NSW, Australia) which allowed the wax to displace the ethanol in the tissue. Finally, the samples were infiltrated with histological wax (paraffin) at 60°C. The stages of tissue processing are shown in table 2.4. The tissue samples were then embedded in paraffin and cut at 4 µm using a microtome (Leica Microsystems, NSW, Australia). The paraffin sections were placed on standard glass and HistoBond+ slides (Paul Marienfeld GmBH & Co. Laude-Konigshofen, Germany) and incubated overnight at 50 °C.

Table 2. 4: The standard protocol for tissue processing

Reagent	Temperature °C	Time (mins)
70% ethanol	Room temperature	30
70% ethanol	Room temperature	60
80% ethanol	30	30
80% ethanol	30	30
90% ethanol	30	30
90% ethanol	30	30
100% ethanol	30	30
100% ethanol	30	60
Xylene	30	30
Xylene	30	30
Xylene	30	120
Paraffin wax	60	120
Paraffin wax	60	120
Paraffin wax	60	120

2.4.2 Haematoxylin and eosin staining (H&E)

In order to deparaffinize the sections, they were immersed in 2 x 2-minute changes of xylene. Xylene was then removed from sections by immersing in 2 changes of 100% ethanol for 2 minutes each, followed by 70% and 30% ethanol for 2 minutes each. The sections were transferred to the water for 4 minutes. Sections were stained by Lillie-Mayer's haematoxylin (Australian Biostain Pty Ltd, Traralgon East, Victoria, Australia) for 6 minutes and rinsed well in tap water. The sections were then placed in 5% bicarbonate solution for 15 seconds (50g sodium bicarbonate ($NaHCO_3$) in 1L H_2O) to blue the sections. The sections were dipped 8 times in 0.25% acid alcohol to differentiate Lillie-Mayer's haematoxylin and remove excess dye background staining. The sections were immersed in a 5% bicarbonate solution for 15 seconds. The sections were then stained in alcoholic eosin (Australian Biostain, Traralgon, VIC, Australia) for 2 minutes and dehydrated by dipping in 70% ethanol and two changes in pure ethanol for 1 minute in each

followed by 2 x 1-minute changes of Xylene for clearing. Finally, the sections were mounted using ClearVue Mountant XYL (Thermo Fisher Scientific, VIC, Australia).

2.4.3 Immunohistochemistry

The sections were dewaxed in two 15-minute changes of xylene. Sections were then immersed in two changes of 100% ethanol for 2 minutes each to remove xylene, followed by immersion in 70% and 30% ethanol for 2 minutes each. The sections were brought and washed in water for 4 minutes and rinsed with PBS. Antigen retrieval was conducted for 10 minutes at 90°C in target retrieval solution (10X Tris: 3.025 g Tris base + 0.925 g Ethylenediaminetetraacetic acid (EDTA) + 1.5 ml Tween 20, make up to 250 ml in H_2O, pH 9) using the decloaking chamber at 90 °C for 10 minutes. The sections were then rinsed with PBS and placed into Trypsin solution (0.0625 g Trypsin in 250 ml 37 °C PBS) for 3 minutes for enzymatic digestion. In order to preserve the tissue structure, the sections were immediately washed with PBS and placed in immunohistochemistry (IHC) black boxes. The sections were blocked for non-specific antibody binding with 3% normal serum from the organism in which secondary antibody was raised in PBS for 30-45 minutes at room temperature. The blocking solution contained antibodies that bind non-specifically to Fc receptors, blocking the primary antibodies from interacting. The blocking solution was replaced with the primary antibody (diluted in 3% blocking serum) and incubated overnight in a moist box at 4^0C. The following day, sections were rinsed 3 times with PBS and incubated with the secondary antibody (diluted in PBS) for 1 hour at room temperature while protected from the light in a moist box. After the removal of the excess secondary antibody, the sections were stained for 3 minutes with 4′,6-diamidino-2-phenylindole (DAPI, 1:5000 of 1 μg/ml stock) for visualization of the nucleus. Sections were then washed 3 times with PBS to remove the excess DAPI, followed by mounted coverslips using Fluorescence Mounting Medium (Agilent Technologies Australia, VIC, Australia). The mounted sections were placed in a -20^0C freezer to dry until imaging using Olympus IX81 microscope (Olympus, Tokyo, Japan) with a 20 x Objective and 0.5 x gain unless otherwise stated. All antibodies used in the studies with the concentration can be found in Table 2.5.

Table 2. 5: List of the primary and secondary antibodies for Fluorescent Immunohistochemistry

Target	Primary Antibody				Secondary Antibody				
	Supplier	Catalogue#	Source	Concentration (ml)	Supplier	Catalogue#	Source	Concentration (ml)	Fluorophore
Flightless I	Thermo Fisher	PA521735	Rabbit	5.8 µg	Life Tech.	A11011	Goat	10 µg	Alexa 594
NIMP-R14	Santa Cruz	sc-59338	Rat	0.5 µg	Life Tech.	A11006	Goat	5 µg	Alexa 488
F4/80	Bio-Rad	MCA4975	Rat	10 µg	Life Tech.	A11006	Goat	5 µg	Alexa 488
YM-1	StemCell	60130	Rabbit	0.37 µg	Life Tech.	A31577	Goat	5 µg	Alexa 633
CD31	Abcam	ab28364	Rabbit	0.2 µg	Life Tech.	A31577	Goat	5 µg	Alexa 633
αSMA	Agilent	GA61161-2	Mouse	0.7 µg	Life Tech.	A11011	Goat	10 µg	Alexa 594
VEGF-A	Abcam	ab46154	Rabbit	0.5 µg	Life Tech.	A11008 A11011	Goat	5 µg	Alexa 488 Alexa 594
FGF-2	Thermo Fisher	PA5116495	Rabbit	8.5 µg	Life Tech.	A11011	Goat	5 µg	Alexa 594
PDGF-BB	Thermo Fisher	PA519524	Rabbit	5.5 µg	Life Tech.	A11011	Goat	5 µg	Alexa 594

2.5 Measurement and analysis

2.5.1 Macroscopic wound measurement

In order to measure the macroscopic area of wounds, a ruler was aligned with each wound, and images were taken on days 0, 2, 4, and 7 for the excisional trial and on days 0, 1, 2, 3, 4, and 7 for the burn antibody localization trial. Photographic images were then imported into Image ProPlus (version 7.0; Media Cybernetics, MD, USA) to determine the macroscopic wound area. Note that measurement tools were calibrated for each image using the ruler in the image and wound areas were normalised to the initial wound area.

2.5.2 IVIS analysis

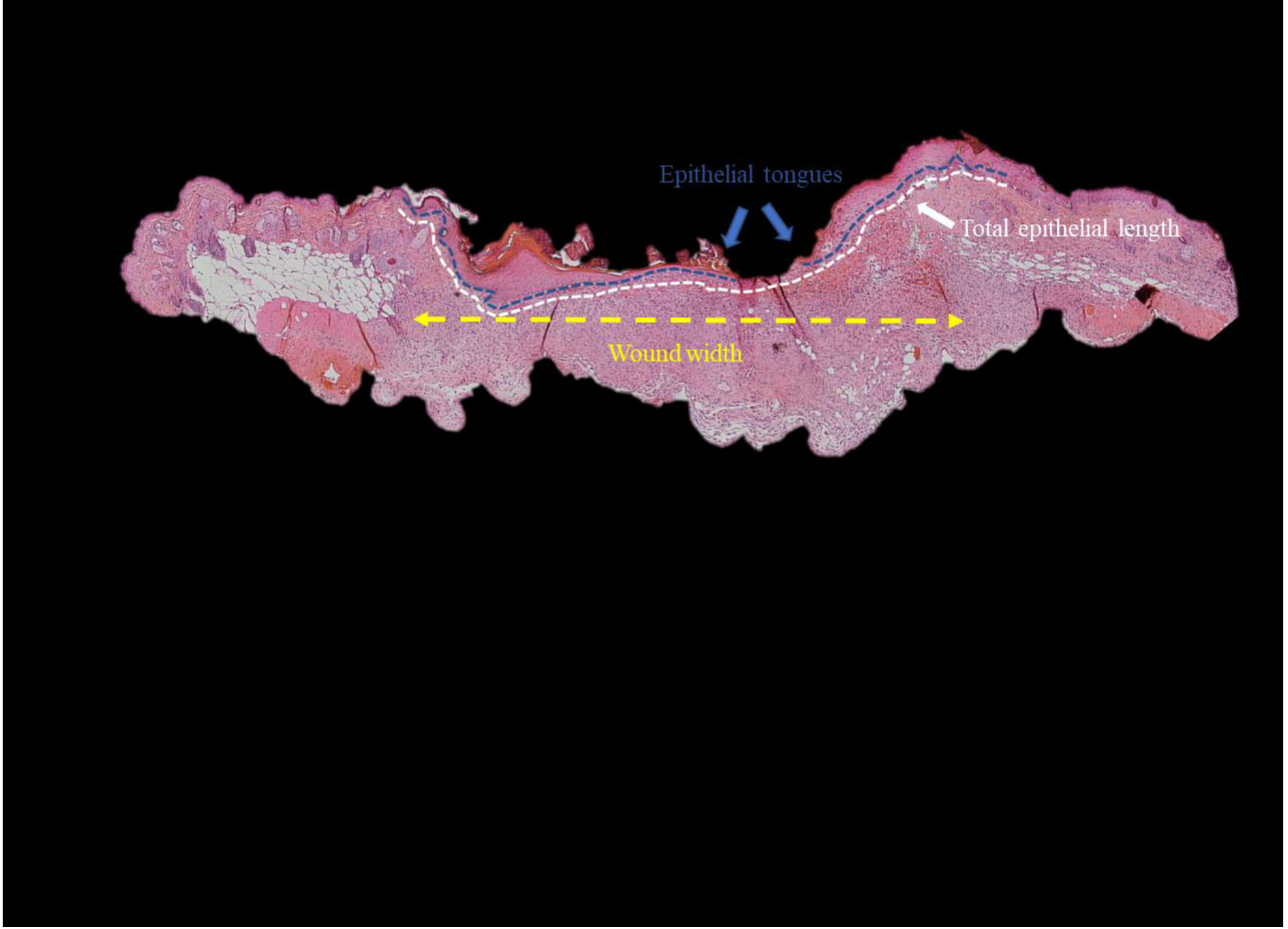
Real-time monitoring of labelled antibodies localization was determined using IVIS Lumina S5 Imaging System (PerkinElmer, Massachusetts, USA) on days 0, 1, 2, 3, 4, and 7. Fluorescence radiance efficiency (p/sec/cm^2/sr) / (μW/ cm^2) was calculated in the burn region in FnAbs treated and IgG treated mice (Figure 2.8).



Figure 2. 8: Fluorescence *in vivo* imaging and analysis by IVIS Lumina S5 Imaging System

2.5.3 Histology and immunohistochemistry measurement/analysis

The histological features of wounds were identified using digital images of stained sections. Histological features were identified manually and quantified using image analysis software (Image Pro Plus, version 7.0; Media Cybernetics, MD, USA). The stained sections were assessed for the percentage of the re-epithelialisation and dermal wound width. The percentage of re-epithelialisation was measured as the percentage of the total wound length covered with migrating tongues of the neoepidermis. Dermal wound width was calculated by measuring the portion between the left and right wound edges where the first hair follicle was observed (Figure 2.9).
Immunohistochemistry analyses were conducted using CellSens Microscope Imaging Software (Olympus, Tokyo, Japan) following capturing images via Olympus IX81 microscope. The number of positively stained cells for F4/80 (as a marker for macrophages), YM-1 (as a marker for chitinase-like protein 3 expressed in M2 macrophages), αSMA (as a marker for alpha smooth muscle actin), CD31(as a marker for endothelial cells), and NIMP-R14 (as a marker for neutrophils) were quantified for the whole wound bed and data presented as positive cells/area mm^2. CD31/αSMA dual positive cells in blood vessel structures were counted to measure blood vessel density as a function of area and data presented as vessels/mm^2. Fluorescence intensity was quantified to measure the amount of Flii, VEGF, FGF-2, and PDGF-BB within the wound area (Figure 2.10). In the analysis of the skin wound sections, measurements were taken throughout the entire wound area, including the depth underneath the epithelium. The entire wound bed was encompassed in the analysis, ensuring a comprehensive assessment of the wound healing process and related changes. The fluorescence intensity was automatically measured by the software as a single gray intensity value which was the mean intensity values of each pixel within the wound bed.


Epithelial tongues
Total epithelial length
Wound width

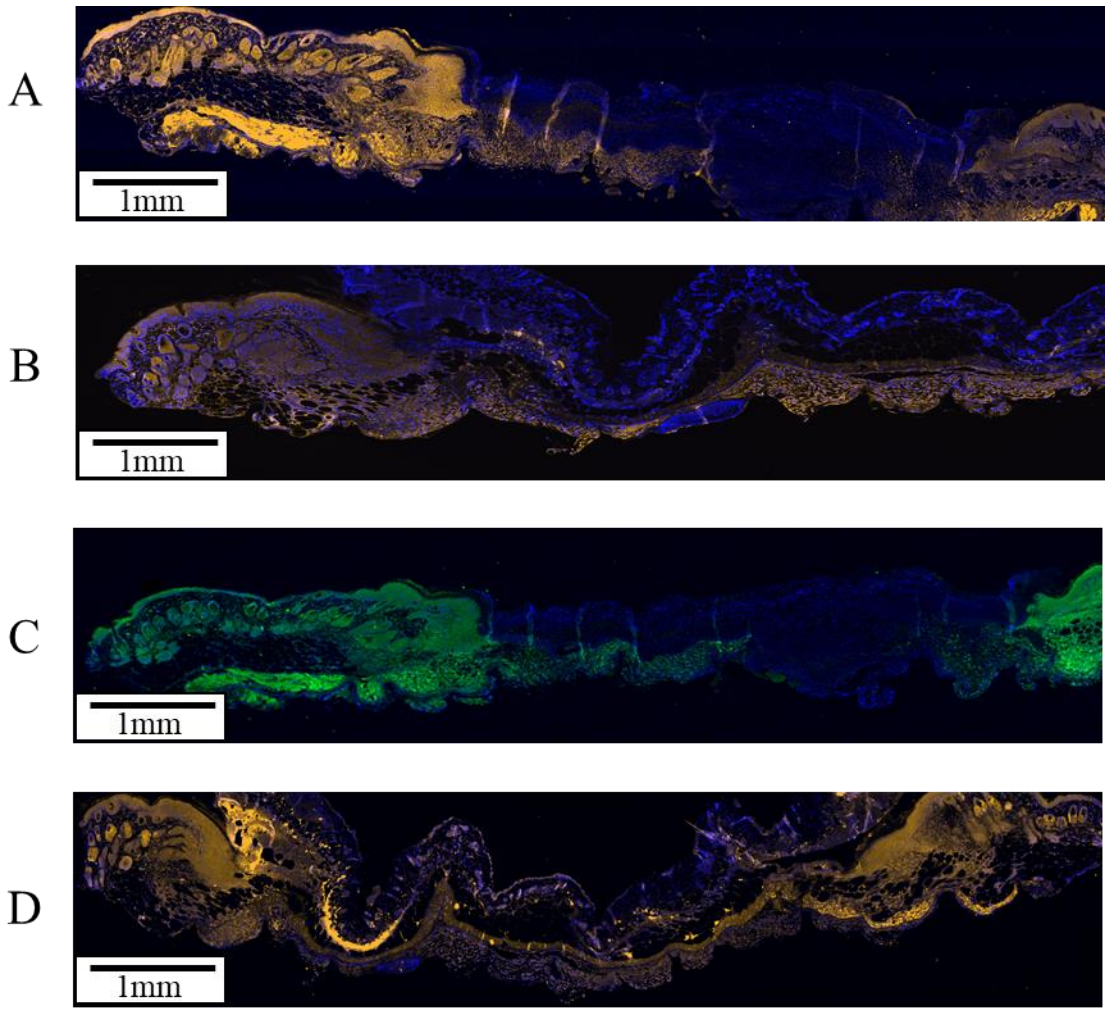


Figure 2. 10: Fluorescent immunohistochemical staining

A) Flii antibody (stained yellow) B) FGF-2 antibody (stained yellow) C) VEGF antibody (stained green) D) PDGF-BB antibody (stained yellow). DAPI nuclear counterstain (pseudo stained blue).

2.6 Preparation of protein lysates

T-per protein extraction reagent (Thermo Fisher Scientific, VIC, Australia) was employed to efficiently obtain tissue lysate from burn wound samples. Tissue samples were homogenized in 1:20 T-per reagent using MoBio BeadMill tubes (Ceramic Bead Tubes, MoBio, CA, USA) placing in the Bullet Blender Storm (Next Advance, NY, USA). In order to pellet tissue debris, the lysate was centrifuged at 14,000 x g for 15 minutes at 4°C. The supernatants were then transferred into new tubes and the total amount of protein was quantified by NanoDrop Lite Spectrophotometer (Thermo Fisher Scientific, VIC, Australia).

2.7 ELISA

The concentration of transforming growth factor beta 1 (TGF-β1) in burn tissue was measured using enzyme-linked immunosorbent assay (ELISA, BioLegend, CA, USA) based on the manufacturer's protocol (LEGEND MAX™ Free Active TGF-β1 ELISA Kit # 437707). The TGF-β1 96-well strip plate was already pre-coated with a mouse monoclonal anti-human free active TGF-β1 antibody. The diluted tissue samples and standards were transferred to appropriate wells in triplicate. The plate was incubated at room temperature for 2 hours while shaking. The plate was then washed, and detection antibody solution was added to each well, followed by incubation at room temperature for 1 hour while shaking. Avidin-HRP D solution was transferred to each well to bind biotin with high affinity and the plate was incubated at room temperature for 30 minutes while shaking. The stop solution was added to each well to stop the reaction and the absorbance was measured at 450 nm on a plate reader (Tecan Group, Mannedorf, Switzerland) to quantify the amount of TGF-β1 as pg/mg of total protein in burn wound tissues.

2.8 Statistical analysis

Power studies were performed using the G Power 3.1.7 statistics package. For animal studies, a reduction in surface area of 20% or more was anticipated to be considered biologically significant (Masson-Meyers *et al*., 2020). Power calculations demonstrated that a sample size of six (for excisional wound healing model) and ten (for the burn mouse model) would give 90% power using a 5% test level and a one-tailed test. Six and ten treatment group were used for the excisional wound healing model and burn mouse model respectively. GraphPad Prism Software (Graphpad, CA, USA) was employed to perform all statistical analysis. For *in vitro* analyses, statistical differences between treatment groups were calculated using a two-way ANOVA with multiple comparisons. Tukey's multiple comparison tests were also employed as post-tests in the statistical analysis of *in vitro* results. For macroscopic comparisons between FnAbs treated and control wounds, statistical differences were determined using a two-way ANOVA with multiple comparisons. For histological and immunohistochemical comparisons between FnAb treated and control wounds, statistical differences were determined using a one-way ANOVA with multiple comparisons. The experiments and the quantitative values were performed three times for *in vitro* studies. Any p-value of < 0.05 was considered significant for all analyses. All data are presented as the mean ± standard error of the mean (SEM), which quantifies the precision of the mean estimate relative to the population mean.

Chapter 3: The impact of LRRFnAb and MFnAb on the function of human skin cells

3.1 Introduction

Fibroblasts and keratinocytes play key roles in the restoration of the barrier function of the skin (Werner *et al*., 2007). Fibroblasts play an important part in breaking down the fibrin clot, producing extracellular matrix, collagen stability to support cells involved in wound contraction and wound repair (Bainbridge, 2013). Keratinocytes cover dermal wounds and create an epithelial barrier (Wang and Graves, 2020). Keratinocytes also secrete several factors to improve re-epithelialization and preserve connective tissue via a complex of mediators that enhance angiogenesis and creation of connective tissue matrix (Wang and Graves, 2020). Angiogenesis is essential for wound healing as it provides new capillaries that are crucial for the formation of granulation tissue (Demidova-Rice *et al*., 2012). In the process of angiogenesis, endothelial cells proliferate and migrate to establish vascular labyrinths that undergo maturation and remodelling to create mature blood capillaries (Wang *et al*., 2008).

Flightless I (Flii) is an actin-binding member of the gelsolin family of cytoskeletal proteins that regulate actin (Claudianos and Campbell, 1995). Flii has been found to be involved in numerous biological processes including those in wound healing (Strudwick and Cowin, 2020). Investigations have revealed that Flii impacts cellular proliferation, inflammation, and cytokine production (Li *et al*., 2008). Studies have shown that Flii is upregulated in wounds, and it inhibits cellular processes including cell migration, proliferation, and adhesion (Cowin *et al*., 2007). Overexpression of Flii has been reported to delay the migration of fibroblasts and keratinocytes which are crucial during wound repair (Cowin *et al*., 2007; Kopecki *et al*., 2009). Studies have demonstrated that attenuating the level of Flii can result in improved wound repair and reduced scar formation (Cameron *et al*., 2016). Reducing the level of Flii using monoclonal antibodies against specific domains of Flii has been investigated in different studies and shown to be a promising approach to inhibit the negative effect of Flii on wound healing (Cowin *et al*., 2007; Jackson *et al*., 2012). Flii is a highly conserved protein across species and has a specific structure with 6 gelsolin domains and also an additional 11 tandem repeats of a 23-amino acid Leucine-Rich Repeat (LRR) motif not observed in other family members (Kobe and Kajava, 2001). Previous studies focused on Flightless I neutralizing antibody (FnAb) which binds to a specific region of the LRR domain of Flii showing that these antibodies have wound healing properties (Jackson *et al*., 2012). The first generation of FnAbs (FliiL FnAb) have been found to increase both

proliferation and migration of cultured keratinocytes and fibroblast *in vitro* (Cowin *et al*., 2007). In addition, treatment of cultured human endothelial cells with FliiL FnAbs led to increased capillary tube formation (Ruzehaji *et al*., 2014).

As previously discussed in Chapter 1, Flii consists of an LRR+ gelsolin domain which is involved in several cellular functions which are critical for wound healing. The LRR domain of Flii enables its effects on cellular apoptosis, TLR4 signalling, and hormone-independent transcriptional regulation (Strudwick and Cowin, 2020). The gelsolin domain of Flii also plays important roles in transcriptional regulation, inflammatory signalling complexes, and regulation of caspase-1 induced cell death (Strudwick and Cowin, 2020).

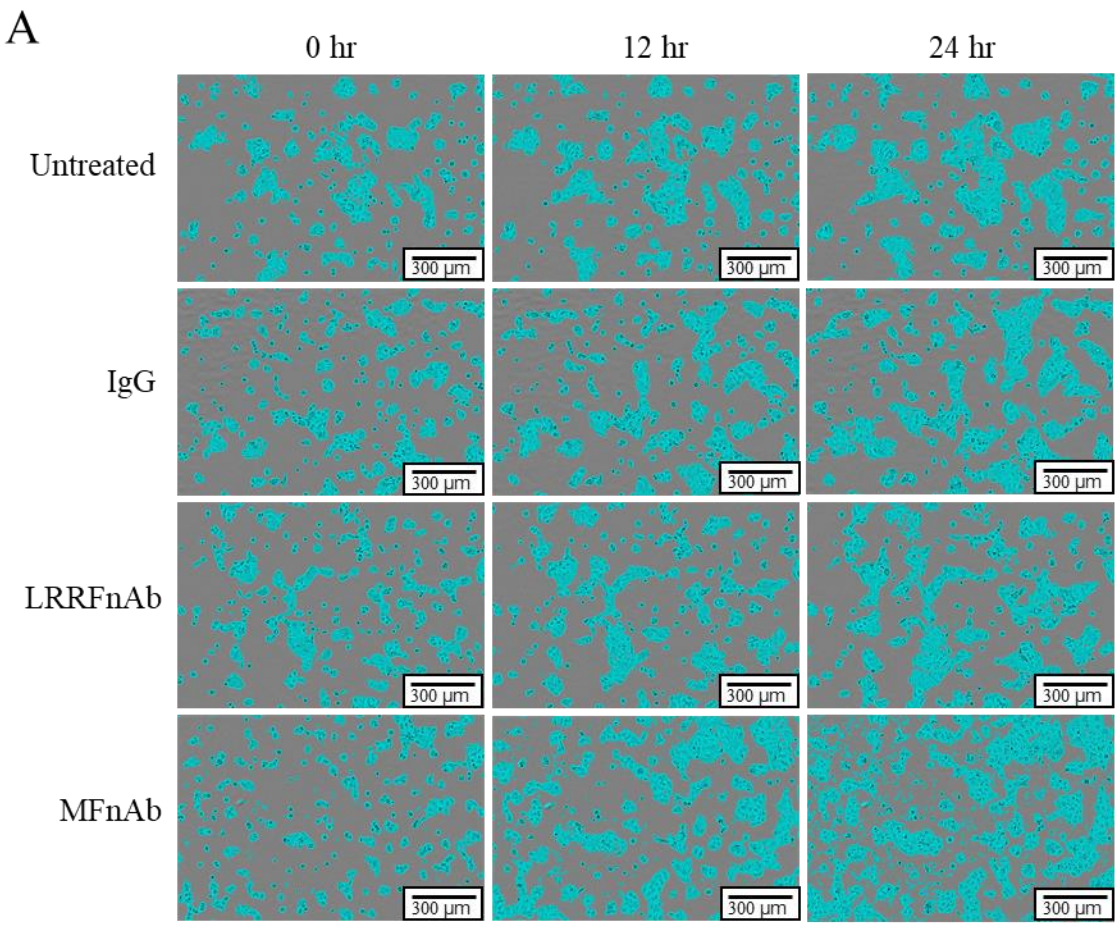
The new generation of FnAbs including LRRFnAb and MFnAb differ from the first version as they bind to a larger portion of Flii protein. These two monoclonal antibodies are generated against LRR domain (LRRFnAb) and middle domain of Flii (MFnAb). The first generation FnAb was designed to target a specific antigen located at the LRR domain of the Flii protein. However, due to its short sequence of only twelve amino acids, the original antibody exhibited limited specificity. In contrast, the new generation of FnAbs employs a mechanism involving induced conformational changes in the protein structure, resulting in improved specificity and enhanced binding affinity. These antibodies effectively bind to their target, thereby obstructing normal protein functions.

The aim of this study was to assess and compare the effect of different FnAbs including MFnAbs and LRRFnAbs that are raised against the LRR and middle domains of Flii protein on cutaneous cells involved in the wound repair process. The impact of these antibodies on the proliferation and migration of keratinocytes and fibroblasts was investigated using proliferation and scratch wound closure assays, respectively. The effect of LRRFnAb and MFnAb on the proliferation and migration of human dermal endothelial cells was also determined. Finally, a Matrigel tube assay was employed to investigate the effect of different antibodies raised against different regions of Flii on angiogenesis.

3.2 Results

3.2.1 MFnAbs improved the proliferation of keratinocytes

The effect of MFnAbs and LRRFnAbs on proliferation of keratinocytes were evaluated using the IncuCyte Live-Cell Imaging System following established protocols as described in Chapter 2. For this purpose, HaCaTs (5×10^3) were incubated in appropriate cell culture media for 24 hours. The media was then replaced with media containing either LRRFnAb or MFnAb (50 μg/ml) and cells were incubated for 24 hours. The standard media and media containing IgG (50 μg/ml) were included as negative controls for the proliferation assessment of keratinocytes treated with LRRFnAbs and MFnAbs (Figure 3.1A). Findings showed that the proliferation of keratinocytes treated with LRRFnAbs was not increased in comparison with cells treated with standard medium and IgG treated cells at each time point of the study (Figure 3.1B). As shown in Figure 3.1B, following 24 hours incubation, the proliferation of HaCaTs was significantly improved after 12 hours of treatment with MFnAb in comparison with untreated cells and cells treated with IgG (Figure 3.1B).


A
0 hr
12 hr
24 hr
Untreated
IgG
LRRFnAb
MFnAb
300 µm

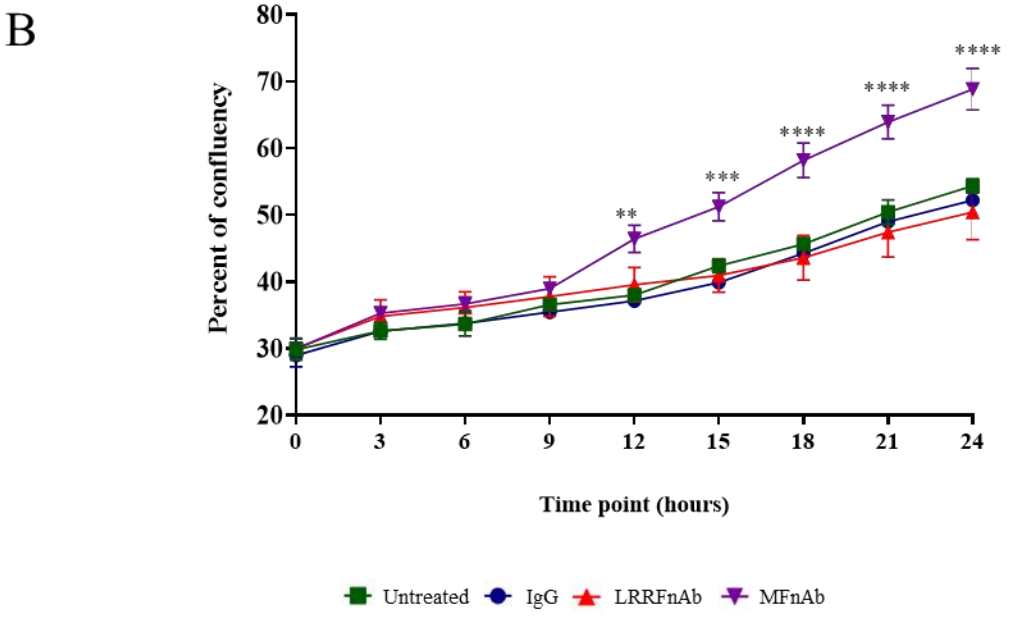
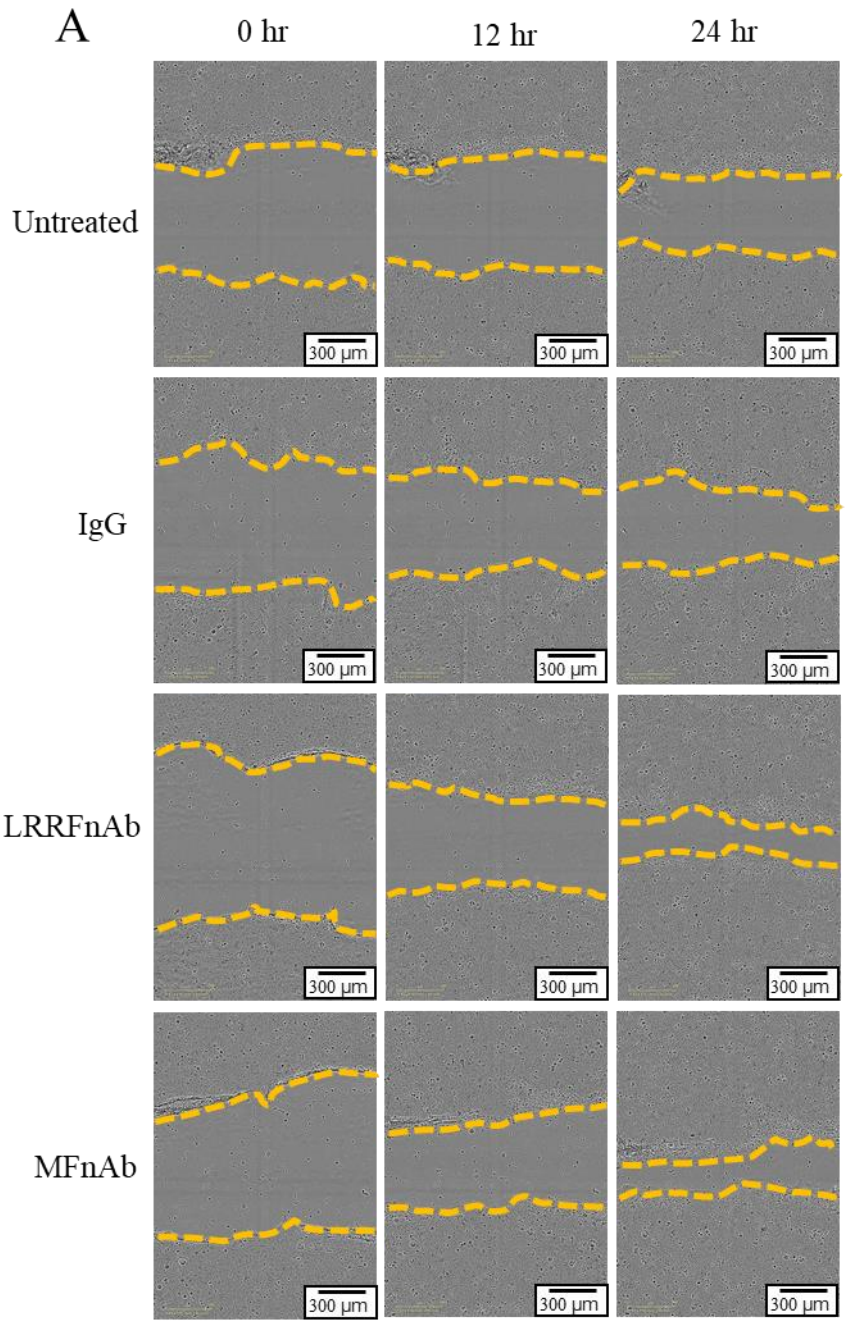

B
Percent of confluency
Time point (hours)
80
70
60
50
40
30
20
0
3
6
9
12
15
18
21
24
**
***
****
****
****
Untreated
IgG
LRRFnAb
MFnAb

Figure 3. 1: Effect of LRRFnAb and MFnAb on the proliferation of keratinocytes

A) Representative images of untreated, IgG (50 μg/ml) treated, LRRFnAb (50 μg/ml) treated, and MFnAb (50 μg/ml) treated keratinocytes at 0, 12, and 24 hours. The cells (blue) are demonstrated with a confluency mask provided by Incucyte zoom software. B) Effect of LRRFnAb and MFnAb on the proliferation of keratinocytes indicating a significant increase in the proliferation of MFnAb treated cells compared to the controls. n = 6. All data are represented as mean ± SEM of 3 independent experiments. Statistical significance was calculated by two-way ANOVA and Tukey's post-tests. **= $p < 0.01$, *** = $p < 0.001$, **** = $p < 0.0001$.

3.2.2 LRRFnAbs and MFnAbs increased the migration of keratinocytes

The migration of keratinocytes was assessed using a wound maker in the IncuCyte Live-Cell Imaging System following established protocols as detailed in Chapter 2. HaCaTs were cultured in standard culture media and the cells were scratched using a Wound Maker™ once they were fully confluent. The media was then removed and LRRFnAb and MFnAb (50 μg/ml) media was added to the cells. The change in the wound width between the two margins of the scratch over time was calculated and normalized to the initial scratch width created at time 0 (Figure 3.2A). The migration of HaCaTs was significantly elevated following 9 hours of treatment with LRRFnAb compared to untreated and IgG treated cells (Figure 3.2B). The migratory ability of cells was significantly increased after 15 hours of treatment with MFnAb in comparison with untreated cells and cells treated with control antibody (Figure 3.2B).


A
0 hr
12 hr
24 hr
Untreated
IgG
LRRFnAb
MFnAb
300 µm

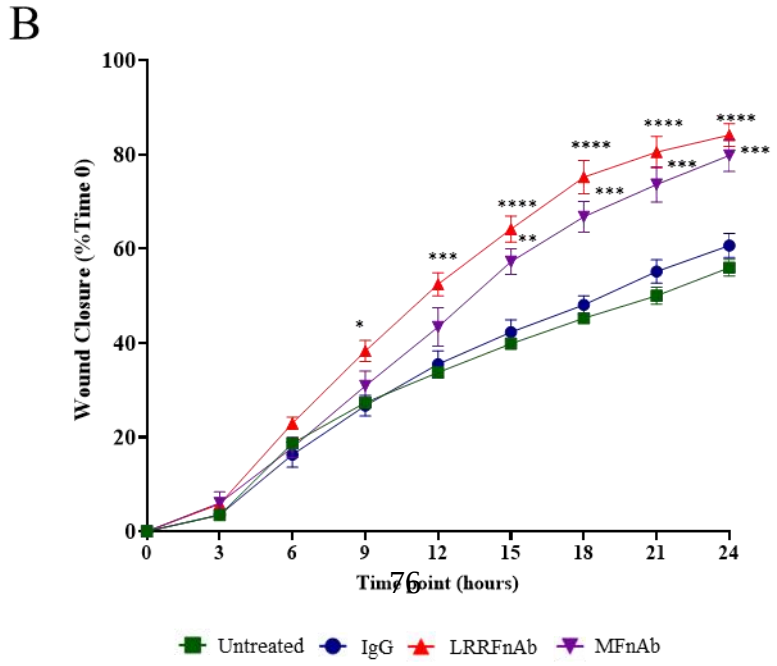
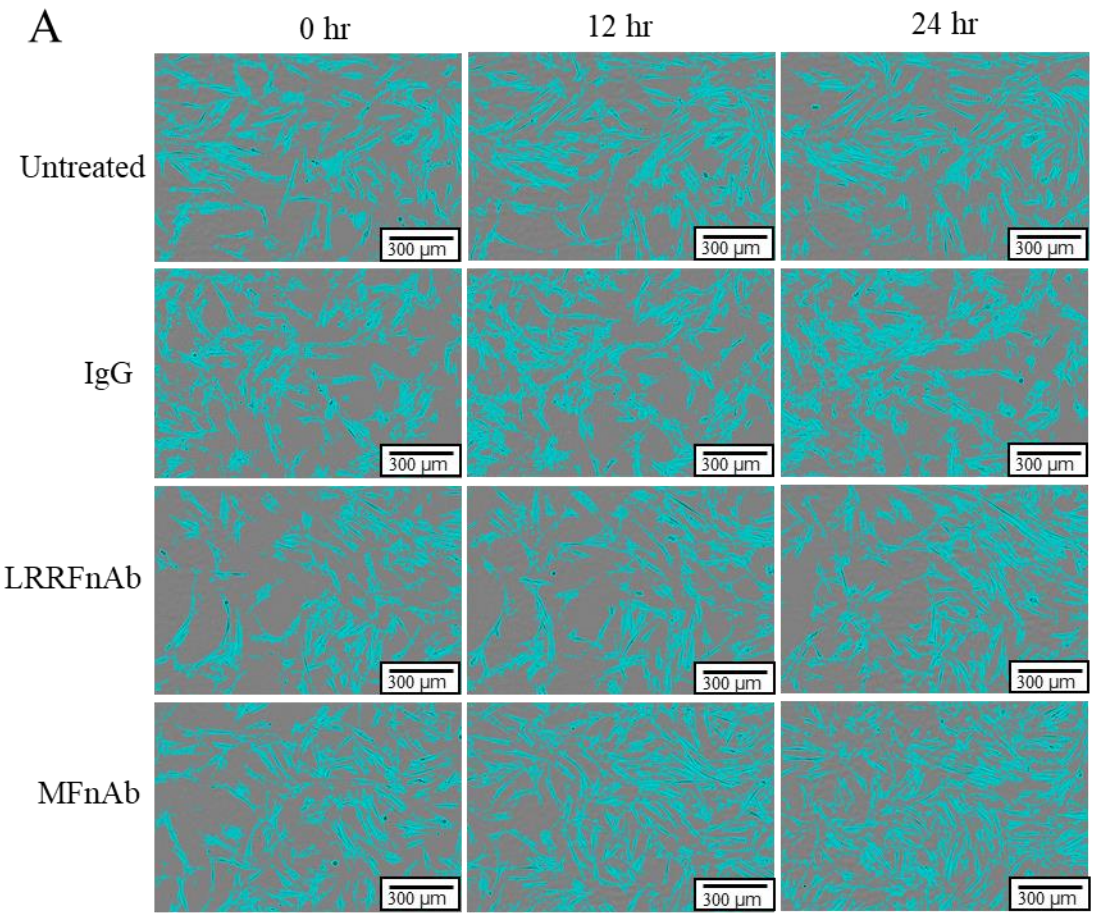

B
Wound Closure (% Time 0)
Time point (hours)
Untreated
IgG
LRRFnAb
MFnAb

Figure 3. 2: Effect of LRRFnAb and MFnAb on the migration of keratinocytes

A) Representative images of untreated, IgG (50 μg/ml) treated, LRRFnAb (50 μg/ml) treated, and MFnAb (50 μg/ml) treated keratinocyte scratch wounds at 0, 12, and 24 hours. Images show the confluency in the wound area 24 hours following making scratches, compared to the initial cell confluency. The migration was measured using Incucyte zoom software. B) Effect of LRRFnAb and MFnAb on the migration ability of keratinocytes indicating a significant increase in the migration of LRRFnAb and MFnAb treated cells compared to the controls. n = 6. All data are represented as mean ± SEM of 3 independent experiments. Statistical significance was calculated by two-way ANOVA and Tukey's post-tests. *= $p < 0.05$, **= $p < 0.01$, *** = $p < 0.001$, **** = $p < 0.0001$.

3.2.3 MFnAbs improved the proliferation of fibroblasts

In order to investigate the impact of LRRFnAb and MFnAb on the proliferation of fibroblasts, HFFs (5×10^3) were cultured in standard culture condition for 24 hours. The media was then replaced with media containing either LRRFnAb or MFnAb (50 μg/ml), standard media, and media containing IgG (50 μg/ml). HFFs were incubated for 24 hours, and the proliferation of fibroblasts was assessed following established protocols as described in chapter 2 (Figure 3.3A). Results indicated that the proliferation of fibroblasts treated with LRRFnAb was not improved compared to untreated and IgG-treated cells at each time point of the study (Figure 3.3B). In contrast, the proliferative ability of fibroblasts was significantly increased following 18 hours of treatment with MFnAb compared to HFFs treated with normal media and IgG (Figure 3.3B).


A
0 hr
12 hr
24 hr
Untreated
IgG
LRRFnAb
MFnAb
300 µm

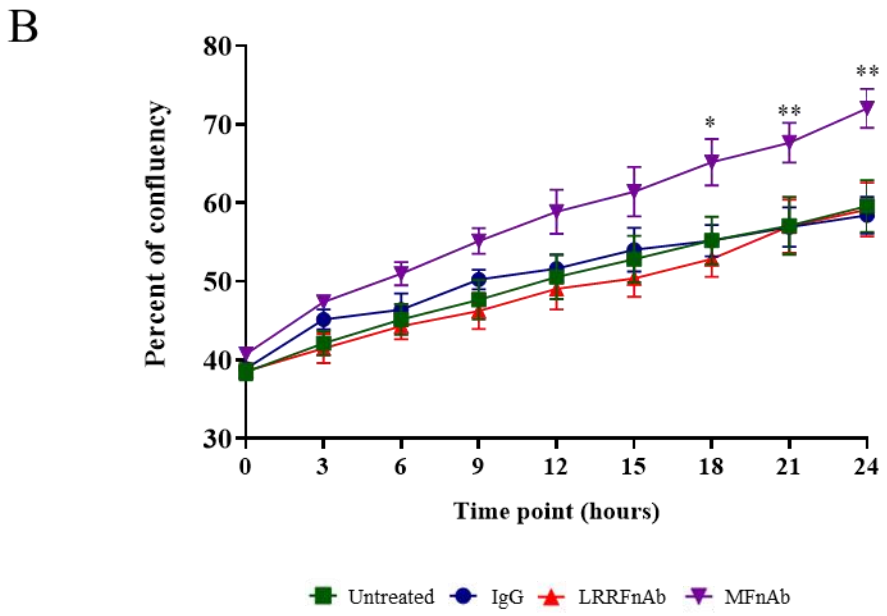
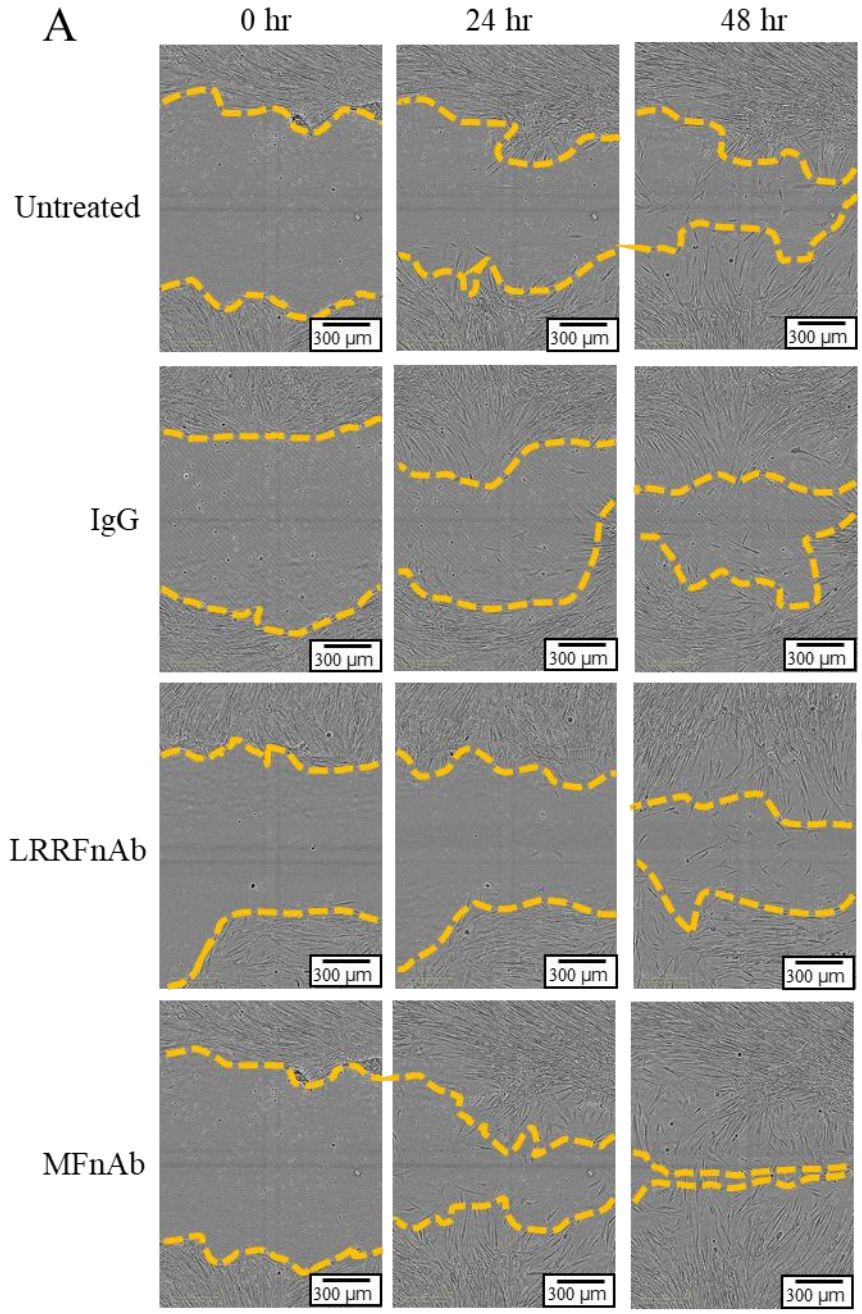

B
Percent of confluency
80
70
60
50
40
30
0
3
6
9
12
15
18
21
24
Time point (hours)
*
**
**
Untreated
IgG
LRRFnAb
MFnAb

Figure 3. 3: Effect of LRRFnAb and MFnAb on the proliferation of fibroblasts

A) Representative images of untreated, IgG treated (50 μg/ml), LRRFnAb (50 μg/ml) treated, and MFnAb (50 μg/ml) treated fibroblasts at 0, 12, and 24 hours. The cells (blue) are demonstrated with a confluency mask provided by Incucyte zoom software. B) Effect of LRRFnAb and MFnAb on the proliferation of fibroblasts indicating a significant increase in the proliferation of MFnAb treated cells compared to the control. n = 6. All data are represented as mean ± SEM of 3 independent experiments. Statistical significance was calculated by two-way ANOVA and Tukey's post-tests. *= $p < 0.05$, **= $p < 0.01$.

3.2.4 MFnAbs improved the migration of fibroblasts

The effect of LRRFnAb and MFnAb on the migration of fibroblasts was explored using a scratch wound closure assay. For this purpose, HFFs were cultured, and scratch wounds were created using a Wound Maker™ at 90% confluency. Immediately after scratching, the HFFs were treated with normal media, LRRFnAb (50 µg/ml), MFnAb (50 µg/ml), and IgG (50 µg/ml). The cells were monitored every 3 hours until 48 hours using Incucyte (Essen bioscience, USA) (Figure 3.4A). The results demonstrated that the migratory ability of LRRFnAb treated cells was not improved compared to cells treated with normal media and IgG treated HFFs (Figure 3.4B). My findings showed that migration of HFFs treated with MFnAb was significantly elevated from 18 hours of treatment with MFnAb in comparison with cells treated with normal media and IgG treated fibroblasts (Figure 3.4B).


A
0 hr
24 hr
48 hr
Untreated
IgG
LRRFnAb
MFnAb
300 µm

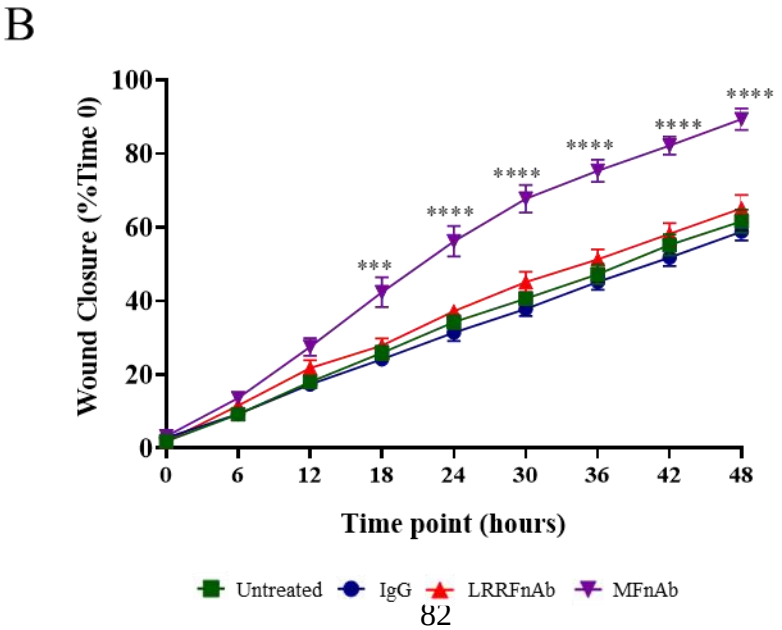

B
Wound Closure (%Time 0)
Time point (hours)
0
20
40
60
80
100
0
6
12
18
24
30
36
42
48
***
****
Untreated
IgG
LRRFnAb
MFnAb

Figure 3. 4: Effect of LRRFnAb and MFnAb on the migration of fibroblasts

A) Representative images of untreated, IgG treated (50 μg/ml), LRRFnAb (50 μg/ml) treated, and MFnAb (50 μg/ml) treated fibroblast scratch wounds at 0, 24, and 48 hours. Images show the confluency in the wound area 48 hours following making scratches, compared to the initial cell confluency. The cell confluency was measured using Incucyte zoom software. B) Effect of LRRFnAb and MFnAb on the migration ability of fibroblasts indicating a significant increase in the migration of MFnAb treated cells compared to the controls. n = 6. All data are represented as mean ± SEM of 3 independent experiments. Statistical significance was calculated by two-way ANOVA and Tukey's post-tests. *** = $p < 0.001$, **** = $p < 0.0001$.

3.2.5 LRRFnAb improved the proliferation of dermal endothelial cells

To investigate the impact of LRRFnAb and MFnAb on the proliferative ability of human dermal endothelial cells, HMDECs (5×10^3) were cultured in standard media for 24 hours. The cells were then treated with FnAbs (50 μg/ml), normal media, and IgG (50 μg/ml). The cells were incubated for 24 hours and the proliferation of HMDECs were assessed using the IncuCyte Live-Cell Imaging System (Figure 3.5A). HMDECs treated with LRRFnAb showed increased confluency at all time points which was significant from 9 hours onwards in comparison with cells treated with normal media and IgG (Figure 3.5B). In contrast, the result indicated that the proliferative ability of HMDECs treated with MFnAb was not improved compared to control groups at each time point of the study (Figure 3.5B).

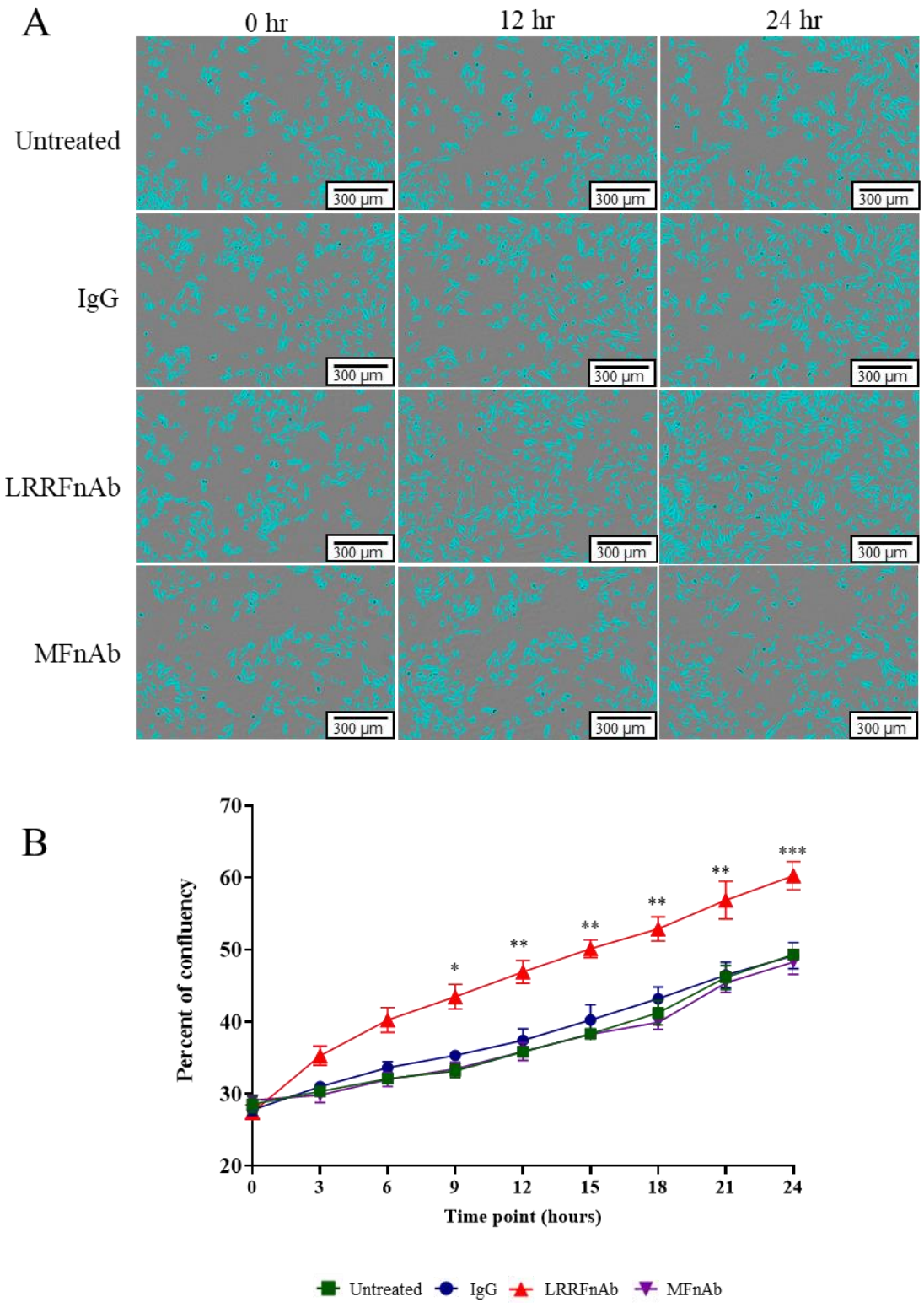
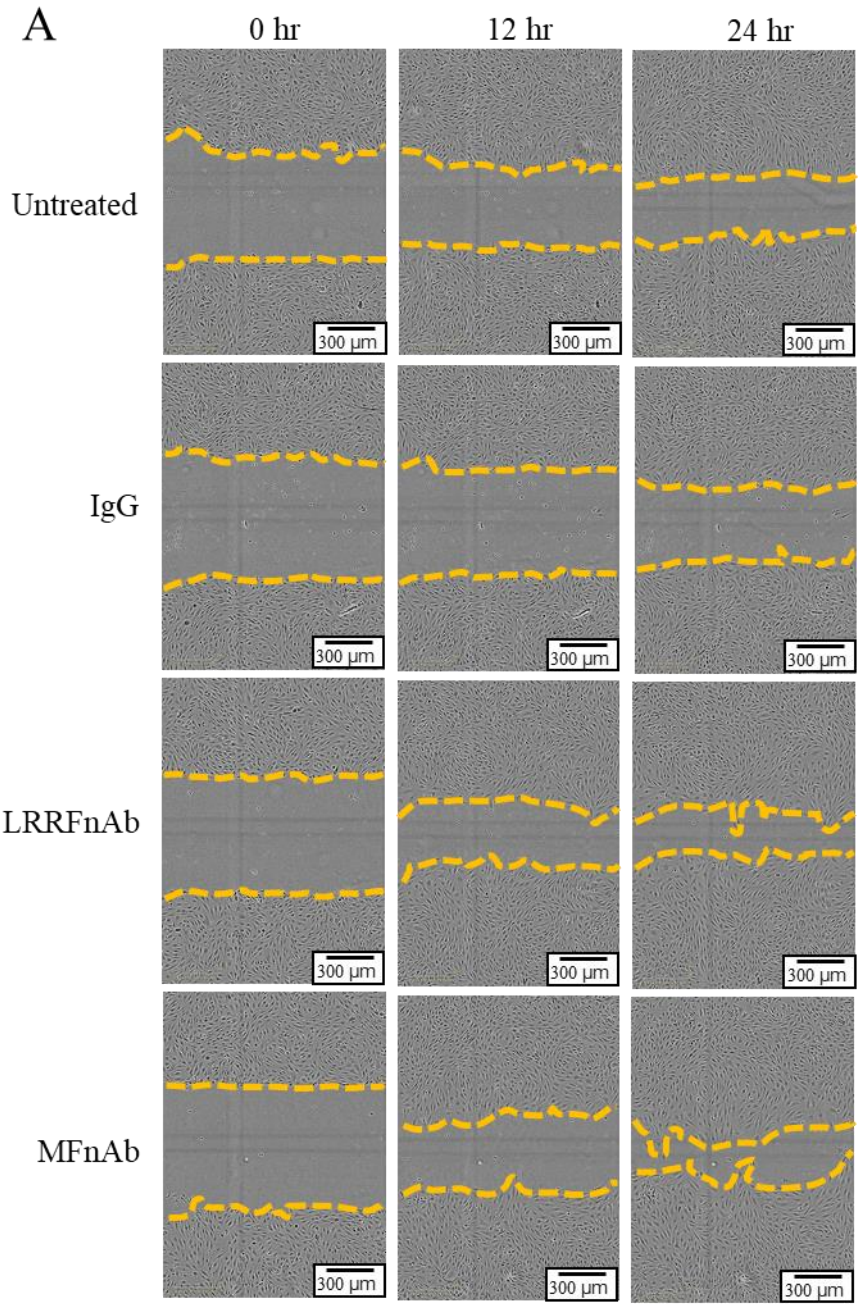

A
0 hr
12 hr
24 hr
Untreated
IgG
LRRFnAb
MFnAb
300 µm
B
Percent of confluency
Time point (hours)
Untreated
IgG
LRRFnAb
MFnAb

Figure 3. 5: Effect of LRRFnAb and MFnAb on the proliferation of endothelial cells

A) Representative images of untreated, IgG (50 μg/ml) treated, LRRFnAb (50 μg/ml) treated, and MFnAb (50 μg/ml) treated endothelial cells at 0, 12, and 24 hours. The cells are demonstrated with a confluency mask provided by Incucyte zoom software. B) Effect of LRRFnAb and MFnAb on the proliferation of endothelial cells indicating a significant increase in confluency of LRRFnAb treated cells compared to the control. n = 6. All data are represented as mean ± SEM of 3 independent experiments. Statistical significance was calculated by two-way ANOVA and Tukey's post-tests. *= $p < 0.05$, **= $p < 0.01$, *** = $p < 0.001$.

3.2.6 LRRFnAb and MFnAb improved the migration of dermal endothelial cells

In order to explore the effect of LRRFnAb and MFnAb on the migratory ability of dermal endothelial cells, HMDECs were grown to confluence in monolayers. The cells were then scratched using a Wound Maker™. The cells were treated with LRRFnAb (50 μg/ml), MFnAb (50 μg/ml), normal media, and IgG (50 μg/ml) immediately after scratching. The HMDECs were then monitored following established protocols in Chapter 2 (Figure 3.6A). The assessment revealed that the migration of HMDECs was elevated after 12 hours of treatment with FnAbs including LRRFnAb and MFnAb compared to untreated cells and HMDECs treated with control antibody (Figure 3.6B).


A
0 hr
12 hr
24 hr
Untreated
IgG
LRRFnAb
MFnAb
300 µm

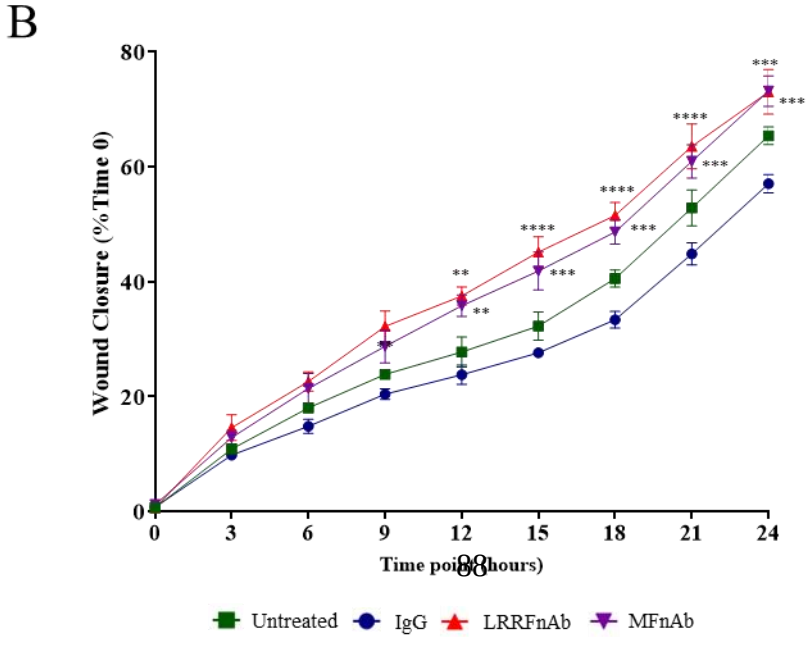

B
Wound Closure (%Time 0)
Time point (hours)
0
20
40
60
80
0
3
6
9
12
15
18
21
24
**
****
***
Untreated
IgG
LRRFnAb
MFnAb

Figure 3. 6: Effect of LRRFnAb and MFnAb on the migration of endothelial cells

A) Representative images of untreated, IgG (50 μg/ml) treated, LRRFnAb (50 μg/ml) treated, and MFnAb (50 μg/ml) treated endothelial cells scratch wounds at 0, 12, and 24 hours. Images illustrate the confluency in the wound area 24 hours following making scratches, compared to the initial cell confluency. The cell confluency was measured using Incucyte zoom software. B) Effect of LRRFnAb and MFnAb on the migratory ability of endothelial cells indicating a significant increase in the migration of LRRFnAb and MFnAb treated cells compared to the control. n = 6. All data are represented as mean ± SEM of 3 independent experiments. Statistical significance was calculated by two-way ANOVA and Tukey's post-tests. **= $p < 0.01$, *** = $p < 0.001$, **** = $p < 0.0001$.

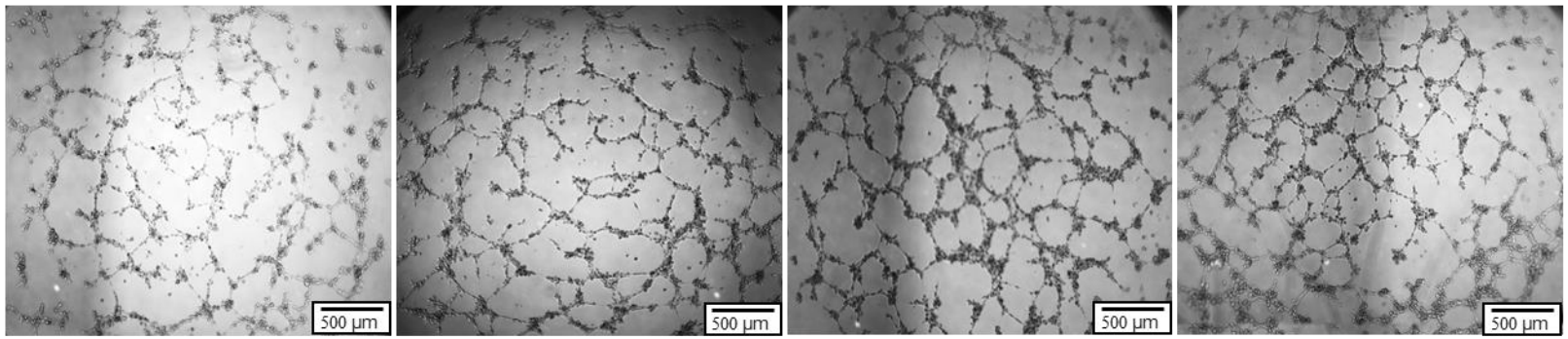
3.2.7 LRRFnAb and MFnAb stimulated tube formation of endothelial cells and increased half-life of formed capillaries

An *in vitro* Matrigel tube formation assay was conducted to investigate the possible effect of LRRFnAb and MFnAb on angiogenesis. A consistent density of HMDECs (1.5×10^4) was suspended in control media, media containing either IgG, LRRFnAb or MFnAb. The cells were then seeded in wells containing Matrigel and were imaged every 3 hours following seeding (Figure 3.7A).

Media containing LRRFnAb and MFnAb significantly accelerated the average number of tubes in comparison with the controls at each time point over the time of the experiment. Specifically, the maximum number of blood vessel-like structures was achieved 6 hours following seeding in LRRFnAb treated cells and was significantly increased compared to both IgG+ media controls. Addition of MFnAb promoted the HMDECS to create significantly higher number of tubes compared to control treated cells incubated in normal and IgG media. The cultured endothelial cells treated with MFnAb formed the maximum number of blood vessel-like structures 9 hours following seeding and these structures exhibited improved stability and degraded more slowly. The average number of tubes was also significantly increased in HMDECs treated with MFnAb compared to LRRFnAb treated cells. This increase was significant at every time point over the course of the experiment. The HMDECs incubated in normal untreated media created the maximum number of tubes 3 hours after seeding and then plateaued to 9 h. The tube-like structures began to degrade 9 hours following seeding in normal treated media. HMDECs treated with IgG created their maximum number 3 hours following seeding cells prior to degradation. (Figure 3.7B). Among all the experimental groups experimented, the maximum number of tubes was achieved 9 hours post seeding when treated with MFnAb (Figure 3.7). The maximum number of capillary-like formations was also achieved 6 hours after seeding when treated with LRRFnAb. As shown in Figure 3.8A, pseudo vascular organization of endothelial cells was assessed using Image J Angiogenesis Analyse as described in Chapter 2. Nodes were identified as pixels that had at least 3 neighbours, corresponding to a bifurcation, while segments were detected as elements delimited by two junctions composed by several nodes. Master junctions were also detected as junctions linking at least three segments and meshes were areas enclosed by large segments. The assessment revealed that in all cases both LRRFnAb and MFnAb improved all parameters (Figure 3.8B-F).

Specifically, the number of nodes (Figure 3.8B), junctions (Figure 3.8C), and segments (Figure 3.8E) of HMDECs structure was significantly increased following 9 hours of treatment with LRRFnAb compared to cells treated with standard media and IgG (Figure 3.8B). The number of master junctions (Figure 3.8D) and meshes (Figure 3.8F) was significantly elevated after 9 hours of treatment with LRRFnAb compared to untreated endothelial cells. The assessments also indicated a trend towards an increase in the number of master junctions (Figure 3.8D) and meshes (Figure 3.8F), in LRRFnAb treated cells in comparison with cells treated with IgG (Figure 3.8B). These findings demonstrated that the number of nodes (Figure 3.8B), junctions (Figure 3.8C), master junctions (Figure 3.8D), segments (Figure 3.8E), and meshes (Figure 3.8F) of the vascular organization was significantly elevated after 9 hours of treatment with MFnAb in comparison with untreated cells and HMDECs treated with IgG.

A


Untreated
IgG
LRRFnAb
MFnAb
500 µm
500 µm
500 µm
500 µm

B

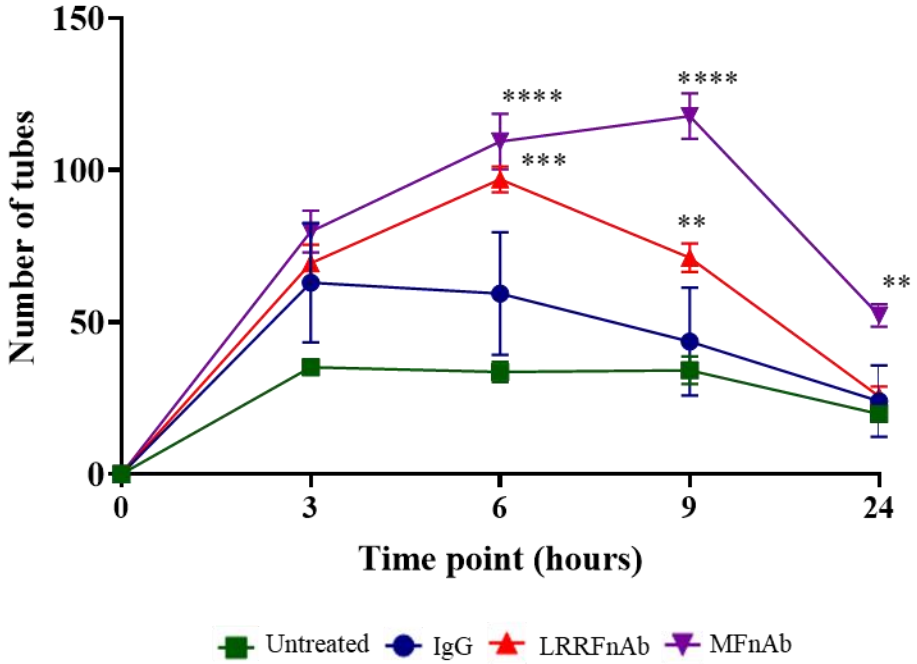
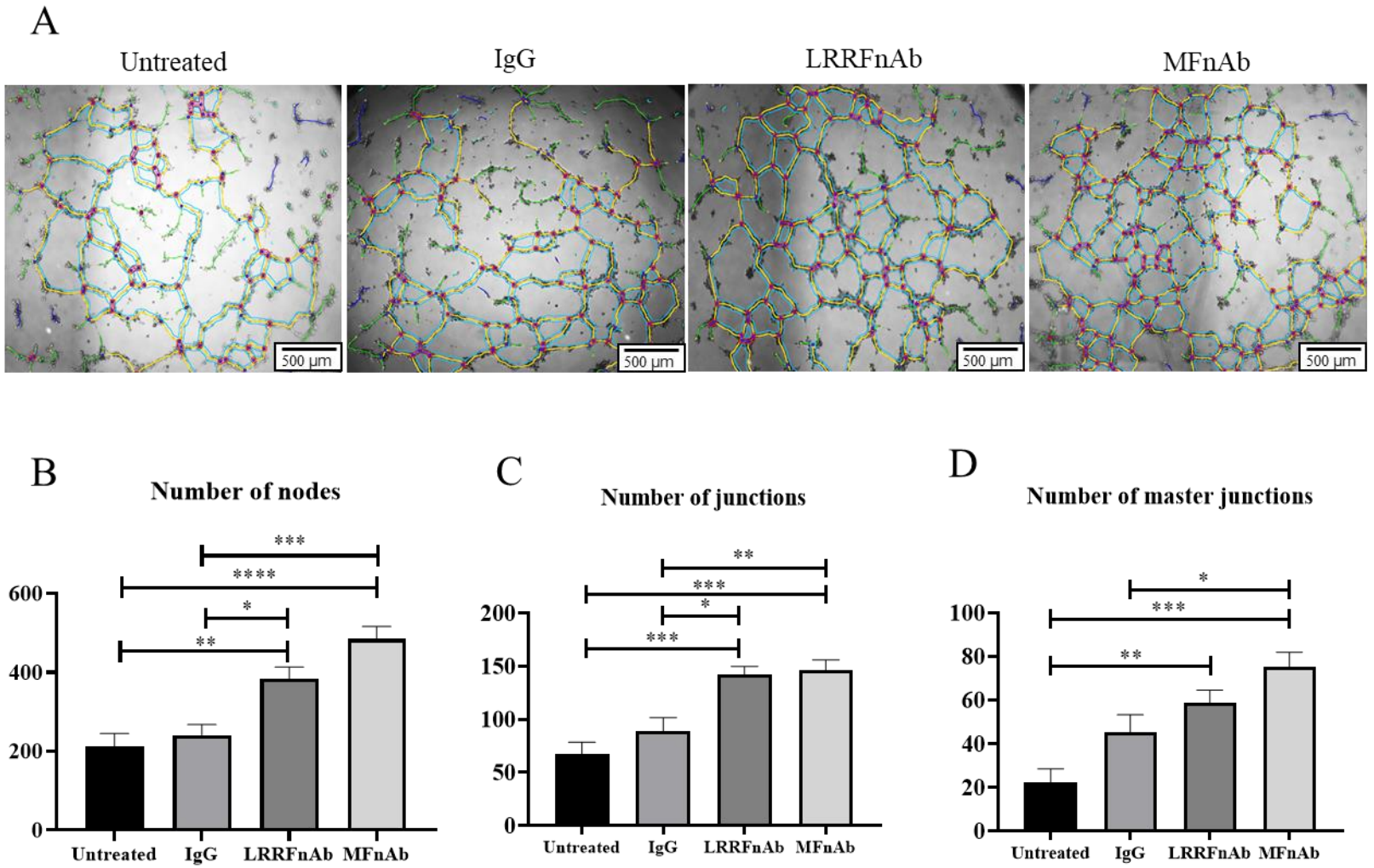

Number of tubes
150
100
50
0
0
3
6
9
24
Time point (hours)
****
****
***
**
**
Untreated
IgG
LRRFnAb
MFnAb

Figure 3. 7: Effect of LRRFnAb and MFnAb on angiogenesic tube formation

A) Representative images of untreated, IgG treated, LRRFnAb treated, and MFnAb treated endothelial cells in tube-like structures 9 hours after seeding onto Matrigel. B) Effect of LRRFnAb and MFnAb on endothelial cell sprouting in a Matrigel tube formation assay. n = 6. All data are represented as mean ± SEM of 3 independent experiments. Statistical significance was calculated by two-way ANOVA and Tukey's post-tests. **= $p < 0.01$, *** = $p < 0.001$, **** = $p < 0.0001$.


A
Untreated
IgG
LRRFnAb
MFnAb
500 μm
500 μm
500 μm
500 μm
B
Number of nodes
600
400
200
0
***
****
*
**
Untreated
IgG
LRRFnAb
MFnAb
C
Number of junctions
200
150
100
50
0
**
***
*
***
Untreated
IgG
LRRFnAb
MFnAb
D
Number of master junctions
100
80
60
40
20
0
*
***
**
Untreated
IgG
LRRFnAb
MFnAb

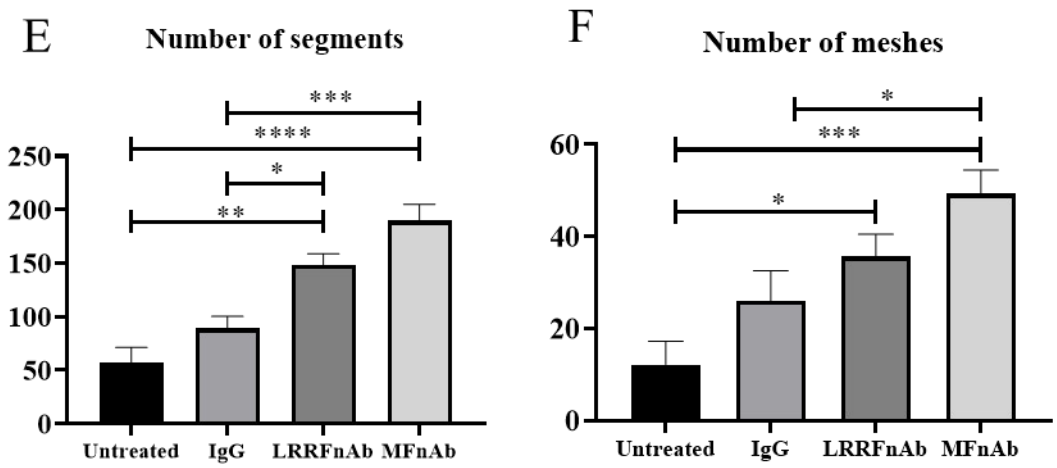


Figure 3. 8: Effect of LRRFnAb and MFnAb on vascular organization

A) Representative images of vascular organization of untreated, IgG treated, LRRFnAb treated, and MFnAb treated endothelial cells in tube-like structures 9 hours after seeding onto Matrigel. Vascular structures are shown by Angiogenesis Analyzer provided by Image J software. Effect of LRRFnAb and MFnAb on the number of nodes (B), junctions (C), master junctions (D), segments (E), and meshes (F) in a Matrigel tube formation assay. n = 6. All data are represented as mean ± SEM of 3 independent experiments. Statistical significance was calculated by two-way ANOVA and Tukey's post-tests. *= $p < 0.05$, **= $p < 0.01$, *** = $p < 0.001$, **** = $p < 0.0001$.

3.3 Discussion

Cutaneous wound healing is a complicated process that can be divided into overlapping phases including haemostasis, inflammation, re-epithelialization/proliferation, and remodelling (Martin, 1997). Multiple biological events including the function of fibroblasts and keratinocytes, expression of growth factors and cytokines, and production of the extracellular matrix are essential for the phases of wound repair (Shaw and Martin, 2009). Any failure to the shift of these phases can considerably delay normal wound healing and result in a chronic or nonhealing wound (Schultz *et al*., 2011; Willenborg *et al*., 2010).

The overlapping functions of keratinocytes including their proliferation and migration are crucial for re-epithelialization during wound healing (Raja *et al*., 2007). Furthermore, the interaction between keratinocytes and fibroblasts plays a key role in the transition from the inflammatory phase of wound healing to the proliferative one (Schmidt-Ullrich and Paus, 2005; Tickle, 2006). Flii has been shown to be involved in cellular proliferation and migration via its interaction with the nuclear hormone receptors including estrogen receptor (ER), androgen receptor (AR), and glucocorticoid receptor (GR) (Archer *et al*., 2004; Jin *et al*., 2017). Flii shifts to the nucleus to prevent β-Catenin dependent transcription of cyclin D1 and inhibits cellular proliferation (Seward *et al*., 2008). The negative effect of Flii on cellular migration and proliferation has been shown in previous investigations (Cowin *et al*., 2007; Kopecki *et al*., 2009). The experiments and analysis of this chapter demonstrate that the treatment of keratinocytes with antibodies raised against LRR domain of Flii *in vitro* had no effect on the proliferation of these cells, however, when treated with antibodies raised against middle domain significantly increased proliferation. Previous studies have reported that FliiL FnAbs or Flii siRNA knockdown increases proliferation of keratinocytes (Cowin *et al*., 2007; Kopecki *et al*., 2009). Collectively, findings in this chapter demonstrate that Flii may affect the proliferation of keratinocytes through its middle domain.

The conducted experiments also revealed that FnAbs raised against either the middle or LRR domain of Flii improved migration in keratinocytes. These findings are in agreement with previous investigation indicating that the addition of FnAbs to the media of keratinocytes increase migration (Cowin *et al*., 2007). Also, these results are consistent with previous studies showing that reducing Flii gene expression improved keratinocyte migration and impaired cell adhesion (Kopecki *et al*.,

2009; Mohammad *et al*., 2012). As mentioned earlier, the FnAbs used in previous studies were generated against a specific antigen sequence in the LRR of Flii, however the binding portion is different from LRRFnAbs used in this study as LRRFnAbs bind to a larger peptide involving all 16 tandem leucine-rich repeats of Flii protein. Flii has been found to modulate cell migration via its localization to focal adhesions and also its capability to cap actin filaments and regulate paxillin signalling (Kopecki *et al*., 2011; Mohammad *et al*., 2012). The results of this chapter suggest that both LRR and middle domain of Flii are involved in controlling the migration of keratinocytes during wound healing as Flii has been previously shown to modulate the F-actin: G-actin ratio which is important in cellular migration (Mohammad *et al*., 2012). Studies have shown that the F-actin: G-actin ratio can be restored by attenuation of Flii in keratinocytes (Kopecki *et al*., 2014).

Different wound healing stages from the inflammatory phase to full epithelialisation highly depend on the role of fibroblasts (Forrest, 1983). Specifically, the proliferation and migration of fibroblasts play a big part in the initiation of the proliferative phase of healing (Ebeling *et al*., 2014; Fronza *et al*., 2009). Fibroblasts migrate to the wound area and proliferate in order to carry out various important biological activities through the secretion of factors present in the injured area (Desmouliere *et al*., 1995). Furthermore, the crosstalk between fibroblasts and keratinocytes through a paracrine loop (Nowinski *et al*., 2004) is crucial for integral dermal remodelling (Ghaffari *et al*., 2009) and re-epithelialization (el-Ghalbzouri *et al*., 2002).

Studies have reported that Flii is secreted into the media of fibroblasts in response to wounding (Cowin *et al*., 2007; Lei *et al*., 2012). The findings of this chapter show that addition of LRRFnAb to fibroblasts *in vitro* had minimal effect on cell proliferation. However, the proliferation of fibroblasts in the presence of MFnAb significantly increased. Moreover, treatment of fibroblasts with FnAb against the LRR domain of Flii had no effect on migratory ability of fibroblasts while the addition of MFnAb to the cultured fibroblasts increased the migration of these cells. These findings are in agreement with the previous work showing that attenuating the expression of Flii using FnAb increase proliferation and migration of fibroblasts (Cowin *et al*., 2007). Another investigation showed that proliferation and migration of human fibroblasts was improved following reducing Flii using siRNA (Jackson *et al*., 2020). The findings of this chapter suggest that Flii may alter the proliferation and migration of fibroblasts through its middle domain. As discussed above, Flii is involved in cellular proliferation through its nuclear receptors, and it

relocates to the nucleus to prevent β-Catenin dependent transcription of cyclin D1 and inhibits cellular proliferation (Archer *et al*., 2004; Jin *et al*., 2017; Seward *et al*., 2008). Flli has been found to be secreted by fibroblasts via a non-classic late endosome/lysosome-mediated pathway (Cowin *et al*., 2007; Lei *et al*., 2012). Flii has been also reported to be a negative regulator of the canonical Wnt signalling pathway which modulates the expression of proliferative genes (Lee and Stallcup, 2006). The canonical Wnt signalling pathway regulates these genes through interfering with the degradation and phosphorylation of cytosolic β-Cat (MacDonald *et al*., 2009). The results suggest that Flii regulates the Wnt signalling pathway through its middle domain by which may affect the expression of proliferative genes including Cyclin D1 and c-myc and genes involved in the degradation and phosphorylation of cytosolic β-Cat (Lecarpentier *et al*., 2019; Lee and Stallcup, 2006; MacDonald *et al*., 2009). Flii is also involved in cellular migration by its regulatory effect on focal adhesion maturation (Strudwick and Cowin, 2020). Cellular migration is also regulated by Flii through its role in binding to the p30 domain of Caspase-11 (Li *et al*., 2008). The gelsolin domain of Flii (targeted by MFnAb) has been found to bind Caspase-11 (Strudwick and Cowin, 2020), suggesting that Flii may regulate the migration of fibroblasts through its middle domain.

During wound healing, new capillaries are created from pre-existing vessels through angiogenesis (Carmeliet and Jain, 2011). The established vessels produce new vessels sprouts in this process (Johnson and Wilgus, 2014). The proliferation and migration of endothelial cells are required for the formation of new vascular structures (Carmeliet and Jain, 2011). Additionally, there are numerous important interactions between endothelial cells, pro-angiogenic factors, and surrounding extracellular matrix during angiogenesis (Gil *et al*., 1996; Morgan *et al*., 2007).

The impact of LRRFnAb and MFnAb on the function of dermal endothelial cells was investigated in this chapter. My results reveal that in contrast to fibroblasts+ keratinocytes the proliferation of endothelial cells was significantly increased following treatment with LRRFnAb. Whereas addition of MFnAb to endothelial cells *in vitro* did not alter the proliferation of these cells. The experiments and assessments of this chapter also demonstrate that treatment of dermal endothelial cells with FnAbs raised against either LRR or middle domain of Flii resulted in improved endothelial cell migration. These findings are in agreement with the previous studies demonstrating that the first generation of FnAbs have the capacity to promote capillary tube formation in endothelial cells and create longer and more mature blood vessels in comparison with

IgG (Ruzehaji *et al*., 2014). Previous studies have also shown that attenuating Flii gene expression using siRNA, resulted in a significant increase in the number of tube formations in human dermal endothelial cells (Thomas *et al*., 2020). These capillary structures lasted much longer than the cells in control groups (Thomas *et al*., 2020). My findings indicate that both LRR and middle domain of Flii are involved in the migration of endothelial cells. Moreover, the results of this chapter suggests that Flii modulates the proliferation of dermal endothelial cells via its LRR domain. Flii has previously been found to bind to Leucine Rich Repeat in Flightless1 (LRRFIP1) through its LRR domain (Strudwick and Cowin, 2020). LRRFIP1 is a cytosolic nucleic-acid sensor that regulates the expression of proangiogenic factors including PDGF involved in the proliferation of endothelial cells (Battegay *et al*., 1994; Jin *et al*., 2013).

The increased capillary tube formation of HDMECs treated with LRRFnAb and MFnAb confirms the previously reported effect of FnAb on tube formation in HUVECs (Ruzehaji *et al*., 2014). My findings show that endothelial cells treated with LRRFnAb+ MFnAb create more capillary tubes and the sprouts last longer than the capillary structures. Overexpression of Flii has been shown *in vivo* to impair the formation of new blood vessels, decrease number of endothelial cells, VEGF, and von Willebrand factor which are critical in angiogenesis (Randi *et al*., 2013; Ruzehaji *et al*., 2014). The assessment of common parameters in tubular structures including nodes, junctions, master junctions, segments, and meshes reveals that both LRRFnAb+ MFnAb treated endothelial cells create more branches that contribute to stable sprout formations. These results suggest that both the middle domain of Flii and the LRR domain are actively involved in the process of angiogenesis during wound healing.

Overall, these findings suggest that both LRR and middle domain of Flii are involved in the process of wound repair through their impact on different cellular activities involved in wound healing. Monoclonal antibodies generated against the middle domain have been shown to have promising effects on cellular activities, however LRRFnAbs also show potential particularly relating to angiogenesis. These *in vitro* results suggest that LRRFnAb+ MFnAb have potential in promoting proliferation, granulation tissue formation, and re-epithelialisation.

Chapter 4: Systemic delivery of FnAbs raised against LRR and middle domains of Flii improves excisional wound healing in an acute wound murine model

4.1 Introduction

One of the major health-related concerns is the burden and incidence of wounds (Sen, 2019). Wounds can be associated with multiple complications such as infection, inflammation and cause burden through, requirement of support, mobility problems, and prolonged hospital stay that can extensively affect quality of life for patients with wounds (Monika *et al*., 2021a; Monika *et al*., 2021b).

Wound repair is a dynamic and complex process by which the injured tissue layers are restored (Brown *et al*., 1988). However, the process of healing can be delayed due to the alterations in the balance between the activation and suppression of mediators during different stages of wound repair (Eming *et al*., 2007). Uncontrolled inflammation is a major cause of delayed healing which can occur when the level of cytokines is altered in the wound area (Singer and Clark, 1999). Impaired healing may also lead to fibrosis and scarring which can cause multiple mental and physical problems for patients (Xue and Jackson, 2015).

Therapeutic monoclonal antibodies (mAbs) are mono-specific antibodies generated to target proteins that are increased in several diseases (Turner *et al*., 2015a). The greatest advantage of these antibodies is their potential to bind to proteins with high specificity and provide direct targeting only to the pathology site/s (Turner *et al*., 2015a). Preclinical and clinical studies have shown roles of therapeutic antibodies for several cutaneous conditions including atopic dermatitis (Kasutani *et al*., 2014), skin cancers (Gilbert *et al*., 2017), psoriasis (Di Lernia, 2017; Kopp *et al*., 2015), and wound healing (Shah *et al*., 1992; Turner *et al*., 2015a). Therapeutic antibodies against wound mediators such as tumour necrosis factor alpha (TNF-α) have been reported to improve healing in different wound types (Streit *et al*., 2006), and therapeutic antibodies against transforming growth factor beta (TGF-β) have been shown to reduce scarring (Mead *et al*., 2003). Flii has been investigated for its function in wound healing and has been shown to be a major inhibitor of wound repair (Cowin *et al*., 2007). In recent years, antibodies against Flii have been used in different models of wound healing and shown to promote repair process (Cowin *et al*., 2007; Ruzehaji *et al*., 2014). Delivery of antibodies can be performed using different routes such as intravenous, subcutaneous, or intramuscular injections (Bruno *et al*., 2013). Flightless I neutralizing antibody (FnAb) has been shown to improve healing outcomes in different animal

models when administered topically and intradermally (Cowin *et al*., 2007; Jackson *et al*., 2012; Ruzehaji *et al*., 2014). Moreover, it has been reported that FnAb treatment enhanced angiogenesis and further contributing to the improved healing process (Ruzehaji *et al*., 2014).

Although administration of FnAbs via topical injection has improved the quality and the rate of healing in preclinical animal models of wound healing, topical application of FnAbs does not appear to be a feasible approach for large skin injuries, particularly for people with extensive wounds that cover large surface areas of their bodies including patients with burn injuries or those suffering from widespread blistering in Epidermolysis Bullosa. Therefore, the systemic delivery of FnAbs could be a highly promising option for patients with extensive wounds, as the potential benefits have not been explored extensively. If investigations into the systemic administration of FnAbs show positive results, it could offer significant advantages and be highly beneficial.

This chapter presents findings from studies investigating whether the systemic delivery of FnAbs could improve cutaneous wound healing *in vivo*. In particular, the effect of LRRFnAbs and MFnAbs generated against specific domains of Flii on excisional wound healing was investigated when systemically administered to mice by intraperitoneal injection. Effect of systemic FnAb administration on wound repair factors including inflammation and angiogenesis were investigated in this study.

4.2 Results

To investigate the effect of LRRFnAb or MFnAb systemic administration on acute wound repair, excisional wounds were created in 18 murine models following established protocols as described in chapter 2. Three groups of mice (n=6) including LRRFnAb, MFnAb, and IgG (as control) groups were used, and the study was conducted for 7 days. Single dose of each treatment including LRRFnAb (5 mg/kg), MFnAb (5 mg/kg), and IgG (5 mg/kg) were delivered to Balb/C mice by Intraperitoneal (IP) injection following wound creation on day 0 of experiment. The optimal dosage and frequency of administration were determined through pilot studies, resulting in an optimized treatment regimen that demonstrated effectiveness. Additionally, it was beneficial to initiate the intervention with a single injection on day 0 as a preliminary measure to assess its response and gauge its viability.

4.2.1 Wound healing was accelerated in LRRFnAb and MFnAb treated mice

Images of wounds were taken on days 0, 2, 4, and 7 and assessed using macroscopic measurements. The wound area at different time points of the trial was measured and normalized to the original wound area at day 0 (Figure 4.1A). As shown in Figure 4.1B, mice treated with LRRFnAb showed a significant reduction by 43.6% ± SEM in wound area in comparison with IgG treated control group on day 2 post-wounding (Figure 4.1B). Mice treated with MFnAb showed a reduction by 12.1% ± SEM in wound size compared to IgG treated mice on day 2 but this difference did not reach statistical significance. The average size of wound area for mice treated with LRRFnAb was significantly decreased by 32.3% ± SEM in comparison to IgG treated mice on day 4 of healing. The macroscopic measurements of wounds in mice treated with MFnAb also showed a significant reduction by 15.1% ± SEM in wound area in comparison with IgG treated control group on day 4 post-wounding. The average size of wound area for mice treated with LRRFnAb was significantly decreased by 30.7% ± SEM compared with IgG control treated mice on days 7 of healing. Wound size for mice treated with MFnAb also significantly reduced by 10.2% ± SEM compared to mice treated with IgG on day 7 post-wounding (Figure 4.1B).

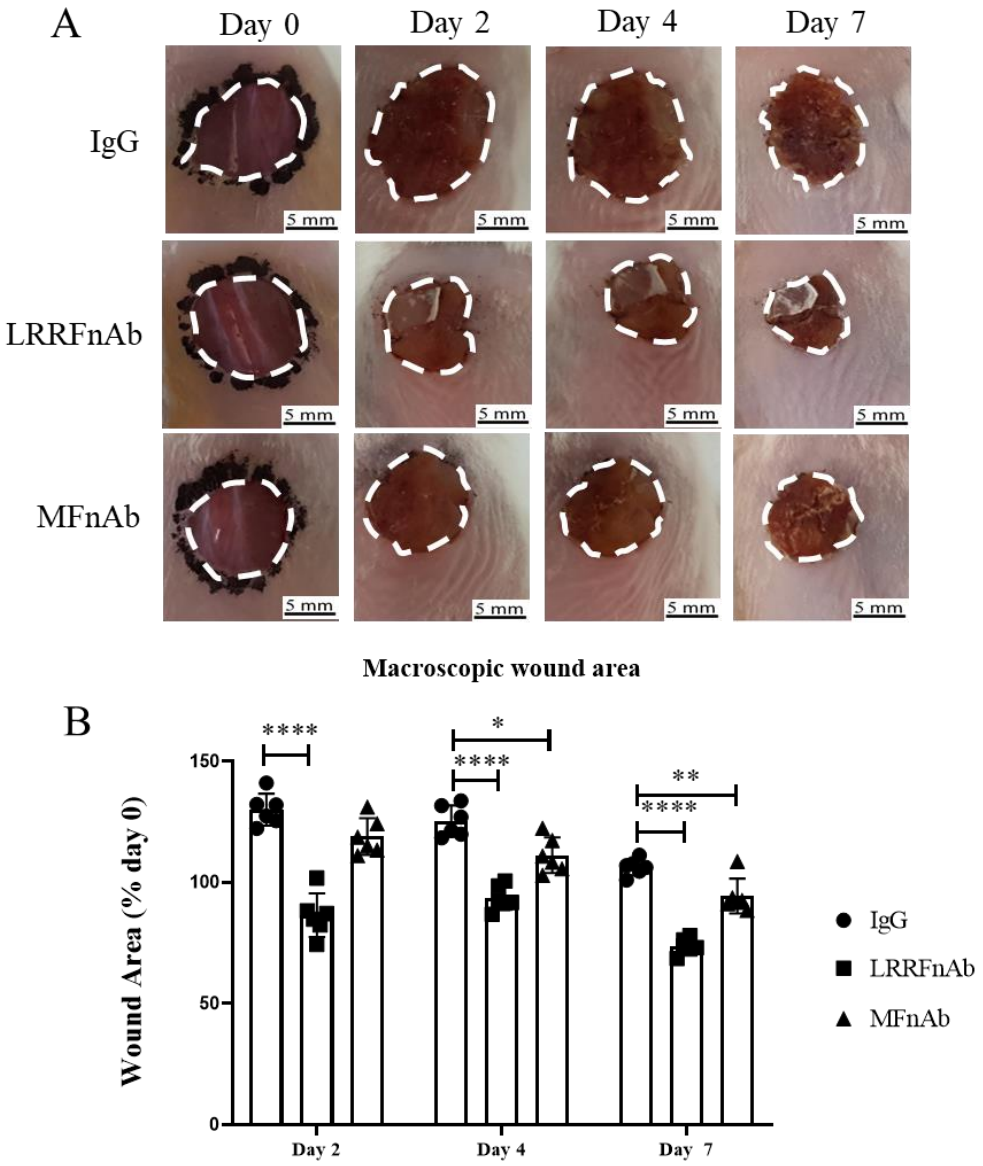


Figure 4. 1: Macroscopic assessment: Effect of LRRFnAb and MFnAb on the rate of murine excisional wound healing

A) Representative images of wounds in mice treated with LRRFnAb, MFnAb, and IgG on days 2, 4 and 7 of healing. Images were captured on days 0, 2, 4, and 7 prior to wound tissue collection. B) Measurement of macroscopic wound area using Image Pro-Plus software illustrates the reduction of macroscopic wound area in LRRFnAb and MFnAb treated mice on days 2, 4, and 7. n = 6. All data are represented as mean ± SEM. Statistical significance was calculated by two-way ANOVA and Tukey's post-tests. *= $p < 0.05$, **= $p < 0.01$, **** = $p < 0.0001$.

Hematoxylin and eosin-stained paraffin embedded 7 day wound tissues were histologically assessed for microscopic measurements of wound healing. The assessment of H&E-stained tissues (Figure 4.2A) revealed that wound width was significantly decreased by 9.5% ± SEM in MFnAb treated mice compared to mice treated with the IgG control group. Additionally, the histological analysis of wounds indicated a non-significant decrease in wound width (7.1% ± SEM) in mice treated with LRRFnAb compared to mice treated with IgG (Figure 4.2B). Histological analysis showed a significant increase by 9.7% ± SEM in the rate of re-epithelialisation in MFnAb treated mice on day 7 of the study compared to the IgG control treated group (Figure 4.2C). Assessment of H&E-stained wounds also demonstrated a non-significant increase by 5.4% ± SEM in the rate of re-epithelialisation in LRRFnAb treated mice compared to the IgG control group (Figure 4.2C).

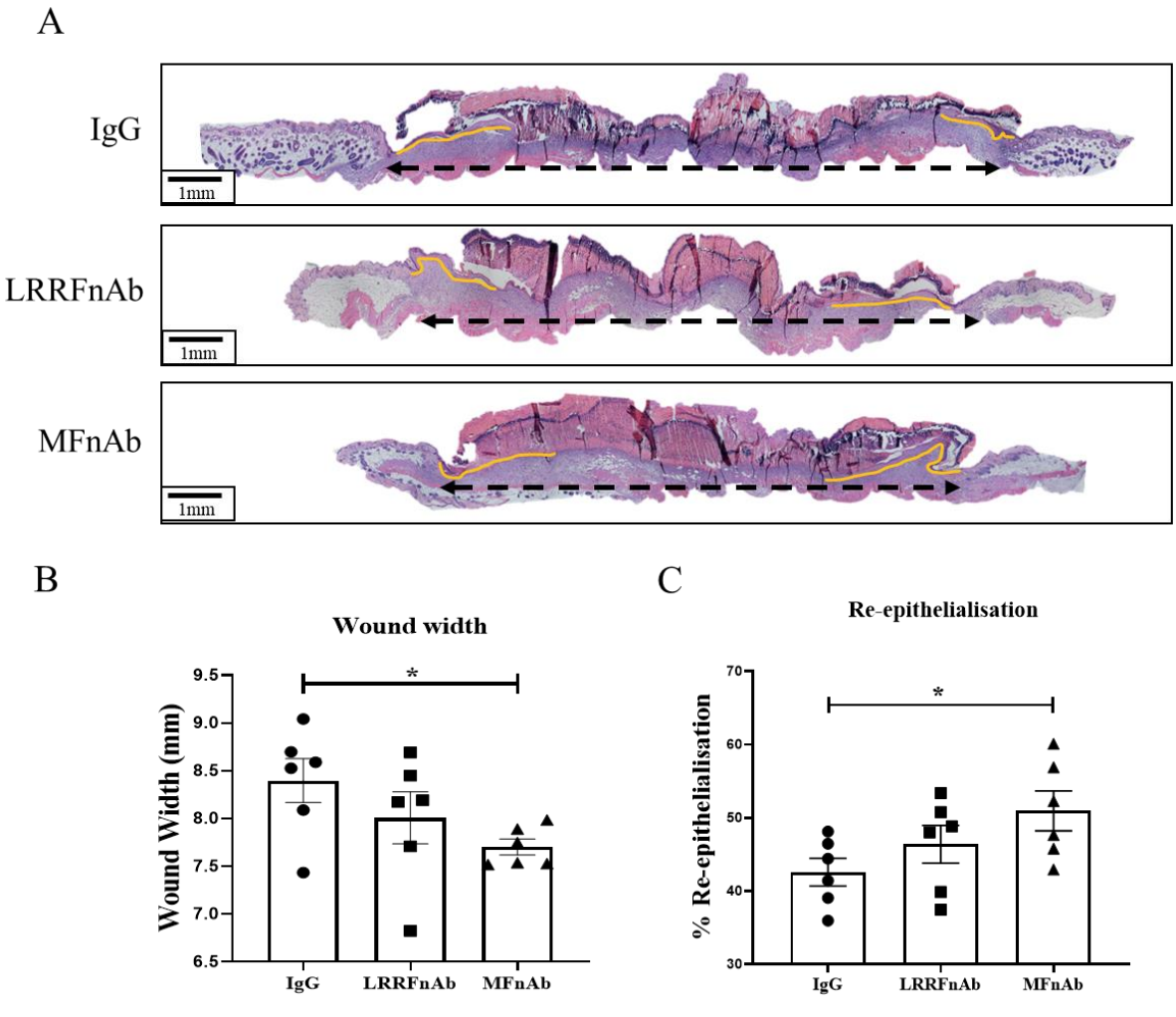


Figure 4. 2: Histological assessment: Effect of LRRFnAb and MFnAb on the rate of excisional wound healing

A) Representative images of LRRFnAb and MFnAb treated and IgG control following hematoxylin and eosin staining, 7 days post-wounding. Images captured using a 10X objective. Black dashed lines demonstrate wound width measured. Yellow lines indicate re-epithelialisation measured B) Histological analysis of wound width MFnAb treated mice. C) Quantification of re-epithelialisation demonstrates increased re-epithelialisation in MFnAb treated mice. n = 6. All data are represented as mean ± SEM. Statistical significance calculated by one-way ANOVA and Dunnett's post-tests. *= $p < 0.05$.

4.2.2 Flii expression was reduced in LRRFnAb and MFnAb treated mice

Studies have shown that Flii is overexpressed in response to wounding, and it impairs the process of healing (Cameron *et al*., 2016; Cowin *et al*., 2007). FnAbs raised against either LRR or middle of Flii protein were used in this study to reduce the negative effect of Flii on wound healing. It was necessary to measure Flii protein following treatment of mice with FnAbs to determine the effectiveness of systemically administered LRRFnAbs and MFnAbs on the expression of Flii.

Immunofluorescent staining assessment for Flii protein in wounds in mice treated with treatment and control antibodies revealed that the expression of Flii was decreased in both LRRFnAb and MFnAb wounds in comparison with mice treated with control antibody 7 days following surgery (Figure 4.3A and B). Both systemically administered LRRFnAb and MFnAb significantly reduced the amount of Flii by 45.4% ± SEM and by 40.2% ± SEM respectively within the wound bed in comparison with IgG in a murine model of excisional wound.

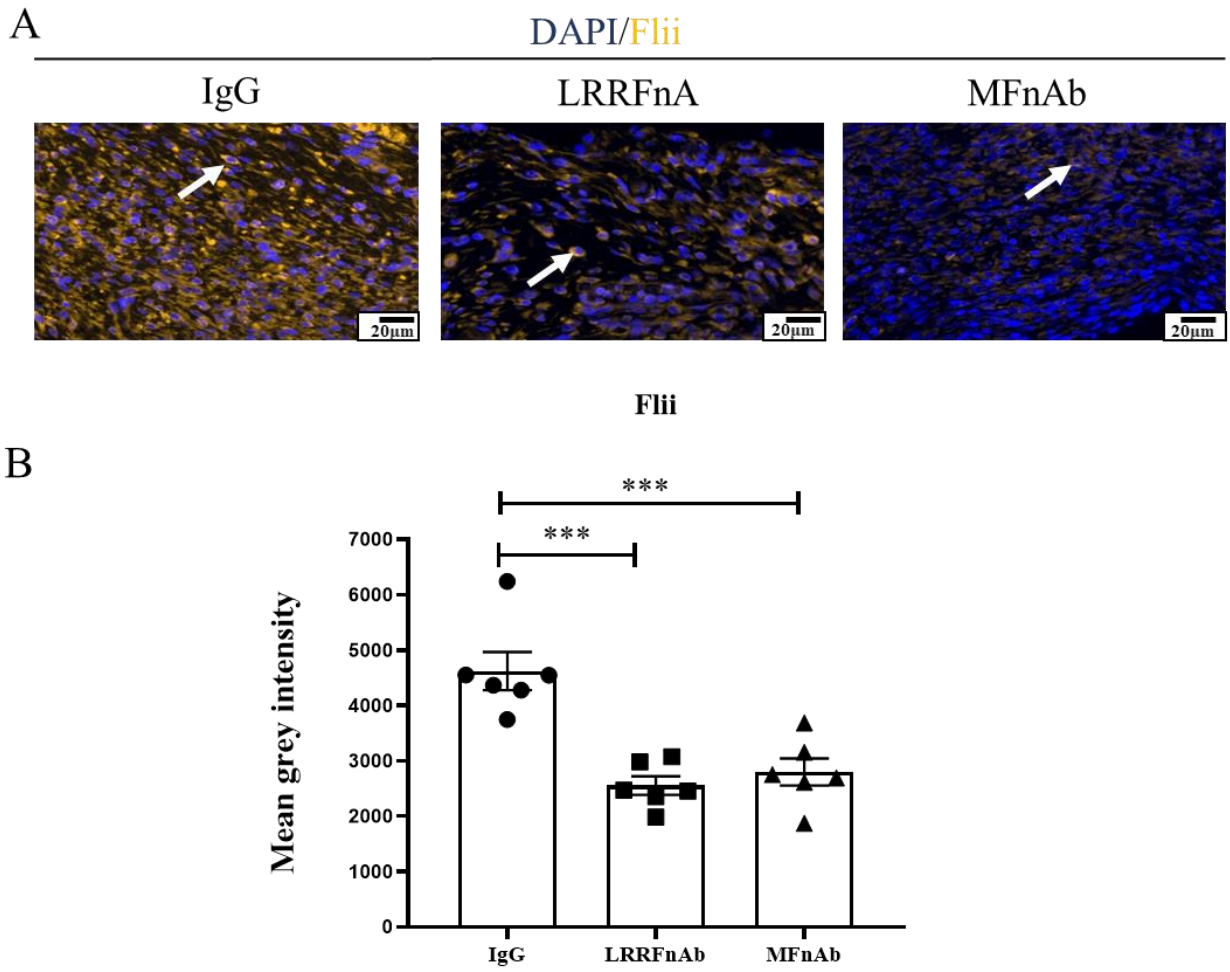


Figure 4. 3: Effect of LRRFnAb and MFnAb on Flii expression

A) Immunofluorescence detection of Flii (yellow) counterstained with DAPI (blue) in LRRFnAb and MFnAb treated mice at day 7 post-injury. The primary antibody used was Rabbit Flii antibody, and for the secondary antibody, Goat anti-Rabbit IgG was employed. The entire wound bed was encompassed in the analysis. Images captured using a 20X objective B) Quantification of Flii expression as mean grey intensity. Flii expression was decreased in LRRFnAb and MFnAb treated mice. n = 6. All data are represented as mean ± SEM. Statistical significance was calculated by one-way ANOVA and Dunnett's post-tests. *** = $p < 0.001$.

4.2.3 Inflammation was reduced in LRRFnAb and MFnAb treated mice

The inflammatory response is crucial for successful haemostasis, control of infection. removal of necrotic tissue, and the entire process of injury repair (Landén *et al*., 2016); however, prolonged, and excessive inflammation can lead to pathogenic conditions with impaired interactions between skin cells including fibroblasts and keratinocytes (Mustoe *et al*., 2006). This can result in impaired proliferation and remodelling phases and defective wound healing processes (Hesketh *et al*., 2017; Mustoe *et al*., 2006). Flii has been reported to be involved in regulating the early phases of inflammation by exerting regulatory effects on neutrophils and macrophages (Mills *et al*., 2022). To explore the impact of LRRFnAbs and MFnAbs on inflammation, the number of neutrophils and macrophages were identified.

Immunofluorescent staining was performed for neutrophil marker NIMP-R14 to assess the possible effect of systemically administered FnAbs generated against different domains of Flii on neutrophil infiltration (Figure 4.4A). The quantification of neutrophil infiltration in treatment and control wounds showed a significant reduction in the neutrophil numbers in LRRFnAb (40.3% ± SEM) and MFnAb (67.3% ± SEM) treated mice in comparison with IgG treated mice 7 days post wounding (Figure 4.4B). The assessment also demonstrated that the number of neutrophil infiltrations was reduced in mice treated with MFnAb compared to LRRFnAb treated mice (Figure 4.4B).

To investigate the effect of LRRFnAb and MFnAb on the quantification of macrophage infiltration, immunofluorescent staining assessment was carried out using macrophage marker (F4/80). The assessment showed a non-significant decrease of 23.1% ± SEM in the number of macrophages with systemically administered LRRFnAb compared to IgG treated mice. The result also demonstrated a significant reduction by 40.5% ± SEM in the total number of macrophages in MFnAb treated mice compared to control group (Figure 4.5B). The percentage of M2 macrophages which are known as anti-inflammatory macrophages (Moreira and Hogaboam, 2011) were quantified using F4/80 and Ym-1 immunofluorescent staining (Figure 4.5A). The findings revealed a non-significant increase of 27.0% ± SEM in the percentage of M2 anti-inflammatory macrophages in mice treated with LRRFnAb compared to the IgG treated group. A significant increase by 39.9% ± SEM in the percentage of M2 anti-inflammatory macrophages observed in

MFnAb treated mice indicated an accelerated rate of macrophage polarization to an anti-inflammatory state (Figure 4.5C).

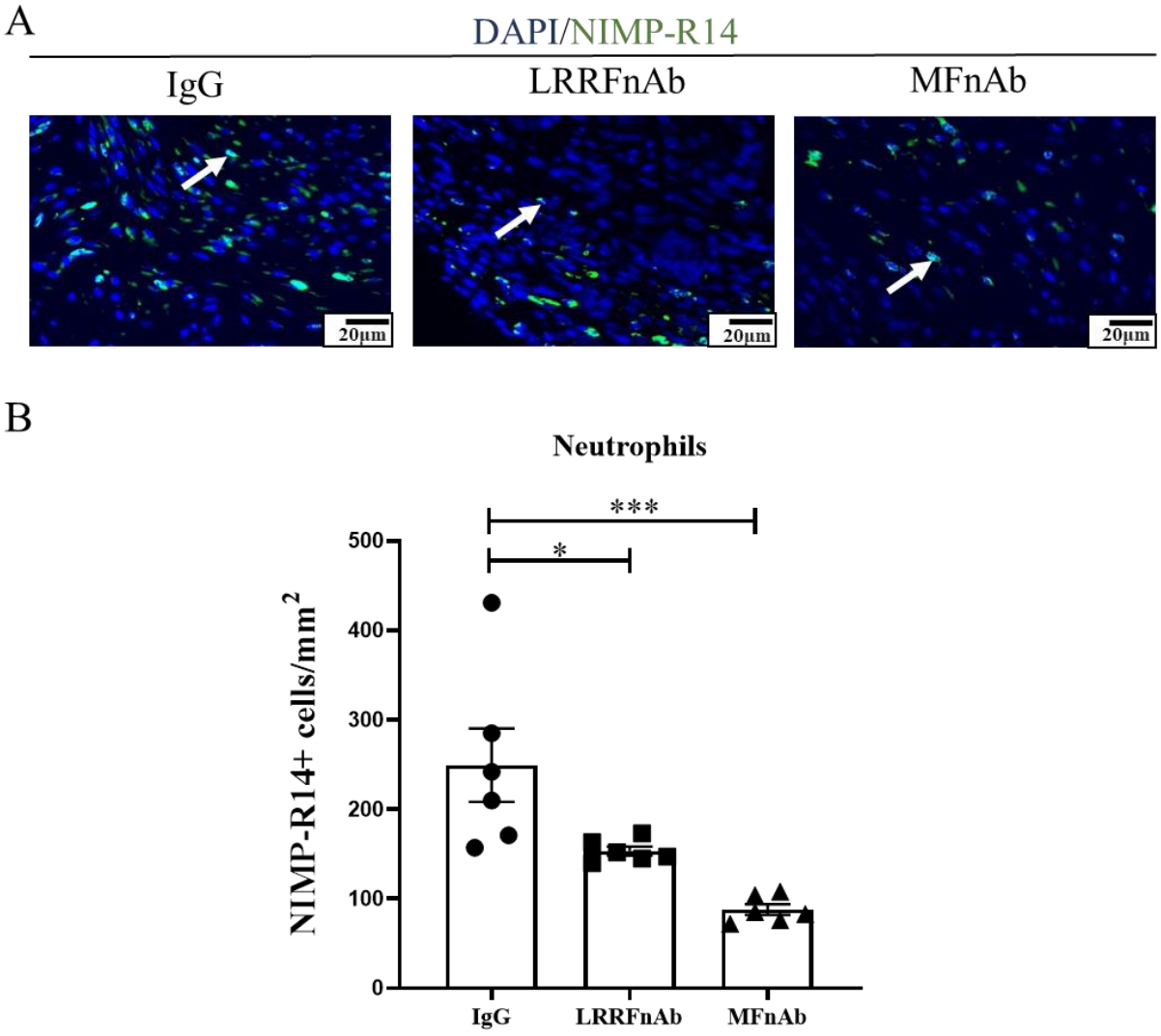


Figure 4. 4: Impact of LRRFnAb and MFnAb on neutrophil infiltration

A) Immunofluorescence detection of neutrophils (green) counterstained with DAPI (blue) in LRRFnAb and MFnAb treated mice at day 7 post-injury. The primary antibody used was Rat monoclonal Neutrophil Marker antibody, and for the secondary antibody, Goat anti-Rat IgG was employed. The entire wound bed was encompassed in the analysis. Images captured using a 20X objective B) Quantification of neutrophil numbers in the wound bed, normalised to area. The number of neutrophils within the wound bed was decreased in LRRFnAb and MFnAb treated mice 7 days post-wounding. n = 6. All data are represented as mean ± SEM. Statistical significance was calculated by one-way ANOVA and Dunnett's post-tests. *= $p < 0.05$, ***= $p < 0.001$.

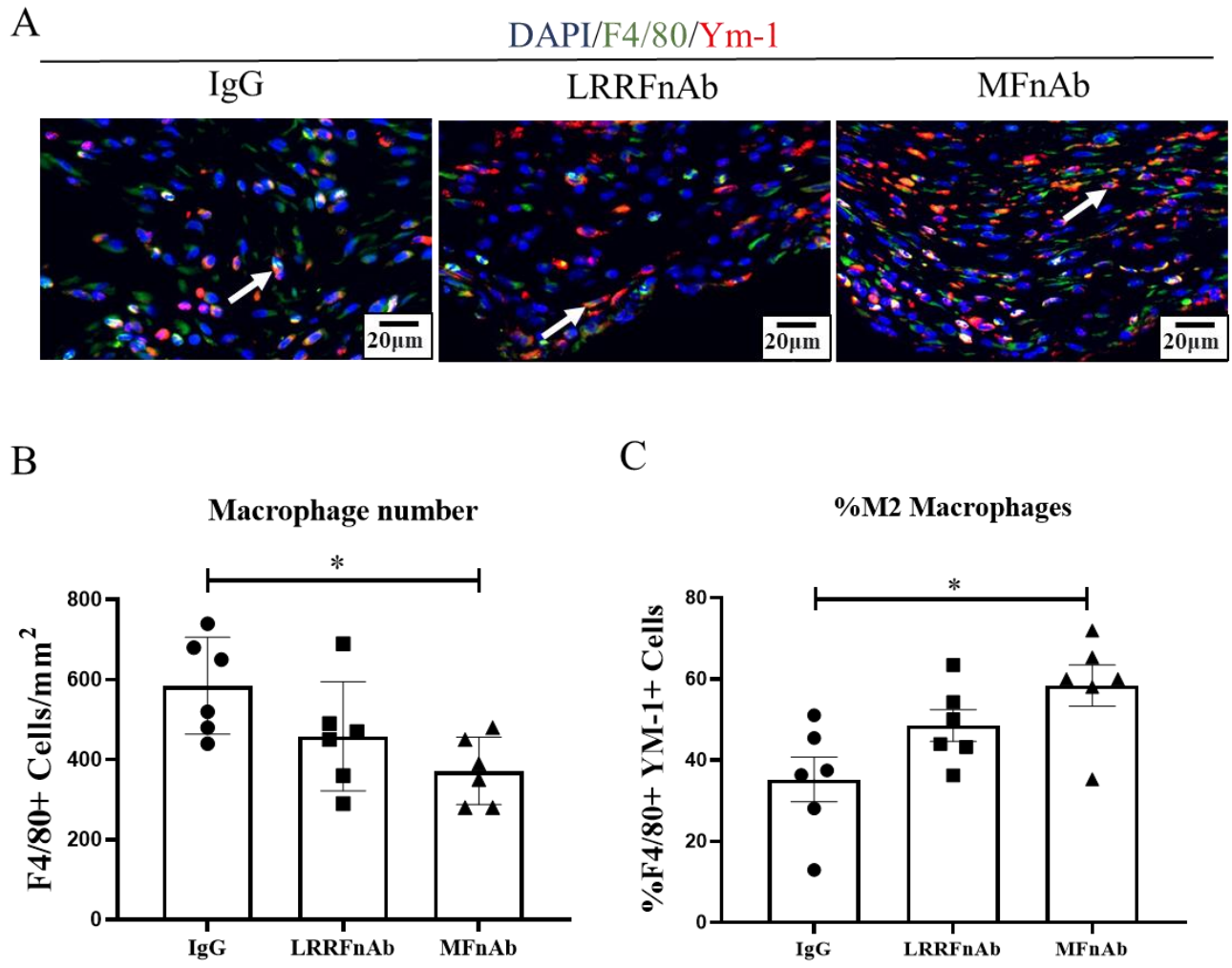


Figure 4. 5: Impact of LRRFnAb and MFnAb on macrophage infiltration and polarization in the wound site

A) Immunofluorescence detection of macrophages using F4/80 (green) and YM-1 (Red) counterstained with DAPI (blue) in LRRFnAb and MFnAb treated mice at day 7 post-injury. In the analysis, the primary antibody used for F4/80 was Rat anti-Mouse F4/80 antibody, and for the secondary antibody, Goat anti-Rat IgG was employed. Additionally, Rabbit anti-Ym1 antibody served as the primary antibody for YM-1, with Goat anti-Rabbit IgG used as the secondary antibody. The entire wound bed was encompassed in the analysis. Images captured using a 20X objective B) Quantification of total macrophage number (F4/80+) within the wound bed normalized to the wound area. The number of macrophages infiltrating to the wound site decreased in MFnAb treated mice C) Quantification of M2 macrophages (F4/80+, YM-1+) as a percentage of total macrophages within the wound bed normalized to the wound area. The ratio of M2

macrophages was increased in MFnAb treated mice. n = 6. All data are represented as mean ± SEM. Statistical significance was calculated by one-way ANOVA and Tukey's post-tests. *= p <0.05.

4.2.4 Angiogenesis was enhanced in LRRFnAb and MFnAb treated mice

Angiogenesis plays an integral role in wound healing as it is the process of re-establishing new blood vessels and contributing to the development of granulation tissue (Saghazadeh *et al*., 2018). New capillaries are formed through the process of angiogenesis, which involves the proliferation of blood vessels. These newly formed capillaries provide a matrix for fibroblast migration and further blood vessel proliferation (Tonnesen *et al*., 2000). Angiogenesis is regulated by different factors including inflammation and growth factors which can stimulate numerous signalling pathways involved in tissue regeneration. Angiogenesis deficiency results in delayed healing and can lead to chronic wounds and scars (Johnson and Wilgus, 2014). The number of mature blood vessels, defined as the larger and more prominent vessels, was measured in mice treated with LRRFnAb and MFnAb to assess the effect of systemic delivery of FnAbs on angiogenesis.

The effect of MFnAb and LRRFnAb on capillary density was assessed using immunohistochemistry for CD31 and α-SMA (Figure 4.6A). CD31 is an endothelial marker which is highly expressed on the surface of these cells (Schlüter *et al*., 2018), while α-SMA is a pericyte marker which is present in mature vessels only (Bergers and Song, 2005). The dual staining of $CD31^{+}$ αSMA^{+} localizes and quantifies the mature blood vessels within the wound bed. The immunofluorescent assessment demonstrated that a significant increase by 33.8% ± SEM in the number of mature blood vessels was observed in wound bed of mice treated with LRRFnAb compared to control mice. The number of mature blood vessels was also increased by 32.2% ± SEM in wound bed of MFnAb treated mice when compared with mice treated with IgG control antibody, indicating a promotion of existing mature blood vessel formation (Figure 4.6B).

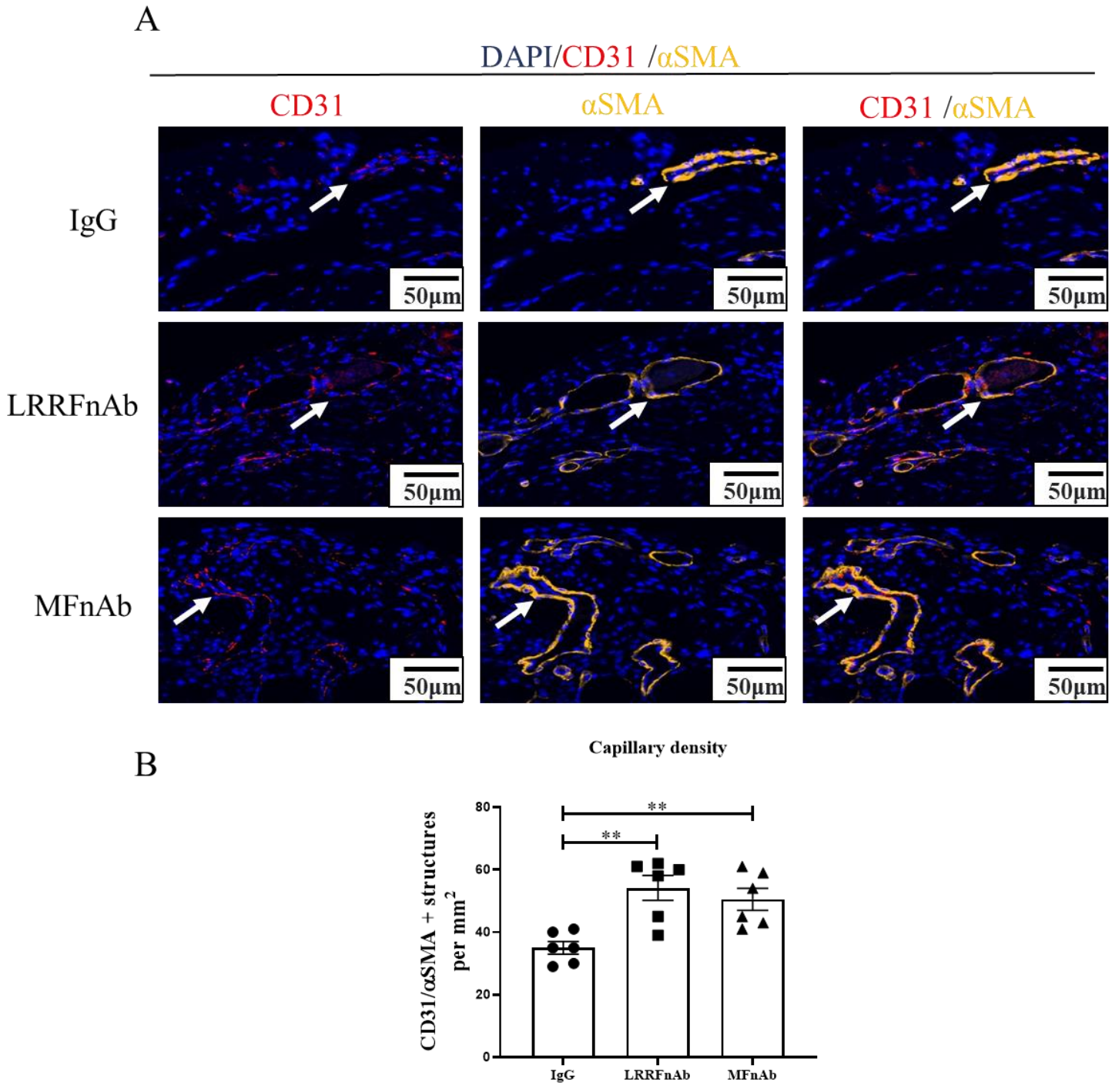

A
DAPI/CD31 /αSMA
CD31
αSMA
CD31 /αSMA
IgG
LRRFnAb
MFnAb
50μm
B
Capillary density
CD31/αSMA + structures per mm2
80
60
40
20
0
**
**
IgG
LRRFnAb
MFnAb

Figure 4. 6: Impact of LRRFnAb and MFnAb on angiogenesis in excisional wounds

A) Immunofluorescence detection of mature blood vessels using staining of CD31 (red) and αSMA (yellow) counterstained with DAPI (blue) in LRRFnAb and MFnAb treated mice at day 7 post-injury. In the analysis, the primary antibody used for CD31 was Rabbit anti- CD31 antibody, and for the secondary antibody, Goat anti-Rabbit IgG was employed. Additionally, Mouse anti- αSMA antibody served as the primary antibody for αSMA, with Goat anti-Mouse IgG used as the secondary antibody. The entire wound bed was encompassed in the analysis. Images captured using a 20X objective B) Quantification of mature blood vessels in the wound bed normalized to the wound area. The average number of blood vessels was increased in LRRFnAb and MFnAb treated mice. n = 6. All data are represented as mean ± SEM. Statistical significance was calculated by one-way ANOVA and Dunnett's post-tests. **= $p < 0.01$.

4.2.5 VEGF expression was elevated in MFnAb treated mice

Various proangiogenic factors trigger the cellular pathways involved in the process of angiogenesis. Vascular endothelial growth factor (VEGF) has been known as the core regulator of angiogenesis since it is precisely involved in the formation of new blood vessels by allowing endothelial cells to migrate, proliferate, and survive. VEGF can trigger downstream signalling transductions involved in angiogenesis (Koch *et al*., 2011). Additionally, reducing the expression of VEGF by neutralizing antibodies or interfering small molecules can impair the wound healing process (Rossiter *et al*., 2004).

In order to determine the impact of MFnAb and LRRFnAb on VEGF expression, immunofluorescent staining was performed, and the expression of VEGF was measured in the wound bed (Figure 4.7A). The amount of VEGF was quantified by assessing total fluorescence revealing significantly higher VEGF expression by 33.3% ± SEM and 51.0% ± SEM in LRRFnAb and MFnAb treated mice respectively compared to IgG control mice (Figure 4.7B). Immunofluorescent assessments also indicated a significant increase by 26.6% ± SEM in the expression of VEGF in mice treated with MFnAb in comparison with LRRFnAb treated mice (Figure 4.7B).

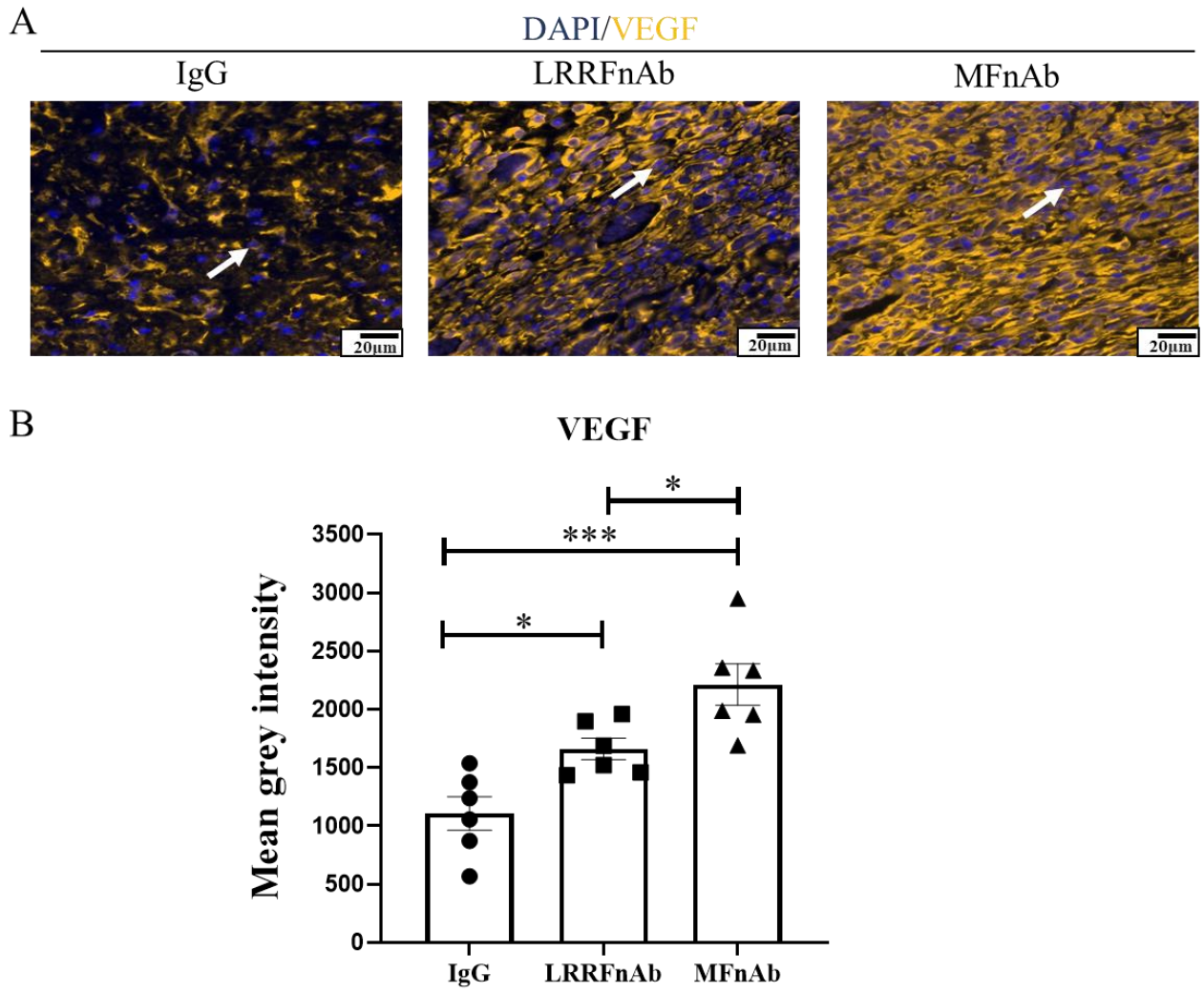


Figure 4. 7: Effect of LRRFnAb and MFnAb on VEGF expression

A) Immunofluorescence detection of VEGF (yellow) counterstained with DAPI (blue) in LRRFnAb and MFnAb treated mice at day 7 post-injury. The primary antibody used was Rabbit anti-VEGFA antibody, and for the secondary antibody, Goat anti-Rabbit IgG was employed. The entire wound bed was encompassed in the analysis. Images captured using a 20X objective B) Quantification of VEGF expression as mean grey intensity in the wound bed normalized to the wound area. The expression of VEGF was elevated in LRRFnAb and MFnAb treated mice. n = 6. All data are represented as mean ± SEM. Statistical significance was calculated by one-way ANOVA and Tukey's post-tests. *= $p < 0.05$, *** = $p < 0.001$.

4.2.6 FGF-2 expression was increased in LRRFnAb treated mice

Basic fibroblast growth factor-2 (FGF-2) is involved in the process of wound repair and is synthesized by numerous cell types including macrophages, monocytes, platelets, and fibroblasts (Matsuoka *et al*., 2006). FGF-2 plays a key role in the formation of new blood vessels and promotes endothelial cell migration and proliferation and stimulates binding of endothelial cells to the ECM (Barrientos *et al*., 2008).

To investigate the effect of MFnAb and LRRFnAb on the expression of FGF-2, wound tissues were immunostained with FGF-2 antibody (Figure 4.8A). The result showed that the expression of FGF-2 was significantly elevated by 28.0% ± SEM in mice treated with LRRFnAb following 7 days after creation of wound. Immunofluorescent assessments also revealed a non-significant increase of 15.0% ± SEM in the expression of FGF-2 in mice treated with MFnAb when compared to the control group. The amount of FGF-2 was measured as mean grey intensity in wound beds followed by normalization to the normal skin (Figure 4.8B).

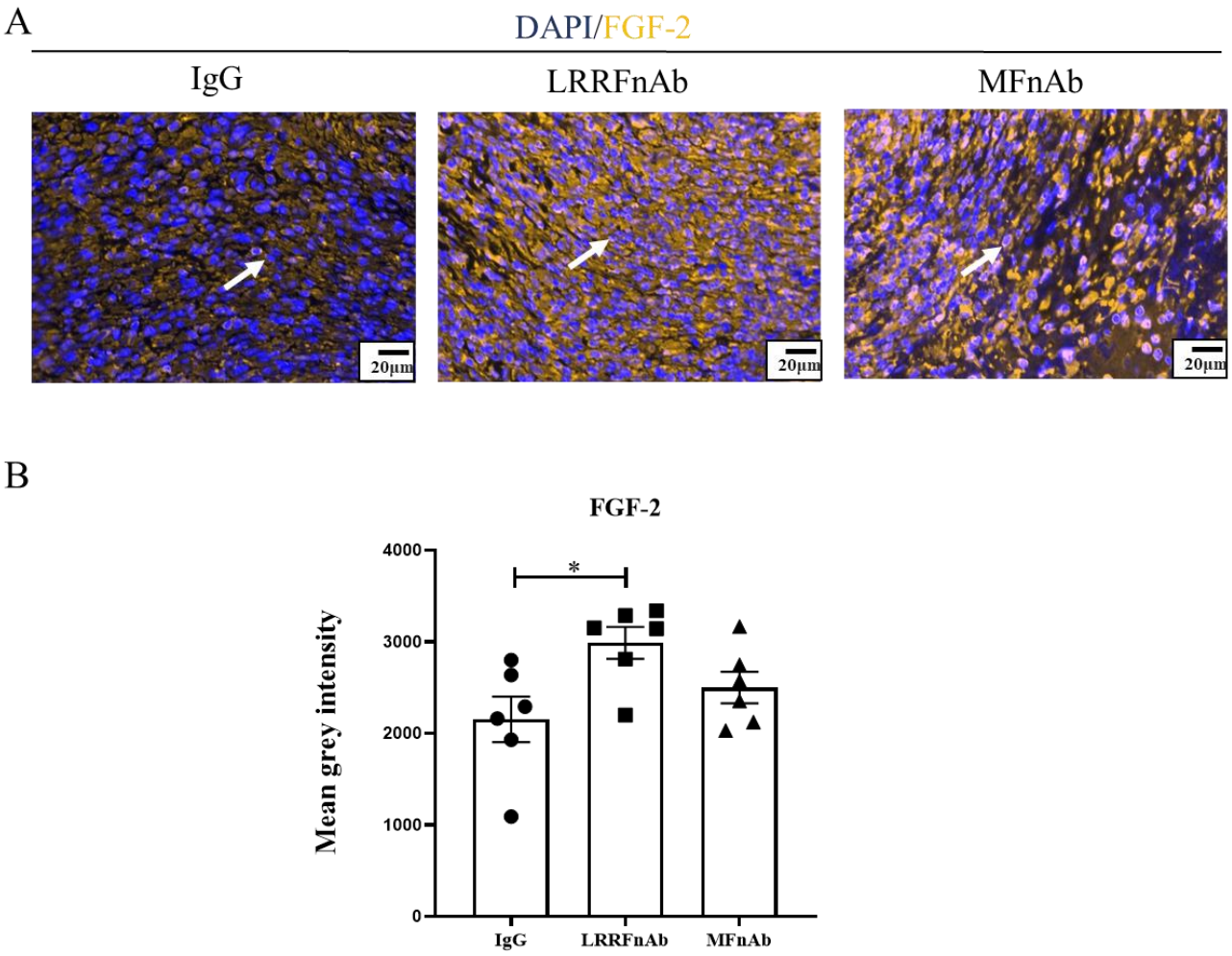


Figure 4. 8: Effect of LRRFnAb and MFnAb on FGF-2 expression in the wound site

A) Immunofluorescence detection of FGF-2 (yellow) counterstained with DAPI (blue) in LRRFnAb and MFnAb treated mice at day 7 post-injury. The primary antibody used was Rabbit anti-FGF-2 antibody, and for the secondary antibody, Goat anti-Rabbit IgG was employed. The entire wound bed was encompassed in the analysis. Images captured using a 20X objective B) Quantification of FGF-2 expression as mean grey intensity in the wound bed normalized to the wound area. The production of FGF-2 was increased in LRRFnAb treated mice. n = 6. All data are represented as mean ± SEM. Statistical significance was calculated by one-way ANOVA and Tukey's post-tests. *= $p < 0.05$.

4.2.7 PDGF-BB expression was stimulated in LRRFnAb treated mice

Platelet-derived growth factor-BB (PDGF-BB) is secreted by different cells including platelets, monocytes, and fibroblasts during wound healing (Barrientos *et al*., 2008; Papanas and Maltezos, 2007). PDGF-BB has a major role in early and later stages of healing process particularly in tube formation during the formation of the granulation tissue (Barrientos *et al*., 2008). PDGF-BB mediates the differentiation of endothelial cells and has been shown that inhibiting the activity of PDGF-BB can result in impaired angiogenesis and consequently delayed wound healing (Onimaru *et al*., 2009).

To investigate the impact of FnAb monoclonal antibodies raised against LRR and middle domain of Flii, immunostaining was performed for PDGF-BB antibody in LRRFnAb and MFnAb treated mice in comparison to mice treated with IgG control antibody (Figure 4.9A). Results showed that the amount of PDGF-BB was significantly higher by 30.2% ± SEM in LRRFnAb treated mice compared to control (Figure 4.9B). Although not statistically significant, an increase of 27.8% ± SEM in PDGF-BB expression was also observed compared to control in MFnAb treated mice. This result indicates that LRRFnAb impacts expression of PDGF-BB more than MFnAb (Figure 4.9B).

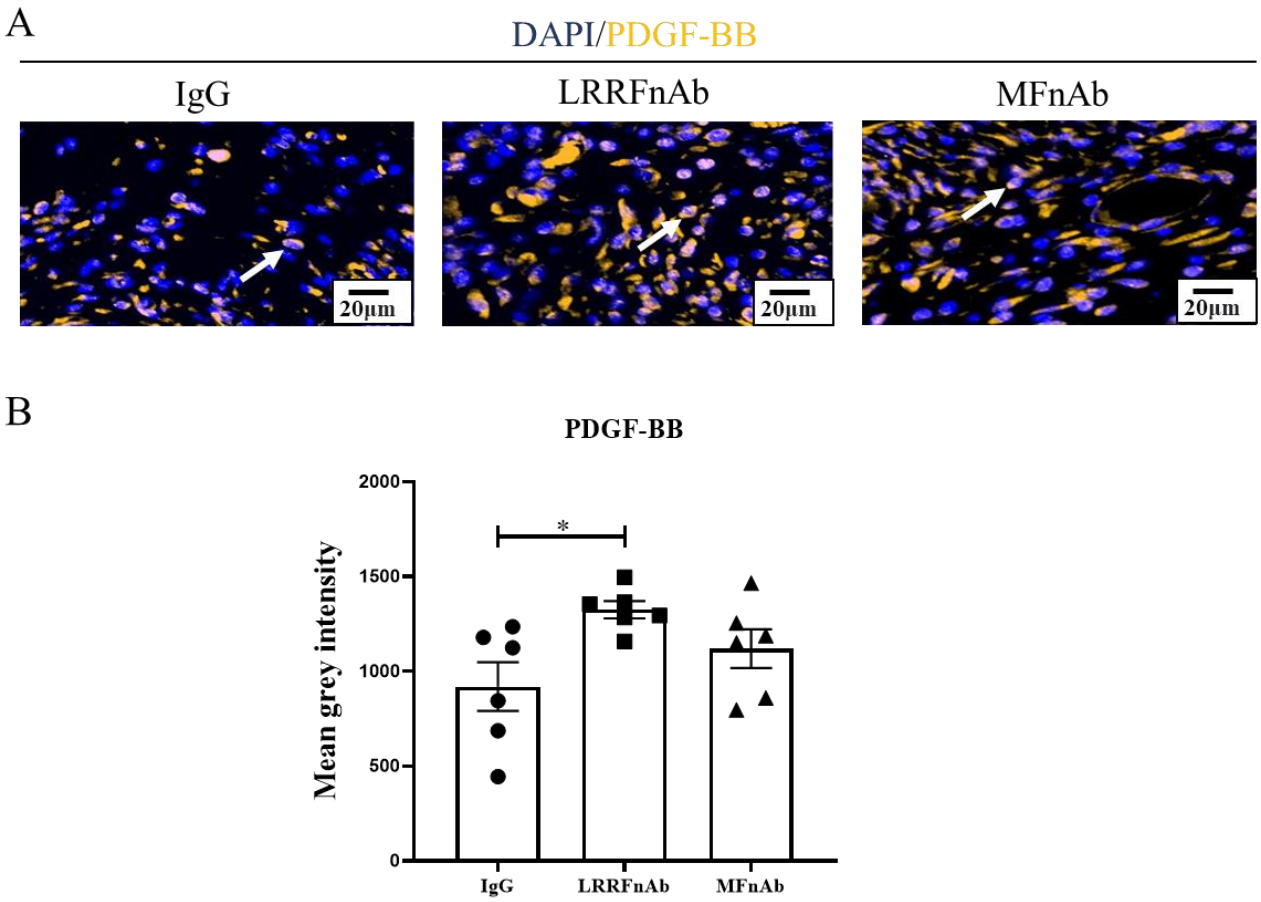


Figure 4. 9: Effect of LRRFnAb and MFnAb on PDGF-BB expression

A) Immunofluorescence detection of PDGF-BB (yellow) counterstained with DAPI (blue) in LRRFnAb and MFnAb treated mice at day 7 post-injury. The primary antibody used was Rabbit anti-PDGF-BB antibody, and for the secondary antibody, Goat anti-Rabbit IgG was employed. The entire wound bed was encompassed in the analysis Images captured using a 20X objective B) Quantification of PDGF-BB expression as mean grey intensity in the wound bed normalized to the wound area. The expression of PDGF-BB is elevated in LRRFnAb treated mice. n = 6. All data are represented as mean ± SEM. Statistical significance was calculated by one-way ANOVA and Dunnett's post-tests. *= $p < 0.05$.

4.3 Discussion

Various cellular processes including cell interactions, cytokine secretion, and growth factor activation are involved in the process of wound healing (Borena *et al*., 2015). Studies have shown that expression of Flii is elevated following injuries and an increased level of Flii has a negative role in the process of wound healing as it negatively affects cellular activities involved in injury repairs (Cowin *et al*., 2007). In this study, the effect of systemic delivery of FnAbs generated against specific domains of Flii on murine excisional wounds was investigated.

Previous published studies have shown that topical and intradermal injections of FnAbs generated against specific Flii peptide attenuated the expression of extracellular Flii and resulted in improved healing in preclinical animal models (Cowin *et al*., 2007; Jackson *et al*., 2012). Flii bound to FnAbs can still be detected through Immunofluorescent staining. In this chapter we showed that systemic injection of antibodies raised against specific domains of the Flii protein effectively reduced the expression of Flii protein in excisional wounds. These findings suggest that the prevention of Flii action by FnAbs may serve as an indication that there is a reduced presence of Flii in the wound at a later stage, suggesting a potential feedback mechanism.

Wound healing analysis showed that the excisional wounds in mice treated with FnAbs raised against either LRR or middle domain improved wound healing as confirmed by faster re-epithelialisation as well as reduced macroscopic wound area, and wound width. My findings also showed reduced neutrophils and higher number of anti-inflammatory M2 macrophages. Mice treated with either LRRFnAb or MFnAb were shown to have accelerated capillary tube formation and increased levels of pro-angiogenic factors including VEGF, FGF-2, and PDGF-BB compared to wounds of IgG treated animals.

The studies reported in this chapter showed that wounds in mice treated with MFnAb have increased rate of wound re-epithalisation and smaller wound width compared to LRRFnAb treated mice. This finding is in agreement with *in vitro* effects of MFnAb observed in studies reported in Chapter 3 where MFnAb treatment of keratinocytes and fibroblasts showed improved cellular healing responses (migration/proliferation) compared to treatment with LRRFnAb. Collectively, these findings suggest that the middle domain of Flii may play an important role in keratinocyte and fibroblasts activity and wound healing, although not all findings reached statistical

significance, certain cellular processes involved in wound repair showed trends suggesting an impact of LRRFnAbs.

Here I also showed that excisional wounds in mice treated with LRRFnAb and MFnAb resulted in a significant reduction in the inflammatory response that occurs during wound healing. Both systemically delivered LRRFnAb and MFnAb were found to reduce the number of neutrophils in the wounds compared to the control. This is consistent with previous studies in diabetic mice wounds which demonstrated that high levels of Flii in wounds result in increased inflammatory responses during healing of acute and chronic wounds. (Ruzehaji *et al*., 2014).

Studies have shown that an increased number of M1 macrophages which are present at the early stage of wound healing can drastically impair the process of injury repair (Hesketh *et al*., 2017). My findings revealed that the total number of macrophages was reduced in MFnAb treated mice, suggesting that Flii may be involved in the inflammatory response through its middle domain. The number of M1 macrophages showed a non-significant increase in LRRFnAb-treated mice, suggesting that the LRR of Flii may have an effect on the activation of M1 macrophages. M1-M2 macrophage polarization has been shown to improve healing and failure in the process of M1-M2 macrophage switch can lead to impaired healing as M2 macrophages are involved in the formation of granulation tissue and angiogenesis processes (Hesketh *et al*., 2017). In this study, the treatment of excisional wounds with systemically administered MFnAb has been associated with an increased presence of M2 macrophages, suggesting a potential promotion of the wound repair process. While the exact mechanisms underlying this observation require further investigation, it could be hypothesized that MFnAb treatment may enhance the retention or clearance dynamics of macrophage subtypes in the tissue, leading to a shift towards an M2 phenotype. Future studies should explore these mechanisms and provide evidence to support this hypothesis. The LRRFnAb treated mice also showed a minimal effect on M1/M2 polarization. These results are consistent with a recent study demonstrating that decreasing Flii levels leads to an earlier shift to M2 macrophages (Mills *et al*., 2022). The findings presented in this chapter showed that Flii may play a key role in inflammation via its middle domain, however, the antibodies against the LRR domain of Flii still had positive impacts on reducing inflammation.

Systemically administered LRRFnAb and MFnAb in mice with excisional wounds resulted in an increased presence of mature capillaries within the wound bed. Angiogenesis is one of the key

stages in wound healing and any failure in the process of angiogenesis results in delayed healing (Johnson and Wilgus, 2014). Previous studies have demonstrated that reducing the level of Flii protein using Matrigel plugs containing first generation FnAbs result in significantly increased development of blood vessels in murine wound models (Ruzehaji *et al*., 2014). My findings now show that systemic delivery of LRRFnAb and MFnAb promote angiogenesis within the wound, and this is supported by *in vitro* results which showed that addition of LRRFnAb and MFnAb to cultured dermal endothelial cells led to increased number of capillary tube formation as observed in Chapter 3.

Angiogenesis plays a key role in the formation of new granulation tissue and the growth of new capillaries. VEGF has a major impact on the proliferation of endothelial cells, and microvascular permeability, and is involved in the regulation of multiple endothelial integrin receptors in the process of new blood vessel formation (Rao *et al*., 2011). VEGF is essential in the survival of endothelial cells and has been found to enhance the migration of endothelial cells (Cascone *et al*., 2003; Soga *et al*., 2001).

My study revealed that mice with excisional wounds systemically treated with LRRFnAb and MFnAb significantly increased the expression of VEGF within the wound. The *in vitro* results demonstrated in Chapter 3 showed that LRRFnAb treatment improved the migration and proliferation of dermal endothelial cells while MFnAb treated endothelial cells showed significantly increased endothelial cell migration, both processes integral to the outcome of angiogenesis during wound repair. This may indicate that the effect upon endothelial cell recruitment could be due to increased VEGF expression.

FGF-2 is one of the most important proangiogenic factors involved in the formation of capillaries which is crucial in the progression of the wound healing (Barrientos *et al*., 2008). Studies have shown that FGF-2 is involved in VEGF expression, and it acts in synergy with multiple growth factors to enable growth of functional blood vessels (Lutolf and Hubbell, 2005). FGF-2 has also been shown to play an important role in wound re-epithelialization by increasing keratinocytes motility (Sogabe *et al*., 2006). Additionally, FGF-2 improves fibroblast migration and acts as a mitogen to produce collagenase which is essential during wound granulation tissue synthesis and collagen remodelling (Sasaki, 1992). FGF-2 has been found to accelerate tissue remodelling which

is vital for the wound healing process (Barrientos *et al*., 2008). Several studies have revealed that FGF-2 stimulates the proliferation of endothelial cells and promotes vessel repair during wound healing (Sahni and Francis, 2004; Seo *et al*., 2016). FGF-2 deficiency in endothelial cells has been shown to result in disruption of endothelial cell integrity (Seo *et al*., 2016).

Following IP injection of mice with LRRFnAb or MFnAb, wounds were found to have increased FGF-2 expression. LRRFnAb treatment promoted FGF-2 expression more effectively than MFnAb. These findings confirm the *in vitro* results which showed that LRRFnAb treated endothelial cells significantly stimulated both migration and proliferation of endothelial cells while the MFnAb treated cells stimulated improved migration of endothelial cells as reported in Chapter 3.

PDGF-BB which is known as the best-defined member of the PDGF family is released from several cells within the wound site. PDGF-BB can regulate the process of wound healing as it is highly involved in modulating inflammatory responses, migration and proliferation of dermal cells, as well as collagen deposition (Jian *et al*., 2022). PDGF-BB acts as a major pro-angiogenic factor by stimulating VEGF production and inducing the regulation of endothelial cell migration and proliferation in the formation of capillaries (Sufen *et al*., 2011).

The expression of PDGF-BB was found to be elevated in excisional wounds of mice treated with LRRFnAb and MFnAb 7 days post-injury showing that inhibiting the activity of Flii using antibodies against different parts of Flii protein can lead to improved production of PDGF-BB which is a major angiogenic factor. FGF-2 and PDGF-BB have a synergistic effect on the expression of VEGF (Sufen *et al*., 2011). Systemic injection of LRRFnAb was shown to promote PDGF-BB expression more effectively in wounds compared to MFnAb treated mice which is consistent with the impact of LRRFnAb on the production of FGF-2 in excisional wounds and *in vitro* findings regarding the effect of this antibody on proliferation and migration of endothelial cells as reported in Chapter 3. Although the higher expression of VEGF was expected due to the higher expression of PDGF-BB and FGF-2 in LRRFnAb treated mice compared to MFnAb treated group, my findings revealed that the production of VEGF was higher in MFnAb treated mice. This may reflect complexity of VEGF expression which has been found to be mediated by multistep mechanisms and various pro-angiogenic factors (Johnson and Wilgus, 2014).

In conclusion, taken together these results suggest that IP injection of either LRRFnAb or MFnAb improve wound healing with reduced dermal wound gape and increased re-epithelialisation. Attenuated Flii provided by antibodies reduced inflammation and stimulated VEGF expression and endothelial capillary tube formation. IP injected MFnAb demonstrated a stronger impact on the reduction of inflammation as this antibody, by acting on Flii, led to a decrease in the number of neutrophils at the wound site and promoted M1-M2 macrophage polarization, which is important in the process of healing. Systemic delivery of LRRFnAb was found to have a more stimulatory impact on the production of pro-angiogenic factors such as FGF-2, and PDGF-BB in comparison with IP injected MFnAb suggesting that the LRR domain of Flii may be involved in the regulation of pro-angiogenic factors during wound healing, although further investigation is needed to fully elucidate the specific binding interactions of Flii with different receptor types.

Overall, these results suggest that systemically administered LRRFnAb and MFnAb can improve healing outcomes via effects on tissue inflammation and angiogenesis and the clinical application of Flii monoclonal antibodies could therefore be a potential approach for accelerating skin wound healing.

Chapter 5: Systemically administered FnAbs are effective at improving burn repair in a mouse model of partial-thickness scald injury

5.1 Introduction

Severe burn injury is one of the most painful and devastating injuries, and it can lead to high rates of morbidity and mortality (Pereira *et al*., 2013). The conventional treatment for severe burn patients is focused on improving overall health outcomes and is comprised of: i) early burn wound excision and ii) skin grafting by which the mortality rate and the length of hospital stay are significantly reduced (Wood, 2014). Despite these health improvements for burn patients, the slow process of healing, infection, pain, and hypertrophic scarring are still considerable clinical challenges in management of burn injuries (Wang *et al*., 2018). Moreover, although advancements in wound dressings have been made in the past, it is important to recognize the inherent challenges of wound healing, particularly in the context of burn injuries. These complex injuries require the exploration of novel approaches to further improve the healing process (Marshall *et al*., 2018).

Increased expression of Flii has been observed in human burn wounds (Cameron *et al*., 2016) and intradermal injection of first generation FnAbs (FliiL FnAbs) to murine partial-thickness scald burns led to a significant improvement in the appearance of the burn wounds (Adams *et al*., 2009). Additionally, the expression of pro-scarring TGF-β1 was reduced, while anti-scarring TGF-β3 was increased following intradermal injection of FliiL FnAbs (Adams *et al*., 2009). The injection of FliiL FnAb into scars induced by bleomycin also improved scar formation and reduced dermal thickness in a murine model of hypertrophic scarring (Cameron *et al*., 2014). Although intradermal delivery of FliiL FnAbs in preclinical animal models of burn and hypertrophic scarring has resulted in improved wound healing, this is not a clinically feasible approach for management of large burn injuries which tend to cover large surface areas of body and affect joints and bony protuberances (Ladak and Tredget, 2009; Marshall *et al*., 2018). Therefore, developing a systemic antibody therapy could improve healing for these patients. Therapeutic monoclonal antibodies (mAbs) provide direct targeting with high specificity for the target protein (Turner *et al*., 2015a); however, systemic administration of these antibodies may increase the risk of off-target effects (Kim and De Jesus, 2022). Systemic administration of FnAbs may be an effective approach for patients with large burn injuries but there is a clear need to determine localization of FnAbs (Kim and De Jesus, 2022).

As previously discussed in Chapter 4, the impact of systemic delivery of FnAbs raised against specific domains of Flii on excisional wounds was investigated. Excisional wounds have been found to heal faster and have a higher rate of re-epithelialisation than burn wounds (Jabeen *et al*., 2019; Monsaingeon and Molimard, 1976). Burns also have more inflammatory cells including neutrophils and macrophages and worse scarring in comparison with excisions of the same depth (Jabeen *et al*., 2019). Mouse burn models are valuable tools for studying wound healing processes. The method used to induce burns plays a significant role in determining the healing outcomes(DiPietro and Burns, 2003). Scalding with constant hot water is particularly advantageous as it uniformly covers the exposed skin surface, regardless of surface variations (DiPietro and Burns, 2003).

This chapter describes the development of a simple systemic, injectable antibody therapy that promotes healing following scald burn injury in mice. Specifically, this study aimed to investigate the ability of systemically delivered LRRFnAbs and MFnAbs to accumulate within burn wounds and then the efficacy of FnAbs generated against different regions of Flii on repair processes while delivered systemically to mice with burns. The effects of systemically administered FnAb on critical wound healing parameters including inflammation and angiogenesis in mice with burn injury was also investigated.

5.2 Results

5.2.1 IP injected FnAbs localized to the site of burn injury

In order to investigate if systemically administered LRRFnAb and MFnAb localised to the burn wound and local surrounding area, the mice were subjected to an antibody localization trial following established protocols as detailed in Chapter 2. Briefly, IgG, LRRFnAb, and MFnAb antibodies were labelled using a Rapid Antibody Labeling Kit, Alexa Fluor™ 680 for *in vivo* imaging of murine burn models when treated with systemic administration of treatment (LRRFnAb and MFnAb) and control (IgG) antibodies. Fluorescence radiance efficiency was then calculated in the burn region in FnAbs treated and IgG treated mice using IVIS Lumina S5 Imaging System.

Fluorescent radiance efficiency measurements showed that both IP injected Alexa-Fluor-680-LRRFnAbs and Alexa-Fluor-680-MFnAbs localized to the site of burn injury from day 1 and remained at site of healing burn wounds for the 7-day study period (Figure 5.1). The yellow colour illustrated that more labelled antibody accumulated within the burn wound, while red colour represented that lower level of antibody localized into the burn site (Figure 5.1). Fluorescent radiance efficiency measurements revealed that fluorescent intensity in Alexa-Fluor-680-LRRFnAb treated mice was significantly increased in comparison with mice treated with Alexa-Fluor-680-IgG antibody on days 1 and 7 of the study (Figure 5.2). Fluorescent intensity was also significantly elevated in burns of mice treated with Alexa-Fluor-680-MFnAb compared to IgG treated controls in burns at each study time point (Figure 5.2). The antibody localization results indicated that higher level of both fluorescently labelled FnAbs raised against either LRR or middle domain of Flii protein were in burn wounds when compared to IgG treated controls over a seven-day study period.

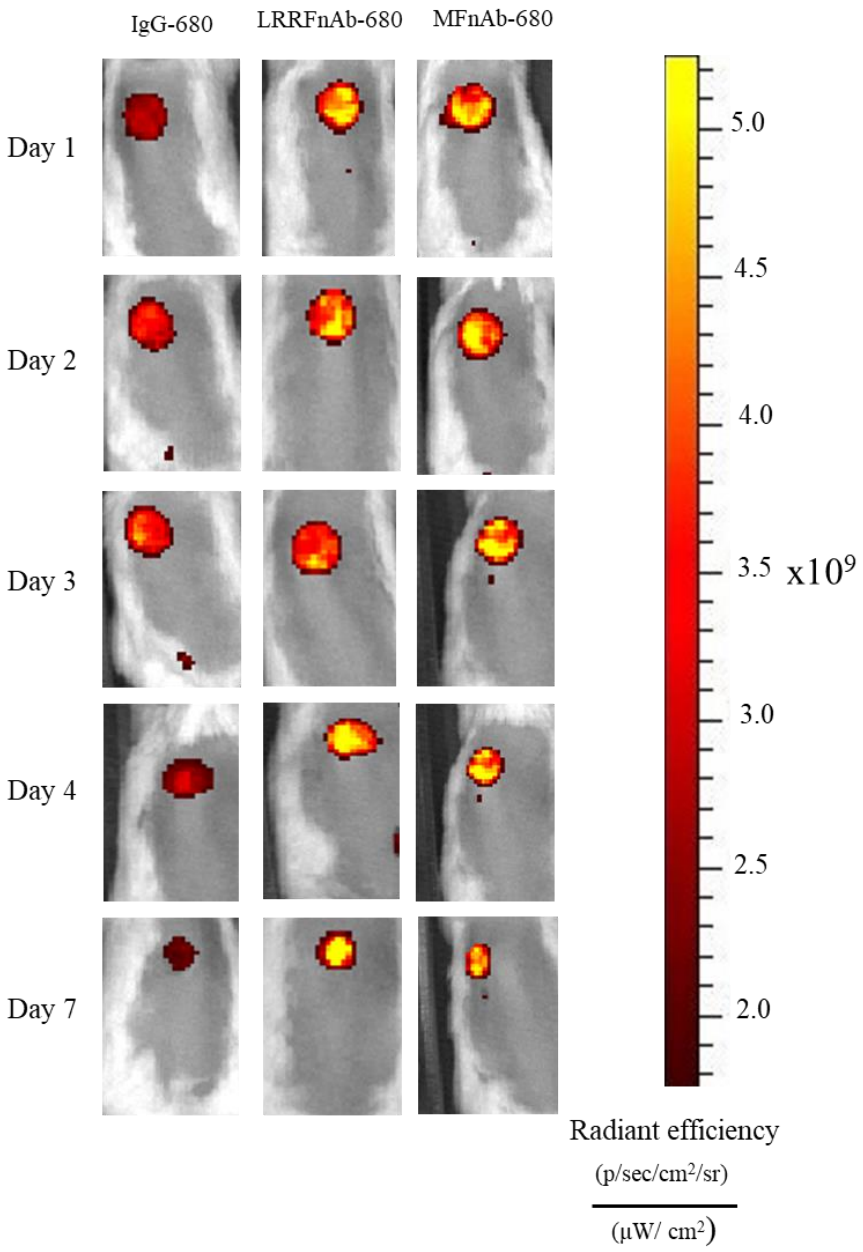


Figure 5. 1: Localization of systemically administered LRRFnAb and MFnAb in murine burn wounds

Representative images of Alexa fluor-680 –labelled LRRFnAb (5 mg/kg), MFnAb (5 mg/kg), and IgG (5 mg/kg) distribution when systemically delivered (single dose on day 0) to murine burn models. Images were captured using the IVIS Lumina imaging system on days 1, 2, 3, 4, and 7 before burn tissue collection. n=10.

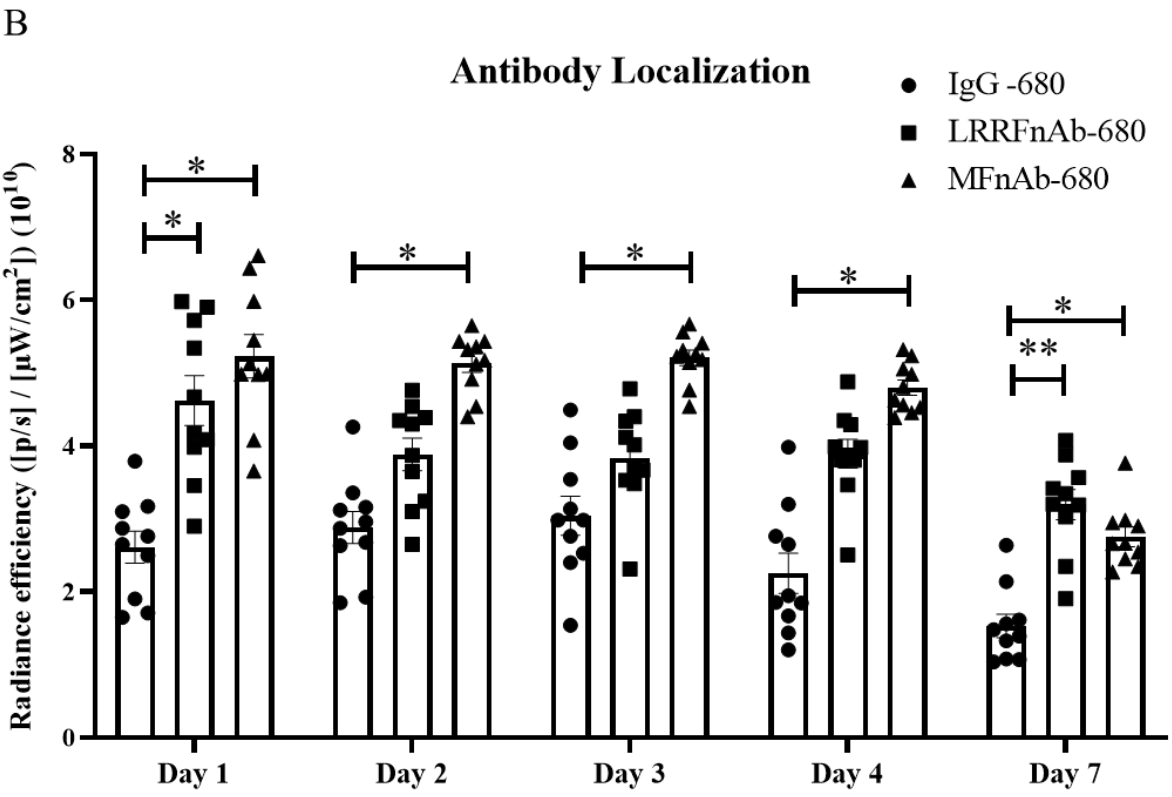


Figure 5. 2: Antibody localization of systemically administered LRRFnAb and MFnAb in murine burn wounds

Measurement of fluorescence radiance efficiency in burn wounds in LRRFnAb and MFnAb treated mice and analysis of wound-specific intensity in comparison with IgG treated mice over the 7-day course of the study. The fluorescent intensity in LRRFnAb and MFnAb treated mice was significantly elevated in comparison with IgG treated mice. n = 10. All data are represented as mean ± SEM. Statistical significance was calculated by two-way ANOVA and Tukey's post-tests. *= $p < 0.05$, **= $p < 0.01$.

5.2.2 Effects of LRRFnAb and MFnAb treatment on wound healing in mice

Wound healing assessments were also carried out on the burns in mice treated systemically with LRRFnAb, MFnAb and compared to IgG control. Macroscopic measurements were performed using digital images taken on days 0, 3, 4, and 7 during the study (Figure 5.3A). The burn wound area at different time points of the trial was measured and normalized to the original burn wound at day 0 for each animal. LRRFnAb treatment did not show significant improvement in healing outcomes. While there was a non-significant increase of 6.0% ± SEM in the average size of burn wound area in animals treated with systemic LRRFnAb compared to IgG treated control mice (Figure 5.3B). In contrast, analysis showed a non-significant reduction of 7.1% ± SEM in the average size of the burn wound area in mice treated with MFnAb compared to the control group at the 7-day post-surgery (Figure 5.3B).

H&E-stained tissue sections were also assessed for microscopic examination of wound healing (Figure 5.4 A). The average wound width was not altered in LRRFnAb treated mice in comparison with IgG treated animals, while the wound width was non-significantly decreased by 8.7% ± SEM in MFnAb treated mice 7 days post-injury (Figure 5.4B). The average percent of re-epithelialisation on day 7 of the study was non-significantly reduced by 9.9% ± SEM in LRRFnAb mice compared to IgG and MFnAb treated mice (Figure 5.4C). H&E measurements also indicated a trend towards an increase by 6.2% ± SEM in the rate of re-epithelialisation in MFnAb treated mice in comparison with mice treated with control antibody on day 7 of healing, although this was not statistically significant (Figure 5.4C).

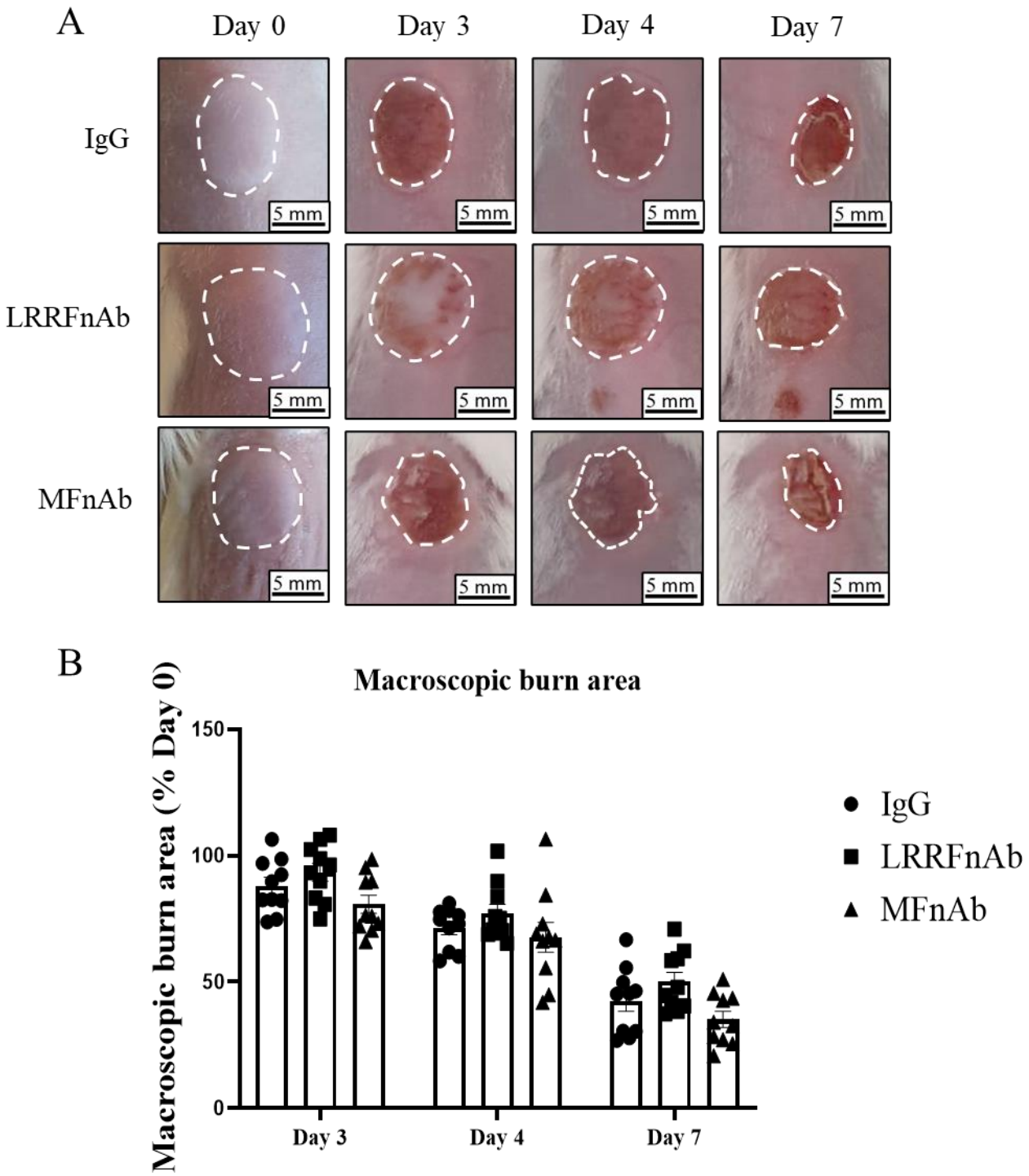

A
Day 0
Day 3
Day 4
Day 7
IgG
LRRFnAb
MFnAb
5 mm
B
Macroscopic burn area
Macroscopic burn area (% Day 0)
150
100
50
0
Day 3
Day 4
Day 7
IgG
LRRFnAb
MFnAb

Figure 5. 3: Macroscopic assessment: Effect of IP injected LRRFnAb and MFnAb on the rate of burn injury healing

A) Representative images of burn wounds in mice treated with LRRFnAb, MFnAb, and IgG on days 0, 3, 4 and 7 of healing. B) Measurement of macroscopic wound area using Image Pro-Plus software illustrates a non-significant decrease in the macroscopic wound area in MFnAb treated mice on days 3,4, and 7. n = 10. All data are represented as mean ± SEM. Statistical significance was calculated by two-way ANOVA and no significant differences were observed.

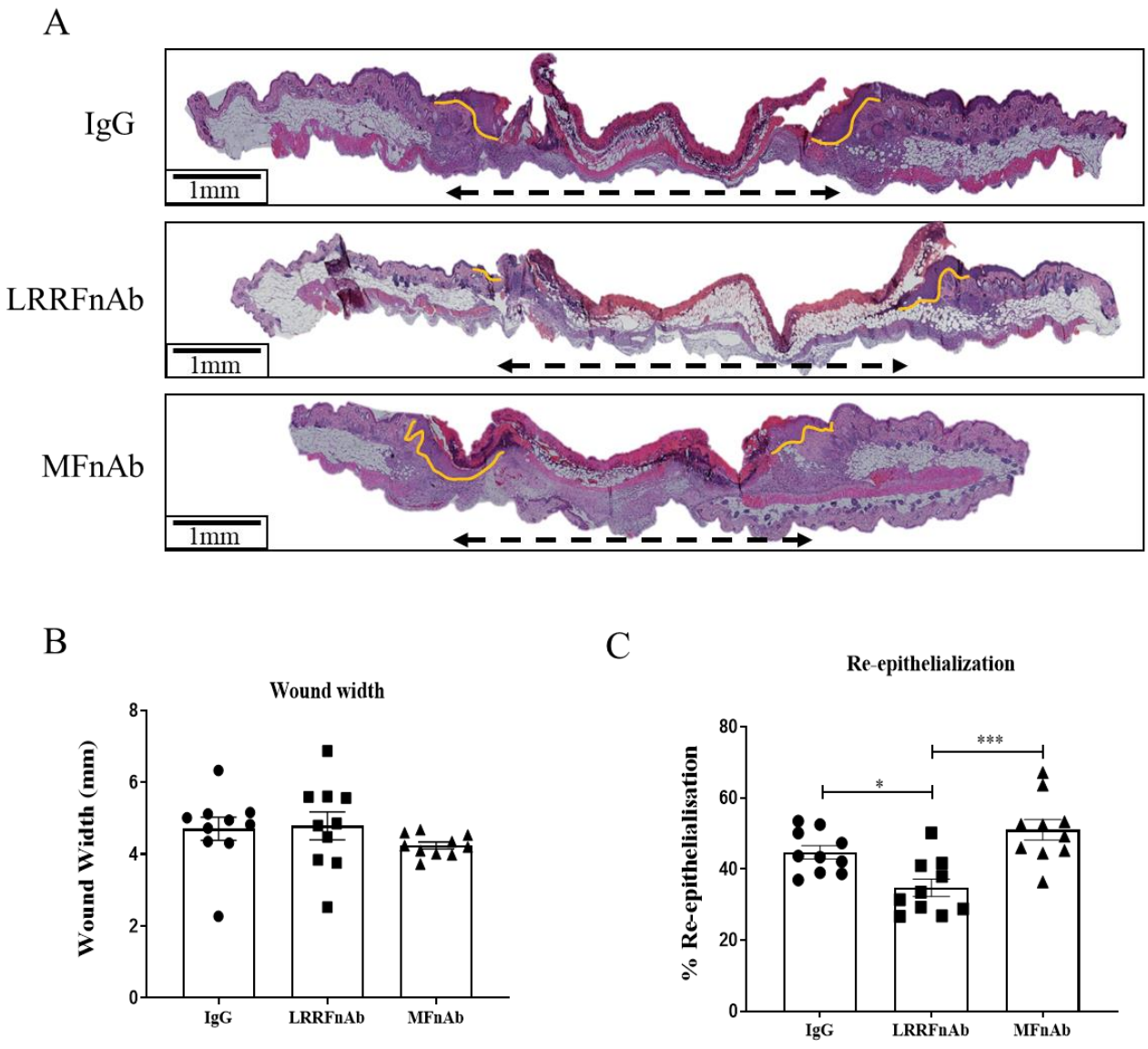


Figure 5. 4: Histological assessment: Effect of LRRFnAb and MFnAb on the rate of burn injury healing

A) Representative images of LRRFnAb and MFnAb treated and control following Hematoxylin and eosin staining, 7 days post-burning. Images captured using a 10X objective. Black dashed lines demonstrate wound width measured. Yellow lines indicate re-epithelialisation measured B) Histological analysis of wounds displays reduced wound width in MFnAb treated mice. C) Quantification of re-epithelialisation demonstrates increased average re-epithelialisation in MFnAb treated mice. n = 10. All data are represented as mean ± SEM. Statistical significance calculated by one-way ANOVA and Tukey's post-tests. *= $p < 0.05$, ***= $p < 0.001$.

5.2.3 Systemically administered MFnAb significantly reduced the expression level of Flii in the burn area

Studies have shown that Flii protein is constitutively secreted by fibroblasts and macrophages and is found in human plasma (Lei *et al*., 2012). Secretion of Flii has been found to be increased in response to injury and this upregulation of Flii impairs the process of healing (Cameron *et al*., 2016; Lei *et al*., 2012). To attenuate the effect of Flii on wound repair, a single dose of LRRFnAbs and MFnAb was delivered systemically to mice following burn creation.

To investigate the effect of systemic administration of LRRFnAbs and MFnAbs on the expression of Flii in mouse burns, immunostaining for Flii was performed (Figure 5.5A). The expression of Flii protein within the wound bed was significantly decreased by 27.2% ± SEM in mice treated with MFnAb compared to IgG control mice (Figure 5.5B). The results also demonstrated a trend towards a 17.0% ± SEM reduction in the expression of Flii in LRRFnAb treated mice compared to mice treated with the IgG antibody (Figure 5.5B).

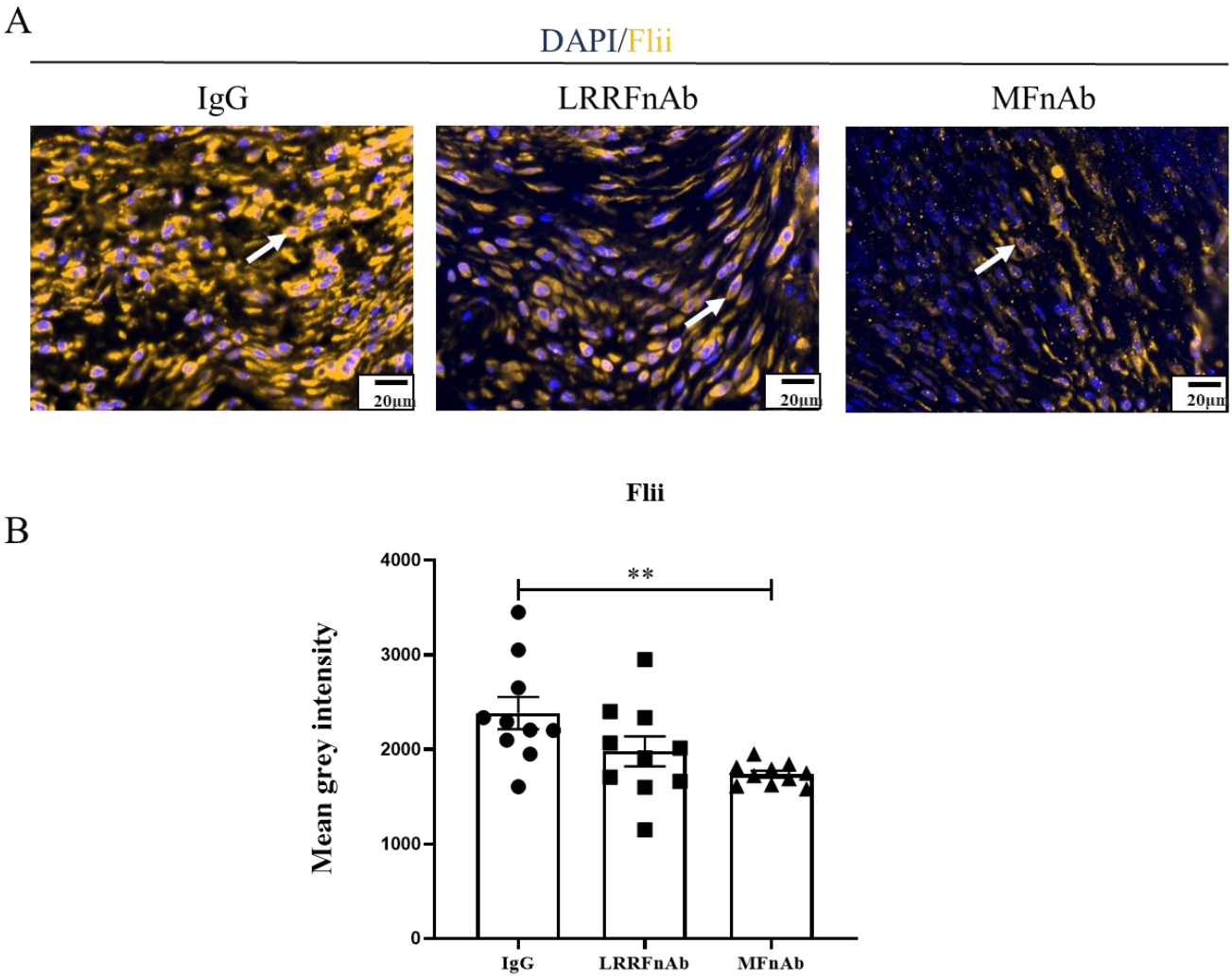


Figure 5. 5: Effect of LRRFnAb and MFnAb on Flii expression

A) Immunofluorescence detection of Flii (yellow) counterstained with DAPI (blue) in LRRFnAb and MFnAb treated mice at day 7 post-injury. The primary antibody used was Rabbit Flii antibody, and for the secondary antibody, goat anti-Rabbit IgG was employed. The entire wound bed was encompassed in the analysis. Images captured using a 20X objective B) Quantification of Flii expression as mean grey intensity. Flii expression was significantly decreased in MFnAb treated mice. n = 10. All data are represented as mean ± SEM. Statistical significance was calculated by one-way ANOVA and Dunnett's post-tests. **= p <0.01.

5.2.4 The number of myofibroblasts was elevated in the dermis of MFnAb treated mice

Myofibroblasts are essential for the wound contraction that takes place in the proliferative phase of the wound healing process (Tomasek *et al*., 2002). To investigate the impact of FnAbs raised against LRR and middle domains of Flii on the number of myofibroblasts, the burn wounds were subsequently stained for α-SMA. Myofibroblasts are responsible for the expression of α-SMA, and this factor has been a consistent marker for myofibroblasts (Sun *et al*., 2016) (Figure 5.6A). Quantification of α-SMA positive cells indicated a significant increase in the number of myofibroblasts in MFnAb treated mice in comparison with mice treated with IgG (Figure 5.6B). Also, immunofluorescent assessments revealed that the number of myofibroblasts were non-significantly elevated by 13.8% ± SEM within the wound bed in LRRFnAb treated mice compared to the control group (Figure 5.6B).

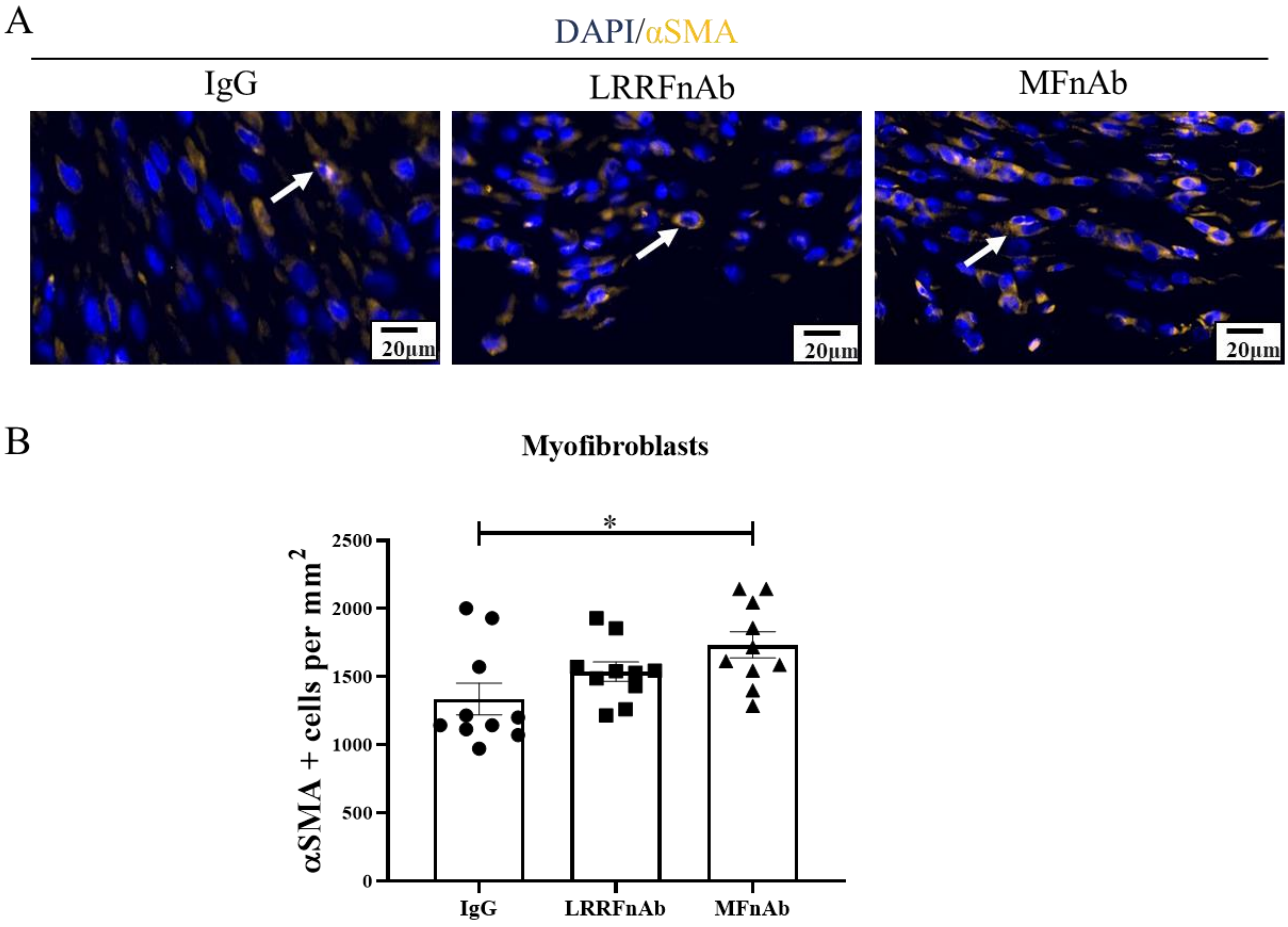


Figure 5. 6: Effect of LRRFnAb and MFnAb on myofibroblasts in the partial-thickness burns

A) Immunofluorescence detection of myofibroblasts using staining of αSMA (yellow) counterstained with DAPI (blue) in LRRFnAb and MFnAb treated mice at day 7 post-injury. Mouse anti- αSMA antibody served as the primary antibody for αSMA, with Goat anti-Mouse IgG used as the secondary antibody. The entire wound bed was encompassed in the analysis. Images captured using a 20X objective B) Quantification of myofibroblasts in the wound bed normalized to the burn area. The number of myofibroblasts was elevated in MFnAb treated mice. n = 10. All data are represented as mean ± SEM. Statistical significance was calculated by one-way ANOVA and Dunnett's post-tests. *= $p < 0.05$.

5.2.5 Systemic delivery of LRRFnAb and MFnAb attenuated local inflammation in burn wounds

NIMP-R14 marker of neutrophils as indicative of inflammation was used to investigate the impact of systemic administration of specific FnAbs generated against different domains of Flii protein on inflammation (Figure 5.7A). As shown in Figure 5.7B, the number of neutrophils was significantly reduced in both LRRFnAb (by 21.3% ± SEM) and MFnAb (by 30.1% ± SEM) treated mice in comparison with control mice at day 7 post burn surgery.

Macrophage infiltration was quantified using immunostaining for F4/80 which is a marker for M1macrophages (Figure 5.8A). Quantification of macrophage infiltration revealed that the total number of F4/80 positive macrophages was significantly reduced in mice treated with both FnAbs raised against either LRR or middle domain (Figure 5.8B). Additionally, examining the macrophage phenotype ratio showed that the percentage of M2 anti-inflammatory macrophages which express both F4/80 and Ym-1 in both LRRFnAb and MFnAb treated mice was significantly elevated by 26.2% ± SEM and 21.0% ± SEM respectively compared to mice treated with IgG (Figure 5.8C).

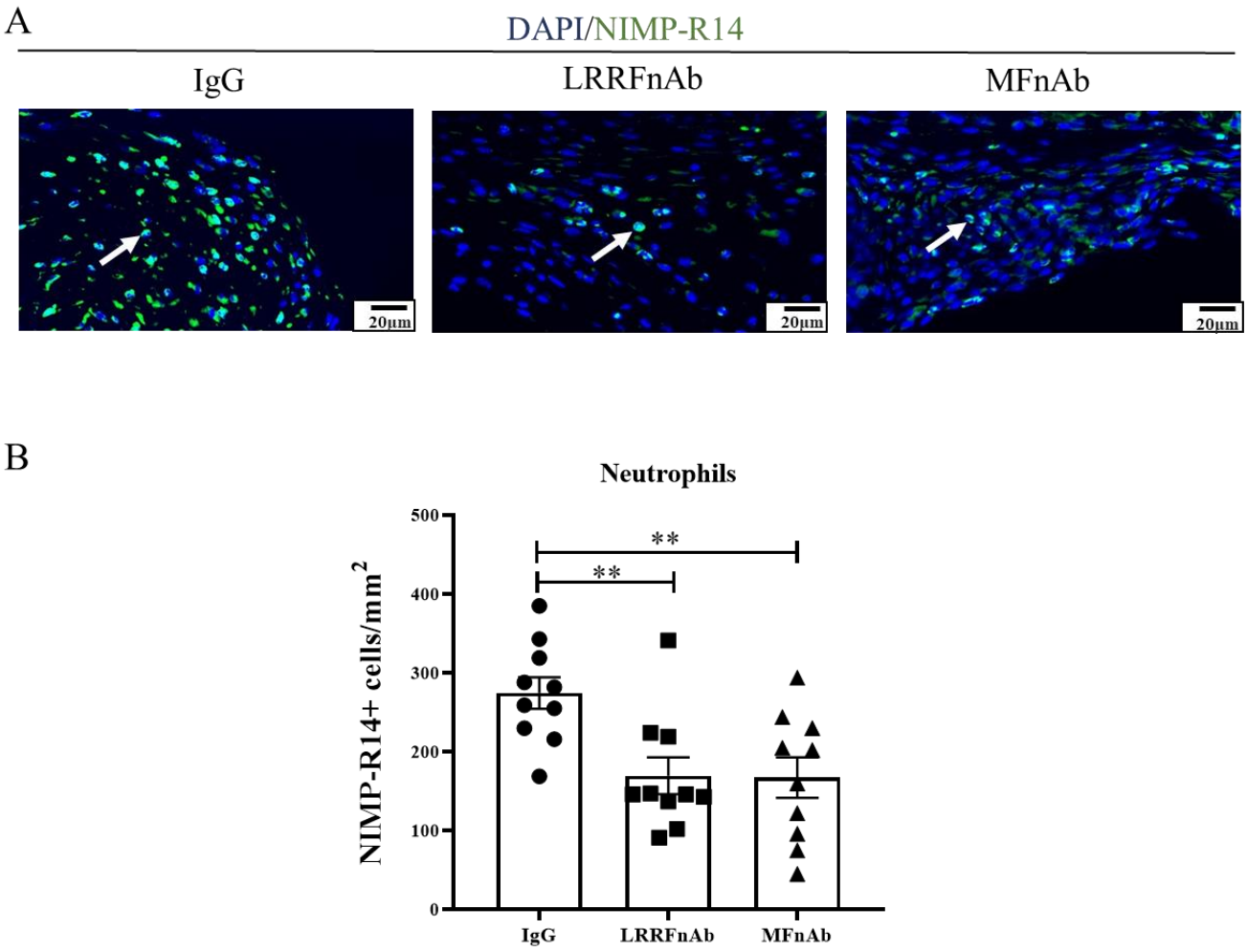


Figure 5. 7: Impact of LRRFnAb and MFnAb on neutrophil infiltration in the deep dermis

A) Immunofluorescence detection of NIMP-R14 neutrophils (green) counterstained with DAPI (blue) in LRRFnAb and MFnAb treated mice at day 7 post-injury. The primary antibody used was Rat monoclonal Neutrophil Marker antibody, and for the secondary antibody, Goat anti-Rat IgG was employed. The entire wound bed was encompassed in the analysis. Images captured using a 20X objective B) Quantification of neutrophil numbers in the wound bed, normalized to area. The number of neutrophils within the wound bed was decreased in LRRFnAb and MFnAb treated mice 7 days post-wounding. n = 10. All data are represented as mean ± SEM. Statistical significance was calculated by one-way ANOVA and Tukey's post-tests. **= $p < 0.01$.

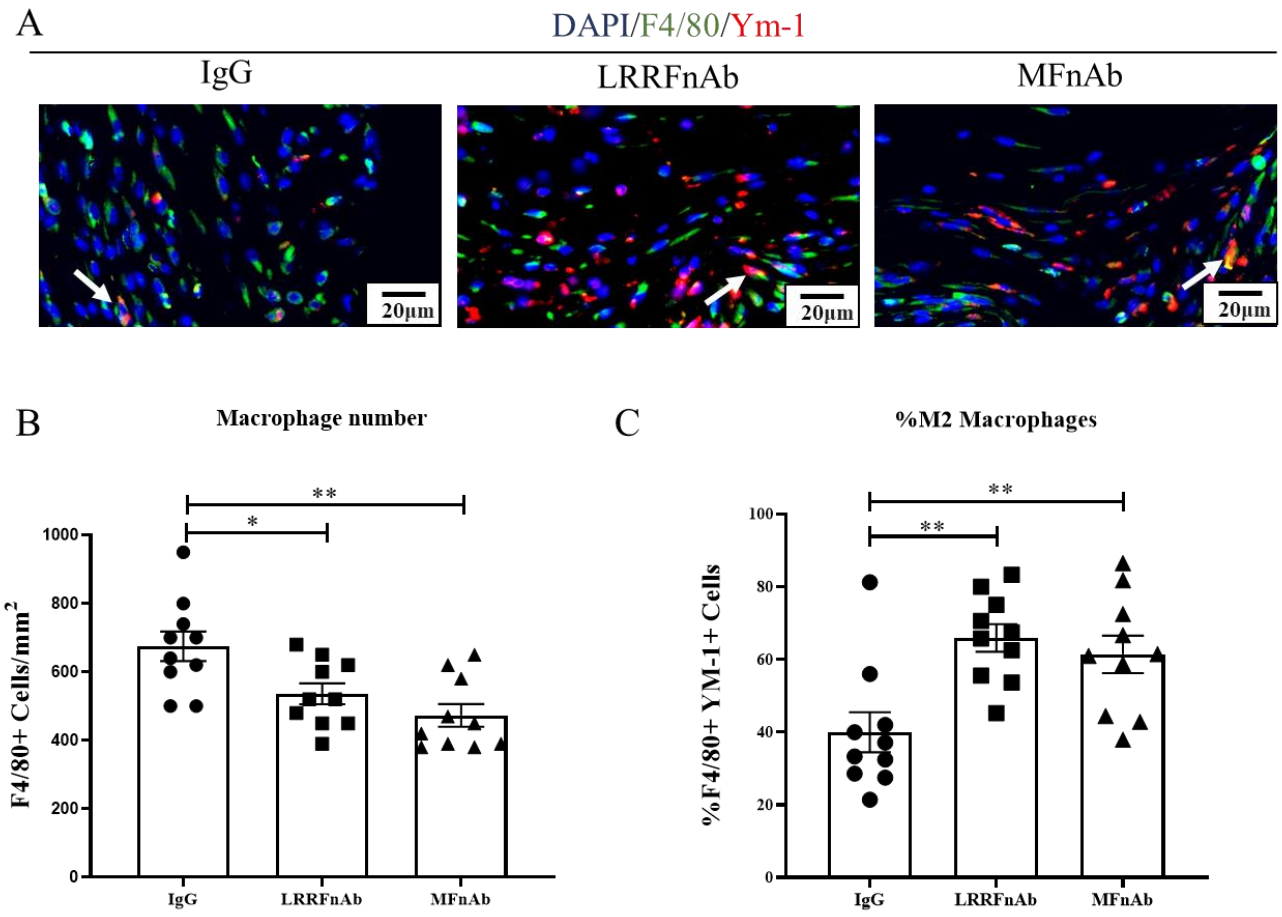


Figure 5. 8: Impact of LRRFnAb and MFnAb on macrophage infiltration and polarization in the burn site

A) Representative images of immunofluorescence staining of macrophages using F4/80 (green) and YM-1 (Red) markers counterstained with DAPI (blue) in LRRFnAb and MFnAb treated mice at day 7 post-burn injury. In the analysis, the primary antibody used for F4/80 was Rat anti-Mouse F4/80 antibody, and for the secondary antibody, Goat anti-Rat IgG was employed. Additionally, Rabbit anti-Ym1 antibody served as the primary antibody for YM-1, with Goat anti-Rabbit IgG used as the secondary antibody. The entire wound bed was encompassed in the analysis. Images captured using a 20X objective B) Quantification of total macrophage number (F4/80+) within the wound bed normalized to the wound area. The number of macrophages infiltrating the wound site decreased in MFnAb and LRRFnAb treated mice C) Quantification of M2 macrophages (F4/80+, YM-1+) as a percentage of total macrophages within the wound bed

normalized to the wound area. The ratio of M2 macrophages was increased in LRRFnAb and MFnAb treated mice. n = 10. All data are represented as mean ± SEM. Statistical significance was calculated by one-way ANOVA and Dunnett's post-tests. *= $p < 0.05$, **= $p < 0.01$.

5.2.6 Systemic delivery of LRRFnAb and MFnAb increased the number of endothelial cells in the burn wounds

In order to explore the effect of systemic delivery of specific FnAbs generated against LRR and middle domain of Flii on the presence of endothelial cells, total number of $CD31^+$ cells within the wound bed was calculated by immunofluorescent staining of CD31 as a marker of endothelial cells (Figure 5.9A). As shown in Figure 5.9B, the quantification of endothelial cells revealed a significant increase in the number of CD31 positive endothelial cells within the wound bed treated with both LRRFnAbs (by 23.9% ± SEM) and MFnAbs (28.5% ± SEM) in comparison with control mice 7 days post-burning.

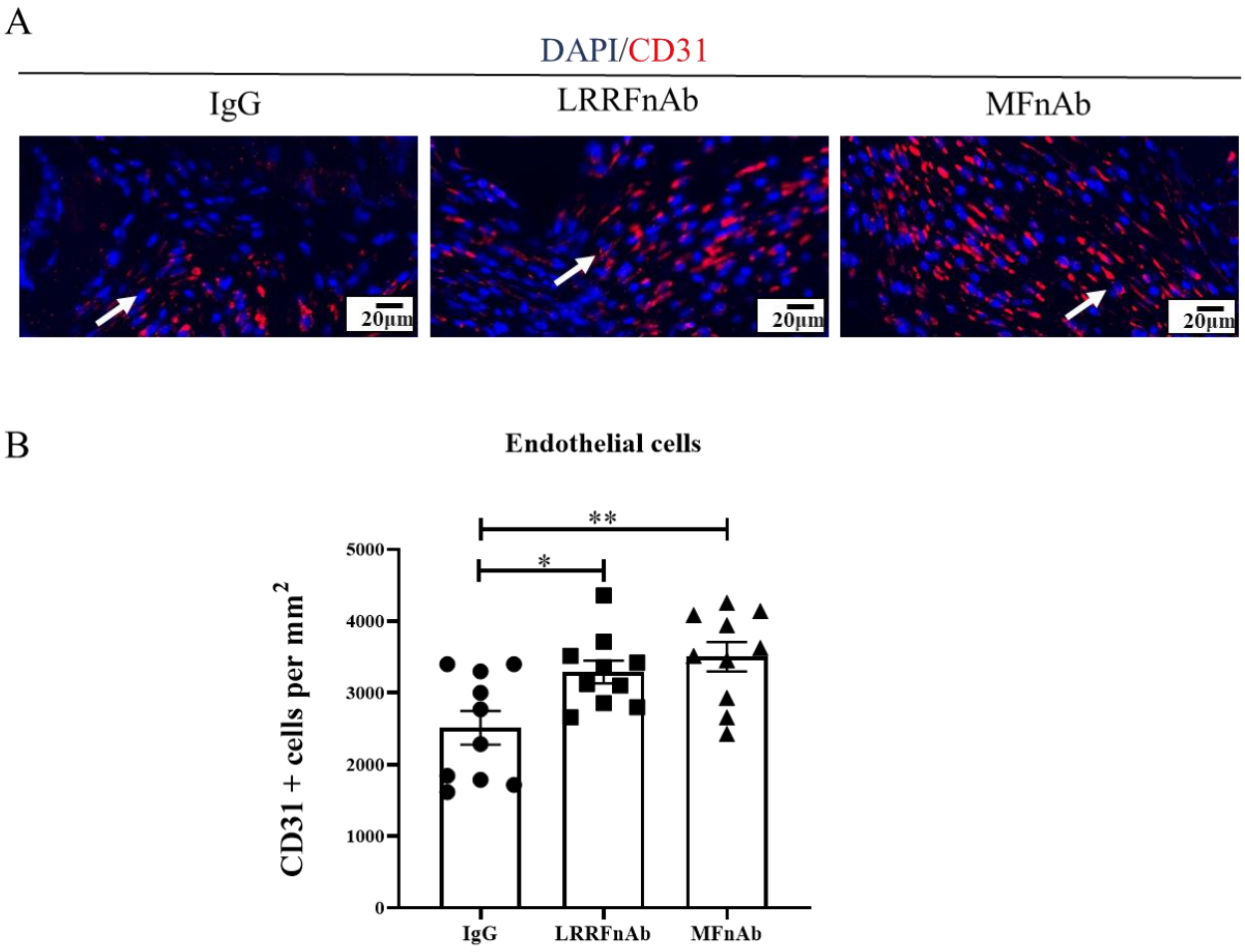


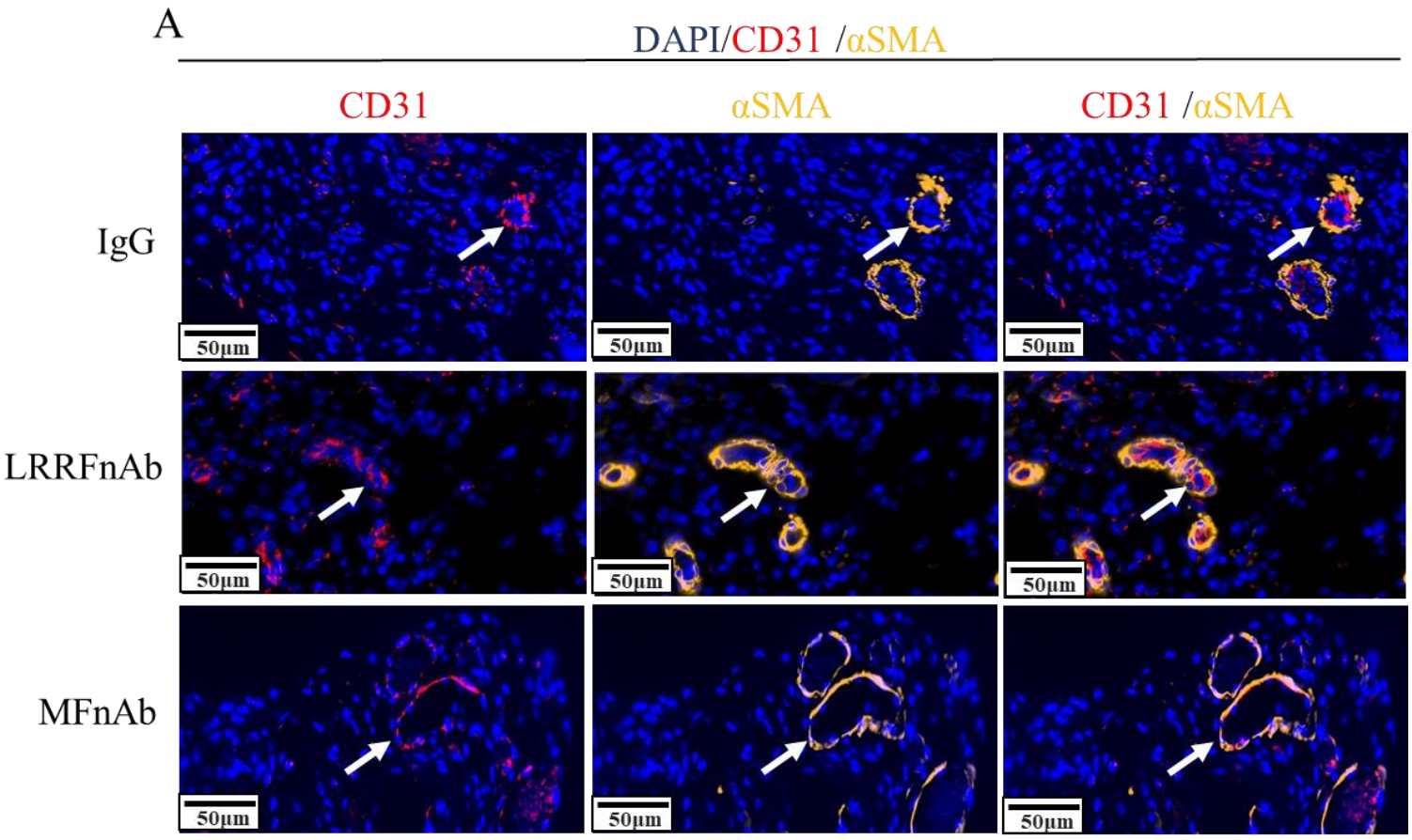
Figure 5. 9: Effect of LRRFnAb and MFnAb on endothelial cells in the partial-thickness burns

A) Immunofluorescence detection of endothelial cells using staining of CD31 (red) counterstained with DAPI (blue) in LRRFnAb and MFnAb treated mice at day 7 post-injury. In the analysis, the primary antibody used for CD31 was Rabbit anti- CD31 antibody, and for the secondary antibody, Goat anti-Rabbit IgG was employed. The entire wound bed was encompassed in the analysis. Images captured using a 20X objective B) Quantification of endothelial cells in the wound bed normalized to the burn area. The number of endothelial cells was elevated in LRRFnAb and MFnAb treated mice. n = 10. All data are represented as mean ± SEM. Statistical significance was calculated by one-way ANOVA and Dunnett's post-tests. *= $p < 0.05$, **= $p < 0.01$.

5.2.7 The number of mature blood vessels was elevated in LRRFnAb treated mice

Re-establishment and creation of new blood vessels play an important role in wound healing as oxygen, nutrients, and immune cells are carried through blood vessels to damaged and infected tissues (Lee *et al*., 2016; Morton and Phillips, 2012). Angiogenesis also plays an important role in the delivery of immune cells during the process of wound healing (Tonnesen *et al*., 2000).

Blood vessels density was quantified using immunohistochemistry for CD31 and α-SMA (Figure 5.10A). Co-staining of cells for both CD31+ α-SMA provide a more specific identification of mature blood vessels as CD31 is expressed by endothelial cells and α-SMA can represent microvascular pericytes (Morikawa *et al*., 2002). The results revealed that systemic delivery of LRRFnAb significantly promoted capillary tube formation by 58.3% ± SEM in the burn area compared to IgG treated mice 7 days post-injury (Figure 5.10B). Angiogenesis was also non-significantly enhanced by 34.7% ± SEM in MFnAb treated mice in comparison with the control group (Figure 5.10B).


A
DAPI/CD31 /αSMA
CD31
αSMA
CD31 /αSMA
IgG
LRRFnAb
MFnAb
50μm

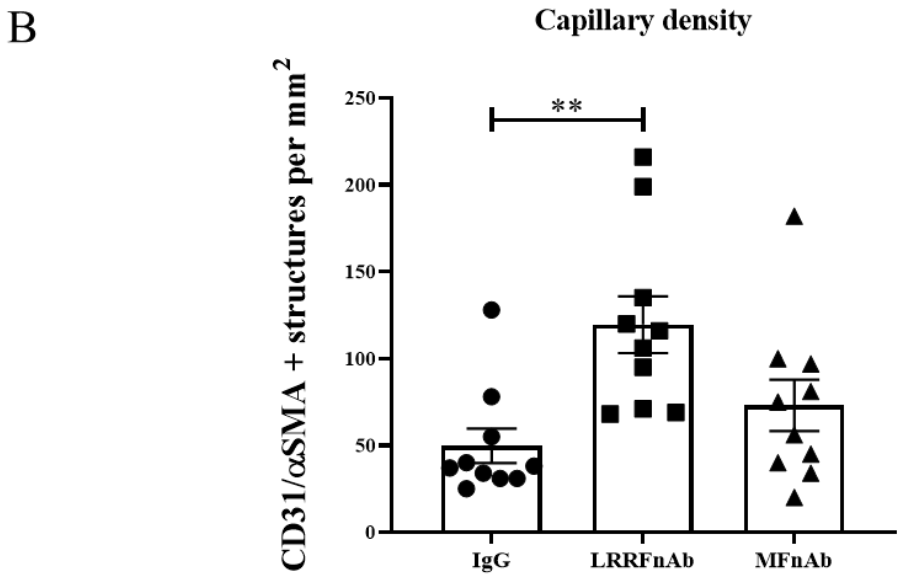

B
Capillary density
CD31/αSMA + structures per mm2
250
200
150
100
50
0
**
IgG
LRRFnAb
MFnAb

Figure 5. 10: Impact of systemic delivery of LRRFnAb and MFnAb on angiogenesis in burns

A) Immunofluorescence detection of mature blood vessels using staining of CD31 (red) and αSMA (yellow) counterstained with DAPI (blue) in LRRFnAb and MFnAb treated mice at day 7 post-injury. In the analysis, the primary antibody used for CD31 was Rabbit anti- CD31 antibody, and for the secondary antibody, Goat anti-Rabbit IgG was employed. Additionally, Mouse anti- αSMA antibody served as the primary antibody for αSMA, with Goat anti-Mouse IgG used as the secondary antibody. The entire wound bed was encompassed in the analysis. Images captured using a 20X objective B) Quantification of mature blood vessels in the wound bed normalized to the wound area. The average number of blood vessels was increased in LRRFnAb burn mice. n = 10. All data are represented as mean ± SEM. Statistical significance was calculated by one-way ANOVA and Dunnett's post-tests. **= $p < 0.01$.

5.2.8 Systemic delivery of LRRFnAb and MFnAb promoted the expression of VEGF within the burn wound

Vascular Endothelial Growth Factor (VEGF) plays a key role in the migration, proliferation, and survival of endothelial cells and is described as the most potent regulator of angiogenesis (Koch *et al*., 2011). The impact of MFnAb and LRRFnAb on VEGF expression was investigated using immunofluorescent staining for VEGF in mouse burns (Figure 5.11A). The amount of VEGF in burn wounds was significantly increased by 20.3% ± SEM in LRRFnAb treated mice in comparison with the control group at day 7 post burn injury (Figure 5.11B). The results also showed that VEGF expression was elevated by 23.0% ± SEM in MFnAb treated mice compared to IgG treated mice (Figure 5.11B).

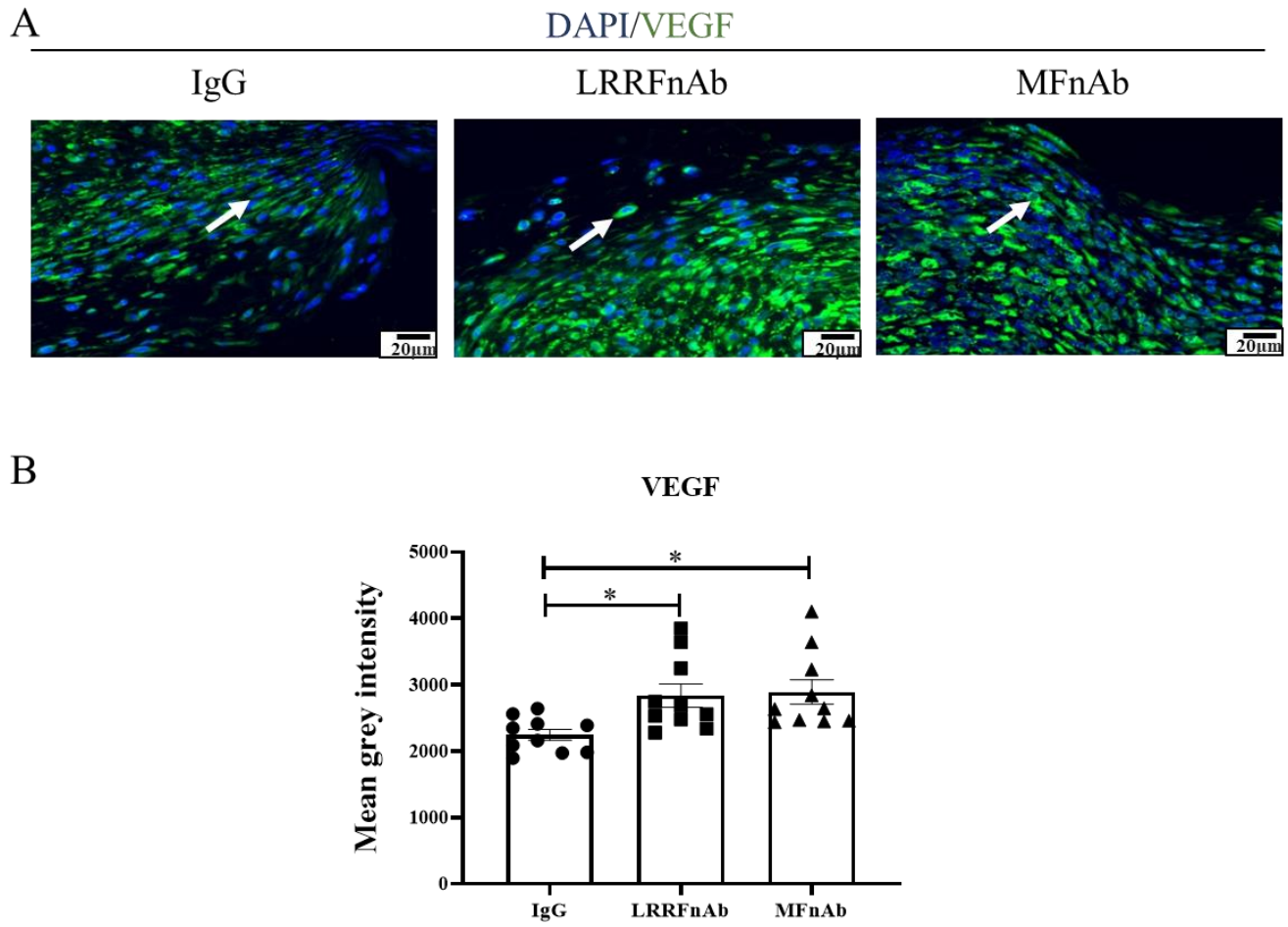


Figure 5. 11: Effect of LRRFnAb and MFnAb on VEGF expression

A) Immunofluorescence detection of VEGF (green) counterstained with DAPI (blue) in LRRFnAb and MFnAb treated mice at day 7 post-injury. The primary antibody used was Rabbit anti-VEGFA antibody, and for the secondary antibody, Goat anti-Rabbit IgG was employed. The entire wound bed was encompassed in the analysis. Images captured using a 20X objective B) Quantification of VEGF expression as mean grey intensity in the wound bed normalized to the burn area. The expression of VEGF was elevated in LRRFnAb and MFnAb treated mice. n = 10. All data are represented as mean ± SEM. Statistical significance was calculated by one-way ANOVA and Dunnett's post-tests. *= $p < 0.05$.

5.2.9 Systemic administration of LRRFnAb and MFnAb increased the expression of FGF-2 within the burn wound

Fibroblast Growth Factor (FGF-2) is elevated in acute wounds and plays an indispensable role in the formation of blood vessels, tissue remodelling, and re-epithelialization (Powers *et al*., 2000). Paraffin-embedded burn tissues were stained by FGF-2 antibody to identify the effect of systemic administration of FnAb on protein expression of FGF-2 within the burn wounds (Figure 5.12A). Results demonstrated that the expression level of FGF-2 was significantly increased in LRRFnAb (by 25.6% ± SEM) and MFnAb (by 23.4% ± SEM) treated mice compared with IgG control counterparts at day 7 post burn injury (Figure 5.12B).

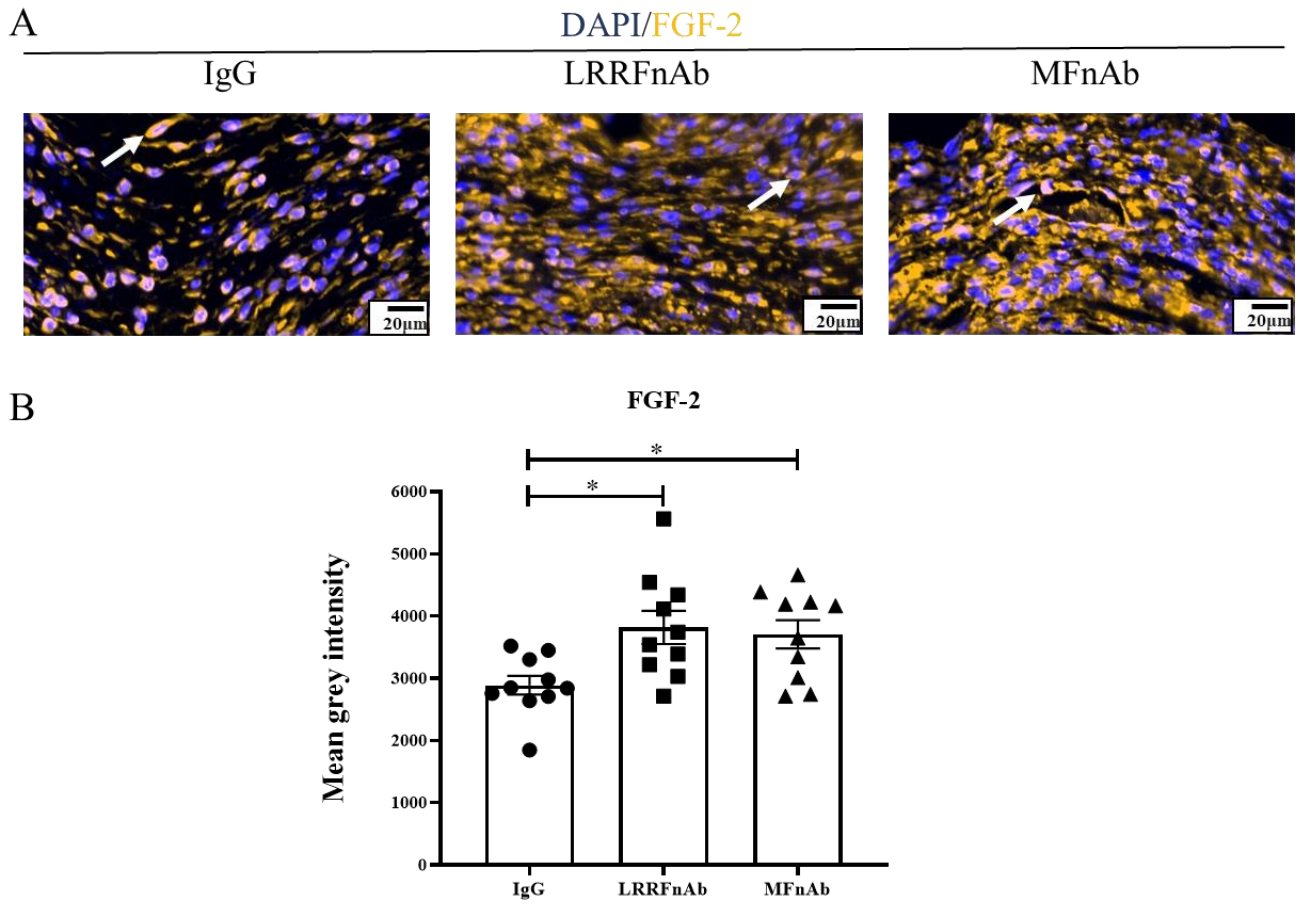


Figure 5. 12: Effect of LRRFnAb and MFnAb on FGF-2 expression in the burn site

A) Immunofluorescence detection of FGF-2 (yellow) counterstained with DAPI (blue) in LRRFnAb and MFnAb treated mice at day 7 post-injury. The primary antibody used was Rabbit anti-FGF-2 antibody, and for the secondary antibody, Goat anti-Rabbit IgG was employed. The entire wound bed was encompassed in the analysis. Images captured using a 20X objective B) Quantification of FGF-2 expression as mean grey intensity in the wound bed normalized to the burn area. The production of FGF-2 was increased in LRRFnAb and MFnAb treated mice. n = 10. All data are represented as mean ± SEM. Statistical significance was calculated by one-way ANOVA and Dunnett's post-tests. *= $p < 0.05$.

5.2.10 TGF-β1 production was significantly reduced in MFnAb treated mice

The transforming growth factor beta 1 (TGF-β1) is a family of growth factors that regulate several cellular functions involved in wound healing (Klass *et al*., 2009). Studies have shown that TGF-β1 plays important roles in inflammatory responses, inducing angiogenesis, collagen synthesis, fibroblasts proliferation, and remodelling of extracellular matrix (Nall *et al*., 1996; Roberts *et al*., 1986). Overactivation of TGF-β1 signalling is a major contributor to fibrosis and scar formation and has been shown to be upregulated in scars (Frangogiannis, 2020). Investigating the possible impact of systemic delivery of LRRFnAb and MFnAb on the production of TGF-β1 could therefore provide beneficial findings related to scar formation.

In order to identify the effect of specific FnAbs on the expression level of TGF-β1, an ELISA assay was used on extracts of wound tissue from FnAb treated and control mice. The finding revealed that the total TGF-β1 ligand levels were significantly reduced by 32.7% ± SEM in MFnAb treated mice compared to IgG treated mice (Figure 5.13). A relative but not significant decrease by 15.6% ± SEM was also observed in mice treated with LRRFnAb (Figure 5.13).

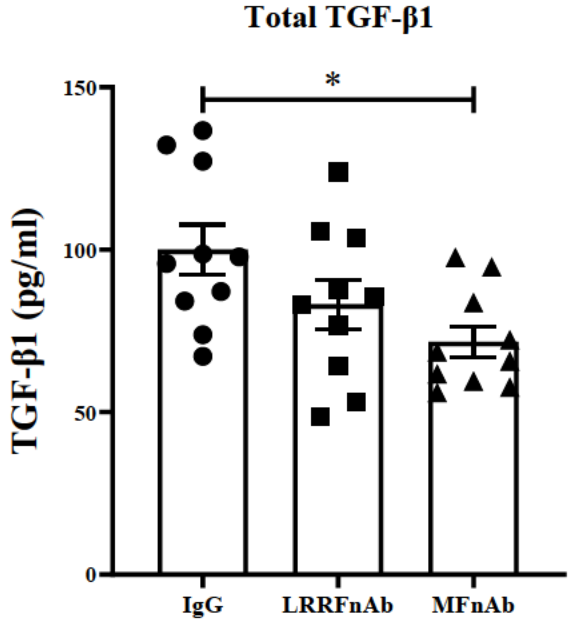


Figure 5. 13: Effect of LRRFnAb and MFnAb on TGF-β1 expression in burn wounds.

TGF-β1 production in the burn wounds was measured using ELISA and expressed as picogram of TGF-β1 in 1 milligram of total protein in burn wounds at day 7 post-burn injury. The expression of TGF-β1was significantly attenuated in MFnAb treated mice. n=10. All data are represented as mean ± SEM. Statistical significance was calculated by one-way ANOVA and Dunnett's post-tests. *= $p < 0.05$.

5.3 Discussion

The current research investigated the localization of systemic injectable therapy of FnAbs generated against specific domains of Flii and explored if systemic administration of these antibodies localizes at the wound site and improves healing following burn injury in mice. Fluorescent radiance efficiency measurements showed that Alexa-Fluor-680-FnAbs including LRRFnAb and MFnAb localized at the site of burn injury from day 1 remaining there for the whole 7-day study. FnAbs against different domains of Flii protein were delivered systemically and results demonstrated that all administered antibodies travel to the burn wound, however FnAbs were present at higher levels and remained longer. The lower signal of IgG suggests that LRRFnAb and MFnAb may be retained within the wound for longer which may be due to the elevated level of Flii within the wound. My results showed that the radiance efficiency was significantly higher in LRRFnAb treated mice compared to the control group on days 1 and 7 of the study. Fluorescent assessments also revealed that burns in mice treated with MFnAb emitted stronger fluorescence compared to IgG treated mice at each time point of the study. These results suggest that FnAbs raised against the middle domain of Flii localize to wound site for a longer period of time during burn wound repair.

Previous investigations have reported that topical and intradermal delivery of FnAbs reduced the expression of Flii and improved healing outcomes in a murine model of partial-thickness scald injury (Adams *et al*., 2009). Upregulation of Flii was also observed in human burns in comparison with human normal skin (Cameron *et al*., 2016). Here we have demonstrated that systemic administration of FnAbs raised against middle domain of Flii resulted in a decreased expression of Flii in mouse burns and this was more effective than burns in mice treated with LRRFnAb. Systemic delivery of LRRFnAb still resulted in a downward trend in the expression of Flii when compared to the IgG control.

Systemic delivery of MFnAb to murine scald burns was found to enhance wound closure and increase the rate of re-epithelialisation while delivery of LRRFnAb did not positively alter the rate of wound closure or the percentage of re-epithelialisation. As previously shown in Chapter 3, addition of MFnAb to cultured fibroblasts and keratinocytes improved cellular proliferation compared to LRRFnAb treatment. These results suggest that binding of an antibody to the middle

domain of Flii reduces its inhibitory effect on the activity of fibroblasts in comparison to binding to the LRR domain of Flii. Additionally, the antibody localization results showed that MFnAbs localized at the site of burn injury during the whole 7-day study. These findings suggest that MFnAbs may target/inhibit Flii more efficiently in comparison with LRRFnAbs as the fluorescent measurements FnAbs raised against the middle domain of Flii are higher within the burn site. This was followed by reduced level of Flii and improved healing outcomes including increased re-epithelialisation and enhanced wound closure time.

Restoring tissue integrity immediately after injury is highly dependent on myofibroblasts which are important in the production of extracellular matrix (Hinz, 2016). Myofibroblasts have a key role during the proliferative phase of wound healing and are important in the process of tissue contraction (Bochaton-Piallat *et al*., 2016). The contraction of a wound, described as one of the crucial stages in wound repair in mice, as it leads to wound closure (Tomasek *et al*., 2002). However, it is important to note that wound healing in humans primarily relies on re-epithelialization, where the primary closure of the wound occurs through the migration and proliferation of epithelial cells (Pastar *et al*., 2014). Additionally, myofibroblasts have been shown to produce α-SMA and play important roles in the synthesis and reorganization of the ECM (Darby *et al*., 1990; Serini and Gabbiani, 1999). My findings have revealed that mice treated with MFnAb had increased numbers of myofibroblasts in the burn which can suggest that the binding of antibody to middle domain interferes with Flii effects on myofibroblast activity during wound repair. However, the binding of antibody to the LRR domain of Flii also showed a relative impact on the myofibroblast assessments as LRRFnAb relatively increased the number of myofibroblasts in burn wounds. These results are in agreement with the previous work indicating that Flii deficiency results in a considerable increase in the myofibroblast marker, α-SMA (Cowin *et al*., 2007). This finding may explain the smaller wound area and increased wound contraction in MFnAb treated mice compared to mice treated with LRRFnAb as myofibroblasts are crucial for wound contraction (Bochaton-Piallat *et al*., 2016).

Flii has been previously found to induce the expression of TLR4 and NF-B which can lead to increased inflammation (Ruzehaji *et al*., 2014). Studies have also reported that attenuation of Flii using topical application of FnAbs decreased the inflammatory response and pro-inflammatory cytokine secretion in a murine model of psoriasiform dermatitis (Chong *et al*., 2017). Neutrophils

remove bacterial and necrotic tissues by phagocytosis and secretion of numerous factors such as reactive oxygen species (ROS), proteolytic enzymes, and antimicrobial peptides (Kolaczkowska and Kubes, 2013; Segel *et al*., 2011). However, uncontrolled inflammation through excessive activation of neutrophils promotes injury and impairs healing (Boniakowski *et al*., 2017). Here I showed that systemic delivery of LRRFnAb and MFnAb resulted in reduced neutrophil infiltration in burns. This suggests that binding of antibodies to LRR and middle of Flii modulates impacts of Flii on inflammation during repair process.

An increased level of M1 macrophages which are active at the early stage of wound healing has been found to impair the healing process (Hesketh *et al*., 2017). Studies have shown that M2 macrophages have anti-inflammatory activities during wound repair and any failure in the shift from M1 to M2 macrophages can negatively impact wound healing outcomes (Hesketh *et al*., 2017). A recent study has also revealed that an increased expression of Flii can lead to elevated inflammation in the wounds by causing a delay in the switch from M1- proinflammatory macrophages to M2- anti-inflammatory macrophages (Mills *et al*., 2022). Results of this chapter indicate that mice treated with systemic injection of FnAbs raised against both LRR and middle domain of Flii resulted in a decreased number of M1 pro-inflammatory macrophages. The findings reported in this chapter also showed that systemic delivery of LRRFnAb and MFnAb increased the level of M2 anti-inflammatory macrophages and therefore improved M1-M2 macrophage polarization and this is in agreement with increased rate of healing observed in MFnAb treated mice and is consistent with the previous work showing that elevated expression of Flii resulted in delayed M1-M2 macrophage polarization (Mills *et al*., 2022).

Endothelial cells are important in the regulation of haemostasis, inflammation, and vascular integrity during wound healing (Johnson and Wilgus, 2014; Verhamme and Hoylaerts, 2006). Haemostasis is immediately triggered after injury and endothelial cells are crucial in restoring vascular integrity (Verhamme and Hoylaerts, 2006). Endothelial cells play a vital role in the preservation and growth of newly formed tissue by facilitating the formation of blood vessels, which are crucial for maintaining adequate blood supply (Velnar and Gradisnik, 2018). During wound healing, endothelial cells undergo morphological alterations and interact with cell surface receptors, contributing to the induction of cell migration (Wilkinson, 1998). The number of

endothelial cells were increased in FnAbs raised against both LRR and middle domain of Flii which indicates that inhibitory effects of Flii on endothelial cells activity during the repair process.

Angiogenesis is one of the major processes during the healing of burn wounds as it provides nutrients for damaged tissues and results in removal of debris (Bodnar, 2015; Busuioc *et al*., 2013). Angiogenesis is also crucial for the delivery of immune cells and the migration of cells involved in the repair process (Tonnesen *et al*., 2000). Newly formed capillaries provide a supportive matrix for fibroblast migration and facilitate the proliferation of additional blood vessels (Tonnesen *et al*., 2000). Following the activity of pro-angiogenic growth factors angiogenesis is promoted during the proliferation stage of healing, however, a low grade of inflammation in the terminal stage of wound healing can lead to attenuated angiogenesis (Kumar *et al*., 2009). Insufficient angiogenesis results in delayed healing and is a major contributor to chronic wounds (Sen, 2021). Results presented in this chapter demonstrated that systemic delivery of LRRFnAb resulted in an increased number of capillaries in the burn wounds. As previously shown in Chapter 3, LRRFnAb treated endothelial cells significantly induced migration and proliferation of dermal endothelial cells. FnAbs against the LRR domain of Flii also improved the tube formation abilities as discussed in Chapter 3. Collectively, binding of antibody to the LRR domain of Flii prevent the function of Flii in angiogenesis, however, the binding of FnAbs to middle domain of Flii FnAbs still had stimulatory effects on the formation of mature blood vessels. As discussed in Chapter 3, treatment with MFnAbs accelerated the migration of endothelial cells and increased the amount of tube formation. This was in agreement with previous work in diabetic mice showing that intradermal delivery of FnAb promoted the angiogenic response through increasing the formation of capillary tubes and mature blood vessels (Ruzehaji *et al*., 2014).

VEGF has been defined as one of the main stimulators of vascular permeability. VEGF plays a key role in inducing endothelial cells to proliferate and migrate, acting as a chemotactic agent (Bao *et al*., 2009). It extensively affects several components of the wound repair cascades such as angiogenesis, re-epithelisation, and collagen deposition (Stojadinovic, 2007). Studies have shown that expression of VEGF in wounds considerably impact healing outcomes and any failure in the expression of VEGF has been found to impair wound repair (Rossiter *et al*., 2004). VEGF has also been shown to be a major stimulator of FGF-2 which is an important pro-angiogenic factor and

neutralizing the activity of VEGF using monoclonal antibodies resulted in inhibited FGF-2–induced endothelial cell proliferation (Seghezzi *et al*., 1998). Results reported in this chapter showed that systemic administration of both FnAbs raised against LRR and middle domain of Flii improved the expression of VEGF. These findings suggest that Flii has a considerable effect on the regulation of VEGF levels during wound healing as *in vitro* studies in Chapter 3 demonstrate the beneficial impact of LRRFnAb on the proliferation and migration of endothelial cells as well as the stimulatory effect of MFnAbs on the migration of endothelial cells.

FGF-2 has been found to activate fibroblasts and stimulate the expression of VEGF and smooth muscle cells in the process of wound repair (Gospodarowicz *et al*., 1987). However, it is important to note that the interplay between FGF-2 and VEGF in wound healing is a dynamic process that may vary based on specific conditions. Several studies have revealed that delivery of recombinant FGF-2 to skin burns results in improved healing (Akita *et al*., 2008; Fu *et al*., 1998; Xiang *et al*., 2011). FGF-2 promotes keratinocyte motility, accelerates the migration of fibroblasts, and increases the production of collagenase (Sasaki, 1992; Sogabe *et al*., 2006). FGF-2 plays an important role in the migration and proliferation of endothelial cells and accelerates the binding of endothelial cells to ECM (Barrientos *et al*., 2008). Moreover, FGF-2 is an important stimulator of VEGF and studies have shown that addition of recombinant FGF-2 to cultured endothelial cells increases the expression of VEGF (Seghezzi *et al*., 1998). Here we showed that the systemic injection of FnAbs raised against LRR and middle domain of Flii increased the expression of FGF-2 in burns. As previously discussed, systemic delivery of both antibodies resulted in elevated VEGF. FGF-2 has been also reported to induce the level of VEGF (Lutolf and Hubbell, 2005). These results suggest that Flii can be a major regulator of pro-angiogenic factors such as VEGF and FGF-2 during burn repair. Treatment with both FnAbs lead to similar VEGF and FGF-2 expression but they had different effects on angiogenesis. This could be a result of numerous molecular and cellular events, growth factors, and extensive signalling pathways involved in angiogenesis as a complex and highly ordered process (Honnegowda *et al*., 2015).

TGF-β1 is involved in many cellular activities including inflammation, angiogenesis, and collagen synthesis during wound healing (Nall *et al*., 1996; Roberts *et al*., 1986). TGF-β1 signalling has been also shown to have beneficial roles in chronic and non-healing wounds (Kim *et al*., 2003; Pastar *et al*., 2010). The relevance of TGF-β1 in the formation of scars has been investigated and

the increased expression of TGF-β1 has been found to promote scarring during wound healing (Le *et al*., 2012). Studies have also reported that upregulation of TGF-β1 can implicate fibrosis and scars following trauma healing (Campaner *et al*., 2006; Le *et al*., 2012). Systemic delivery of FnAbs raised against the middle domain of Flii attenuated the apparent expression of TGF-β1 in burns, while the administration of LRRFnAbs resulted in a relative decrease in the level of TGF-β1 protein. As discussed in the antibody localization section, MFnAbs were found to be localized for a more prolonged time within the burn area compared to LRRFnAb during the whole study suggesting that MFnAb may have more effects on TGF-β1 activity during burn repair. This is in agreement with a previous study that showed wounds with decreased expression of Flii resulted in reduced expression of pro-scarring TGF-β (Adams *et al*., 2009; Chan *et al*., 2014). Studies have previously reported that Flii influences the non-classical TGF-β signalling transduction containing nuclear and activating proteins-1 (AP-1), Akt, c-fos, and c-jun (Chan *et al*., 2014). Furthermore, reducing the gene expression of Flii decreases the level of TGF-β1 and Smad 3 gene expression and also increases inhibitory Smad 7 gene expression (Chan *et al*., 2014). Collectively, findings in this chapter are consistent with previous works suggesting decreasing the expression of Flii lead to attenuated responses of TGF-β signals (Chan *et al*., 2014).

Overall, the findings presented in this chapter suggest that the treatment of mice with systemic delivery of FnAbs raised against the middle domain of Flii may have the potential to improve healing outcomes. These findings are associated with observed correlations between the use of FnAbs and various processes such as reduced inflammation and TGF-β1 expression, as well as enhanced angiogenesis and the production of pro-angiogenic factors VEGF and FGF-2. However, further in-depth experimentation is necessary to determine the precise mechanisms and to clearly establish a cause-and-effect connection.

Chapter 6: Investigating the signalling pathways that lead to the pro-angiogenic effects of intracellular and extracellular Flii

6.1 Introduction:

The repair of a cutaneous wound is an extremely complex process that incorporates multiple stages including haemostasis, inflammation, proliferation, and matrix remodelling. The proliferative phase of wound repair is highly dependent on the development and formation of blood vessels which is known as the process of angiogenesis (Das and Baker, 2016). VEGF-A, FGF-2, and PDGF-BB have all been identified as key pro-angiogenic stimulators that play major roles in the process of healing (Kano *et al*., 2005). VEGF-A acts as a mitogen for endothelial cells as it promotes proliferation and migration of endothelial cells and inhibits apoptosis (Ferrari *et al*., 2006). FGF-2 not only activates fibroblasts but also stimulates the vascular endothelial cells during wound healing and tissue remodelling (Koike *et al*., 2020). PDGF-BB is secreted by skin cells and is known as an important regulator of angiogenesis as it plays a key role in the proliferation and migration of endothelial cells (Jian *et al*., 2022). The expression of PDGF-BB has been shown to increase both vascularity and maturation of blood vessels, while PDGF-BB deficiency results in poorly formed and immature capillaries (Onimaru *et al*., 2009; Raica and Cimpean, 2010). Several cellular sources including keratinocytes, fibroblasts, and endothelial cells contribute to increased expression of VEGF post injury (Johnson and Wilgus, 2014). FGF-2 has been reported to induce the expression of VEGF through autocrine and paracrine mechanisms (Seghezzi *et al*., 1998). PDGF-BB and FGF-2 have been reported to interact mutually and contribute their impacts to angiogenesis (Cao *et al*., 2008).

Previous studies have reported the negative effect of both intracellular and extracellular Flightless I (Flii) on angiogenesis (Ruzehaji *et al*., 2014; Thomas *et al*., 2020). Heterozygous knockout of Flii leads to an increase in the expression of pro-angiogenic factor VEGF, and elevated numbers of endothelial cells in diabetic mouse models (Ruzehaji *et al*., 2014; Thomas *et al*., 2020). In contrast, endothelial cells from mice with elevated Flii exhibited attenuated micro vessels sprouting and impaired tight junction formation (Ruzehaji *et al*., 2014). *In vitro*, addition of the first generation Flii neutralizing antibodies (FliiL FnAb) to HUVEC cells resulted in increased capillary tube formation (Ruzehaji *et al*., 2014). Moreover, in the Matrigel plug assay cells treated with FliiL FnAb were found to develop more mature blood vessels when placed under the skin of murine models (Ruzehaji *et al*., 2014).

In vitro and *in vivo* results reported in this thesis have demonstrated that LRRFnAb and MFnAb have the potential to stimulate angiogenesis. *In vitro*, addition of LRRFnAbs increased both proliferation and migration of dermal endothelial cells, as well as capillary tube formation (Chapter 2). The *in vitro* results of Chapter 2 also revealed that MFnAbs improve the migration of endothelial cells and endothelial capillary tube formation. While both FnAbs generated against either the LRR or the middle domain of Flii promoted the number of mature blood vessels in an acute wound murine model (Chapters 3), LRRFnAb was shown to increase mature blood vessels in burns (Chapter 4). The expression of pro-angiogenic VEGF, FGF-2, and PDGF-BB was also elevated in excisional wounds in LRRFnAb treated mice, while the level of VEGF was higher in MFnAb treated mice compared to LRRFnAb treated animals. Both antibodies increased the expression of VEGF and FGF-2 in partial-thickness scald injury murine models.

The purpose of this study was to investigate the influence of extracellular and intracellular Flii on angiogenesis signalling pathways in skin cells *in vitro* following alteration of Flii levels. Specifically, the effect of recombinant Flii protein (rFlii), LRRFnAb and MFnAb on the gene expression of key pro-angiogenic factors including VEGF-A, FGF-2, and PDGF-BB was investigated to determine the impact of extracellular Flii on angiogenesis signalling pathways. Additionally, to investigate the role of intracellular Flii in angiogenesis, the gene expression of pro-angiogenic factors secreted by skin cells was evaluated following knockdown of Flii gene expression by siRNA.

6.2 Results

6.2.1 VEGF-A was upregulated in both LRRFnAb and MFnAb treated endothelial cells while the expression of PDGF-BB was downregulated in LRRFnAb and MFnAb treated endothelial cells

To determine the effect of reducing extracellular Flii levels in endothelial cells on gene expression of key pro-angiogenic factors, qRT-PCR of VEGF-A, FGF-2, and PDGF-BB genes was carried out following LRRFnAb or MFnAb treatment. The findings of the experiments showed that the level of pro-angiogenic factor VEGF-A was significantly elevated in both LRRFnAb and MFnAb treated cells compared to control (Figure 6.1A). Additionally, there was a significant increase in VEGF-A levels in MFnAb treated endothelial cells when compared to LRRFnAb treated cells (Figure 6.1A). Treatment of endothelial cells with either LRRFnAb or MFnAb did not alter the FGF-2 levels in comparison with untreated cells (Figure 6.1B), however, as illustrated in Figure 6.1C, PDGF-BB levels were significantly downregulated in cells treated with either LRRFnAb or MFnAb. Additionally, the level of PDGF-BB was significantly increased in MFnAb endothelial cells compared to LRRFnAb treated cells (Figure 6.1C).

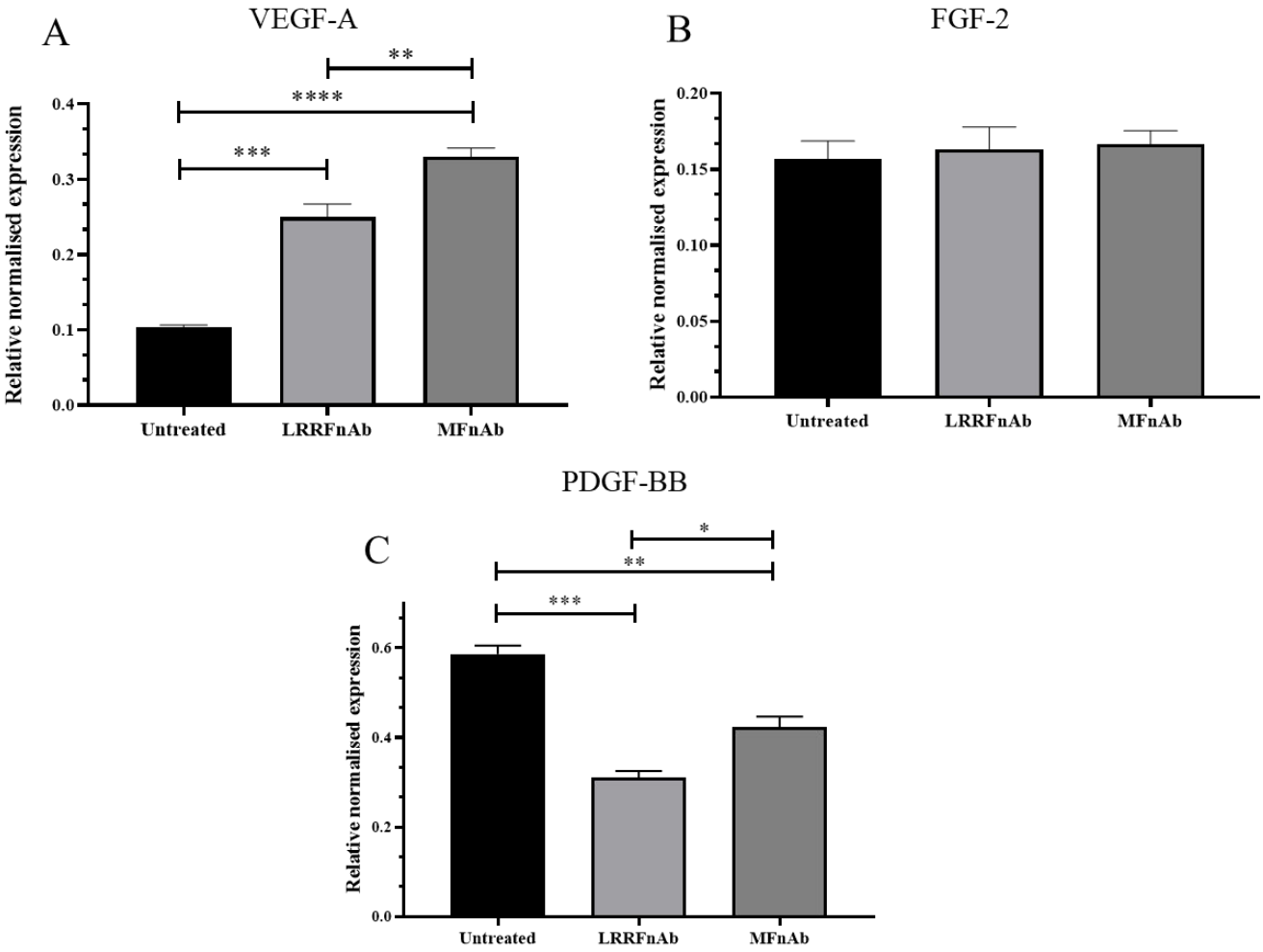


Figure 6. 1: Effect of LRRFnAb and MFnAb on mRNA expression of pro-angiogenic factors in dermal endothelial cells

qRT-PCR results of A) VEGF-A, B) FGF-2, C) PDGF-BB in HDMECs treated with either normal media, or LRRFnAb (50 μg/ml), or MFnAb (50 μg/ml). Values of relative mRNA levels were normalised to reference gene CypA. All data are represented as mean ± SEM of 3 independent experiments. Statistical significance was calculated by one-way ANOVA and Tukey's post-tests. *= $p < 0.05$, **= $p < 0.01$, ***= $p < 0.001$, ****= $p < 0.0001$.

6.2.2 The effect of rFlii on the expression of pro-angiogenic genes in dermal endothelial cells

To determine the effect of extracellular Flii levels in endothelial cells on the expression of key pro-angiogenic factors, qRT-PCR of VEGF-A, FGF-2, and PDGF-BB was performed following rFlii treatment. Pre-incubated LRRFnAbs/MFnAbs with rFlii was also added to endothelial cells to identify the impact of antibodies against different domains of Flii on possible gene-expression effects of rFlii.

The results demonstrated that addition of rFlii significantly increased VEGF-A levels compared to untreated cells (Figure 6.2A). Pre-incubating rFlii with LRRFnAb reduced the upregulation of VEGF-A, while pre-incubation with MFnAb was unable to prevent the upregulation of VEGF-A by rFlii (Figure 6.2A). qRT-PCR analysis also showed that FGF-2 was significantly elevated in response to rFlii (Figure 6.2B). Pre-incubating rFlii with LRRFnAb was found to reduce the effect of rFlii, however the difference was not statistically significant (Figure 6.2B). Surprisingly, addition of rFlii+MFnAb treatment further elevated levels of FGF-2 compared to untreated endothelial cells (Figure 6.2B). The level of pro-angiogenic PDGF-BB was also significantly increased in response to rFlii (Figure 6.2C). The results showed that pre-incubation with LRRFnAb neutralized the effect of rFlii on the expression of PDGF-BB, whilst pre-incubation with MFnAb had minimal effect on this upregulation. (Figure 6.2C).

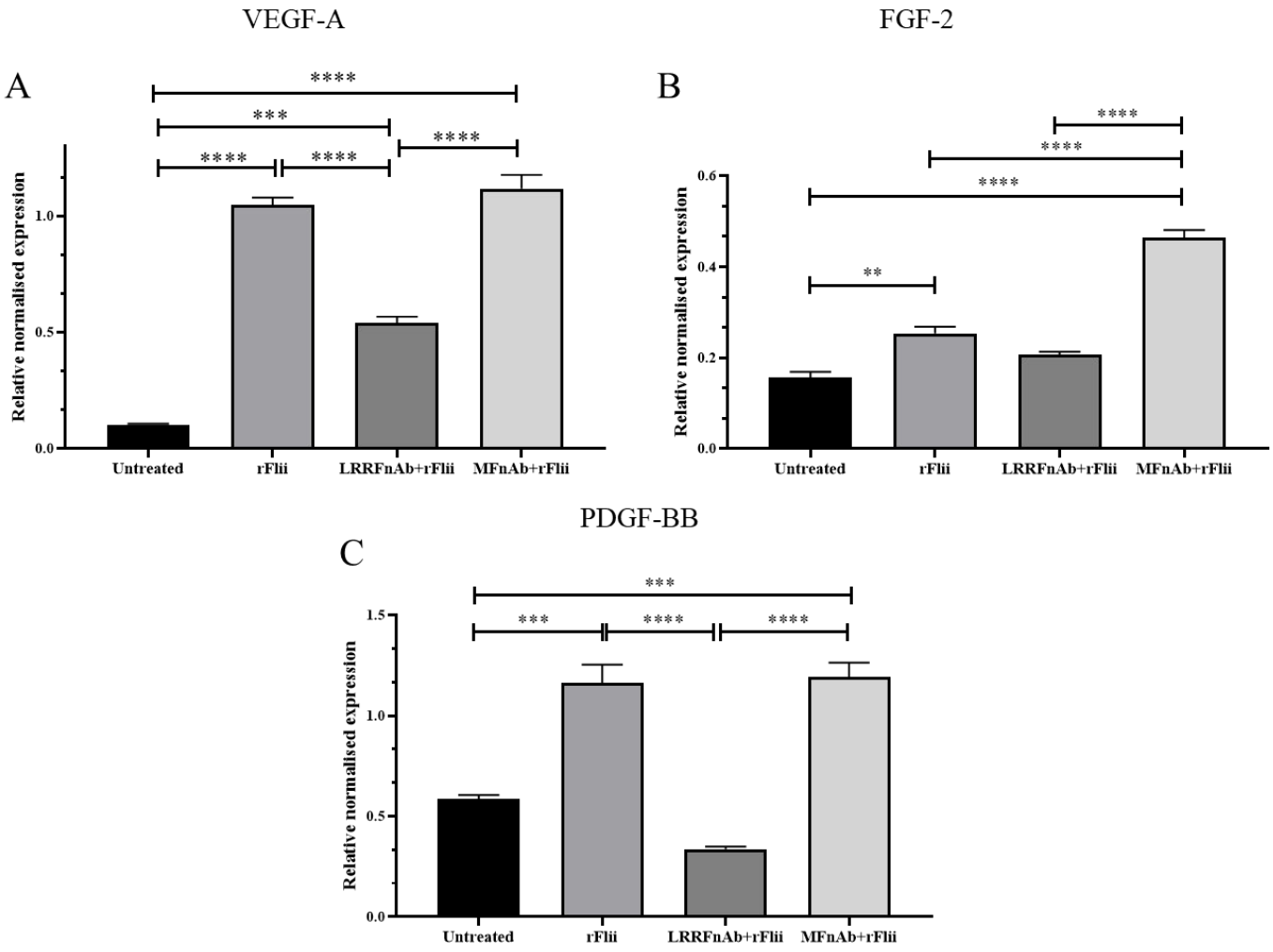


Figure 6. 2: Impact of rFlii and FnAb neutralizing rFlii on mRNA expression of pro-angiogenic factors in dermal endothelial cells

qRT-PCR results of A) VEGF-A, B) FGF-2, C) PDGF-BB in HDMECs treated with either normal media, or rFlii (5 µg/ ml), or rFlii (5 µg/ ml) +LRRFnAb (50 µg/ml), or rFlii (5 µg/ ml) +MFnAb (50 µg/ml). Values of relative mRNA levels were normalized to reference gene CypA. All data are represented as mean ± SEM of 3 independent experiments. Statistical significance was calculated by one-way ANOVA and Tukey's post-tests. **= $p < 0.01$, ***= $p < 0.001$, ****= $p < 0.0001$.

6.2.3 Knockdown of Flii by siRNA significantly decreased Flii RNA in dermal endothelial cells

To determine the effect of Flii on the expression of pro-angiogenic factors, it was essential to first demonstrate effective knockdown of intracellular Flii expression. siRNA knockdown of Flii was performed in endothelial cells as previously described in Chapter 2. The impact of siFlii treatment was evaluated in endothelial cells (Figure 6.3). qRT-PCR analysis showed that Flii levels were significantly attenuated in endothelial cells within 6 hours of siFlii administration compared with untreated and siControl treated cells (Figure 6.3).

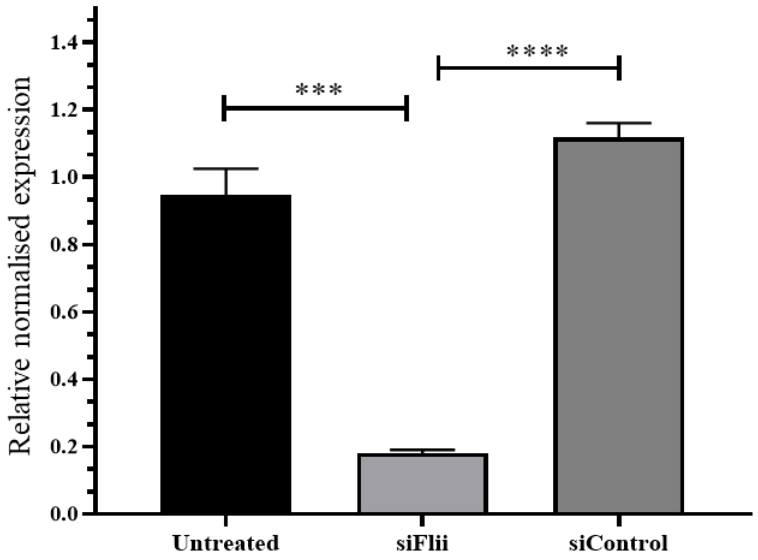


Figure 6. 3: Flii knockdown by siRNA significantly decreased Flii in dermal endothelial cells

Flii knockdown by siRNA as illustrated by qPCR for Flii levels in siControl treated and siFlii treated HDMECs lysates. Flii mRNA levels were normalised to reference gene CypA. All data are represented as mean ± SEM of 3 independent experiments. Statistical significance was calculated by one-way ANOVA and Tukey's post-tests. ***= $p < 0.001$, ****= $p < 0.0001$.

6.2.4 Flii Knockdown attenuated intracellular Flii protein level in dermal endothelial cells

To investigate the effect of Flii knockdown on the intracellular Flii protein level in dermal endothelial cells, Western blotting was carried out as previously detailed in Chapter 2 (Figure 6.4A). siFlii treated cells exhibited depleted Flii protein levels within 6 hours of siFlii administration compared to untreated and scrambled control siRNA (siControl) treated endothelial cells (Figure 6.4B). Additionally, Flii protein in siControl treated cells was no different to untreated endothelial cells.

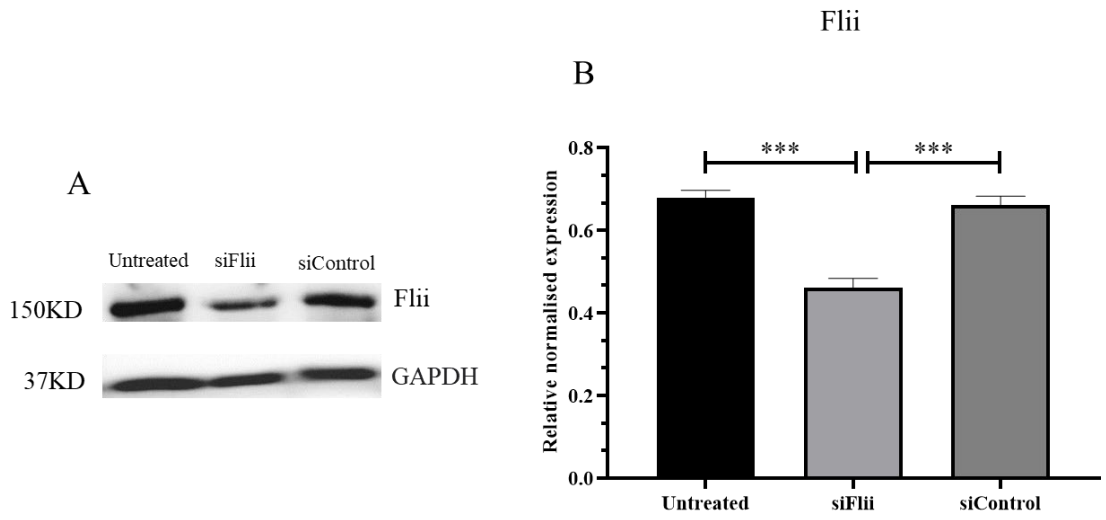


Figure 6. 4: Impact of Flii knockdown on protein level of Flii in dermal endothelial cells

A) Western blotting of untreated, siFlii, siControl, and rFlii treated dermal endothelial cells. B) Band densitometry analysis of relative expression of Flii protein normalised to GAPDH. All data are represented as mean ± SEM of 3 independent experiments. Statistical significance was calculated by one-way ANOVA and Tukey's post-tests. ***= $p < 0.001$.

6.2.5 Flii knockdown by siRNA significantly upregulates FGF-2 and PDGF-BB levels in dermal endothelial cells

In order to investigate the effect of intracellular Flii on the regulation of pro-angiogenic factors in endothelial cells, qRT-PCR of VEGF-A, FGF-2, and PDGF-BB genes was carried out following Flii knockdown. The analysis demonstrated that there were no considerable changes in the expression of VEGF-A in siFlii treated cells in comparison with untreated cells and endothelial cells treated with siControl (Figure 6.5A). On the other hand, the qRT-PCR results showed that FGF-2 was significantly upregulated in siFlii treated cells when compared with both control groups including untreated and siControl treated cells (Figure 6.5B). Lastly, PDGF-BB levels were also significantly increased in response to Flii knockdown in siFlii treated endothelial cells compared to untreated cells and endothelial cells treated with siControl (Figure 6.5C).

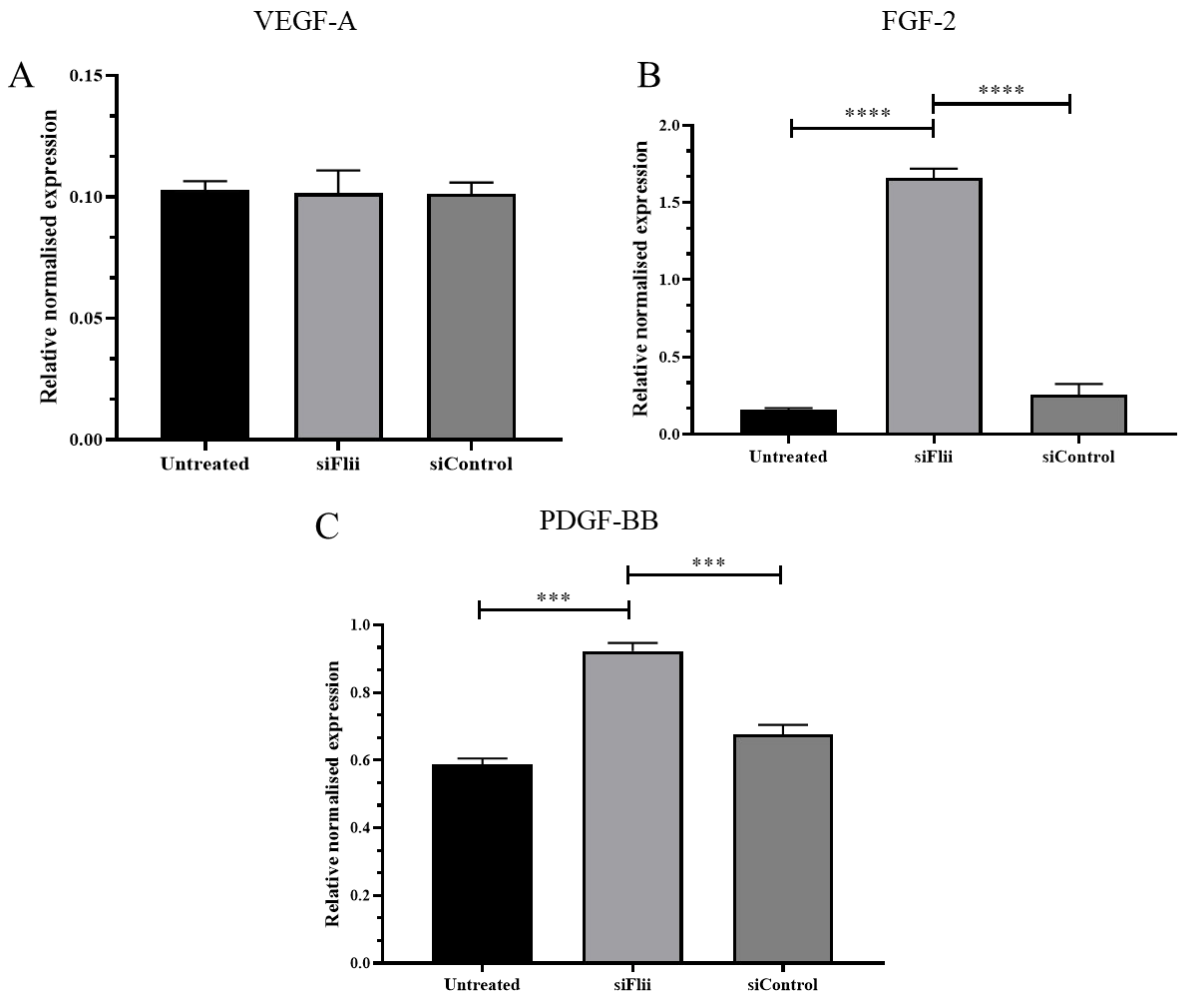


Figure 6. 5: Effect of Flii knockdown on mRNA expression of pro-angiogenic factors in dermal endothelial cells

qRT-PCR results of A) VEGF-A, B) FGF-2, C) PDGf-BB in HDMECs treated with either normal media, or siFlii, or siControl. Values of relative mRNA levels were normalized to reference gene CypA. All data are represented as mean ± SEM of 3 independent experiments. Statistical significance was calculated by one-way ANOVA and Tukey's post-tests. ***= $p < 0.001$, ****= $p < 0.0001$.

6.2.6 VEGF-A was elevated in MFnAb treated keratinocytes and FGF-2 was upregulated in LRRFnAb treated keratinocytes

To determine the effect of attenuating extracellular Flii levels in keratinocytes on gene expression of key pro-angiogenic factors, qRT-PCR of VEGF-A, FGF-2, and PDGF-BB genes was carried out following LRRFnAb or MFnAb treatment. The findings revealed that VEGF-A was significantly upregulated in MFnAb treated cells. Additionally, a similar although not significant trend towards increased VEGF-A was observed in LRRFnAb treated keratinocytes when compared with untreated cells (Figure 6.6A). The assessments of qRT-PCR results demonstrated that the level of FGF-2 gene expression was significantly higher in keratinocytes treated with LRRFnAb in comparison with both untreated and MFnAb treated cells (Figure 6.6B). There was a trend towards an increase in the expression of FGF-2 in MFnAb treated keratinocytes compared to untreated cells, however, this was not significant (Figure 6.6B). As shown in Figure 6.6C, PDGF-BB was significantly increased in cells with LRRFnAb compared to MFnAb treated cells and there was a slight trend towards an increase in the level of PDGF-BB in cells treated with LRRFnAb when compared to untreated group although this was not significant (Figure 6.6C).

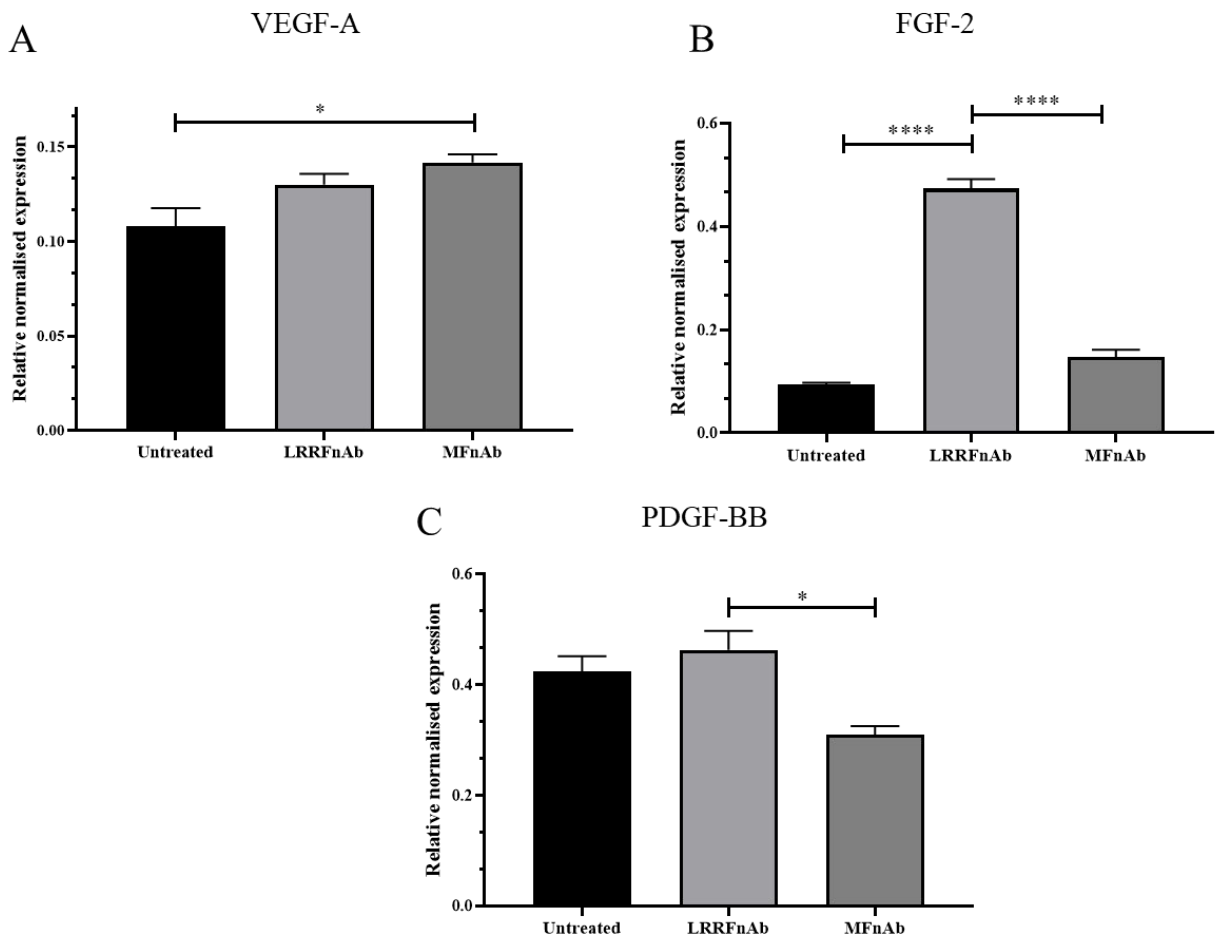


Figure 6. 6: Impact of LRRFnAb and MFnAb on mRNA expression of pro-angiogenic factors in keratinocytes

qRT-PCR results of A) VEGF-A, B) FGF-2, C) PDGf-BB in HaCaTs treated with either normal media, or LRRFnAb (50 μg/ml), or MFnAb (50 μg/ml). Values of relative mRNA levels were normalised to reference gene CypA. All data are represented as mean ± SEM of 3 independent experiments. Statistical significance was calculated by one-way ANOVA and Tukey's post-tests. *= $p < 0.05$, ****= $p < 0.0001$.

6.2.7 The effect of rFlii on the expression of pro-angiogenic genes in keratinocytes

In order to examine the role of extracellular Flii in the regulation of angiogenesis, keratinocytes were treated with rFlii. In addition to the individual treatment of rFlii, either LRRFnAbs or MFnAbs were also added to rFlii treated cells to assess the effects of FnAb-mediated neutralization of rFlii on the expression of angiogenesis-related genes. The qRT-PCR results indicated that the level of VEGF-A was significantly higher in rFlii treated keratinocytes (Figure 6.7A). Pre-incubation with either LRRFnAb or MFnAb had minimal effect on this upregulation (Figure 6.7A). As shown in Figure 6.7B, FGF-2 was detected at a significantly higher level in rFlii treated cells. The results showed that pre-incubation with either LRRFnAb or MFnAb neutralized the effect of rFlii on the expression of FGF-2 (Figure 6.7B). The findings also revealed that addition of rFlii significantly increased PDGF-BB levels in keratinocytes (Figure 6.7C). Pre-incubating rFlii with LRRFnAb and MFnAb was found to significantly reduce the effect of rFlii on the expression of PDGF-BB in keratinocytes (Figure 6.7C). However, LRRFnAbs were shown to have more effects than MFnAbs on neutralizing the activity of rFlii (Figure 6.7C).

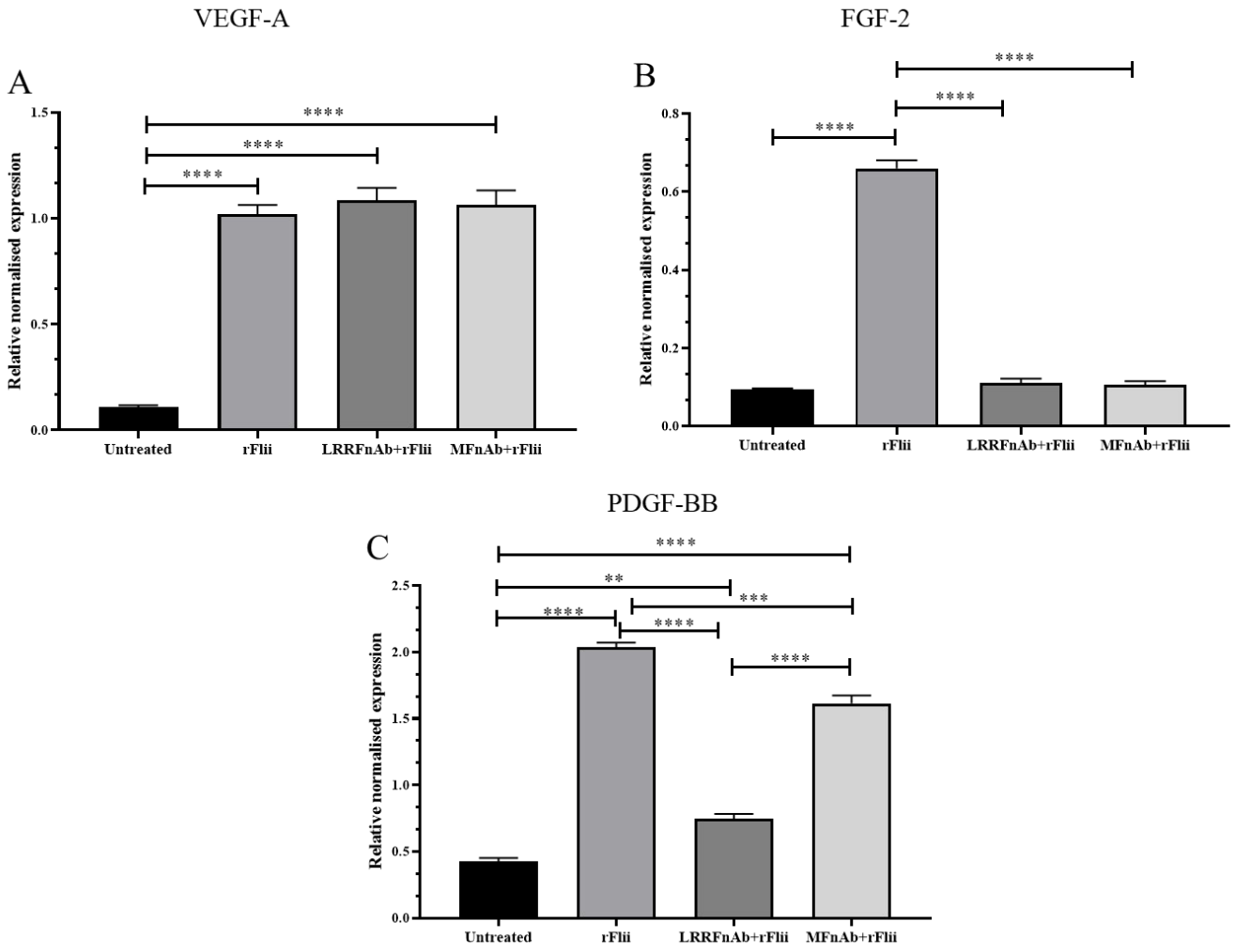


Figure 6. 7: Impact of rFlii and FnAb binding rFlii on mRNA expression of pro-angiogenic factors in keratinocytes

qRT-PCR results of A) VEGF-A, B) FGF-2, C) PDGf-BB in HaCaTs treated with either normal media, or rFlii (5 μg/ml), or rFlii (5 μg/ml) +LRRFnAb (50 μg/ml), or rFlii (5 μg/ml) +MFnAb (50 μg/ml). Values of relative mRNA levels were normalised to reference gene CypA. All data are represented as mean ± SEM of 3 independent experiments. Statistical significance was calculated by one-way ANOVA and Tukey's post-tests. **= $p < 0.01$, ***= $p < 0.001$, ****= $p < 0.0001$.

6.2.8 Knockdown of Flii by siRNA significantly attenuated Flii RNA in keratinocytes

As previously described in Chapter 2, siRNA knockdown of Flii was performed in keratinocytes to determine Flii gene level following siRNA knockdown. As illustrated in Figure 6.8, the effect of siFlii treatment was evaluated in keratinocytes. qRT-PCR analysis showed that Flii level was significantly attenuated in keratinocytes within 6 hours of siFlii administration compared to untreated and siControl treated keratinocytes (Figure 6.8).

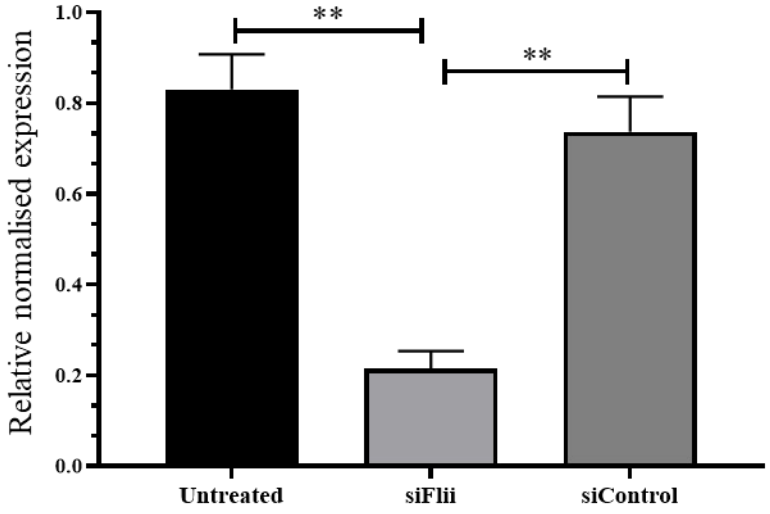


Figure 6. 8: Flii knockdown by siRNA significantly attenuated Flii in keratinocytes

Flii knockdown by siRNA as illustrated by qPCR for Flii levels in siControl treated and siFlii treated HaCaTs lysates. Flii mRNA levels were normalised to reference gene CypA. All data are represented as mean ± SEM of 3 independent experiments. Statistical significance was calculated by one-way ANOVA and Tukey's post-tests. **= $p < 0.01$.

6.2.9 Flii knockdown by siRNA promoted VEGF-A and FGF-2 expression and attenuated the PDGF-BB levels in skin keratinocytes

In order to determine the effect of intracellular Flii on the regulation of pro-angiogenic factors in keratinocytes, qRT-PCR of VEGF-A, FGF-2, and PDGF-BB genes was carried out following Flii knockdown.

As illustrated in Figure 6.9, VEGF-A expression was significantly upregulated in siFlii treated cells when compared to untreated keratinocytes (Figure 6.9A). The qRT-PCR analysis revealed that FGF-2 levels were significantly higher in siFlii keratinocytes in comparison with untreated cells. There was also a non-significant increase in the expression of FGF-2 in siFlii cells when compared to siControl, however, this was not statistically significant (Figure 6.9B). In contrast, the qRT-PCR analysis showed that PDGF-BB was significantly downregulated in siFlii treated keratinocytes in comparison to untreated control cells (Figure 6.9C).

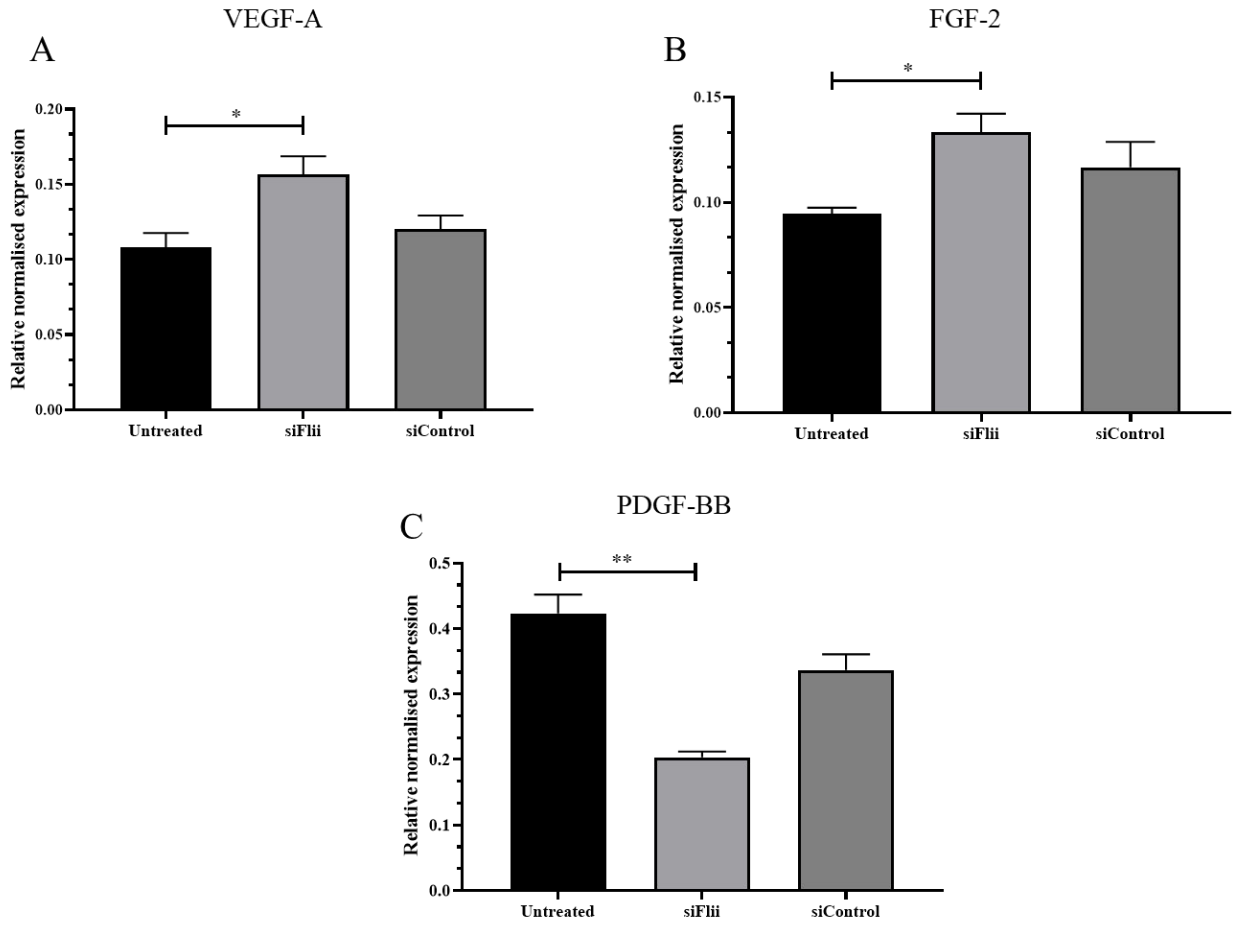


Figure 6. 9: Effect of Flii knockdown on mRNA expression of pro-angiogenic factors in keratinocytes

qRT-PCR results of A) VEGF-A, B) FGF-2, C) PDGf-BB in HaCaTs treated with either normal media, or siFlii, or siControl. Values of relative mRNA levels were normalised to reference gene CypA. All data are represented as mean ± SEM of 3 independent experiments. Statistical significance was calculated by one-way ANOVA and Tukey's post-tests. *= $p < 0.05$, **= $p < 0.01$.

6.2.10 The effect of rFlii and MFnAb on the gene expression of pro-angiogenic factors in fibroblasts

The impact of MFnAb, rFlii, and MFnAb neutralization of rFlii on the expression of pro-angiogenic factors VEGF-A, FGF-2, and PDGF-BB was investigated in fibroblasts. The qRT-PCR analysis demonstrated that MFnAb alone had little effect on VEGF-A expression (Figure 6.10A). Addition of rFlii significantly increased the levels of VEGF-A compared with untreated fibroblasts, while pre-incubation with MFnAb significantly reduced the effect of rFlii on the expression of VEGF-A (Figure 6.10A). qRT-PCR assessments showed that FGF-2 was significantly elevated in MFnAb treated cells compared to untreated fibroblasts (Figure 6.10B). The levels of FGF-2 were also detected at significantly higher levels in rFlii treated fibroblasts (Figure 6.10B). The results showed that pre-incubation with MFnAb neutralized the effect of rFlii on the expression of FGF-2 (Figure 6.10B). Addition of MFnAb had minimal effect on the expression of PDGF-BB in fibroblasts (Figure 6.10C). The results revealed that the expression of PDGF-BB was significantly elevated following treatment of cells with rFlii (Figure 6.10C). Pre-incubating rFlii with MFnAb significantly decreased the effect of rFlii on the expression of PDGF-BB in fibroblasts (Figure 6.10C).

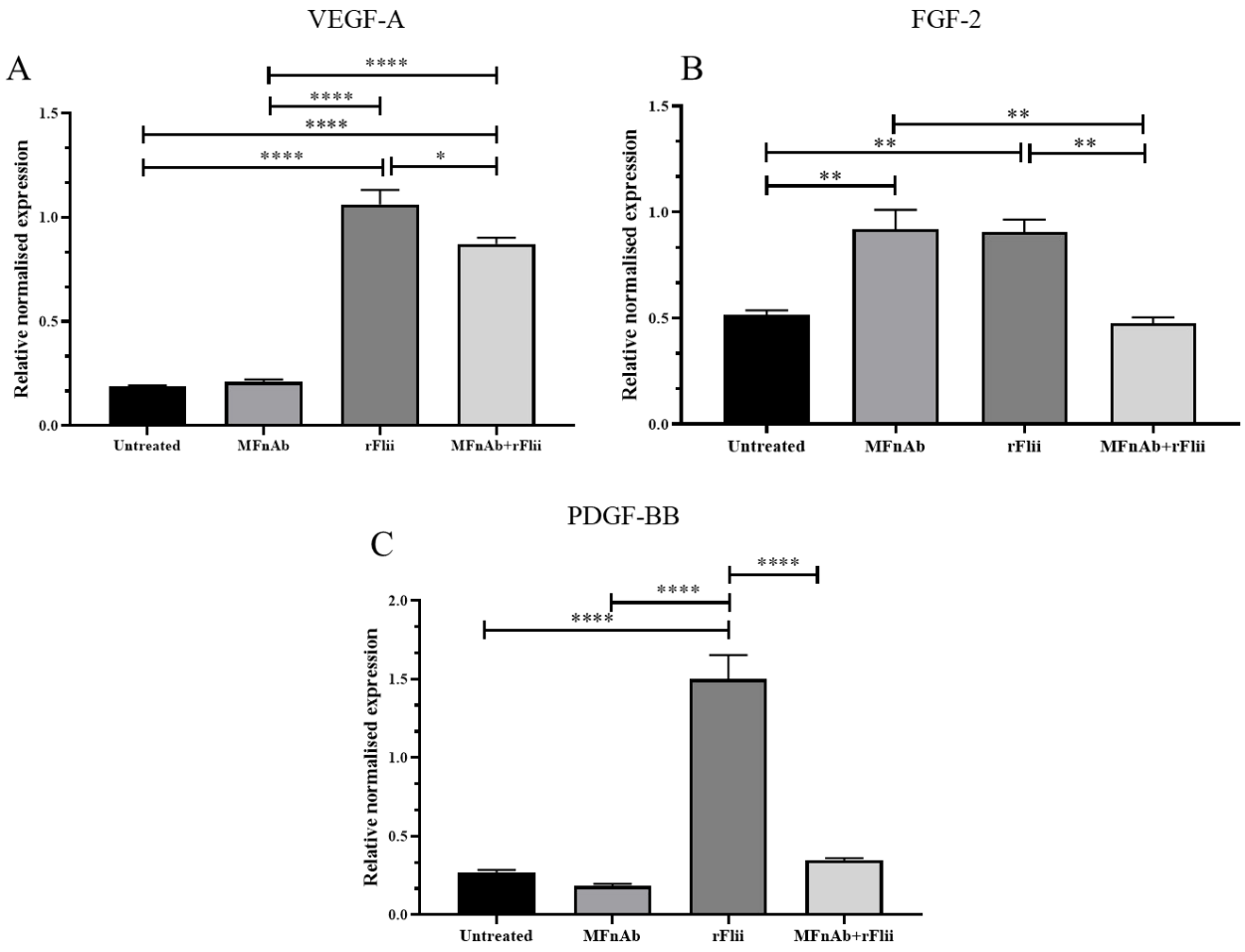


Figure 6. 10: Impact of MFnAb, rFlii, and MFnAb binding rFlii on mRNA expression of pro-angiogenic factors in fibroblasts

qRT-PCR results of A) VEGF-A, B) FGF-2, C) PDGF-BB in HFFs treated with either normal media, or MFnAb (50 µg/ml), or rFlii (5 µg/ml), or rFlii (5 µg/ml) +MFnAb (50 µg/ml). Values of relative mRNA levels were normalised to reference gene CypA. All data are represented as mean ± SEM of 3 independent experiments. Statistical significance was calculated by one-way ANOVA and Tukey's post-tests. *= $p < 0.05$, **= $p < 0.01$, ****= $p < 0.0001$.

6.3 Discussion

The outcome of angiogenesis widely regulated by the function of cytokines, growth factors, and chemokines, which intricately coordinate and modulate cellular processes during wound repair and tissue regeneration (Raja *et al*., 2007). The gene expression of pro-angiogenic factors (including VEGF-A, FGF-2, and PDGF-BB) following alteration of Flii levels was investigated in this study to determine the pro-angiogenic effects of intracellular and extracellular Flii protein.

VEGF-A is secreted by different skin cells including keratinocytes, fibroblasts, and endothelial cells (Barrientos *et al*., 2008; Namiki *et al*., 1995). VEGF-A is a key trigger factor for the migration of endothelial cells which has a major contribution to angiogenesis during healing processes (Abhinand *et al*., 2016). *In vivo*, the extracellular effect of Flii protein (previously discussed in Chapter 3 and 4) using the new generation of FnAbs including LRRFnAb and MFnAb showed that attenuating Flii resulted in increased expression of VEGF. Moreover, studies have previously reported that healing in mice with attenuated Flii is associated with elevated VEGF and endothelial cells (Ruzehaji *et al*., 2014; Thomas *et al*., 2020). Herein, the PCR assessments revealed that reducing Flii, following LRRFnAb and MFnAb treatment, upregulated VEGF-A gene expression in endothelial cells. The dose of LRRFnAb and MFnAb in these experiments was selected based on the studies carried out in Chapter 3 that showed the potential effects of these FnAbs on angiogenesis *in vitro*. VEGF-A was elevated more in MFnAb treated endothelial cells when compared to LRRFnAb treated cells (Figure 6.1A), suggesting that binding of antibody to the middle domain of Flii was more effective at neutralizing its effects on the expression of VEGF-A. Pro-angiogenic FGF-2 is produced by different cells including keratinocytes, fibroblasts, and endothelial cells and plays major roles in the formation of granulation tissue (Robson, 1997). Neither LRRFnAb nor MFnAb treatment affected the expression of FGF-2 gene in endothelial cells (Figure 6.1B), however, both MFnAb and LRRFnAb led to attenuated level of PDGF-BB in endothelial cells (Figure 6.1C), suggesting that extracellular Flii may play an important role in the pathway that regulates the level of PDGF-BB gene expression. PDGF-BB is secreted by skin cells including endothelial cells and is highly involved in different stages of wound healing, particularly in angiogenesis (Heldin and Westermark, 1999; Lederle *et al*., 2006; Uutela *et al*., 2004). Interestingly, addition of rFlii to dermal endothelial cells resulted in a significant upregulation in the expression of VEGF-A gene (Figure 6.2A). While the influence of extracellular Flii on VEGF

expression has been indirectly demonstrated, further investigation is necessary to determine the direct impact on the pathways that are associated with the pro-angiogenic factor VEGF-A gene level, such as VEGF-A/VEGFR2 and Ras/MAPK (Abhinand *et al*., 2016; Ichise *et al*., 2012). Interestingly, pre-incubation of rFlii with LRRFnAb neutralized the ability of rFlii to induce an increase in VEGF-A expression (Figure 6.2A). Addition of rFlii to the media increased the level of FGF-2 in endothelial cells (Figure 6.2B), suggesting that the elevated extracellular Flii in response to injury stimulates the expression of FGF-2 which is necessary for improvement of granulation tissue formation, re-epithelialization, and matrix formation and remodelling (Robson, 1997). The level of FGF-2 did not change when LRRFnAb was added to rFlii treated endothelial cells (Figure 6.2B), but interestingly, treating with MFnAb and rFlii potentiated FGF2 expression. rFlii also increased PDGF-BB expression (Figure 6.2C), which was prevented when LRRFnAb was added, but the effect of rFlii was not neutralized by MFnAb (Figure 6.2C), which suggesting a potentially complex relationship between MFnAb dose and its ability to counteract rFlii. A dose response experiment may determine the effective dose of MFnAb for attenuating rFlii activity. Flii knockdown by siRNA was found to significantly attenuate Flii gene (Figure 6.3) and protein (Figure 6.4) in dermal endothelial cells. The expression of VEGF-A was detected at similar level compared to the control in endothelial cells (Figure 6.5A), while the expression of both FGF-2 (Figure 6.5B) and PDGF-BB (Figure 6.5C) was elevated following Flii knockdown and attenuation of intracellular Flii protein. These results suggest that intracellular Flii may play an important role in signalling pathways including FGF-2–FGFR1–PDGF-BB and FGF-2–FGFR2–PDGFRβ that are involved in the expression of pro-angiogenic factors FGF-2 and PDGF-BB (Hosaka *et al*., 2018).

The PCR analysis revealed that the VEGF-A gene was upregulated in keratinocytes following MFnAb treatment (Figure 6.6A), however, LRRFnAb did not neutralize the effect of extracellular Flii in keratinocytes (Figure 6.6A). These findings revealed that binding of antibody to the middle domain of Flii neutralizes its activity better than binding to the LRR domain. On the other hand, LRRFnAb was shown to increase FGF-2 in keratinocytes (Figure 6.6B), while MFnAb did not effectively change the expression of FGF-2 (Figure 6.6B). This suggests that the interaction between Flii and LRRFnAb modulates Flii impacts on the expression of FGF-2. MFnAb was found to slightly decrease PDGF-BB expression in keratinocytes (Figure 6.6C), while LRRFnAb did not

change PDGF-BB compared to normal cells (Figure 6.6C). These findings suggest that Flii may affect the expression of PDGF-BB in keratinocytes through its middle domain. The PCR results demonstrated that rFlii increased all three pro-angiogenic factors VEGF-A, FGF-2, and PDGF-BB in keratinocytes (Figure 6.7A-C), suggesting that extracellular Flii may play a key role in the regulation of signalling pathways involved in the expression of these factors. Treatment with FnAb either LRRFnAb or MFnAb did not alter the effect of rFlii on the expression of VEGF-A in keratinocytes (Figure 6.7A) while, both antibodies reduced FGF-2 when added to rFlii (Figure 6.7B). LRRFnAb was found to effectively reduce the increased PDGF expression brought about by extracellular Flii in keratinocytes (Figure 6.7C), however, MFnAb also neutralized the effect of rFlli on the expression of PDGF-BB in keratinocytes (Figure 6.7C). It is possible that the effect of LRRFnAb on the impact of rFlii may be dose dependent. To explore this further, conducting a dose-response experiment with LRRFnAb would be valuable in determining if there exists an optimal dosage for its efficacy. A dose response experiment would identify the optimum dose of LRRFnAb for neutralizing rFlii activity. Flii knockdown by siRNA was found to significantly attenuate Flii gene (Figure 6.8) but upregulate the expression of VEGF-A gene in keratinocytes (Figure 6.9A). Studies have reported that keratinocytes derived VEGF-A binds to VEGFR-2 (kinase insert-domain containing receptor (KDR) or fetal liver kinase (Flk-1)) and regulate vascular permeability, angiogenesis, and cellular migration, proliferation, and survival (Bae *et al*., 2015). Therefore, the interaction of Flii with VEGF-A signalling pathway in keratinocytes can be one of the mechanisms of action of Flii in the regulation of angiogenesis. Attenuated Flii gene also resulted in a significant upregulation in the expression of FGF-2 gene in keratinocytes (Figure 6.9B). FGF-2 and VEGF-A has been shown to synergistically stimulate angiogenesis by promoting migration of smooth muscle cells and pericytes of the vasculature and their attachment to endothelial cells (Kano *et al*., 2005). The synergistic effect observed between FGF-2 and VEGF-A, along with the findings presented in this chapter, indicates a potential involvement of the Flii gene in the regulation of keratinocyte-derived VEGF-A and FGF-2 expression. However, it is important to note that the functional consequences of VEGF-A and FGF-2 expression, such as their synergistic effect on angiogenesis, do not directly demonstrate the role of Flii in regulating their expression. Further investigations are needed to establish a definitive link between Flii and the regulation of VEGF-A and FGF-2 expression. In contrast to VEGF-A and FGF-2, the expression of PDGF-BB gene was significantly downregulated in keratinocytes following Flii

knockdown (Figure 6.9C). This suggests that Flii is required in a signalling pathway that produces PDGF-BB in keratinocytes. Keratinocyte derived Flii may have a different binding partner from those in endothelial cells (PDGF-BB was elevated after Flii knockdown in endothelial cells) that underpin the angiogenic signalling and wound healing outcomes. Further studies could explore this by conducting comparative binding assays or protein-protein interaction experiments specific to keratinocytes and endothelial cells. These additional investigations would help show the significance of the observed elevation of PDGF-BB following Flii knockdown in endothelial cells and its implications for angiogenic signalling and wound healing outcomes.

Neutralizing Flii activity with MFnAb was shown to increase the level of FGF-2 in fibroblasts (Figure 6.10B) but had no effect on the expression of pro-angiogenic VEGF-A (Figure 6.10A) and PDGF-BB (Figure 6.10C). This suggests that binding of antibody to the middle domain of Flii may inhibit Flii effects on FGF-2 expression. rFlii increased all three pro-angiogenic factors VEGF-A, FGF-2, and PDGF-BB in fibroblasts (Figure 6.10A-C), suggesting that extracellular Flii may directly affect in fibroblasts. Extracellular Flii could be a key factor involved in the expression of pro-angiogenic genes including VEGF-A, FGF-2, and PDGF-BB, all of which have previously been shown to have synergistic effects on enhancing angiogenesis during tissue repair (Kano *et al*., 2005). Interestingly, the effect of rFlii on the expression of pro-angiogenic factors was prevented when MFnAb was added as the levels of VEGF-A, FGF-2, and PDGF-BB were decreased in rFlii+ MFnAb treated fibroblasts (Figure 6.10A-C).

Overall, the results reported in this chapter suggest that both intracellular and extracellular Flii levels are implicated in controlling the expression of pro-angiogenic factors including VEGF-A, FGF-2, and PDGF-BB that are heavily involved in process of angiogenesis during wound repair. Based on the available evidence, it is suggested that decreased expression of Flii at the gene and protein levels leads to alterations in the expression of key pro-angiogenic genes. These findings imply that Flii may play a significant role in angiogenesis. However, further investigation is required to determine the specific mechanisms through which Flii influences angiogenesis, including any potential interactions with signalling pathways such as VEGF-A, FGF-2, and PDGF-BB. The binding of the LRRFnAb to the LRR domain of Flii may potentially disrupt its interactions with other molecules involved in regulating VEGF-A expression in both keratinocytes and endothelial cells. While this suggests that the LRR domain may play a role in VEGF

regulation, further investigation is needed to identify the specific molecules involved and confirm its regulatory function. Additionally, the binding of the LRRFnAb to the LRR domain of Flii may potentially interfere with the FGF-2 signalling pathway in keratinocytes and the PDGF-BB signalling pathway in endothelial cells, warranting further investigation.

On the other hand, the middle domain of Flii was found to play a significant role in the regulation of VEGF-A in both keratinocytes and endothelial cells. The middle domain of Flii may potentially influence angiogenesis through FGF-2-related signalling pathways in fibroblasts and PDGF-BB signalling in endothelial cells, necessitating further investigation. Dose response experiments can be considered for further investigations as one dose of FnAbs (based on results in Chapter 3) was used in experiments conducted in this research. rFlii could be also pre-incubated with both LRRFnAb and MFnAb simultaneously in further studies to neutralize LRR + middle domains of Flii protein. More studies are required to further confirm these results and investigate the exact mechanism of Flii in the regulation of angiogenesis. The inclusion of other genes and proteins including cyclooxygenase-2, hypoxia-inducible factor 1-alpha, and prostaglandin receptors that are involved in the signalling pathways related to VEGF-A, FGF-2, and PDGF-BB (Ahluwalia and Tarnawski, 2012; Lim, 2003; Mao *et al*., 2018; Tamura *et al*., 2006) are necessary to better investigate the function of Flii in the process of angiogenesis during tissue regeneration. Additionally, the study of VEGF-A receptors including VEGFR-1 and VEGFR-2 (Shibuya, 2011), the receptors of FGF-2 including FGFR1-3 (Koledova *et al*., 2019), and PDGF-BB receptors including PDGFRα and PDGFRβ can be carried out following the alteration of Flii levels to better investigate the role of Flii in the regulation of angiogenesis processes during wound healing (Heldin, 2013).

Chapter 7: General Discussion

7.1 Project significance

There have been many advances in burns research during recent decades, however, management of burn injuries remains a challenge as pain, slow process of healing, and hypertrophic scarring are continued causes of ongoing patient morbidity (Finnerty *et al*., 2016). The Flii protein has been identified to be a negative regulator of wound repair and it is elevated in response to wounding, including burn injury (Adams *et al*., 2009; Cowin *et al*., 2007; Kopecki *et al*., 2016). Impaired burn healing is observed in Flii overexpressing mice, while Flii heterozygous knockout mice show a significant improvement in healing of burn wounds (Adams *et al*., 2009). Flii protein is highly conserved across species and consists of a classic 6-fold gelsolin repeat at the C-terminal and 16 tandem leucine-rich repeats (LRR) at the N-terminus (Liu and Yin, 1998). This LRR domain enables Flii to interact with numerous binding partners (Strudwick and Cowin, 2020). The first Flii neutralizing antibodies (FliiL FnAbs) were generated against a specific antigen sequence corresponding to aa57-66 in the LRR of human Flii (Cowin *et al*., 2007; Strudwick and Cowin, 2020). Studies have reported that the gelsolin domain of Flii also plays a role in facilitating interactions with various cellular processes (Strudwick and Cowin, 2020). A new generation of FnAbs were subsequently raised against larger regions of Flii compared to FliiL FnAb. These FnAbs were generated against the LRR (LRRFnAb) and middle domains of Flii (MFnAb). The topical and intradermal applications of FliiL FnAb have been investigated in both acute and burn wounds, indicating wound healing promoting properties (Adams *et al*., 2009; Cowin *et al*., 2007). However, topical and intradermal applications are not clinically feasible approaches, particularly for people with extensive burns where burn injuries cover large surface areas of the body. The research presented in this thesis therefore aimed to develop a simple, effective, systemic delivery of FnAbs generated against either LRR or the middle domain of Flii for the treatment of wounds and burns. The effect of intracellular and extracellular Flii on healing parameters was also investigated in this research to better understand the effect of neutralizing extracellular Flii on the wound microenvironment.

7.2 Systemic delivery of LRRFnAb in wound healing

This research aimed to determine whether blocking different parts of the Flii protein would result in different cell functions so specific FnAbs were employed as a tool to target against LRR and middle domains of Flii. The effect of LRRFnAbs on the function of human skin cells *in vitro* was determined (Chapter 3). These antibodies were then tested systemically in an acute wound murine model (Chapter 4). The effect of systemic administration of LRRFnAbs was also investigated in a mouse model of partial-thickness scald injury (Chapter 5). Finally, the impact of LRRFnAbs on the expression of key pro-angiogenic factors were determined to better understand the role of extracellular Flii in angiogenesis (Chapter 6).

FliiL FnAb was shown to have healing outcomes using both *in vitro* and *in vivo* in topical and intradermal delivery applications (Adams *et al*., 2009; Cowin *et al*., 2007; Jackson *et al*., 2012). The results of the research presented in this thesis revealed that the new generation of antibodies targeting the LRR of Flii improved cellular functions in keratinocytes and endothelial cells *in vitro*. Additionally, systemic delivery of the LRRFnAb improved the appearance of wounds in an excisional model of wound healing. LRRFnAbs administration increased both the rate and quality of healing, confirming the negative impact of extracellular Flli on the repair process.

The findings reported in this thesis showed that systemic delivery of LRRFnAbs reduced the extracellular Flii within the wound bed in a murine model of excisional wound. Systemic administration of LRRFnAbs also exhibited a trend towards a decrease in the expression of Flii in in burn wounds. The findings of Chapter 5 demonstrated that systemically delivered LRRFnAbs travel to the wound site and localise at the site of injury from the first day, remaining there until the last day of the study (day 7).

Histology assessments of H&E-stained tissues showed that wound length and re-epithelialisation were enhanced in excisional wounds in LRRFnAb treated mice. As demonstrated in Chapter 3, LRRFnAbs increased the migration of keratinocytes, demonstrating the effect of these antibodies on wound length and re-epithelialisation. The migration of basal keratinocytes from the wound edge plays a key role in re-epithelialisation during wound healing (Wang and Graves, 2020). Flii protein regulates cell extensions in the first stage of migration as Flii recruits R-Ras in spreading cells (Arora *et al*., 2018). Flii also is an adaptor protein which links the GTPase-activating protein

SH3 domain-binding protein (G3BP1), and R-Ras facilitating downstream signalling driving cell migration (Arora *et al*., 2018). The LRR domain of Flii has been shown to bind R-Ras, Ras GAP, and G3BP, acting as a trigger factor for Rac1-mediated cell extension formation (Arora *et al*., 2018). Furthermore, The LRR of Flii interacts with Rac1 and the interaction is enhanced by P-Rex bound to the gelsolin domain of Flii, increasing the activation of myosin II (Strudwick and Cowin, 2020). The RhoA-ROCK-independent myosin II activation is facilitated by the LRR of Flii, resulting in the regulation of cell adhesion and migration (Strudwick and Cowin, 2020). Flii interaction with p-pax also affects adhesion processes including formation of focal contacts, and turnover of adhesion structures (Kopecki *et al*., 2011). These cellular events that are mediated by the LRR of Flii may explain the improvement in the re-epithelialization of excisional wounds in LRRFnAb treated mice shown in Chapter 4 of this thesis.

Despite the importance of inflammation in wound healing, an uncontrolled inflammatory response negatively impacts repair and regeneration (Boniakowski *et al*., 2017). The prolonged and systemic inflammation resulting from the excessive activation of neutrophils and macrophages has been shown to cause considerable tissue damage during tissue repair (Wilgus *et al*., 2013). As demonstrated in Chapters 4 and 5, the systemic administration of LRRFnAb resulted in a decreased number of neutrophils in the wound bed and this finding is consistent with previous studies which showed that decreasing Flii using FliiL FnAbs attenuated the number of wound bed neutrophils (Ruzehaji *et al*., 2014). Toll-like receptors (TLRs) are essential in the inflammatory burst and the TLR4 signal pathway plays a pivotal role in activating the innate immune response (Chen and DiPietro, 2017; Davis *et al*., 2019; Orr *et al*., 2012). Studies have reported that TLR4 and NF-κB expression is decreased in Flii-deficient mice and also in diabetic wounds treated with FliiL FnAb (Ruzehaji *et al*., 2013). Moreover, *in vitro* investigations have demonstrated that Flii LRR has 42% similarity and also shares 29% sequence identity with TLR4 (Wang *et al*., 2006), indicating that Flii may affect the TLR4 signalling via its LRR domain association with the TLR4 receptor as they could compete for the same ligands. Moreover, an interaction between Flii and MyD88-TLR4 has been reported in previous studies (Mogensen, 2009; Wang *et al*., 2005). Flii utilizes its gelsolin domain to bind with MyD88, thereby disrupting the MyD88-TLR4 inflammatory pathway complex after injury (Mogensen, 2009; Wang *et al*., 2005). The findings presented in this thesis showed that the systemic delivery of LRRFnAbs to both excisional and burn wounds led to a

significant decrease in M1 macrophages present in the wound bed and a concurrent increase in M2 macrophage phenotype. M1 macrophages are activated at the early phases of wound healing and have been found to delay healing, while M2 macrophages have anti-inflammatory promoting effects during repair process (Hassanshahi *et al*., 2022). The TLR4 signalling pathway and its downstream outputs facilitate the polarization of Macrophage M1/M2 (Chen *et al*., 2013). While the investigation of TLR4 and NF-κB expression was not conducted in the current study, several factors could explain this omission. The primary focus of this research was to examine the effects of extracellular and intracellular Flii on angiogenesis and key pro-angiogenic factors. Limited resources, time constraints, and previous studies already establishing the association between Flii and TLR4/NF-κB are among the reasons for not investigating these pathways in this specific context. However, future investigations could consider examining TLR4 and NF-κB expression to provide further mechanistic insights into the impacts of Flii and the potential effect of FnAb treatment. A recent study showed that elevated Flii negatively affects TLR4 and NF-κB pathways, resulting in promotion of inflammation, impaired macrophage polarization, and subsequent delayed wound healing outcomes (Mills *et al*., 2022). Collectively, LRRFnAbs appear to positively regulate inflammation during wound injury by decreasing the activity of Flii potentially by interfering with signalling pathways involved in the activation of neutrophils and macrophage responses during healing.

Angiogenesis plays a major role in process of healing as oxygen, nutrients, and immune cells are carried via blood vessels to damaged tissues (Bodnar, 2015). Flii has been reported to delay the process of angiogenesis in diabetic wounds as endothelial cells isolated from mice with overexpressed Flii lead to attenuated micro vessel sprouting (Ruzehaji *et al*., 2014). The results in Chapters 4 and 5 for the first time now show that the systemic administration of LRRFnAb to excisional wounds and burns in mice increased capillary tube formation. The *in vitro* findings in Chapter 3 also revealed that the treatment of dermal endothelial cells with LRRFnAbs led to enhanced cellular proliferation and migration. As discussed in Chapter 3, tube formation and capillary structures were improved in endothelial cells following LRRFnAb treatment *in vitro*. Results presented in this thesis are in agreement with earlier studies which showed that FliiL FnAbs stimulated HUVEC cells to form capillaries *in vitro* (Ruzehaji *et al*., 2014). Angiogenesis is highly dependent on the proliferation and migration of endothelial cells and VEGF has a major

contribution to the proliferative and migratory ability of endothelial cells (Wang *et al*., 2008). The findings of this research revealed that the improved angiogenesis in both burn, and excisional wounds in mice treated with LRRFnAbs were associated with increased VEGF. These findings are consistent with previous studies showing that mice with heterozygous knockout of Flii resulted in the elevated expression of VEGF (Ruzehaji *et al*., 2014; Thomas *et al*., 2020). Other pro-angiogenic factors including FGF-2 and PDGF-BB also influence the migration and proliferation of endothelial cells (Tonnesen *et al*., 2000; Wang *et al*., 2008). The systemic administration of LRRFnAbs was shown to increase FGF-2 in burn and excisional models of wound healing (Chapter 4 and 5). Moreover, as discussed in Chapter 4 the expression of PDGF-BB was elevated following systemic delivery of LRRFnAb to wounds. Additionally, the promoted angiogenesis was associated with the increased number of endothelial cells in burn injuries which is in agreement with the previous study revealing that Flii heterozygous mice for Flii had increased numbers of endothelial cells in wounds *in vivo* (Ruzehaji *et al*., 2014). Collectively, the results of this thesis show that LRRFnAb improves angiogenesis both *in vitro* and *in vivo*.

Overall, the systemic administration of LRRFnAbs display promising regulatory and regenerative potential as they improve various cellular functions involved in wound healing. LRRFnAbs were shown to decrease Flii and subsequently affect wound healing by enhancing re-epithelialization, angiogenesis and pro-angiogenic factors, and decreasing inflammation.

7.3 Systemic delivery of MFnAb in wound healing

The first generation of FnAbs was against a specific antigen sequence in the LRR of Flii, while MFnAbs are generated against the gelsolin domains of Flii protein. As previously discussed, the gelsolin domain of Flii is involved in various cellular events by mediating specific processes such as binding to specific receptors, regulating signalling pathways, modulating cell contractility, migration, actin dynamics, apoptosis, and inflammatory responses (Strudwick and Cowin, 2020). The effect of systemic administration of MFnAbs on the healing process was then investigated in this research *in vitro* and *in vivo*.

The systemic administration of MFnAbs resulted in attenuated Flii expression in both excisional and burn wounds. Additionally, the results of Chapter 5 confirmed that MFnAbs localized at the site of burn injury with high specificity and remained at the wound region until the last day of the study (day 7). This suggests that MFnAbs may be retained within the wound which may be due to the increased Flii expression within the wound. Taken together, systemic administration of MFnAb was shown to reduce the overall levels of Flii within the wounds and appeared to reduce Flii activity during wound healing.

Flii interacts with caspase 1 through its gelsolin domains to restrict caspase 1-induced cell death (Li *et al*., 2008). In addition to the previously discussed inflammatory effects of Flii, the binding of Flii to caspase has been suggested to play a pivotal role in the inflammatory response (Li *et al*., 2008; Strudwick and Cowin, 2020). Inflammation was dampened following systemic administration of MFnAbs to the excisional and burn models of healing. Excessive activation of neutrophils and M1 macrophages is responsible for the uncontrolled inflammation (Boniakowski *et al*., 2017) and the findings of this research revealed that both inflammatory factors (neutrophils and M1 macrophages) were attenuated in MFnAb treated mice. The number of M2 anti-inflammatory macrophages was also decreased following treatment with MFnAb in animal models of wound healing. These findings indicate that the gelsolin domains of Flii may play a major role in promotion of exacerbated inflammation during the repair process.

The systemic delivery of MFnAbs was shown to improve the macroscopic appearance of the wounds in both excisional wounds and burn injuries in mice. Additionally, the rate of wound re-epithelialization was enhanced in the mice treated with MFnAbs. Systemic administration of MFnAbs increased the number of myofibroblasts in wound bed which may explain the smaller burn wounds in MFnAb treated mice. Myofibroblasts are critical factors in the proliferative phase of wound healing as they are crucial for wound contraction and the restoration of tissue integrity and ECM depends on myofibroblasts roles (Chitturi *et al*., 2015). The overlapping function of keratinocytes and fibroblasts including cellular proliferation and migration is necessary for re-epithelialization (Raja *et al*., 2007). As mentioned in Chapter 3, the addition of MFnAbs to keratinocytes and fibroblasts resulted in increased migration and proliferation. The effects of MFnAbs on keratinocytes and fibroblast cell function suggest a potential mechanism of action of Flii during healing. Previous studies have shown the beneficial effects of FliiL FnAbs in cellular

proliferation and migration of keratinocytes and fibroblasts (Cowin *et al*., 2007) and the findings presented in this research reveal that neutralizing Flii by antibodies against the gelsolin domains also have the potential to improve healing properties *in vitro*. Additionally, the positive impacts of topical and intradermal applications of FliiL FnAbs in various healing models have been reported in several studies *in vivo* (Cowin *et al*., 2007; Haidari *et al*., 2017; Jackson *et al*., 2012; Kopecki *et al*., 2013; Ruzehaji *et al*., 2014). The results of this research also showed that systemic delivery of FnAbs against the gelsolin domains of Flii improve healing outcomes *in vivo* (Chapter 4 and 5). To date, studies have reported that the gelsolin domain of Flii is involved in the regulation of cellular migration via its interaction with the p30 domain of Caspase 11 (Li *et al*., 2008). Given the fact that MFnAbs improve cellular activities involved in wound healing this data suggests that Flii negatively affects the proliferation and migration of skin cells through its gelsolin domains, however, further studies are required to investigate exact downstream signalling pathways. Taken together, MFnAbs were found to improve the appearance of the wound as these antibodies increase migration/proliferation of keratinocytes and fibroblasts, resulting in faster re-epithelialization. The increased number of myofibroblasts by MFnAbs also suggests that middle domain of Flii may have negative effects on wound contraction.

Angiogenesis is an important process in wound healing as it plays a key role during granulation tissue formation (Guerra *et al*., 2018). The results of this thesis have demonstrated that the systemic delivery of MFnAbs led to improved angiogenesis in excisional and burn wounds. As discussed in Chapter 3, the treatment of dermal endothelial cells with MFnAbs increased cellular migration. The migration of endothelial has a great contribution to the reestablishment of new capillaries during wound repair (Lamalice *et al*., 2007). Moreover, *in vitro* Matrigel tube assay using endothelial cells treated with MFnAb showed that capillary tube formation was significantly enhanced. The findings presented in this research also revealed that the expression of proangiogenic factors VEGF and FGF-2 were increased in MFnAb treated mice. FGF-2 is a major stimulator for the expression of VEGF and plays a key role in the migration of endothelial cells (Barrientos *et al*., 2008). Collectively, results of this thesis suggests that middle domain of extracellular Flii negatively regulates angiogenesis and pro-angiogenic factors during healing.

The production of collagen is regulated by TGF-β1 which is known as a core mediator of fibrogenesis and scarring (Biernacka *et al*., 2011). An interplay between Flii and TGF-β1 is

reported and FliiL FnAb has been found to decrease gel contraction *in vitro*, while treatment with TGF-β1 restore collagen contraction (Kopecki *et al*., 2011). MFnAbs were shown to attenuate the expression of TGF-β1 following burn injury (Chapter 5). Flii has been reported to regulate TGFβ/Smad-Dependent Signalling Pathway (Chan *et al*., 2014; Kopecki *et al*., 2013). The co-precipitation of Flii and TGF-β family and Akt has been described and Flii has been found to co-localizes with Smad 2, 3, 7, AP-1, Akt, c-fos, and c-jun (Chan *et al*., 2014). Furthermore, previous studies showed that the attenuation of Flii using siRNA in fibroblasts led to a decreased level of TGF-β1 (Adams *et al*., 2008). The elevated Flii is indicated in human burns and hypertrophic scars and a previous study revealed that intradermal injection of FliiL FnAb into the wound bed resulted in reduced expression of TGF-β1 levels (Adams *et al*., 2009). The results of Chapter 5 demonstrated that systemic delivery of MFnAbs resulted in a similar impact on the expression of TGF-β1 and suggest that the middle domain of Flii interferes with a signalling pathway involved in TGF-β1expression during healing.

Overall, findings of this thesis suggest that binding of antibody to the middle domain of Flii interfere with Flii effects on different cellular events in the process of wound repair. Systemically administered MFnAbs reduced the expression of Flii and improved healing in an excisional and a scald burn model. This was mediated by reduced inflammation, increased production of pro-angiogenic factors VEGF and FGF-2, and improved angiogenesis. Additionally, MFnAbs injected systemically localised at the site of burn injury and resulted in decreased expression of pro-scarring TGF-β1 resulting in improved wound healing outcomes.

7.4 LRRFnAbs vs MFnAbs in wound healing

The new generations of FnAbs used in this research were generated against different portions of Flii as these parts of Flii have different binding partners and functions (Strudwick and Cowin, 2020). The healing effect of LRRFnAbs and MFnAbs on wound healing were investigated in this research both *in vitro* and *in vivo* while compared to the effect of IgG antibody control (Table 7.1 and Figure 7.1). As illustrated in Table 6.1, *in vitro* results reveals that MFnAbs improve healing promoting cellular functions of keratinocytes and fibroblasts more effectively than LRRFnAbs. While addition of LRRFnAbs to cultured keratinocytes and fibroblasts did not alter cellular

proliferation, cellular proliferation was significantly enhanced in keratinocytes and fibroblasts treated with MFnAbs. These results may explain the increased rate of re-epithelialization observed in excisional and burn models following systemic administration of MFnAbs. Proliferation of keratinocytes and fibroblasts and the overlapping function of these cells are critical for successful re-epithelialization and wound resolution (Raja *et al*., 2007). Moreover, the wound length was decreased in burn and excisional wounds in mice treated with MFnAb and this might be correlated to the more positive impact of MFnAbs on the proliferation of keratinocytes and fibroblasts. Both LRRFnAb and MFnAb had similar effect on the migration of keratinocytes, while MFnAb was shown to have greater effect on the migration of fibroblasts than cells treated with LRRFnAb, indicating the possible explanation for the better wound appearance in MFnAb treated mice (Chapter 5). The increased number of myofibroblasts in burns in MFnAb treated mice also suggests that MFnAbs enhance wound contraction more effectively than LRRFnAbs.

As discussed in Chapter 4, the systemic administration of both LRRFnAbs and MFnAbs decreased the expression of Flii in acute and excisional wounds, while the expression of Flii was reduced more effectively in burn wounds in MFnAb treated mice compared to mice treated with LRRFnAb (Chapter 5). These results may also explain the more improved appearance of burns in mice that received MFnAbs systemically compared to LRRFnAb treated mice. In addition, the antibody localization analysis conducted in Chapter 5 revealed that MFnAbs localized to the wound site with stronger signals in comparison with LRRFnAb over the course of the study. MFnAbs appear to have stronger binding affinity to the extracellular Flii elevated in the wound site particularly in the early days post injury, however, further research is required to determine antibody affinity and strength of interaction or binding kinetics using Biacore analysis. The stronger interaction between MFnAbs and Flii might underpin a mechanism of action of these antibodies during burn injury repair.

The excisional models treated with MFnAb resulted in decreased inflammation within the wound bed which was mediated by a reduced number of neutrophils and M1 macrophages and elevated M2 anti-inflammatory macrophages. According to Table 7.1, systemic delivery of LRRFnAb was shown to reduce inflammation less effectively compared to MFnAb in excisional wounds, while the findings of Chapter 5 revealed that both LRRFnAb and MFnAb had very similar impact on wound inflammation. The number of neutrophils was equally decreased and M2 anti-inflammatory

macrophages were similarly increased in burns in mice treated with both types of FnAbs. As previously discussed, previous studies suggest the involvement of Flii LRR domain in regulating the TLR4 signalling pathway, potentially through interaction with the TLR4 receptor and modulation of downstream signalling event (Ruzehaji *et al*., 2013). Furthermore, the interaction between Flii and MyD88-TLR4 has been reported (Mogensen, 2009; Wang *et al*., 2005). Flii binds MyD88 via its gelsolin domain to interfere with the MyD88-TLR4 inflammatory pathway complex following injury (Mogensen, 2009; Wang *et al*., 2005). The gelsolin domain of Flii was also suggested to influence inflammation through the interaction of Flii with caspase (Strudwick and Cowin, 2020). Both LRR and gelsolin domain of Flii interact with caspase 1 and caspase 11 and regulate the inflammatory response (Li *et al*., 2008). The findings of this thesis suggest that Flii can interfere with the inflammatory signalling pathways through its LRR, and gelsolin domains, however, the middle domain has greater regulatory effect on wound inflammation during wound repair process.

In vitro Matrigel tube assay showed that cells treated with MFnAb resulted in more capillary formations compared to LRRFnAb treated cells, but the cells treated with LRRFnAb still formed significantly more capillaries compared to IgG over the course of the study. *In vitro* results also demonstrated that migration of endothelial cells was increased in endothelial cells treated with either LRRFnAb or MFnAb, while the proliferative ability of endothelial cells was increased only in LRRFnAb treated cells. This may explain the increased numbers of mature blood vessels in burns in mice treated with LRRFnAb compared with MFnAb treated mice. Moreover, the pro-angiogenic factors FGF-2 and PDGF-BB were elevated in wounds in LRRFnAb treated mice (Chapter 4). However, MFnAb was found to stimulate the expression of VEGF more effectively compared to LRRFnAb treated mice. The number of mature blood vessels was significantly elevated in excisional wounds in animals administered with systemic delivery of both LRRFnAb and MFnAb. The expression of pro-angiogenic factors including VEFG and FGF-2 was equally increased in burn wounds in mice treated with either LRRFnAb or MFnAb and the number of endothelial cells was similar in both FnAbs treated mice. Collectively, both the LRR and middle domains of Flii appear to interact with specific molecules and have the potential to interfere with the binding of molecules to cell surface receptors that initiate intracellular signalling events

involved in angiogenesis during wound healing. Notably, the use of LRRFnAbs demonstrated a greater angiogenic potential in both models of wound healing.

As shown in Table 7.1, the production of pro-scarring TGF-β1 was decreased in MFnAb treated mice compared to mice treated with LRRFnAb. TGF-β1 is one of the binding partners of Flii which has been upregulated in hypertrophic scarring and human burn samples, resulting in increased expression of collagen (Adams *et al*., 2009; Strudwick and Cowin, 2020). The findings of this thesis suggest that Flii may regulate the level of pro-scarring TGF-β1 via its middle domain.

Overall, the results of this thesis have revealed the significant role of extracellular Flii in wounds including burn injuries. The systemic delivery of LRRFnAbs and MFnAbs generated against the LRR and middle domains of Flii respectively resulted in significantly improved wound healing. LRRFnAbs displayed a significant healing effect on the excisional model of wound healing while administered systemically. Angiogenesis was promoted using LRRFnAbs in both *in vitro* and *in vivo* studies. The significant angiogenic effects of LRRFnAbs in the mouse model of partial-thickness scald should be considered in the future generation of antibody-based therapies. MFnAbs were found to have strong regenerative potential including in both cell-based studies and excisional and burn models of wound healing. MFnAbs displayed a significant potential in the proliferation and migration studies of skin cells including keratinocytes and fibroblasts and accelerated re-epithelialization in both animal models. The clinical application of systemically injected Flii monoclonal antibodies could therefore be a potential approach for promoting healing of large surface area injuries including burns immediately after injury.

Table 7. 1. *In vitro* and *in vivo* effects of LRRFnAb and MFnAb compared to IgG antibody control.

Note that * shows the level of significance, NS stands for not significant difference, - indicates there is no difference, ↑ shows the increase, and ↓ shows the decrease.

Experiment	Functional outcome	LRRFnAb	MFnAb
In vitro **(24 hours)**	Keratinocyte proliferation	-	**** ↑
	Keratinocyte migration	**** ↑	*** ↑
	Fibroblast proliferation	-	** ↑
	Fibroblast migration	-	**** ↑
	Endothelial cell proliferation	*** ↑	-
	Endothelial cell migration	*** ↑	*** ↑
	Tube formation (Over the course of the experiment)	** ↑	*** ↑
Excisional wound Day 7	Macro measurements	**** ↓	** ↓
	Re-epithelialization	NS ↑	* ↑
	The wound width	NS ↓	* ↓
	Flii expression	*** ↓	*** ↓
	Neutrophil infiltration	* ↓	** ↓
	M1 macrophages	NS ↓	* ↓
	M2 macrophages	NS ↑	* ↑
	Angiogenesis	** ↑	** ↑
	VEGF	* ↑	*** ↑
	FGF-2	* ↑	NS ↑
	PDGF-BB	* ↑	NS ↑

Experiment	Effect	LRRFnAb	MFnAb
Burn wound **Day 7**	Antibody localization	** ↑	* ↑
	Macro measurements	NS ↑	NS ↓
	Re-epithelialization	* ↓	NS ↑
	The wound width	-	NS ↓
	Flii expression	NS ↓	** ↓
	Myofibroblasts	NS ↑	* ↑
	Neutrophil infiltration	** ↓	** ↓
	M1 macrophages	* ↓	** ↓
	M2 macrophages	** ↑	** ↑
	Angiogenesis	** ↑	NS ↑
	Endothelial cells	* ↑	** ↑
	VEGF	* ↑	* ↑
	FGF-2	* ↑	* ↑
	TGF-β1	NS ↓	* ↓

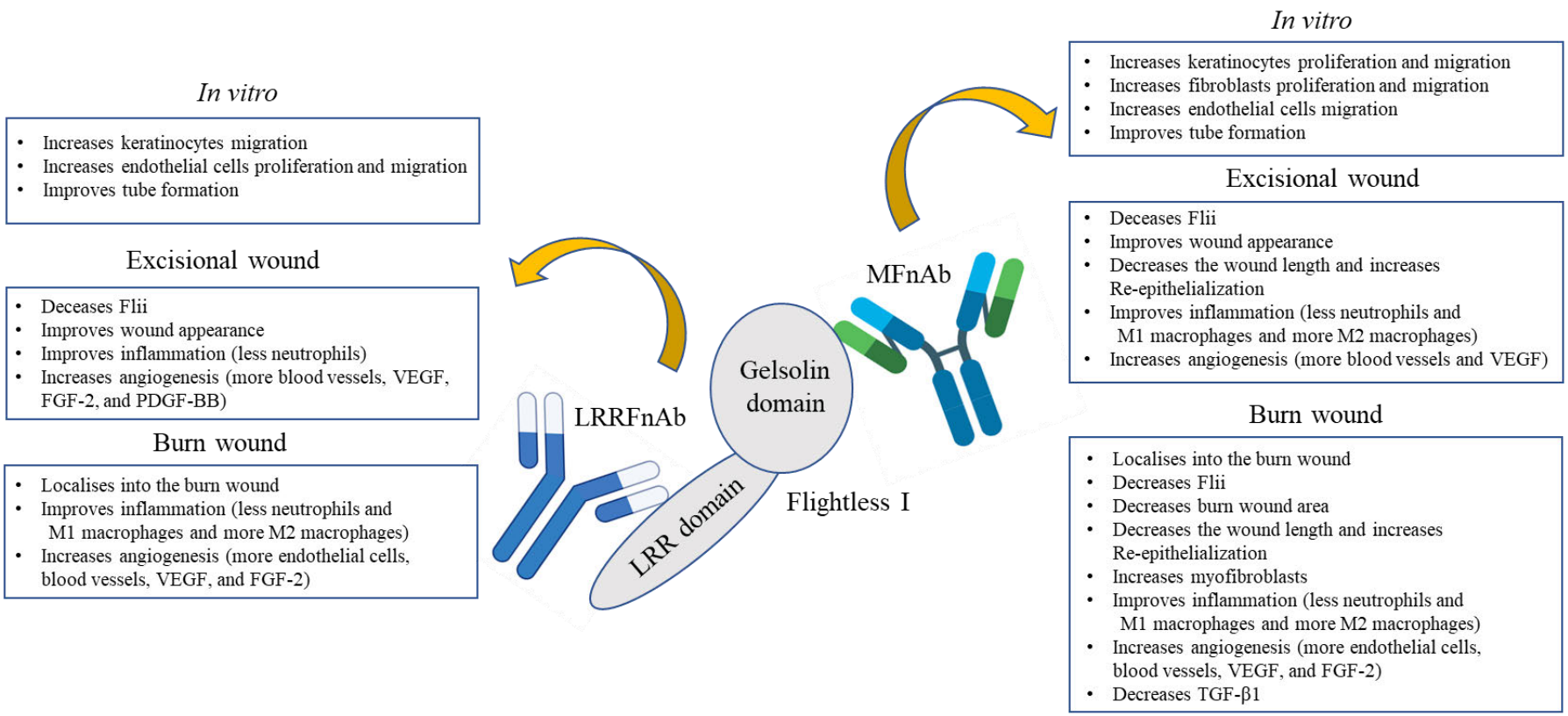


Figure 7. 1: *In vitro* and *in vivo* effects of LRRFnAb and MFnAb on wound healing compared to IgG antibody control

Binding of FnAbs to either the LRR or the middle domain of extracellular Flii have different healing outcomes both *in vitro* and *in vivo*

7.5 Extracellular and intracellular Flii interfere with the expression of pro-angiogenic factors and regulate angiogenesis

Previous studies have reported that attenuation of intracellular and extracellular Flii improves angiogenesis (Ruzehaji *et al*., 2014; Thomas *et al*., 2020). The expression of key pro-angiogenic factors VEGF-A, FGF-2, and PDGF-BB was investigated following alteration of Flii levels at gene and protein levels in skin cells *in vitro*.

7.5.1 The effect of extracellular Flii on the expression of pro-angiogenic factors

VEGF-A plays an important role in the migration of endothelial cells and is highly involved in the promotion of angiogenesis (Abhinand *et al*., 2016). The PCR findings revealed that VEGF-A gene was elevated in endothelial cells following LRRFnAb and MFnAb treatment as shown in Chapter 6. The results of Chapter 3 also showed that both LRRFnAb and MFnAb increased migration of endothelial cells. Additionally, both FnAbs increased the expression of VEGF within the wound in excisional and burn model of healing (Chapter 4 and 5). These suggested that binding of FnAbs to Flii alter Flii angiogenic functions through increased VEGF-A expression. Interestingly, addition of rFlii to endothelial cells also increased the levels of VEGF-A, indicating the complex regulation and interactions between extracellular Flii and VEGF-A which require further investigations. Pre-incubation of rFlii with LRRFnAb was shown to neutralize the effect of rFlii on the expression of VEGF-A in endothelial cells. Both LRRFnAb and MFnAb were found to have no effect on the levels of FGF-2, while treatment of endothelial cells treated with rFlii led to increased expression of FGF-2. These results show that elevated extracellular Flii may trigger signalling pathways involved in the expression of FGF-2 in endothelial cells. Pro-angiogenic factor PDGF-BB plays important roles in the maturation of blood vessels during angiogenesis (Raica and Cimpean, 2010). LRRFnAb and MFnAb decreased the expression of PDGF-BB in endothelial cells (Chapter 6). In contrast, endothelial cells treated with rFlii decreased the expression of PDGF-BB. This suggests that extracellular Flii may have a stimulatory effect on the levels of PDGF-BB at gene level in endothelial cells. Pre-incubating rFlii with LRRFnAb reduced the upregulation of PDGF-BB, while pre-incubation with MFnAb was unable to prevent the upregulation of PDGF-

BB by rFlii. This suggests that binding of antibody to LRR domain interfere with Flii effects on the expression of PDGF-BB in endothelial cells.

Addition of MFnAb to keratinocytes led to increased levels of VEGF-A (Chapter 6) which may explain the elevated expression of VEGF in the excisional wounds in mice treated with MFnAb compared to LRRFnAb treated mice (Chapter 5). Interestingly, rFlii also increased the expression of VEGF-A in keratinocytes which indicates the complexity of correlation which may exist between extracellular Flii and VEGF-A in keratinocytes. LRRFnAb was found to increase the expression of FGF-2 in keratinocytes compared to both MFnAb and IgG control antibody. This suggests that the binding of antibody to the LRR of Flii modulates the Flii effects on the expression of FGF-2 in keratinocytes and may explain the more expression of FGF-2 within the excisional wounds in LRRFnAb treated mice compared to MFnAb treated mice (Chapter 4). Additionally, the levels of FGF-2 and PDGF-BB gene were elevated in rFlii treated keratinocytes (Chapter 6). These findings suggest that increased expression of extracellular Flii may stimulate FGF-2 and PDGF-BB in keratinocytes.

Results presented in this thesis showed that MFnAb increased the expression of FGF-2 gene in fibroblasts, while MFnAb had no effect on the levels of VEGF-A and PDGF-BB in fibroblasts. Theses suggest that extracellular Flii may affect the expression of FGF-2 through its middle domain in fibroblasts. Additionally, the expression of all three pro-angiogenic factors VEGF-A, FGF-2, and PDGF-BB was significantly increased in rFlii treated fibroblasts (Chapter 6). These findings suggest that extracellular Flii may have an important regulator of pro-angiogenic factors VEGF-A, FGF-2, and PDGF-BB in fibroblasts.

7.5.2 The effect of intracellular Flii on the expression of pro-angiogenic factors

In order to investigate the effect of intracellular Flii on the expression of important pro-angiogenic factors, attenuation of Flii gene was performed using siRNA. Decreased levels of Flii gene was confirmed in endothelial cells by PCR assessments. Attenuated Flii gene resulted in decreased intracellular Flii protein in endothelial cells. Findings in Chapter 6 also revealed that siFlii had no effect on the expression of VEGF-A in endothelial cells. In contrast, siFlii treated endothelial cells showed a significant increase in the levels of FGF-2. These results suggest that intracellular Flii

gene may play a major role in signalling pathways involved in the expression of FGF-2 in endothelial cells. Similarly, the expression of PDGF-BB was elevated following treatment of endothelial cells with siFlii. Studies have demonstrated that FGF-2 and PDGF-BB have clear synergistic effect to stimulate angiogenesis (Li *et al*., 2010; Nissen *et al*., 2007). The results presented in Chapter 6 of this thesis suggest that intracellular Flii gene and protein may be involved in the signalling pathways that activate FGF-2 and PDGF-BB in endothelial cells, however, more investigations are needed to confirm the role of intracellular Flii in the expression of FGF-2 and PDGF-BB.

As shown in Chapter 6, the expression of Flii gene was significantly attenuated following siRNA knockdown of Flii in keratinocytes. Decreased Flii gene resulted in elevated expression of pro-angiogenic factors VEGF-A and FGF-2 in keratinocytes. FGF-2 acts synergistically with VEGF-A to induce angiogenesis *in vitro* and *in vivo* (Kano *et al*., 2005; Nissen *et al*., 2007). The results presented in Chapter 6 suggest that VEGF-2 and FGF-2 signalling pathways may be regulated by intracellular Flii in keratinocytes. In contrast to VEGF-A and FGF-2 findings, attenuation of Flii gene significantly decreased the levels of pro-angiogenic factor PDGF-BB, showing that intracellular Flii may be required for the expression of PDGF-BB in keratinocytes. Further investigations are necessary to determine the effect of intracellular Flii on the expression of pro-angiogenic factors in keratinocytes.

Unfortunately, there was an unexpected problem with growing fibroblasts and some results are not included in this research, particularly the experiments on siFlii treated fibroblasts. The effects of LRRFnAb on the expression of pro-angiogenic factors were not also performed due to poor fibroblasts growth.

In general, both intracellular and extracellular Flii have the potential to interact with molecules involved in angiogenic signalling pathways and interfere with their functions. Upstream/downstream relationship between interacting proteins involved in pro-angiogenic factors VEGF-A, FGF-2, and PDGF-BB can be further investigated in skin cells with altered levels of Flii to better understand the role of Flii in the regulation of angiogenesis.

7.6 Limitations and Future Outlook

This study showed that the systemic administration of LRRFnAbs and MFnAbs is a possible approach for the improvement of wound healing. Additionally, findings presented from this research demonstrated that altered intracellular and extracellular Flii have the potential to modulate healing factors, however, several aspects remained unknown and there are many areas to be further examined and considered before the translation of this antibody therapy into clinical applications. This study revealed that both LRRFnAb and MFnAb result in improved overall healing outcomes including reduced wound inflammation and anti-scarring factors, which can decrease post-repair scarring. Despite these results showing clear improvements in wound healing, further studies would be required to more clearly determine the role of systemically administered LRRFnAb or MFnAb in scarring using murine models of fibrosis and hypertrophic scarring respectively (Cameron *et al*., 2014). A porcine model of wound healing would also be needed to determine the effect of LRRFnAb and MFnAb on the repair process. As murine models are easy to handle and cost-effective, these models are the common models for animal studies. However, porcine skin is considered to most closely resemble that of humans and studies on pigs are the high standard preclinical evidence prior to commencing human trials. Porcine models are the most appropriate preclinical approach due to the physiological and anatomical similarities with humans including thick epidermis, extensive thermoregulatory vasculature, and sparse hair (Grada *et al*., 2018).

A major concern in the development of systemic antibody treatment for burns would be if there were adverse effects of the systemic treatment on patients who are critically ill. Studies show that even a 50% attenuation of Flii in mice has no detrimental effect on health (Campbell *et al*., 2002). Moreover, Flii heterozygous mice are phenotypically normal with no effects observed on lifespan, breeding, or general health (Cowin *et al*., 2007). However, a transient reduction in plasma Flii levels should be further investigated in the clinic to identify the possible effect of attenuated Flii on human health.

As shown in this thesis, the injections of both LRRFnAb and MFnAb were carried out on day 0 immediately after creating wounds. However, wound healing stages including inflammatory, proliferative, and remodelling phases take place within different timeframes. For example, the inflammatory phase initiates at the time of injury and lasts up to three to four days, while the

proliferative phase of wound healing begins about three days following injury in human (Gonzalez *et al*., 2016). Therefore, further studies are required to investigate whether delivering LRRFnAbs and MFnAbs on other days than day 0 results in different healing responses. Moreover, the effects of repeated treatment with FnAbs can be investigated (e.g., day 0, day 1, and day 3). These approaches may aid to better investigate effects and functions of Flii in wound healing outcomes and also potential adverse effects/toxicity of FnAbs.

Optimizing the dose of FnAbs *in vivo* is another required investigation which can be considered for further studies. In this study each mouse received a single 5 mg/kg of candidate FnAb for excisional and partial-thickness scald injury model. Either increasing or decreasing the dose of candidate FnAb might be associated with different healing outcomes. The expression level of Flii following excision acute wounds and burn injuries also requires further investigations to deliver the appropriate dose of FnAbs to attenuate elevated Flii in response to injuries.

Expanding the scope of the antibody tracking study to include other organs such as the liver, spleen, lungs, etc., and examining the presence of fluorescent LRRRFnAb and MFnAb (LRRRFnAb labeled with a fluorescent marker) at the endpoint would provide valuable insights into the biodistribution patterns. This comprehensive approach would enhance the characterization of the biodistribution study by assessing the distribution of antibodies in multiple organs.

Instability and poor affinity of monoclonal antibodies are known as highly significant problems in different aspects of utilisation an production of these antibodies (Joshi *et al*., 2014). Instability of antibodies may lead to decreased production yields, lost or attenuated antibody efficacy, and harmful immune reactions (Gébleux *et al*., 2015; Laptoš and Omersel, 2018). Optimizing FnAbs affinity and stability should be considered in further investigations. Multiple tests can be employed to check and monitor stability, performance, and affinity of antibodies (Ma *et al*., 2020). ELISA, and affinity assessments using SPR/Biacore can be utilised to determine the retention of biological functions including antigen binding and specificity (Ma *et al*., 2020). Moreover, circular dichroism, mass spectroscopy, and nuclear magnetic resonance have been employed to probe stability of antibodies (Guo and Carta, 2015; Nokwe *et al*., 2014). Methods based on computational design have been also developed to boost affinity and stability of antibodies (Lippow *et al*., 2007). These methods are based on the Fv complementarity determining regions which are normally in

contact with antigen (Lippow *et al*., 2007; Warszawski *et al*., 2019). FnAb specificity can be also assessed by comparing binding signals in cells with different levels of Flii or cells with targeted gene knockout by clustered regularly interspaced short palindromic repeats (CRISPR) or RNA interference (RNAi) (Boettcher and McManus, 2015).

In vitro and *in vivo* results revealed that both LRRFnAb and MFnAb affected inflammation and angiogenesis which might be the major mechanisms of action of Flii in wound healing. Future work should focus on experiments to investigate the role of Flii in modulating specific signalling pathways involved in angiogenesis and inflammation. As this thesis has briefly investigated, expression of pro-angiogenic factors VEGF-A, FGF-2, and PDGF-BB were modulated following alteration of Flii levels at protein and gene levels. Extracellular Flii protein can be inhibited using FnAbs generated against different domain of Flii to identify key downstream effectors in the expression of investigated pro-angiogenic factors using Western blotting and PCR assessments. The expression of Flii genes in skin cells can also be attenuated using siRNA knockdown to determine the effect of Flii gene on downstream and upstream of effectors involved in VEGF-A, FGF-2, and PDGF-BB signalling pathways.

Overall, the findings of this thesis support the negative effects of extracellular Flii in wound healing including burn injury repair. The results have laid the foundation for further work aiming to develop a simple, systemic, injectable antibody therapy that promotes healing and reduces scarring after extensive injury with potential applications in personalised patient approaches for acute or chronic wounds of different pathology and degree of injury.

References

Abazari, M., Ghaffari, A., Rashidzadeh, H., Badeleh, S.M., Maleki, Y., 2022. A Systematic Review on Classification, Identification, and Healing Process of Burn Wound Healing. Int J Low Extrem Wounds 21, 18-30.

Abhinand, C.S., Raju, R., Soumya, S.J., Arya, P.S., Sudhakaran, P.R., 2016. VEGF-A/VEGFR2 signaling network in endothelial cells relevant to angiogenesis. J Cell Commun Signal 10, 347-354.

Adams, D.H., Ruzehaji, N., Strudwick, X.L., Greenwood, J.E., Campbell, H.D., Arkell, R., Cowin, A.J., 2009. Attenuation of Flightless I, an actin-remodelling protein, improves burn injury repair via modulation of transforming growth factor (TGF)-beta1 and TGF-beta3. Br J Dermatol 161, 326-336.

Adams, D.H., Strudwick, X.L., Kopecki, Z., Hooper-Jones, J.A., Matthaei, K.I., Campbell, H.D., Powell, B.C., Cowin, A.J., 2008. Gender specific effects on the actin-remodelling protein Flightless I and TGF-beta1 contribute to impaired wound healing in aged skin. Int J Biochem Cell Biol 40, 1555-1569.

Ahluwalia, A., Tarnawski, A.S., 2012. Critical role of hypoxia sensor--HIF-1α in VEGF gene activation. Implications for angiogenesis and tissue injury healing. Curr Med Chem 19, 90-97.

Ahmed, N., 2011. Effectiveness of 0.025% Dakin's Solution Versus 1% Silver Sulphadiazine for Treatment of Partial Thickness Burns. 7, 94-96.

Akita, S., Akino, K., Imaizumi, T., Hirano, A., 2008. Basic fibroblast growth factor accelerates and improves second-degree burn wound healing. Wound Repair Regen 16, 635-641.

Aranez, V., Ambrus, J., Jr., 2020. Immunologic Adverse Effects of Biologics for the Treatment of Atopy. Clin Rev Allergy Immunol 59, 220-230.

Archer, S.K., Behm, C.A., Claudianos, C., Campbell, H.D., 2004. The flightless I protein and the gelsolin family in nuclear hormone receptor-mediated signalling. Biochem Soc Trans 32, 940-942.

Archer, S.K., Claudianos, C., Campbell, H.D., 2005. Evolution of the gelsolin family of actin-binding proteins as novel transcriptional coactivators. Bioessays 27, 388-396.

Arora, P.D., He, T., Ng, K., McCulloch, C.A., 2018. The leucine-rich region of Flightless I interacts with R-ras to regulate cell extension formation. Mol Biol Cell 29, 2481-2493.

Arora, P.D., Nakajima, K., Nanda, A., Plaha, A., Wilde, A., Sacks, D.B., McCulloch, C.A., 2020. Flightless anchors IQGAP1 and R-ras to mediate cell extension formation and matrix remodeling. Mol Biol Cell 31, 1595-1610.

Arturson, G., 2000. Forty years in burns research - the postburn inflammatory response. Burns 26, 599-604.

Auger, C., Samadi, O., Jeschke, M.G., 2017. The biochemical alterations underlying post-burn hypermetabolism. Biochimica et Biophysica Acta (BBA)-Molecular Basis of Disease 1863, 2633-2644.

Augustin, H.G., Kozian, D.H., Johnson, R.C., 1994. Differentiation of endothelial cells: analysis of the constitutive and activated endothelial cell phenotypes. Bioessays 16, 901-906.

Aziz, Z., Abdul Rasool Hassan, B., 2017. The effects of honey compared to silver sulfadiazine for the treatment of burns: A systematic review of randomized controlled trials. Burns 43, 50-57.

Bae, O.N., Noh, M., Chun, Y.J., Jeong, T.C., 2015. Keratinocytic vascular endothelial growth factor as a novel biomarker for pathological skin condition. Biomol Ther (Seoul) 23, 12-18.

Bainbridge, P., 2013. Wound healing and the role of fibroblasts. J Wound Care 22, 407-408, 410-412.

Bao, P., Kodra, A., Tomic-Canic, M., Golinko, M.S., Ehrlich, H.P., Brem, H., 2009. The role of vascular endothelial growth factor in wound healing. J Surg Res 153, 347-358.

Barret, J.P., Herndon, D.N., 2003. Effects of burn wound excision on bacterial colonization and invasion. Plast Reconstr Surg 111, 744-750; discussion 751-742.

Barrientos, S., Stojadinovic, O., Golinko, M.S., Brem, H., Tomic-Canic, M., 2008. Growth factors and cytokines in wound healing. Wound Repair Regen 16, 585-601.

Battegay, E.J., Rupp, J., Iruela-Arispe, L., Sage, E.H., Pech, M., 1994. PDGF-BB modulates endothelial proliferation and angiogenesis in vitro via PDGF beta-receptors. J Cell Biol 125, 917-928.

Baum, C.L., Arpey, C.J., 2005. Normal cutaneous wound healing: clinical correlation with cellular and molecular events. Dermatol Surg 31, 674-686; discussion 686.

Bell, J.K., Mullen, G.E.D., Leifer, C.A., Mazzoni, A., Davies, D.R., Segal, D.M., 2003. Leucine-rich repeats and pathogen recognition in Toll-like receptors. Trends in Immunology 24, 528-533.

Bergers, G., Song, S., 2005. The role of pericytes in blood-vessel formation and maintenance. Neuro Oncol 7, 452-464.

Bernad, R., Engelsma, D., Sanderson, H., Pickersgill, H., Fornerod, M., 2006. Nup214-Nup88 nucleoporin subcomplex is required for CRM1-mediated 60 S preribosomal nuclear export. J Biol Chem 281, 19378-19386.

Biernacka, A., Dobaczewski, M., Frangogiannis, N.G., 2011. TGF-β signaling in fibrosis. Growth Factors 29, 196-202.

Block, L., Gosain, A., King, T.W., 2015. Emerging Therapies for Scar Prevention. Adv Wound Care (New Rochelle) 4, 607-614.

Bloemsma, G.C., Dokter, J., Boxma, H., Oen, I.M., 2008. Mortality and causes of death in a burn centre. Burns 34, 1103-1107.

Bochaton-Piallat, M.L., Gabbiani, G., Hinz, B., 2016. The myofibroblast in wound healing and fibrosis: answered and unanswered questions. F1000Res 5.

Bodnar, R.J., 2015. Chemokine Regulation of Angiogenesis During Wound Healing. Adv Wound Care (New Rochelle) 4, 641-650.

Boettcher, M., McManus, M.T., 2015. Choosing the Right Tool for the Job: RNAi, TALEN, or CRISPR. Mol Cell 58, 575-585.

Boniakowski, A.E., Kimball, A.S., Jacobs, B.N., Kunkel, S.L., Gallagher, K.A., 2017. Macrophage-Mediated Inflammation in Normal and Diabetic Wound Healing. J Immunol 199, 17-24.

Borena, B.M., Martens, A., Broeckx, S.Y., Meyer, E., Chiers, K., Duchateau, L., Spaas, J.H., 2015. Regenerative Skin Wound Healing in Mammals: State-of-the-Art on Growth Factor and Stem Cell Based Treatments. Cell Physiol Biochem 36, 1-23.

Boulais, N., Misery, L., 2007. Merkel cells. Journal of the American Academy of Dermatology 57, 147-165.

Bran, G.M., Goessler, U.R., Schardt, C., Hormann, K., Riedel, F., Sadick, H., 2010. Effect of the abrogation of TGF-beta1 by antisense oligonucleotides on the expression of TGF-beta-isoforms and their receptors I and II in isolated fibroblasts from keloid scars. Int J Mol Med 25, 915-921.

Branski, L.K., Al-Mousawi, A., Rivero, H., Jeschke, M.G., Sanford, A.P., Herndon, D.N., 2009. Emerging infections in burns. Surg Infect (Larchmt) 10, 389-397.

Broughton, G., 2nd, Janis, J.E., Attinger, C.E., 2006. Wound healing: an overview. Plast Reconstr Surg 117, 1e-S-32e-S.

Brown, G.L., Curtsinger, L.J., White, M., Mitchell, R.O., Pietsch, J., Nordquist, R., von Fraunhofer, A., Schultz, G.S., 1988. Acceleration of tensile strength of incisions treated with EGF and TGF-beta. Ann Surg 208, 788-794.

Bruno, B.J., Miller, G.D., Lim, C.S., 2013. Basics and recent advances in peptide and protein drug delivery. Ther Deliv 4, 1443-1467.

Buckley, C.D., Ross, E.A., McGettrick, H.M., Osborne, C.E., Haworth, O., Schmutz, C., Stone, P.C., Salmon, M., Matharu, N.M., Vohra, R.K., Nash, G.B., Rainger, G.E., 2006. Identification of a phenotypically and functionally distinct population of long-lived neutrophils in a model of reverse endothelial migration. J Leukoc Biol 79, 303-311.

Burger, D., Fickentscher, C., de Moerloose, P., Brandt, K.J., 2016. F-actin dampens NLRP3 inflammasome activity via Flightless-I and LRRFIP2. Sci Rep 6, 29834.

Busuioc, C.J., Mogoşanu, G.D., Popescu, F.C., Lascăr, I., Pârvănescu, H., Mogoantă, L., 2013. Phases of the cutaneous angiogenesis process in experimental third-degree skin burns: histological and immunohistochemical study. Rom J Morphol Embryol 54, 163-171.

Cai, J., Ahmad, S., Jiang, W.G., Huang, J., Kontos, C.D., Boulton, M., Ahmed, A., 2003. Activation of vascular endothelial growth factor receptor-1 sustains angiogenesis and Bcl-2 expression via the phosphatidylinositol 3-kinase pathway in endothelial cells. Diabetes 52, 2959-2968.

Cameron, A.M., Adams, D.H., Greenwood, J.E., Anderson, P.J., Cowin, A.J., 2014. A novel murine model of hypertrophic scarring using subcutaneous infusion of bleomycin. Plast Reconstr Surg 133, 69-78.

Cameron, A.M., Turner, C.T., Adams, D.H., Jackson, J.E., Melville, E., Arkell, R.M., Anderson, P.J., Cowin, A.J., 2016. Flightless I is a key regulator of the fibroproliferative process in hypertrophic scarring and a target for a novel antiscarring therapy. Br J Dermatol 174, 786-794.

Campaner, A.B., Ferreira, L.M., Gragnani, A., Bruder, J.M., Cusick, J.L., Morgan, J.R., 2006. Upregulation of TGF-β1 Expression May Be Necessary but Is Not Sufficient for Excessive Scarring. Journal of Investigative Dermatology 126, 1168-1176.

Campbell, H.D., Fountain, S., McLennan, I.S., Berven, L.A., Crouch, M.F., Davy, D.A., Hooper, J.A., Waterford, K., Chen, K.S., Lupski, J.R., Ledermann, B., Young, I.G., Matthaei, K.I., 2002. Fliih, a gelsolin-related cytoskeletal regulator essential for early mammalian embryonic development. Mol Cell Biol 22, 3518-3526.

Campbell, H.D., Schimansky, T., Claudianos, C., Ozsarac, N., Kasprzak, A.B., Cotsell, J.N., Young, I.G., de Couet, H.G., Miklos, G.L., 1993. The Drosophila melanogaster flightless-I gene involved in gastrulation and muscle degeneration encodes gelsolin-like and leucine-rich repeat domains and is conserved in Caenorhabditis elegans and humans. Proc Natl Acad Sci U S A 90, 11386-11390.

Campbell, L., Saville, C.R., Murray, P.J., Cruickshank, S.M., Hardman, M.J., 2013. Local arginase 1 activity is required for cutaneous wound healing. J Invest Dermatol 133, 2461-2470.

Cao, Y., Cao, R., Hedlund, E.-M., 2008. R Regulation of tumor angiogenesis and metastasis by FGF and PDGF signaling pathways. Journal of molecular medicine 86, 785-789.

Carmeliet, P., Jain, R.K., 2011. Molecular mechanisms and clinical applications of angiogenesis. Nature 473, 298-307.

Cascone, I., Audero, E., Giraudo, E., Napione, L., Maniero, F., Philips, M.R., Collard, J.G., Serini, G., Bussolino, F., 2003. Tie-2-dependent activation of RhoA and Rac1 participates in endothelial cell motility triggered by angiopoietin-1. Blood 102, 2482-2490.

Chambers, A., 2020. Treatment of Immature Scars with Botulinum Toxin. Textbook on Scar Management: State of the Art Management and Emerging Technologies, 219-226.

Chames, P., Van Regenmortel, M., Weiss, E., Baty, D., 2009. Therapeutic antibodies: successes, limitations and hopes for the future. Br J Pharmacol 157, 220-233.

Chan, H., Kopecki, Z., Waters, J.M., Powell, B.C., Arkell, R.M., Cowin, A.J., 2014. Cytoskeletal protein flightless I differentially affects TGF-beta isoform expression in both in vitro and in vivo wound models. Wound Practice & Research: Journal of the Australian Wound Management Association 22, 169-181.

Chen, L., DiPietro, L.A., 2017. Toll-like receptor function in acute wounds. Advances in wound care 6, 344-355.

Chen, L., Guo, S., Ranzer, M.J., DiPietro, L.A., 2013. Toll-like receptor 4 has an essential role in early skin wound healing. Journal of Investigative Dermatology 133, 258-267.

Chitturi, R.T., Balasubramaniam, A.M., Parameswar, R.A., Kesavan, G., Haris, K.T., Mohideen, K., 2015. The role of myofibroblasts in wound healing, contraction and its clinical implications in cleft palate repair. J Int Oral Health 7, 75-80.

Choe, N., Kwon, J.S., Kim, J.R., Eom, G.H., Kim, Y., Nam, K.I., Ahn, Y., Kee, H.J., Kook, H., 2013. The microRNA miR-132 targets Lrrfip1 to block vascular smooth muscle cell proliferation and neointimal hyperplasia. Atherosclerosis 229, 348-355.

Chong, H.T., Yang, G.N., Sidhu, S., Ibbetson, J., Kopecki, Z., Cowin, A.J., 2017. Reducing Flightless I expression decreases severity of psoriasis in an imiquimod-induced murine model of psoriasiform dermatitis. Br J Dermatol 176, 705-712.

Church, D., Elsayed, S., Reid, O., Winston, B., Lindsay, R., 2006. Burn wound infections. Clin Microbiol Rev 19, 403-434.

Claudianos, C., Campbell, H.D., 1995. The novel flightless-I gene brings together two gene families, actin-binding proteins related to gelsolin and leucine-rich-repeat proteins involved in Ras signal transduction. Mol Biol Evol 12, 405-414.

Clayton, K., Vallejo, A.F., Davies, J., Sirvent, S., Polak, M.E., 2017. Langerhans Cells-Programmed by the Epidermis. Front Immunol 8, 1676.

Cowin, A.J., Adams, D.H., Strudwick, X.L., Chan, H., Hooper, J.A., Sander, G.R., Rayner, T.E., Matthaei, K.I., Powell, B.C., Campbell, H.D., 2007. Flightless I deficiency enhances wound repair by increasing cell migration and proliferation. J Pathol 211, 572-581.

Cowin, A.J., Lei, N., Franken, L., Ruzehaji, N., Offenhäuser, C., Kopecki, Z., Murray, R.Z., 2012. Lysosomal secretion of Flightless I upon injury has the potential to alter inflammation. Commun Integr Biol 5, 546-549.

D'Avignon, L.C., Hogan, B.K., Murray, C.K., Loo, F.L., Hospenthal, D.R., Cancio, L.C., Kim, S.H., Renz, E.M., Barillo, D., Holcomb, J.B., Wade, C.E., Wolf, S.E., 2010. Contribution of bacterial and viral infections to attributable mortality in patients with severe burns: an autopsy series. Burns 36, 773-779.

Dai, P., Jeong, S.Y., Yu, Y., Leng, T., Wu, W., Xie, L., Chen, X., 2009. Modulation of TLR signaling by multiple MyD88-interacting partners including leucine-rich repeat Fli-I-interacting proteins. J Immunol 182, 3450-3460.

Darby, I., Skalli, O., Gabbiani, G., 1990. Alpha-smooth muscle actin is transiently expressed by myofibroblasts during experimental wound healing. Lab Invest 63, 21-29.

Darby, I.A., Laverdet, B., Bonté, F., Desmoulière, A., 2014. Fibroblasts and myofibroblasts in wound healing. Clin Cosmet Investig Dermatol 7, 301-311.

Das, A., Sinha, M., Datta, S., Abas, M., Chaffee, S., Sen, C.K., Roy, S., 2015. Monocyte and macrophage plasticity in tissue repair and regeneration. Am J Pathol 185, 2596-2606.

Das, S., Baker, A.B., 2016. Biomaterials and nanotherapeutics for enhancing skin wound healing. Frontiers in bioengineering and biotechnology 4, 82.

Davis, F.M., Kimball, A., Joshi, A.D., Boniakowski, A.E., Nysz, D., Allen, R.M., Obi, A., Singer, K., Henke, P.K., Moore, B.B., 2019. Histone methylation directs myeloid TLR4 expression and regulates wound healing following cutaneous tissue injury. The Journal of Immunology 202, 1777-1785.

Demidova-Rice, T.N., Durham, J.T., Herman, I.M., 2012. Wound Healing Angiogenesis: Innovations and Challenges in Acute and Chronic Wound Healing. Adv Wound Care (New Rochelle) 1, 17-22.

Desai, M.H., Herndon, D.N., Broemeling, L., Barrow, R.E., Nichols, R.J., Jr., Rutan, R.L., 1990. Early burn wound excision significantly reduces blood loss. Ann Surg 211, 753-759; discussion 759-762.

Desmouliere, A., Redard, M., Darby, I., Gabbiani, G., 1995. Apoptosis mediates the decrease in cellularity during the transition between granulation tissue and scar. The American journal of pathology 146, 56.

Di Lernia, V., 2017. Adalimumab for treating childhood plaque psoriasis: a clinical trial evaluation. Expert Opin Biol Ther 17, 1553-1556.

Diegelmann, R.F., Evans, M.C., 2004. Wound healing: an overview of acute, fibrotic and delayed healing. Front Biosci 9, 283-289.

DiPietro, L.A., Burns, A.L., 2003. Wound healing: methods and protocols. Springer.

Du Cheyne, C., Tay, H., De Spiegelaere, W., 2020. The complex TIE between macrophages and angiogenesis. Anat Histol Embryol 49, 585-596.

Ebeling, S., Naumann, K., Pollok, S., Wardecki, T., Vidal, Y.S.S., Nascimento, J.M., Boerries, M., Schmidt, G., Brandner, J.M., Merfort, I., 2014. From a traditional medicinal plant to a rational drug: understanding the clinically proven wound healing efficacy of birch bark extract. PLoS One 9, e86147.

Eccleston, D.S., Horrigan, M.C., Ellis, S.G., 1996. Rationale for local drug delivery. Semin Interv Cardiol 1, 8-16.

Edgar, D.W., Fish, J.S., Gomez, M., Wood, F.M., 2011. Local and systemic treatments for acute edema after burn injury: a systematic review of the literature. J Burn Care Res 32, 334-347.

el-Ghalbzouri, A., Gibbs, S., Lamme, E., Van Blitterswijk, C.A., Ponec, M., 2002. Effect of fibroblasts on epidermal regeneration. Br J Dermatol 147, 230-243.

Eming, S.A., Krieg, T., Davidson, J.M., 2007. Inflammation in wound repair: molecular and cellular mechanisms. J Invest Dermatol 127, 514-525.

Engrav, L.H., Heimbach, D.M., Reus, J.L., Harnar, T.J., Marvin, J.A., 1983. Early excision and grafting vs. nonoperative treatment of burns of indeterminant depth: a randomized prospective study. J Trauma 23, 1001-1004.

Farina, J.A., Jr., Rosique, M.J., Rosique, R.G., 2013. Curbing inflammation in burn patients. Int J Inflam 2013, 715645.

Ferguson, M.W., Duncan, J., Bond, J., Bush, J., Durani, P., So, K., Taylor, L., Chantrey, J., Mason, T., James, G., Laverty, H., Occleston, N.L., Sattar, A., Ludlow, A., O'Kane, S., 2009. Prophylactic administration of avotermin for improvement of skin scarring: three double-blind, placebo-controlled, phase I/II studies. Lancet 373, 1264-1274.

Ferrante, C.J., Leibovich, S.J., 2012. Regulation of Macrophage Polarization and Wound Healing. Adv Wound Care (New Rochelle) 1, 10-16.

Ferrari, G., Pintucci, G., Seghezzi, G., Hyman, K., Galloway, A.C., Mignatti, P., 2006. VEGF, a prosurvival factor, acts in concert with TGF-beta1 to induce endothelial cell apoptosis. Proc Natl Acad Sci U S A 103, 17260-17265.

Finnerty, C.C., Jeschke, M.G., Branski, L.K., Barret, J.P., Dziewulski, P., Herndon, D.N., 2016. Hypertrophic scarring: the greatest unmet challenge after burn injury. Lancet 388, 1427-1436.

Forrest, L., 1983. Current concepts in soft connective tissue wound healing. Journal of British Surgery 70, 133-140.

Frangogiannis, N., 2020. Transforming growth factor-β in tissue fibrosis. J Exp Med 217, e20190103.

Franz, M.G., Steed, D.L., Robson, M.C., 2007. Optimizing healing of the acute wound by minimizing complications. Curr Probl Surg 44, 691-763.

Fronza, M., Heinzmann, B., Hamburger, M., Laufer, S., Merfort, I., 2009. Determination of the wound healing effect of Calendula extracts using the scratch assay with 3T3 fibroblasts. J Ethnopharmacol 126, 463-467.

Fu, X., Shen, Z., Chen, Y., Xie, J., Guo, Z., Zhang, M., Sheng, Z., 1998. Randomised placebo-controlled trial of use of topical recombinant bovine basic fibroblast growth factor for second-degree burns. Lancet 352, 1661-1664.

Gabbiani, G., 2003. The myofibroblast in wound healing and fibrocontractive diseases. The Journal of Pathology: A Journal of the Pathological Society of Great Britain and Ireland 200, 500-503.

Gassner, H.G., Sherris, D.A., 2003. Chemoimmobilization: improving predictability in the treatment of facial scars. Plast Reconstr Surg 112, 1464-1466.

Gauglitz, G.G., Korting, H.C., Pavicic, T., Ruzicka, T., Jeschke, M.G., 2011. Hypertrophic scarring and keloids: pathomechanisms and current and emerging treatment strategies. Mol Med 17, 113-125.

Gébleux, R., Wulhfard, S., Casi, G., Neri, D., 2015. Antibody Format and Drug Release Rate Determine the Therapeutic Activity of Noninternalizing Antibody–Drug ConjugatesNoninternalizing Antibody–Drug Conjugates. Molecular cancer therapeutics 14, 2606-2612.

Gettemans, J., Van Impe, K., Delanote, V., Hubert, T., Vandekerckhove, J., De Corte, V., 2005. Nuclear actin-binding proteins as modulators of gene transcription. Traffic 6, 847-857.

Ghaffari, A., Kilani, R.T., Ghahary, A., 2009. Keratinocyte-Conditioned Media Regulate Collagen Expression in Dermal Fibroblasts. Journal of Investigative Dermatology 129, 340-347.

Gil, K.M., Wilson, J.J., Edens, J.L., Webster, D.A., Abrams, M.A., Orringer, E., Grant, M., Clark, W.C., Janal, M.N., 1996. Effects of cognitive coping skills training on coping strategies and experimental pain sensitivity in African American adults with sickle cell disease. Health Psychol 15, 3-10.

Gilaberte, Y., Prieto-Torres, L., Pastushenko, I., Juarranz, Á., 2016. Chapter 1 - Anatomy and Function of the Skin, in: Hamblin, M.R., Avci, P., Prow, T.W. (Eds.), Nanoscience in Dermatology. Academic Press, Boston, pp. 1-14.

Gilbert, S.M., Gidley Baird, A., Glazer, S., Barden, J.A., Glazer, A., Teh, L.C., King, J., 2017. A phase I clinical trial demonstrates that nfP2X(7) -targeted antibodies provide a novel, safe and tolerable topical therapy for basal cell carcinoma. Br J Dermatol 177, 117-124.

Golay, J., Introna, M., 2012. Mechanism of action of therapeutic monoclonal antibodies: promises and pitfalls of in vitro and in vivo assays. Arch Biochem Biophys 526, 146-153.

Gonzalez, A.C., Costa, T.F., Andrade, Z.A., Medrado, A.R., 2016. Wound healing - A literature review. An Bras Dermatol 91, 614-620.

Gospodarowicz, D., Ferrara, N., Schweigerer, L., Neufeld, G., 1987. Structural characterization and biological functions of fibroblast growth factor. Endocr Rev 8, 95-114.

Grada, A., Mervis, J., Falanga, V., 2018. Research Techniques Made Simple: Animal Models of Wound Healing. Journal of Investigative Dermatology 138, 2095-2105.e2091.

Guerra, A., Belinha, J., Jorge, R.N., 2018. Modelling skin wound healing angiogenesis: A review. Journal of Theoretical Biology 459, 1-17.

Guo, J., Carta, G., 2015. Unfolding and aggregation of monoclonal antibodies on cation exchange columns: effects of resin type, load buffer, and protein stability. Journal of Chromatography A 1388, 184-194.

Haensel, D., Dai, X., 2018. Epithelial-to-mesenchymal transition in cutaneous wound healing: Where we are and where we are heading. Dev Dyn 247, 473-480.

Haidari, H., Zhang, Q., Melville, E., Kopecki, Z., Song, Y., Cowin, A.J., Garg, S., 2017. Development of Topical Delivery Systems for Flightless Neutralizing Antibody. J Pharm Sci 106, 1795-1804.

Hassanshahi, A., Moradzad, M., Ghalamkari, S., Fadaei, M., Cowin, A.J., Hassanshahi, M., 2022. Macrophage-Mediated Inflammation in Skin Wound Healing. Cells 11.

Heldin, C.-H., 2013. Targeting the PDGF signaling pathway in tumor treatment. Cell Communication and Signaling 11, 97.

Heldin, C.H., Westermark, B., 1999. Mechanism of action and in vivo role of platelet-derived growth factor. Physiol Rev 79, 1283-1316.

Heng, J.S., Clancy, O., Atkins, J., Leon-Villapalos, J., Williams, A.J., Keays, R., Hayes, M., Takata, M., Jones, I., Vizcaychipi, M.P., 2015. Revised Baux Score and updated Charlson comorbidity index are independently associated with mortality in burns intensive care patients. Burns 41, 1420-1427.

Hermans, M.H., 2011. Preservation methods of allografts and their (lack of) influence on clinical results in partial thickness burns. Burns 37, 873-881.

Hesketh, M., Sahin, K.B., West, Z.E., Murray, R.Z., 2017. Macrophage Phenotypes Regulate Scar Formation and Chronic Wound Healing. Int J Mol Sci 18.

Higashi, T., Ikeda, T., Murakami, T., Shirakawa, R., Kawato, M., Okawa, K., Furuse, M., Kimura, T., Kita, T., Horiuchi, H., 2010. Flightless-I (Fli-I) regulates the actin assembly activity of diaphanous-related formins (DRFs) Daam1 and mDia1 in cooperation with active Rho GTPase. J Biol Chem 285, 16231-16238.

Hinz, B., 2007. Formation and function of the myofibroblast during tissue repair. J Invest Dermatol 127, 526-537.

Hinz, B., 2016. The role of myofibroblasts in wound healing. Curr Res Transl Med 64, 171-177.

Honnegowda, T.M., Kumar, P., Udupa, E.G.P., Kumar, S., Kumar, U., Rao, P., 2015. Role of angiogenesis and angiogenic factors in acute and chronic wound healing. Plastic and Aesthetic Research 2, 243-249.

Hosaka, K., Yang, Y., Nakamura, M., Andersson, P., Yang, X., Zhang, Y., Seki, T., Scherzer, M., Dubey, O., Wang, X., Cao, Y., 2018. Dual roles of endothelial FGF-2–FGFR1–PDGF-BB and perivascular FGF-2–FGFR2–PDGFRβ signaling pathways in tumor vascular remodeling. Cell Discovery 4, 3.

Huang, G., Liang, B., Liu, G., Liu, K., Ding, Z., 2015. Low dose of glucocorticoid decreases the incidence of complications in severely burned patients by attenuating systemic inflammation. J Crit Care 30, 436.e437-411.

Hutten, S., Kehlenbach, R.H., 2006. Nup214 is required for CRM1-dependent nuclear protein export in vivo. Mol Cell Biol 26, 6772-6785.

Hwa, C., Bauer, E.A., Cohen, D.E., 2011. Skin biology. Dermatol Ther 24, 464-470.

Ichise, T., Yoshida, N., Ichise, H., 2012. Ras/MAPK signaling modulates VEGFR-3 expression through Ets-mediated p300 recruitment and histone acetylation on the Vegfr3 gene in lymphatic endothelial cells. PLoS One 7, e51639.

Ishikawa, J., Shimotoyodome, Y., Chen, S., Ohkubo, K., Takagi, Y., Fujimura, T., Kitahara, T., Takema, Y., 2012. Eucalyptus increases ceramide levels in keratinocytes and improves stratum corneum function. International journal of cosmetic science 34, 17-22.

Jabeen, S., Clough, E.C.S., Thomlinson, A.M., Chadwick, S.L., Ferguson, M.W.J., Shah, M., 2019. Partial thickness wound: Does mechanism of injury influence healing? Burns 45, 531-542.

Jackson, J.E., Kopecki, Z., Adams, D.H., Cowin, A.J., 2012. Flii neutralizing antibodies improve wound healing in porcine preclinical studies. Wound Repair Regen 20, 523-536.

Jackson, J.E., Kopecki, Z., Anderson, P.J., Cowin, A.J., 2020. Increasing the level of cytoskeletal protein Flightless I reduces adhesion formation in a murine digital flexor tendon model. Journal of Orthopaedic Surgery and Research 15, 362.

Jeong, K.W., Lee, Y.H., Stallcup, M.R., 2009. Recruitment of the SWI/SNF chromatin remodeling complex to steroid hormone-regulated promoters by nuclear receptor coactivator flightless-I. J Biol Chem 284, 29298-29309.

Jeschke, M.G., Chinkes, D.L., Finnerty, C.C., Kulp, G., Suman, O.E., Norbury, W.B., Branski, L.K., Gauglitz, G.G., Mlcak, R.P., Herndon, D.N., 2008. The pathophysiologic response to severe burn injury. Annals of surgery 248, 387.

Jeschke, M.G., van Baar, M.E., Choudhry, M.A., Chung, K.K., Gibran, N.S., Logsetty, S., 2020. Burn injury. Nature Reviews Disease Primers 6, 11.

Jian, K., Yang, C., Li, T., Wu, X., Shen, J., Wei, J., Yang, Z., Yuan, D., Zhao, M., Shi, J., 2022. PDGF-BB-derived supramolecular hydrogel for promoting skin wound healing. Journal of Nanobiotechnology 20, 201.

Jin, H.L., Yang, L., Jeong, K.W., 2017. Flightless-I homolog regulates glucocorticoid receptor-mediated transcription via direct interaction of the leucine-rich repeat domain. Mol Biol Rep 44, 243-250.

Jin, J., Yu, Q., Han, C., Hu, X., Xu, S., Wang, Q., Wang, J., Li, N., Cao, X., 2013. LRRFIP2 negatively regulates NLRP3 inflammasome activation in macrophages by promoting Flightless-I-mediated caspase-1 inhibition. Nature Communications 4, 2075.

Johnson, K.E., Wilgus, T.A., 2014. Vascular Endothelial Growth Factor and Angiogenesis in the Regulation of Cutaneous Wound Repair. Adv Wound Care (New Rochelle) 3, 647-661.

Joshi, V., Shivach, T., Kumar, V., Yadav, N., Rathore, A., 2014. Avoiding antibody aggregation during processing: establishing hold times. Biotechnology journal 9, 1195-1205.

Jull, A.B., Cullum, N., Dumville, J.C., Westby, M.J., Deshpande, S., Walker, N., 2015. Honey as a topical treatment for wounds. Cochrane Database Syst Rev 2015, Cd005083.

Kalebic, T., Garbisa, S., Glaser, B., Liotta, L.A., 1983. Basement membrane collagen: degradation by migrating endothelial cells. Science 221, 281-283.

Kano, M.R., Morishita, Y., Iwata, C., Iwasaka, S., Watabe, T., Ouchi, Y., Miyazono, K., Miyazawa, K., 2005. VEGF-A and FGF-2 synergistically promote neoangiogenesis through enhancement of endogenous PDGF-B-PDGFRbeta signaling. J Cell Sci 118, 3759-3768.

Kasutani, K., Fujii, E., Ohyama, S., Adachi, H., Hasegawa, M., Kitamura, H., Yamashita, N., 2014. Anti-IL-31 receptor antibody is shown to be a potential therapeutic option for treating itch and dermatitis in mice. Br J Pharmacol 171, 5049-5058.

Khallou-Laschet, J., Varthaman, A., Fornasa, G., Compain, C., Gaston, A.T., Clement, M., Dussiot, M., Levillain, O., Graff-Dubois, S., Nicoletti, A., Caligiuri, G., 2010. Macrophage plasticity in experimental atherosclerosis. PLoS One 5, e8852.

Kim, B.C., Kim, H.T., Park, S.H., Cha, J.S., Yufit, T., Kim, S.J., Falanga, V., 2003. Fibroblasts from chronic wounds show altered TGF-beta-signaling and decreased TGF-beta Type II receptor expression. J Cell Physiol 195, 331-336.

Kim, D.H., Xing, T., Yang, Z., Dudek, R., Lu, Q., Chen, Y.H., 2017. Epithelial Mesenchymal Transition in Embryonic Development, Tissue Repair and Cancer: A Comprehensive Overview. J Clin Med 7.

Kim, J., De Jesus, O., 2022. Medication routes of administration, StatPearls [Internet]. StatPearls Publishing.

Kim, M.H., Liu, W., Borjesson, D.L., Curry, F.R., Miller, L.S., Cheung, A.L., Liu, F.T., Isseroff, R.R., Simon, S.I., 2008. Dynamics of neutrophil infiltration during cutaneous wound healing and infection using fluorescence imaging. J Invest Dermatol 128, 1812-1820.

Klass, B.R., Grobbelaar, A.O., Rolfe, K.J., 2009. Transforming growth factor beta1 signalling, wound healing and repair: a multifunctional cytokine with clinical implications for wound repair, a delicate balance. Postgrad Med J 85, 9-14.

Kobe, B., Kajava, A.V., 2001. The leucine-rich repeat as a protein recognition motif. Current Opinion in Structural Biology 11, 725-732.

Koch, S., Tugues, S., Li, X., Gualandi, L., Claesson-Welsh, L., 2011. Signal transduction by vascular endothelial growth factor receptors. Biochem J 437, 169-183.

Kocik, J., 1996. Udział cytokin i innych mediatorów w procesie gojenia rany. Postępy Biol. Komórki 23, 63-92.

Koike, Y., Yozaki, M., Utani, A., Murota, H., 2020. Fibroblast growth factor 2 accelerates the epithelial–mesenchymal transition in keratinocytes during wound healing process. Scientific Reports 10, 18545.

Kolaczkowska, E., Kubes, P., 2013. Neutrophil recruitment and function in health and inflammation. Nat Rev Immunol 13, 159-175.

Koledova, Z., Sumbal, J., Rabata, A., de La Bourdonnaye, G., Chaloupkova, R., Hrdlickova, B., Damborsky, J., Stepankova, V., 2019. Fibroblast Growth Factor 2 Protein Stability Provides Decreased Dependence on Heparin for Induction of FGFR Signaling and Alters ERK Signaling Dynamics. Front Cell Dev Biol 7, 331.

Kopecki, Z., Arkell, R., Powell, B.C., Cowin, A.J., 2009. Flightless I regulates hemidesmosome formation and integrin-mediated cellular adhesion and migration during wound repair. J Invest Dermatol 129, 2031-2045.

Kopecki, Z., Arkell, R.M., Strudwick, X.L., Hirose, M., Ludwig, R.J., Kern, J.S., Bruckner-Tuderman, L., Zillikens, D., Murrell, D.F., Cowin, A.J., 2011. Overexpression of the Flii gene increases dermal-epidermal blistering in an autoimmune ColVII mouse model of epidermolysis bullosa acquisita. J Pathol 225, 401-413.

Kopecki, Z., Ludwig, R.J., Cowin, A.J., 2016. Cytoskeletal Regulation of Inflammation and Its Impact on Skin Blistering Disease Epidermolysis Bullosa Acquisita. Int J Mol Sci 17.

Kopecki, Z., Ruzehaji, N., Turner, C., Iwata, H., Ludwig, R.J., Zillikens, D., Murrell, D.F., Cowin, A.J., 2013. Topically applied flightless I neutralizing antibodies improve healing of blistered skin in a murine model of epidermolysis bullosa acquisita. J Invest Dermatol 133, 1008-1016.

Kopecki, Z., Yang, G.N., Arkell, R.M., Jackson, J.E., Melville, E., Iwata, H., Ludwig, R.J., Zillikens, D., Murrell, D.F., Cowin, A.J., 2014. Flightless I over-expression impairs skin barrier development, function and recovery following skin blistering. J Pathol 232, 541-552.

Kopp, T., Riedl, E., Bangert, C., Bowman, E.P., Greisenegger, E., Horowitz, A., Kittler, H., Blumenschein, W.M., McClanahan, T.K., Marbury, T., Zachariae, C., Xu, D., Hou, X.S., Mehta, A., Zandvliet, A.S., Montgomery, D., van Aarle, F., Khalilieh, S., 2015. Clinical improvement in psoriasis with specific targeting of interleukin-23. Nature 521, 222-226.

Krausz, A.E., Adler, B.L., Cabral, V., Navati, M., Doerner, J., Charafeddine, R.A., Chandra, D., Liang, H., Gunther, L., Clendaniel, A., Harper, S., Friedman, J.M., Nosanchuk, J.D., Friedman, A.J., 2015. Curcumin-encapsulated nanoparticles as innovative antimicrobial and wound healing agent. Nanomedicine 11, 195-206.

Kumar, I., Staton, C.A., Cross, S.S., Reed, M.W., Brown, N.J., 2009. Angiogenesis, vascular endothelial growth factor and its receptors in human surgical wounds. Br J Surg 96, 1484-1491.

Ladak, A., Tredget, E.E., 2009. Pathophysiology and management of the burn scar. Clin Plast Surg 36, 661-674.

Lamalice, L., Le Boeuf, F., Huot, J., 2007. Endothelial cell migration during angiogenesis. Circ Res 100, 782-794.

Landén, N.X., Li, D., Ståhle, M., 2016. Transition from inflammation to proliferation: a critical step during wound healing. Cell Mol Life Sci 73, 3861-3885.

Laptoš, T., Omersel, J., 2018. The importance of handling high-value biologicals: Physico-chemical instability and immunogenicity of monoclonal antibodies. Experimental and Therapeutic Medicine 15, 3161-3168.

Larouche, J., Sheoran, S., Maruyama, K., Martino, M.M., 2018. Immune Regulation of Skin Wound Healing: Mechanisms and Novel Therapeutic Targets. Adv Wound Care (New Rochelle) 7, 209-231.

Lateef, Z., Stuart, G., Jones, N., Mercer, A., Fleming, S., Wise, L., 2019. The Cutaneous Inflammatory Response to Thermal Burn Injury in a Murine Model. Int J Mol Sci 20.

Le, M., Naridze, R., Morrison, J., Biggs, L.C., Rhea, L., Schutte, B.C., Kaartinen, V., Dunnwald, M., 2012. Transforming growth factor Beta 3 is required for excisional wound repair in vivo. PLoS One 7, e48040.

Lecarpentier, Y., Schussler, O., Hébert, J.L., Vallée, A., 2019. Multiple Targets of the Canonical WNT/β-Catenin Signaling in Cancers. Front Oncol 9, 1248.

Lederle, W., Stark, H.J., Skobe, M., Fusenig, N.E., Mueller, M.M., 2006. Platelet-derived growth factor-BB controls epithelial tumor phenotype by differential growth factor regulation in stromal cells. Am J Pathol 169, 1767-1783.

Lee, D.E., Ayoub, N., Agrawal, D.K., 2016. Mesenchymal stem cells and cutaneous wound healing: novel methods to increase cell delivery and therapeutic efficacy. Stem Cell Res Ther 7, 37.

Lee, R.C., 1997. Injury by electrical forces: pathophysiology, manifestations, and therapy. Curr Probl Surg 34, 677-764.

Lee, Y.H., Campbell, H.D., Stallcup, M.R., 2004. Developmentally essential protein flightless I is a nuclear receptor coactivator with actin binding activity. Mol Cell Biol 24, 2103-2117.

Lee, Y.H., Stallcup, M.R., 2006. Interplay of Fli-I and FLAP1 for regulation of beta-catenin dependent transcription. Nucleic Acids Res 34, 5052-5059.

Lei, N., Franken, L., Ruzehaji, N., Offenhäuser, C., Cowin, A.J., Murray, R.Z., 2012. Flightless, secreted through a late endosome/lysosome pathway, binds LPS and dampens cytokine secretion. J Cell Sci 125, 4288-4296.

Li, J., Chen, J., Kirsner, R., 2007. Pathophysiology of acute wound healing. Clin Dermatol 25, 9-18.

Li, J., Wei, Y., Liu, K., Yuan, C., Tang, Y., Quan, Q., Chen, P., Wang, W., Hu, H., Yang, L., 2010. Synergistic effects of FGF-2 and PDGF-BB on angiogenesis and muscle regeneration in rabbit hindlimb ischemia model. Microvasc Res 80, 10-17.

Li, J., Yin, H.L., Yuan, J., 2008. Flightless-I regulates proinflammatory caspases by selectively modulating intracellular localization and caspase activity. J Cell Biol 181, 321-333.

Liao, D.J., Thakur, A., Wu, J., Biliran, H., Sarkar, F.H., 2007. Perspectives on c-Myc, Cyclin D1, and their interaction in cancer formation, progression, and response to chemotherapy. Crit Rev Oncog 13, 93-158.

Liao, S., Wang, C., Tang, D., Wei, J., He, Y., Xiong, H., Xu, F., Gao, X., Liu, X., Liu, L., 2015. [Interaction of Flightless I with Nup88 and Importin β]. Sheng Wu Gong Cheng Xue Bao 31, 1247-1254.

Lim, S.C., 2003. Role of COX-2, VEGF and cyclin D1 in mammary infiltrating duct carcinoma. Oncol Rep 10, 1241-1249.

Lin, Q., Fang, D., Fang, J., Ren, X., Yang, X., Wen, F., Su, S.B., 2011. Impaired wound healing with defective expression of chemokines and recruitment of myeloid cells in TLR3-deficient mice. J Immunol 186, 3710-3717.

Lippow, S.M., Wittrup, K.D., Tidor, B., 2007. Computational design of antibody-affinity improvement beyond in vivo maturation. Nat Biotechnol 25, 1171-1176.

Liu, J., Bang, A.G., Kintner, C., Orth, A.P., Chanda, S.K., Ding, S., Schultz, P.G., 2005. Identification of the Wnt signaling activator leucine-rich repeat in Flightless interaction protein 2 by a genome-wide functional analysis. Proc Natl Acad Sci U S A 102, 1927-1932.

Liu, Y., Zou, Z., Zhu, B., Hu, Z., Zeng, P., Wu, L., 2015. LRRFIP1 inhibits hepatitis C virus replication by inducing type I interferon in hepatocytes. Hepatitis Monthly 15.

Liu, Y.T., Yin, H.L., 1998. Identification of the binding partners for flightless I, A novel protein bridging the leucine-rich repeat and the gelsolin superfamilies. J Biol Chem 273, 7920-7927.

Lu, R.M., Hwang, Y.C., Liu, I.J., Lee, C.C., Tsai, H.Z., Li, H.J., Wu, H.C., 2020. Development of therapeutic antibodies for the treatment of diseases. J Biomed Sci 27, 1.

Lutolf, M.P., Hubbell, J.A., 2005. Synthetic biomaterials as instructive extracellular microenvironments for morphogenesis in tissue engineering. Nature Biotechnology 23, 47-55.

Ma, H., Ó'Fágáin, C., O'Kennedy, R., 2020. Antibody stability: A key to performance - Analysis, influences and improvement. Biochimie 177, 213-225.

MacDonald, B.T., Tamai, K., He, X., 2009. Wnt/beta-catenin signaling: components, mechanisms, and diseases. Dev Cell 17, 9-26.

Madison, K.C., 2003. Barrier Function of the Skin: "La Raison d'Être" of the Epidermis. Journal of Investigative Dermatology 121, 231-241.

Mahdavian Delavary, B., van der Veer, W.M., van Egmond, M., Niessen, F.B., Beelen, R.H., 2011. Macrophages in skin injury and repair. Immunobiology 216, 753-762.

Mantovani, A., Sica, A., Locati, M., 2005. Macrophage polarization comes of age. Immunity 23, 344-346.

Mao, Y., Liu, X., Song, Y., Zhai, C., Zhang, L., 2018. VEGF-A/VEGFR-2 and FGF-2/FGFR-1 but not PDGF-BB/PDGFR-β play important roles in promoting immature and inflammatory intraplaque angiogenesis. PLoS One 13, e0201395.

Marei, H., Carpy, A., Woroniuk, A., Vennin, C., White, G., Timpson, P., Macek, B., Malliri, A., 2016. Differential Rac1 signalling by guanine nucleotide exchange factors implicates FLII in regulating Rac1-driven cell migration. Nat Commun 7, 10664.

Markiewicz-Gospodarek, A., Kozioł, M., Tobiasz, M., Baj, J., Radzikowska-Büchner, E., Przekora, A., 2022. Burn Wound Healing: Clinical Complications, Medical Care, Treatment, and Dressing Types: The Current State of Knowledge for Clinical Practice. International Journal of Environmental Research and Public Health 19, 1338.

Marshall, C.D., Hu, M.S., Leavitt, T., Barnes, L.A., Lorenz, H.P., Longaker, M.T., 2018. Cutaneous Scarring: Basic Science, Current Treatments, and Future Directions. Adv Wound Care (New Rochelle) 7, 29-45.

Martens, P.J., Ly, M., Adams, D.H., Penzkover, K.R., Strudwick, X., Cowin, A.J., Poole-Warren, L.A., 2015. In vivo delivery of functional Flightless I siRNA using layer-by-layer polymer surface modification. Journal of Biomaterials Applications 30, 257-268.

Martin, P., 1997. Wound healing--aiming for perfect skin regeneration. Science 276, 75-81.

Martin, P., Leibovich, S.J., 2005. Inflammatory cells during wound repair: the good, the bad and the ugly. Trends Cell Biol 15, 599-607.

Masson-Meyers, D.S., Andrade, T.A.M., Caetano, G.F., Guimaraes, F.R., Leite, M.N., Leite, S.N., Frade, M.A.C., 2020. Experimental models and methods for cutaneous wound healing assessment. Int J Exp Pathol 101, 21-37.

Matsuoka, H., Sisson, T.H., Nishiuma, T., Simon, R.H., 2006. Plasminogen-mediated activation and release of hepatocyte growth factor from extracellular matrix. Am J Respir Cell Mol Biol 35, 705-713.

Mead, A.L., Wong, T.T., Cordeiro, M.F., Anderson, I.K., Khaw, P.T., 2003. Evaluation of anti-TGF-beta2 antibody as a new postoperative anti-scarring agent in glaucoma surgery. Invest Ophthalmol Vis Sci 44, 3394-3401.

Mills, S.J., Ahangar, P., Thomas, H.M., Hofma, B.R., Murray, R.Z., Cowin, A.J., 2022. Flightless I Negatively Regulates Macrophage Surface TLR4, Delays Early Inflammation, and Impedes Wound Healing. Cells 11.

Mogensen, T.H., 2009. Pathogen recognition and inflammatory signaling in innate immune defenses. Clin Microbiol Rev 22, 240-273, Table of Contents.

Mohammad, I., Arora, P.D., Naghibzadeh, Y., Wang, Y., Li, J., Mascarenhas, W., Janmey, P.A., Dawson, J.F., McCulloch, C.A., 2012. Flightless I is a focal adhesion-associated actin-capping protein that regulates cell migration. Faseb j 26, 3260-3272.

Molina, E.A., Hartmann, B., Oliver, M.A., Kirkpatrick, L.D., Keyloun, J.W., Moffatt, L.T., Shupp, J.W., Travis, T.E., Carney, B.C., 2022. Angiogenic gene characterization and vessel permeability of dermal microvascular endothelial cells isolated from burn hypertrophic scar. Scientific Reports 12, 12222.

Monika, P., Chandraprabha, M.N., Rangarajan, A., Waiker, P.V., Chidambara Murthy, K.N., 2021a. Challenges in Healing Wound: Role of Complementary and Alternative Medicine. Front Nutr 8, 791899.

Monika, P., Waiker, P.V., Chandraprabha, M.N., Rangarajan, A., Murthy, K.N.C., 2021b. Myofibroblast progeny in wound biology and wound healing studies. Wound Repair Regen 29, 531-547.

Monsaingeon, A., Molimard, R., 1976. Wound healing. Comparison of healing rates of burn wounds and of excisional wounds. Eur Surg Res 8, 337-343.

Moreira, A.P., Hogaboam, C.M., 2011. Macrophages in allergic asthma: fine-tuning their pro- and anti-inflammatory actions for disease resolution. J Interferon Cytokine Res 31, 485-491.

Morgan, M.R., Humphries, M.J., Bass, M.D., 2007. Synergistic control of cell adhesion by integrins and syndecans. Nat Rev Mol Cell Biol 8, 957-969.

Morikawa, S., Baluk, P., Kaidoh, T., Haskell, A., Jain, R.K., McDonald, D.M., 2002. Abnormalities in pericytes on blood vessels and endothelial sprouts in tumors. Am J Pathol 160, 985-1000.

Morton, L.M., Phillips, T.J., 2012. Wound healing update. Semin Cutan Med Surg 31, 33-37.

Murray, P.J., Allen, J.E., Biswas, S.K., Fisher, E.A., Gilroy, D.W., Goerdt, S., Gordon, S., Hamilton, J.A., Ivashkiv, L.B., Lawrence, T., Locati, M., Mantovani, A., Martinez, F.O., Mege, J.L., Mosser, D.M., Natoli, G., Saeij, J.P., Schultze, J.L., Shirey, K.A., Sica, A., Suttles, J., Udalova, I., van Ginderachter, J.A., Vogel, S.N., Wynn, T.A., 2014. Macrophage activation and polarization: nomenclature and experimental guidelines. Immunity 41, 14-20.

Mustoe, T.A., O'Shaughnessy, K., Kloeters, O., 2006. Chronic wound pathogenesis and current treatment strategies: a unifying hypothesis. Plast Reconstr Surg 117, 35s-41s.

Nag, S., Larsson, M., Robinson, R.C., Burtnick, L.D., 2013. Gelsolin: the tail of a molecular gymnast. Cytoskeleton (Hoboken) 70, 360-384.

Nall, A.V., Brownlee, R.E., Colvin, C.P., Schultz, G., Fein, D., Cassisi, N.J., Nguyen, T., Kalra, A., 1996. Transforming growth factor beta 1 improves wound healing and random flap survival in normal and irradiated rats. Arch Otolaryngol Head Neck Surg 122, 171-177.

Namdar, T., Stollwerck, P.L., Stang, F.H., Siemers, F., Mailänder, P., Lange, T., 2010. Transdermal fluid loss in severely burned patients. Ger Med Sci 8, Doc28.

Namiki, A., Brogi, E., Kearney, M., Kim, E.A., Wu, T., Couffinhal, T., Varticovski, L., Isner, J.M., 1995. Hypoxia induces vascular endothelial growth factor in cultured human endothelial cells. J Biol Chem 270, 31189-31195.

Nielson, C.B., Duethman, N.C., Howard, J.M., Moncure, M., Wood, J.G., 2017. Burns: Pathophysiology of Systemic Complications and Current Management. J Burn Care Res 38, e469-e481.

Nissen, L.J., Cao, R., Hedlund, E.M., Wang, Z., Zhao, X., Wetterskog, D., Funa, K., Bråkenhielm, E., Cao, Y., 2007. Angiogenic factors FGF2 and PDGF-BB synergistically promote murine tumor neovascularization and metastasis. J Clin Invest 117, 2766-2777.

Nokwe, C.N., Zacharias, M., Yagi, H., Hora, M., Reif, B., Goto, Y., Buchner, J., 2014. A residue-specific shift in stability and amyloidogenicity of antibody variable domains. Journal of Biological Chemistry 289, 26829-26846.

Norbury, W., Herndon, D.N., Tanksley, J., Jeschke, M.G., Finnerty, C.C., 2016. Infection in Burns. Surg Infect (Larchmt) 17, 250-255.

Norman, D., 2003. The use of povidone-iodine in superficial partial-thickness burns. Br J Nurs 12, S30-36.

Norman, G., Christie, J., Liu, Z., Westby, M.J., Jefferies, J.M., Hudson, T., Edwards, J., Mohapatra, D.P., Hassan, I.A., Dumville, J.C., 2017. Antiseptics for burns. Cochrane Database Syst Rev 7, Cd011821.

Nowinski, D., Lysheden, A.S., Gardner, H., Rubin, K., Gerdin, B., Ivarsson, M., 2004. Analysis of gene expression in fibroblasts in response to keratinocyte-derived factors in vitro: potential implications for the wound healing process. J Invest Dermatol 122, 216-221.

Ohtsuka, H., Oikawa, M., Ariake, K., Rikiyama, T., Motoi, F., Katayose, Y., Unno, M., Johnson, A.C., 2011. GC-binding factor 2 interacts with dishevelled and regulates Wnt signaling pathways in human carcinoma cell lines. Int J Cancer 129, 1599-1610.

Olson, M.F., Marais, R., 2000. Ras protein signalling. Semin Immunol 12, 63-73.

Ong, Y.S., Samuel, M., Song, C., 2006. Meta-analysis of early excision of burns. Burns 32, 145-150.

Onimaru, M., Yonemitsu, Y., Fujii, T., Tanii, M., Nakano, T., Nakagawa, K., Kohno, R., Hasegawa, M., Nishikawa, S., Sueishi, K., 2009. VEGF-C regulates lymphangiogenesis and capillary stability by regulation of PDGF-B. Am J Physiol Heart Circ Physiol 297, H1685-1696.

Ordás, I., Mould, D.R., Feagan, B.G., Sandborn, W.J., 2012. Anti-TNF monoclonal antibodies in inflammatory bowel disease: pharmacokinetics-based dosing paradigms. Clin Pharmacol Ther 91, 635-646.

Orr, J.S., Puglisi, M.J., Ellacott, K.L., Lumeng, C.N., Wasserman, D.H., Hasty, A.H., 2012. Toll-like receptor 4 deficiency promotes the alternative activation of adipose tissue macrophages. Diabetes 61, 2718-2727.

Papanas, N., Maltezos, E., 2007. Growth factors in the treatment of diabetic foot ulcers: new technologies, any promises? Int J Low Extrem Wounds 6, 37-53.

Pastar, I., Stojadinovic, O., Krzyzanowska, A., Barrientos, S., Stuelten, C., Zimmerman, K., Blumenberg, M., Brem, H., Tomic-Canic, M., 2010. Attenuation of the transforming growth factor beta-signaling pathway in chronic venous ulcers. Mol Med 16, 92-101.

Pastar, I., Stojadinovic, O., Yin, N.C., Ramirez, H., Nusbaum, A.G., Sawaya, A., Patel, S.B., Khalid, L., Isseroff, R.R., Tomic-Canic, M., 2014. Epithelialization in Wound Healing: A Comprehensive Review. Adv Wound Care (New Rochelle) 3, 445-464.

Pedrosa, A.F.B., Rodrigues, A.G., 2011. Candidemia in Burn Patients: Figures and Facts. Journal of Trauma and Acute Care Surgery 70.

Pereira, C.T., Herndon, D.N., 2005. The pharmacologic modulation of the hypermetabolic response to burns. Adv Surg 39, 245-261.

Pereira, R.F., Barrias, C.C., Granja, P.L., Bartolo, P.J., 2013. Advanced biofabrication strategies for skin regeneration and repair. Nanomedicine (Lond) 8, 603-621.

Periayah, M.H., Halim, A.S., Mat Saad, A.Z., 2017. Mechanism Action of Platelets and Crucial Blood Coagulation Pathways in Hemostasis. Int J Hematol Oncol Stem Cell Res 11, 319-327.

Plikus, M.V., Gay, D.L., Treffeisen, E., Wang, A., Supapannachart, R.J., Cotsarelis, G., 2012. Epithelial stem cells and implications for wound repair. Semin Cell Dev Biol 23, 946-953.

Porter, C., Tompkins, R.G., Finnerty, C.C., Sidossis, L.S., Suman, O.E., Herndon, D.N., 2016. The metabolic stress response to burn trauma: current understanding and therapies. The Lancet 388, 1417-1426.

Powers, C.J., McLeskey, S.W., Wellstein, A., 2000. Fibroblast growth factors, their receptors and signaling. Endocr Relat Cancer 7, 165-197.

Procter, F., 2010. Rehabilitation of the burn patient. Indian J Plast Surg 43, S101-113.

Pucułek, M., Baj, J., Portincasa, P., Sitarz, M., Grochowski, C., Radzikowska, E., 2021. The morphology and application of stem cells in digestive system surgery. Folia Morphologica 80, 13-19.

Puri, V., Khare, N.A., Chandramouli, M.V., Shende, N., Bharadwaj, S., 2016. Comparative Analysis of Early Excision and Grafting vs Delayed Grafting in Burn Patients in a Developing Country. J Burn Care Res 37, 278-282.

Raica, M., Cimpean, A.M., 2010. Platelet-Derived Growth Factor (PDGF)/PDGF Receptors (PDGFR) Axis as Target for Antitumor and Antiangiogenic Therapy. Pharmaceuticals (Basel) 3, 572-599.

Raja, Sivamani, K., Garcia, M.S., Isseroff, R.R., 2007. Wound re-epithelialization: modulating keratinocyte migration in wound healing. Front Biosci 12, 2849-2868.

Randi, A.M., Laffan, M.A., Starke, R.D., 2013. Von Willebrand factor, angiodysplasia and angiogenesis. Mediterr J Hematol Infect Dis 5, e2013060.

Rao, X., Zhong, J., Zhang, S., Zhang, Y., Yu, Q., Yang, P., Wang, M.H., Fulton, D.J., Shi, H., Dong, Z., Wang, D., Wang, C.Y., 2011. Loss of methyl-CpG-binding domain protein 2 enhances endothelial angiogenesis and protects mice against hind-limb ischemic injury. Circulation 123, 2964-2974.

Reinke, J.M., Sorg, H., 2012. Wound repair and regeneration. Eur Surg Res 49, 35-43.

Roberts, A.B., Sporn, M.B., Assoian, R.K., Smith, J.M., Roche, N.S., Wakefield, L.M., Heine, U.I., Liotta, L.A., Falanga, V., Kehrl, J.H., *et al*., 1986. Transforming growth factor type beta: rapid induction of fibrosis and angiogenesis in vivo and stimulation of collagen formation in vitro. Proc Natl Acad Sci U S A 83, 4167-4171.

Robson, M.C., 1997. The role of growth factors in the healing of chronic wounds. Wound Repair Regen 5, 12-17.

Rodero, M.P., Licata, F., Poupel, L., Hamon, P., Khosrotehrani, K., Combadiere, C., Boissonnas, A., 2014. In vivo imaging reveals a pioneer wave of monocyte recruitment into mouse skin wounds. PLoS One 9, e108212.

Rossiter, H., Barresi, C., Pammer, J., Rendl, M., Haigh, J., Wagner, E.F., Tschachler, E., 2004. Loss of vascular endothelial growth factor a activity in murine epidermal keratinocytes delays wound healing and inhibits tumor formation. Cancer Res 64, 3508-3516.

Rowan, M.P., Cancio, L.C., Elster, E.A., Burmeister, D.M., Rose, L.F., Natesan, S., Chan, R.K., Christy, R.J., Chung, K.K., 2015. Burn wound healing and treatment: review and advancements. Crit Care 19, 243.

Ruzehaji, N., Kopecki, Z., Melville, E., Appleby, S.L., Bonder, C.S., Arkell, R.M., Fitridge, R., Cowin, A.J., 2014. Attenuation of flightless I improves wound healing and enhances angiogenesis in a murine model of type 1 diabetes. Diabetologia 57, 402-412.

Ruzehaji, N., Mills, S.J., Melville, E., Arkell, R., Fitridge, R., Cowin, A.J., 2013. The influence of Flightless I on Toll-like-receptor-mediated inflammation in a murine model of diabetic wound healing. Biomed Res Int 2013, 389792.

Saghazadeh, S., Rinoldi, C., Schot, M., Kashaf, S.S., Sharifi, F., Jalilian, E., Nuutila, K., Giatsidis, G., Mostafalu, P., Derakhshandeh, H., Yue, K., Swieszkowski, W., Memic, A., Tamayol, A., Khademhosseini, A., 2018. Drug delivery systems and materials for wound healing applications. Advanced Drug Delivery Reviews 127, 138-166.

Sahni, A., Francis, C.W., 2004. Stimulation of endothelial cell proliferation by FGF-2 in the presence of fibrinogen requires αvβ3. Blood 104, 3635-3641.

Sakallioglu, A.E., Basaran, O., Karakayali, H., Ozdemir, B.H., Yucel, M., Arat, Z., Haberal, M., 2006. Interactions of systemic immune response and local wound healing in different burn depths: an experimental study on rats. J Burn Care Res 27, 357-366.

Sakimoto, T., Sugaya, S., Ishimori, A., Sawa, M., 2012. Anti-inflammatory effect of IL-6 receptor blockade in corneal alkali burn. Exp Eye Res 97, 98-104.

Sasaki, T., 1992. The effects of basic fibroblast growth factor and doxorubicin on cultured human skin fibroblasts: relevance to wound healing. J Dermatol 19, 664-666.

Schlüter, A., Weller, P., Kanaan, O., Nel, I., Heusgen, L., Höing, B., Haßkamp, P., Zander, S., Mandapathil, M., Dominas, N., Arnolds, J., Stuck, B.A., Lang, S., Bankfalvi, A., Brandau, S., 2018. CD31 and VEGF are prognostic biomarkers in early-stage, but not in late-stage, laryngeal squamous cell carcinoma. BMC Cancer 18, 272.

Schmidt-Ullrich, R., Paus, R., 2005. Molecular principles of hair follicle induction and morphogenesis. Bioessays 27, 247-261.

Schultz, G.S., Davidson, J.M., Kirsner, R.S., Bornstein, P., Herman, I.M., 2011. Dynamic reciprocity in the wound microenvironment. Wound Repair Regen 19, 134-148.

Schultz, G.S., Wysocki, A., 2009. Interactions between extracellular matrix and growth factors in wound healing. Wound Repair Regen 17, 153-162.

Schwanholt, C., Greenhalgh, D.G., Warden, G.D., 1993. A comparison of full-thickness versus split-thickness autografts for the coverage of deep palm burns in the very young pediatric patient. J Burn Care Rehabil 14, 29-33.

Segel, G.B., Halterman, M.W., Lichtman, M.A., 2011. The paradox of the neutrophil's role in tissue injury. J Leukoc Biol 89, 359-372.

Seghezzi, G., Patel, S., Ren, C.J., Gualandris, A., Pintucci, G., Robbins, E.S., Shapiro, R.L., Galloway, A.C., Rifkin, D.B., Mignatti, P., 1998. Fibroblast growth factor-2 (FGF-2) induces vascular endothelial growth factor (VEGF) expression in the endothelial cells of forming capillaries: an autocrine mechanism contributing to angiogenesis. J Cell Biol 141, 1659-1673.

Sen, C.K., 2019. Human Wounds and Its Burden: An Updated Compendium of Estimates. Adv Wound Care (New Rochelle) 8, 39-48.

Sen, C.K., 2021. Human Wound and Its Burden: Updated 2020 Compendium of Estimates. Adv Wound Care (New Rochelle) 10, 281-292.

Seo, H.-R., Jeong, H.E., Joo, H.J., Choi, S.-C., Park, C.-Y., Kim, J.-H., Choi, J.-H., Cui, L.-H., Hong, S.J., Chung, S., Lim, D.-S., 2016. Intrinsic FGF2 and FGF5 promotes angiogenesis of human aortic endothelial cells in 3D microfluidic angiogenesis system. Scientific Reports 6, 28832.

Serini, G., Gabbiani, G., 1999. Mechanisms of myofibroblast activity and phenotypic modulation. Exp Cell Res 250, 273-283.

Serrano, C., Boloix-Tortosa, R., Gómez-Cía, T., Acha, B., 2015. Features identification for automatic burn classification. Burns 41, 1883-1890.

Seward, M.E., Easley, C.A.t., McLeod, J.J., Myers, A.L., Tombes, R.M., 2008. Flightless-I, a gelsolin family member and transcriptional regulator, preferentially binds directly to activated cytosolic CaMK-II. FEBS Lett 582, 2489-2495.

Shah, M., Foreman, D.M., Ferguson, M.W., 1992. Control of scarring in adult wounds by neutralising antibody to transforming growth factor beta. Lancet 339, 213-214.

Shah, M., Foreman, D.M., Ferguson, M.W., 1994. Neutralising antibody to TGF-beta 1,2 reduces cutaneous scarring in adult rodents. J Cell Sci 107 (Pt 5), 1137-1157.

Shaw, T.J., Martin, P., 2009. Wound repair at a glance. J Cell Sci 122, 3209-3213.

Shaw, T.J., Martin, P., 2016. Wound repair: a showcase for cell plasticity and migration. Curr Opin Cell Biol 42, 29-37.

Shibuya, M., 2011. Vascular Endothelial Growth Factor (VEGF) and Its Receptor (VEGFR) Signaling in Angiogenesis: A Crucial Target for Anti- and Pro-Angiogenic Therapies. Genes Cancer 2, 1097-1105.

Shin, D., Minn, K.W., 2004. The effect of myofibroblast on contracture of hypertrophic scar. Plastic and reconstructive surgery 113, 633-640.

Shpichka, A., Butnaru, D., Bezrukov, E.A., Sukhanov, R.B., Atala, A., Burdukovskii, V., Zhang, Y., Timashev, P., 2019. Skin tissue regeneration for burn injury. Stem Cell Res Ther 10, 94.

Shupp, J.W., Pavlovich, A.R., Jeng, J.C., Pezzullo, J.C., Oetgen, W.J., Jaskille, A.D., Jordan, M.H., Shoham, S., 2010. Epidemiology of bloodstream infections in burn-injured patients: a review of the national burn repository. J Burn Care Res 31, 521-528.

Silva, J.P., Dhall, S., Garcia, M., Chan, A., Costa, C., Gama, M., Martins-Green, M., 2015. Improved burn wound healing by the antimicrobial peptide LLKKK18 released from conjugates with dextrin embedded in a carbopol gel. Acta Biomater 26, 249-262.

Singer, A.J., Clark, R.A., 1999. Cutaneous wound healing. N Engl J Med 341, 738-746.

Singh, M., Nuutila, K., Kruse, C., Robson, M.C., Caterson, E., Eriksson, E., 2015. Challenging the Conventional Therapy: Emerging Skin Graft Techniques for Wound Healing. Plast Reconstr Surg 136, 524e-530e.

Singh, S., Kumar, N.K., Dwiwedi, P., Charan, J., Kaur, R., Sidhu, P., Chugh, V.K., 2018. Monoclonal Antibodies: A Review. Curr Clin Pharmacol 13, 85-99.

Snowden, J.M., 1984. Wound closure: an analysis of the relative contributions of contraction and epithelialization. J Surg Res 37, 453-463.

Soga, N., Connolly, J.O., Chellaiah, M., Kawamura, J., Hruska, K.A., 2001. Rac regulates vascular endothelial growth factor stimulated motility. Cell Commun Adhes 8, 1-13.

Sogabe, Y., Abe, M., Yokoyama, Y., Ishikawa, O., 2006. Basic fibroblast growth factor stimulates human keratinocyte motility by Rac activation. Wound Repair Regen 14, 457-462.

Sommer, K., Sander, A.L., Albig, M., Weber, R., Henrich, D., Frank, J., Marzi, I., Jakob, H., 2013. Delayed wound repair in sepsis is associated with reduced local pro-inflammatory cytokine expression. PLoS One 8, e73992.

Stanojcic, M., Abdullahi, A., Rehou, S., Parousis, A., Jeschke, M.G., 2018. Pathophysiological response to burn injury in adults. Annals of surgery 267, 576.

Steen, M., 1993. Review of the use of povidone-iodine (PVP-I) in the treatment of burns. Postgrad Med J 69 Suppl 3, S84-92.

Stojadinovic, O., 2007. A novel non-angiogenic mechanism of VEGF : stimulation of keratinocyte and fibroblast migration. Wound Repair Regen 15, A30.

Straub, K.L., Stella, M.C., Leptin, M., 1996. The gelsolin-related flightless I protein is required for actin distribution during cellularisation in Drosophila. J Cell Sci 109 (Pt 1), 263-270.

Streit, M., Beleznay, Z., Braathen, L.R., 2006. Topical application of the tumour necrosis factor-alpha antibody infliximab improves healing of chronic wounds. Int Wound J 3, 171-179.

Strom, A., Weis, K., June 2001, posting date. Importin-beta-like nuclear transport receptors. Genome Biol 2.

Strudwick, X., Cowin, A., 2018. The Role of the Inflammatory Response in Burn Injury.

Strudwick, X.L., Cowin, A.J., 2020. Multifunctional Roles of the Actin-Binding Protein Flightless I in Inflammation, Cancer and Wound Healing. Frontiers in Cell and Developmental Biology 8.

Stubhaug, A., Romundstad, L., Kaasa, T., Breivik, H., 2007. Methylprednisolone and ketorolac rapidly reduce hyperalgesia around a skin burn injury and increase pressure pain thresholds. Acta Anaesthesiol Scand 51, 1138-1146.

Sufen, G., Xianghong, Y., Yongxia, C., Qian, P., 2011. bFGF and PDGF-BB have a synergistic effect on the proliferation, migration and VEGF release of endothelial progenitor cells. Cell Biol Int 35, 545-551.

Sun, K.H., Chang, Y., Reed, N.I., Sheppard, D., 2016. α-Smooth muscle actin is an inconsistent marker of fibroblasts responsible for force-dependent TGFβ activation or collagen production across multiple models of organ fibrosis. Am J Physiol Lung Cell Mol Physiol 310, L824-836.

Suzuki, M., Kato, C., Kato, A., 2015. Therapeutic antibodies: their mechanisms of action and the pathological findings they induce in toxicity studies. J Toxicol Pathol 28, 133-139.

Tamura, K., Sakurai, T., Kogo, H., 2006. Relationship between prostaglandin E2 and vascular endothelial growth factor (VEGF) in angiogenesis in human vascular endothelial cells. Vascul Pharmacol 44, 411-416.

Thomas, H.M., Ahangar, P., Hofma, B.R., Strudwick, X.L., Fitridge, R., Mills, S.J., Cowin, A.J., 2020. Attenuation of Flightless I Increases Human Pericyte Proliferation, Migration and Angiogenic Functions and Improves Healing in Murine Diabetic Wounds. Int J Mol Sci 21.

Tickle, C., 2006. Making digit patterns in the vertebrate limb. Nature reviews Molecular cell biology 7, 45-53.

Tiwari, V.K., 2012. Burn wound: How it differs from other wounds? Indian J Plast Surg 45, 364-373.

Tomasek, J.J., Gabbiani, G., Hinz, B., Chaponnier, C., Brown, R.A., 2002. Myofibroblasts and mechano-regulation of connective tissue remodelling. Nat Rev Mol Cell Biol 3, 349-363.

Tonnesen, M.G., Feng, X., Clark, R.A., 2000. Angiogenesis in wound healing. J Investig Dermatol Symp Proc 5, 40-46.

Tsatmali, M., Ancans, J., Thody, A.J., 2002. Melanocyte Function and Its Control by Melanocortin Peptides. Journal of Histochemistry & Cytochemistry 50, 125-133.

Turner, C.T., Hasanzadeh Kafshgari, M., Melville, E., Delalat, B., Harding, F., Mäkilä, E., Salonen, J.J., Cowin, A.J., Voelcker, N.H., 2016. Delivery of Flightless I siRNA from Porous Silicon Nanoparticles Improves Wound Healing in Mice. ACS Biomater Sci Eng 2, 2339-2346.

Turner, C.T., McInnes, S.J., Cowin, A.J., 2015a. Therapeutic antibodies for improved wound healing. Wound Practice & Research: Journal of the Australian Wound Management Association 23, 16-24.

Turner, C.T., McInnes, S.J., Melville, E., Cowin, A.J., Voelcker, N.H., 2017. Delivery of Flightless I Neutralizing Antibody from Porous Silicon Nanoparticles Improves Wound Healing in Diabetic Mice. Adv Healthc Mater 6.

Turner, C.T., McInnes, S.J.P., Voelcker, N.H., Cowin, A.J., 2015b. Therapeutic Potential of Inorganic Nanoparticles for the Delivery of Monoclonal Antibodies. Journal of Nanomaterials 2015, 309602.

Turner, C.T., Waters, J.M., Jackson, J.E., Arkell, R.M., Cowin, A.J., 2015c. Fibroblast-specific upregulation of Flightless I impairs wound healing. Exp Dermatol 24, 692-697.

Uutela, M., Wirzenius, M., Paavonen, K., Rajantie, I., He, Y., Karpanen, T., Lohela, M., Wiig, H., Salven, P., Pajusola, K., Eriksson, U., Alitalo, K., 2004. PDGF-D induces macrophage recruitment, increased interstitial pressure, and blood vessel maturation during angiogenesis. Blood 104, 3198-3204.

van Baar, M.E., Essink-Bot, M.L., Oen, I.M., Dokter, J., Boxma, H., van Beeck, E.F., 2006. Functional outcome after burns: a review. Burns 32, 1-9.

Veith, A.P., Henderson, K., Spencer, A., Sligar, A.D., Baker, A.B., 2019. Therapeutic strategies for enhancing angiogenesis in wound healing. Adv Drug Deliv Rev 146, 97-125.

Velnar, T., Bailey, T., Smrkolj, V., 2009. The wound healing process: an overview of the cellular and molecular mechanisms. J Int Med Res 37, 1528-1542.

Velnar, T., Gradisnik, L., 2018. Tissue Augmentation in Wound Healing: the Role of Endothelial and Epithelial Cells. Med Arch 72, 444-448.

Verhamme, P., Hoylaerts, M.F., 2006. The pivotal role of the endothelium in haemostasis and thrombosis. Acta Clin Belg 61, 213-219.

Vermeulen, H., Westerbos, S.J., Ubbink, D.T., 2010. Benefit and harm of iodine in wound care: a systematic review. J Hosp Infect 76, 191-199.

Vestweber, D., 2015. How leukocytes cross the vascular endothelium. Nat Rev Immunol 15, 692-704.

Viera, M.H., Amini, S., Valins, W., Berman, B., 2010. Innovative therapies in the treatment of keloids and hypertrophic scars. J Clin Aesthet Dermatol 3, 20-26.

Vos, A.C., Wildenberg, M.E., Duijvestein, M., Verhaar, A.P., van den Brink, G.R., Hommes, D.W., 2011. Anti-tumor necrosis factor-α antibodies induce regulatory macrophages in an Fc region-dependent manner. Gastroenterology 140, 221-230.

Wall, S.L., Clarke, D.L., Allorto, N.L., 2019. Analgesia protocols for burns dressings: Challenges with implementation. Burns 45, 1680-1684.

Wang, J., Hossain, M., Thanabalasuriar, A., Gunzer, M., Meininger, C., Kubes, P., 2017. Visualizing the function and fate of neutrophils in sterile injury and repair. Science 358, 111-116.

Wang, S., Li, X., Parra, M., Verdin, E., Bassel-Duby, R., Olson, E.N., 2008. Control of endothelial cell proliferation and migration by VEGF signaling to histone deacetylase 7. Proc Natl Acad Sci U S A 105, 7738-7743.

Wang, T., Chuang, T.H., Ronni, T., Gu, S., Du, Y.C., Cai, H., Sun, H.Q., Yin, H.L., Chen, X., 2006. Flightless I homolog negatively modulates the TLR pathway. J Immunol 176, 1355-1362.

Wang, T., Gu, S., Ronni, T., Du, Y.C., Chen, X., 2005. In vivo dual-tagging proteomic approach in studying signaling pathways in immune response. J Proteome Res 4, 941-949.

Wang, T., Song, W., Chen, Y., Chen, R., Liu, Z., Wu, L., Li, M., Yang, J., Wang, L., Liu, J., Ye, Z., Wang, C., Chen, K., 2016. Flightless I Homolog Represses Prostate Cancer Progression through Targeting Androgen Receptor Signaling. Clin Cancer Res 22, 1531-1544.

Wang, Y., Beekman, J., Hew, J., Jackson, S., Issler-Fisher, A.C., Parungao, R., Lajevardi, S.S., Li, Z., Maitz, P.K.M., 2018. Burn injury: Challenges and advances in burn wound healing, infection, pain and scarring. Adv Drug Deliv Rev 123, 3-17.

Wang, Y., Graves, D.T., 2020. Keratinocyte Function in Normal and Diabetic Wounds and Modulation by FOXO1. Journal of Diabetes Research 2020, 3714704.

Warszawski, S., Borenstein Katz, A., Lipsh, R., Khmelnitsky, L., Ben Nissan, G., Javitt, G., Dym, O., Unger, T., Knop, O., Albeck, S., Diskin, R., Fass, D., Sharon, M., Fleishman, S.J., 2019. Optimizing antibody affinity and stability by the automated design of the variable light-heavy chain interfaces. PLoS Comput Biol 15, e1007207.

Wasiak, J., Cleland, H., Campbell, F., Spinks, A., 2013. Dressings for superficial and partial thickness burns. Cochrane Database Syst Rev 2013, Cd002106.

Wehrhan, F., Rödel, F., Grabenbauer, G.G., Amann, K., Brückl, W., Schultze-Mosgau, S., 2004. Transforming growth factor beta 1 dependent regulation of Tenascin-C in radiation impaired wound healing. Radiother Oncol 72, 297-303.

Werner, S., Krieg, T., Smola, H., 2007. Keratinocyte-fibroblast interactions in wound healing. J Invest Dermatol 127, 998-1008.

West, H.C., Bennett, C.L., 2018. Redefining the role of langerhans cells as immune regulators within the skin. Frontiers in Immunology 8, 1941.

Wickett, R.R., Visscher, M.O., 2006. Structure and function of the epidermal barrier. American Journal of Infection Control 34, S98-S110.

Widgerow, A.D., 2011. Cellular/extracellular matrix cross-talk in scar evolution and control. Wound Repair Regen 19, 117-133.

Wilgus, T.A., Roy, S., McDaniel, J.C., 2013. Neutrophils and Wound Repair: Positive Actions and Negative Reactions. Adv Wound Care (New Rochelle) 2, 379-388.

Wilkinson, H.N., Hardman, M.J., 2020. Wound healing: cellular mechanisms and pathological outcomes. Open Biol 10, 200223.

Wilkinson, P.C., 1998. Assays of leukocyte locomotion and chemotaxis. J Immunol Methods 216, 139-153.

Willenborg, S., Knipper, J., Ranjan, R., Krieg, T., Eming, S., 2010. Advances in Wound Care.

Wilson, S.A., Brown, E.C., Kingsman, A.J., Kingsman, S.M., 1998. TRIP: a novel double stranded RNA binding protein which interacts with the leucine rich repeat of flightless I. Nucleic Acids Res 26, 3460-3467.

Witte, M.B., Barbul, A., 1997. General principles of wound healing. Surg Clin North Am 77, 509-528.

Wong, R., Geyer, S., Weninger, W., Guimberteau, J.C., Wong, J.K., 2016. The dynamic anatomy and patterning of skin. Exp Dermatol 25, 92-98.

Wood, F.M., 2014. Skin regeneration: the complexities of translation into clinical practise. Int J Biochem Cell Biol 56, 133-140.

Wu, L., Chen, H., Zhu, Y., Meng, J., Li, Y., Li, M., Yang, D., Zhang, P., Feng, M., Tong, X., 2013. Flightless I homolog negatively regulates ChREBP activity in cancer cells. Int J Biochem Cell Biol 45, 2688-2697.

Xiang, Q., Xiao, J., Zhang, H., Zhang, X., Lu, M., Zhang, H., Su, Z., Zhao, W., Lin, C., Huang, Y., Li, X., 2011. Preparation and characterisation of bFGF-encapsulated liposomes and evaluation of wound-healing activities in the rat. Burns 37, 886-895.

Xiao, Z., Zhang, F., Lin, W., Zhang, M., Liu, Y., 2010. Effect of botulinum toxin type A on transforming growth factor beta1 in fibroblasts derived from hypertrophic scar: a preliminary report. Aesthetic Plast Surg 34, 424-427.

Xue, M., Jackson, C.J., 2015. Extracellular Matrix Reorganization During Wound Healing and Its Impact on Abnormal Scarring. Adv Wound Care (New Rochelle) 4, 119-136.

Yamaguchi, Y., Mann, D.M., Ruoslahti, E., 1990. Negative regulation of transforming growth factor-beta by the proteoglycan decorin. Nature 346, 281-284.

Yang, C.M., Ji, S., Li, Y., Fu, L.Y., Jiang, T., Meng, F.D., 2017. β-Catenin promotes cell proliferation, migration, and invasion but induces apoptosis in renal cell carcinoma. Onco Targets Ther 10, 711-724.

Yang, G.N., Strudwick, X.L., Bonder, C., Kopecki, Z., Cowin, A.J., 2020. Effect of Flightless I Expression on Epidermal Stem Cell Niche During Wound Repair. Adv Wound Care (New Rochelle) 9, 161-173.

Yang, P., An, H., Liu, X., Wen, M., Zheng, Y., Rui, Y., Cao, X., 2010. The cytosolic nucleic acid sensor LRRFIP1 mediates the production of type I interferon via a beta-catenin-dependent pathway. Nat Immunol 11, 487-494.

Yoo, S.K., Huttenlocher, A., 2011. Spatiotemporal photolabeling of neutrophil trafficking during inflammation in live zebrafish. J Leukoc Biol 89, 661-667.

Zaidi, A., Green, L., 2019. Physiology of haemostasis. Anaesthesia & Intensive Care Medicine 20, 152-158.

Zhang, J., Wong, M.G., Wong, M., Gross, S., Chen, J., Pollock, C., Saad, S., 2015. A cationic-independent mannose 6-phosphate receptor inhibitor (PXS64) ameliorates kidney fibrosis by inhibiting activation of transforming growth factor-β1. PLoS One 10, e0116888.

Zhibo, X., Miaobo, Z., 2009. Intralesional botulinum toxin type A injection as a new treatment measure for keloids. Plast Reconstr Surg 124, 275e-277e.